

Aus der Klinik für Allgemeine, Unfall- und Wiederherstellungschirurgie
– Innenstadt, der Ludwig-Maximilians-Universität zu München
Direktor: Prof. Dr. med. Wolfgang Böcker

The role of NF- κ B signaling in cartilage development and function

Dissertation
zum Erwerb des Doktorgrades der Humanbiologie
an der Medizinischen Fakultät der
Ludwig-Maximilians-Universität zu München

vorgelegt von
Feng-Koo, Hsieh

aus
Taipei, Taiwan

Jahr
2017

Mit Genehmigung der Medizinischen Fakultät
der Universität München

Berichterstatter: Prof. Dr. med. Matthias Schieker

Mitberichterstatter: Priv.-Doz. Dr. med. Jörg Hausdorf

Prof. Dr. Marcus Schmitt-Sody

Mitbetreuung durch den
promovierten Mitarbeiter:

Priv.-Doz. Attila Aszoi

Dekan: Prof. Dr. med. dent. Reinhard HICKEL

Tag der mündlichen Prüfung: 23.10.2017

Table of Contents

1	Introduction	1
1.1.	Forward	1
1.2.	Clinical relevance of cartilage disorders	1
1.3.	Structure of articular cartilage	4
1.4.	Composition of articular cartilage	5
1.4.1.	Chondrocyte	5
1.4.2.	Water	5
1.4.3.	Collagens	6
1.4.4.	Proteoglycans	7
1.4.5.	Noncollagenous glycoproteins	8
1.5.	Function of articular cartilage	9
1.5.1.	Biomechanical function	9
1.6.	Metabolism within the cartilage	11
1.7.	The development of bone	12
1.7.1.	Cartilage differentiation during endochondral bone formation	13
1.7.2.	Intramembranous ossification	14
1.7.3.	Endochondral ossification	14
1.7.4.	Growth plate	15
1.7.4.1.	Structure and function of the cartilaginous growth plate	15
1.7.4.2.	Metaphysis	19
1.7.4.3.	Peripheral ossification groove of Ranvier	19
1.8.	Chronic cartilage disorders	20
1.8.1.	Aetiology of cartilage lesions	20
1.8.2.	Cartilage injuries among athletes	20
1.8.3.	Osteoarthritis	22
1.8.4.	Current, non-surgical treatment options for cartilage injury	26
1.8.5.	Inhibition of NF- κ B pathway by pharmacologic agents	28
1.8.6.	Operative treatment options	30
1.9.	The NF- κ B/Rel family of transcription factors	30
1.9.1.	The NF- κ B signaling pathways	32
1.9.2.	Activation of the IKK complex	34
1.9.3.	NF- κ B pathway in skeletal development and arthritis	35
1.10.	Model to study NF- κ B canonical pathway in cartilage development	37
2.	Aim and milestones of the thesis	38
3.	Materials and Methods	39
3.1.	Animal	39
3.1.1.	Mouse housing and breeding	39
3.1.2.	Mouse genotyping	39
3.2.	Primary chondrocyte isolation	41
3.3.	Cell culture	42
3.3.1.	Primary cells and culture media	42
3.3.2.	Passaging and counting cells	42
3.3.3.	Cryopreservation and thawing of cells	42

3.4. Tissue culture techniques	43
3.4.1. Femoral head explant culture	43
3.4.2. Mechanically-induced hip injury	44
3.4.3. Metatarsal explant culture.....	44
3.5. mRNA analysis	45
3.5.1. Total RNA isolation	45
3.5.2. Complementary DNA (cDNA) synthesis	46
3.5.3. Polymerase chain reaction (PCR)	46
3.6. Western blotting.....	47
3.6.1. Protein extraction from monolayer culture.....	47
3.6.2. Protein quantification	48
3.6.3. SDS-Polyacrylamide gel electrophoresis (PAGE).....	48
3.6.4. Protein transfer	50
3.6.5. Protein immunodetection	51
3.6.6. Gelatin/collagen Zymography.....	51
3.7. NF-κB reporter assay.....	53
3.7.1. Transfection	53
3.7.2. Dual-Luciferase assay	53
3.8. Time-lapse migration and adhesion assay	53
3.9. Cell attachment assay	54
3.10. Immunofluorescence staining	54
3.11. Whole-mount skeletal staining	56
3.12. Histology	57
3.12.1. Fixation.....	57
3.12.2. Decalcification	58
3.12.3. Embedding	58
3.12.4. Sectioning	58
3.12.5. Hematoxyllin and eosin (H&E) staining	59
3.12.6. Safranin orange staining	59
3.12.7. Von Kossa staining	59
3.12.8. Toluidin blue staining.....	60
3.12.9. Tartrate-resistant acid phosphatase staining (TRAP).....	60
3.12.10. Immunohistochemistry staining (IHC).....	60
3.12.11. Measurement of growth plate	61
3.12.12. Analysis of proliferating columns in growth plate	61
3.13. Non-radioactive <i>in situ</i> hybridization.....	62
3.14. Sulpated glycosaminoglycan (sGAG) assay	65
3.15. Pathological Scoring System of Articular Cartilage.....	65
X-ray imaging	66
3.16. Proliferation and Apoptosis Assays	66
3.17. Atomic force microscopy (AFM).....	67
3.18. Taqman Low-Density Array (TLDA) microfluidic cards	67
3.19. Microscopy.....	69
3.20. Computer software and statistical analysis	70
4. Results	71

4.1. Characterization of <i>NEMO^{fl/Y} Col2a1Cre</i> mice	71
4.1.1. RNA and protein expression of NEMO in <i>NEMO^{fl/Y} Col2a1Cre</i> chondrocytes were completely inhibited	72
4.1.2. Activation of NF- κ B canonical pathway was diminished in <i>NEMO^{fl/Y} Col2a1Cre</i> chondrocytes.....	73
4.1.3. I κ B α sequestered p65 dimers in cytoplasm of <i>NEMO^{fl/Y} Col2a1Cre</i> chondrocytes.	74
4.1.4. p65 in <i>NEMO^{fl/Y} Col2a1Cre</i> chondrocyte failed to relocate into nucleus.....	74
4.1.5. Expression of NEMO was specifically prohibited in cartilage tissue of <i>NEMO^{fl/Y} Col2a1Cre</i> mice	75
4.2. The influence of NEMO-deficiency on the skeleton development of the embryonic stage	76
4.2.1. <i>NEMO^{fl/Y} Col2a1Cre</i> mice displayed similar skeleton development at embryonic stage	76
4.2.2. Length and ossification of NEMO-deficient long bone were similar to wild-type	77
4.2.3. Skeleton differentiation in <i>NEMO^{fl/Y} Col2a1Cre</i> mice during embryo stage were fairly the same as wild-type	78
4.2.4. No difference was noticed in long bone morphology and proliferation.....	79
4.2.5. Vascular invasion and intramembranous ossification of NEMO-deficient skeleton were comparable to wild-type.....	81
4.2.6. In cytokine-induced growth, NEMO-deficient metatarsals demonstrated comparable growth pattern as wild-type	82
4.3. The impact of NEMO-deficiency to skeleton development at postnatal stage .	84
4.3.1. Post-natal skeletal phenotype of <i>NEMO^{fl/Y} Col2a1Cre</i> mice.....	84
4.3.2. Length of NEMO-deficient long bones was significantly shorten	85
4.3.3. Metaphysis of NEMO-deficient long bone was characterized with shorten growth plate.....	86
4.3.4. NEMO-deficient chondrocytes displayed reduced proliferation activity	87
4.3.5. Apoptotic cells were found in NEMO-deficient growth plate	88
4.3.6. In proinflammatory cytokine induced apoptosis, primary NEMO-deficient chondrocytes were more sensitive to TNF- α -induced apoptosis	89
4.3.7. Disoriented columns in proliferating zone of <i>NEMO^{fl/Y} Col2a1Cre</i> mice	90
4.3.8. Fat-oval-shaped proliferating columns were pronounced in NEMO-deficient growth plate.....	92
4.3.9. NEMO-deficient chondrocytes displayed a reduced migration activity	93
4.3.10. NEMO-deficient chondrocytes possess higher adhesion to cartilage ECM	94
4.3.11. The stiffness of cartilage ECM from <i>NEMO^{fl/Y} Col2a1Cre</i> mice was fairly the same as wild-type	95
4.3.12. NEMO-deficient chondrocytes displayed larger spreading area in vitro	96
4.4. The role of NF-κB canonical pathway in cartilage metabolism using hip explant culture	98
Degradation of proteoglycans and glycosaminoglycans breakdown were partially eased in hip cap of <i>NEMO^{fl/Y} Col2a1Cre</i> mice	98
4.5. Regulation of NF-κB in cartilage responses upon ex vivo induced hip injury 103	
Against mechanical stress, ARG-1, HAS-2, IL-18 and MMP-3 were significantly regulated in hip cap of <i>NEMO^{fl/Y} Col2a1Cre</i> mice compare to wild-type.....	103
4.6. The role of NF-κB canonical pathway in spontaneous OA model	109

<i>NEMO</i> -deficiency has no impact on age-associated, spontaneous osteoarthritis in mice	109
5. Discussion	115
5.1. The <i>NEMO</i>-mediated, canonical NF-κB pathway regulates postnatal growth of endochondral bones via the control of growth plate functions	115
5.2. <i>NEMO</i>/canonical NF-κB signaling modulates chondrocyte survival in postnatal growth plate	117
5.3. Primary <i>NEMO</i>^{fl/y} <i>Col2a1Cre</i> chondrocytes exhibit severe death phenotype upon exposure to TNF-α	118
5.4. <i>NEMO</i> modulates growth plate architecture.....	121
5.5. Efficient ablation of <i>NEMO</i> in chondrocytes alleviate proteoglycan loss upon pro-inflammatory cytokine treatment in hip explant culture.....	123
5.6. An <i>ex vivo</i> hip avulsion model does not indicate a particular importance of NF-κB canonical signaling in injury induced activation of inflammatory gene expression.....	125
5.7. <i>NEMO</i>/canonical NF-κB-deficiency has no apparent consequence on spontaneous, age-associated OA progression in mice.....	127
6. Conclusion	129
7. Summary.....	131
8. Zusammenfassung	132
9. Reference.....	134
10. List of abbreviations.....	154
11. Acknowledgement	158
12. Declaration	159

1 Introduction

1.1. Forward

Signaling through the family of nuclear factor- κ B (NF- κ B) transcription factors is involved in the regulation of numerous genes that are activated in response to stressful conditions such as infection, inflammation or injury. Inflammation processes play pivotal roles in detrimental joint disorders including osteoarthritis (OA) and rheumatoid arthritis (RA), the most common degenerative conditions of the skeletal system. NF- κ B signaling pathways have been indicated to control inflammation and cartilage destruction, which are participating in the pathogenesis of rheumatic diseases. Consequently, the blockade of NF- κ B pathways through pharmacological or gene therapeutic inhibition has been suggested as a potential strategy as treatment of OA and RA. Although blocking the components of NF- κ B signaling cascades are attractive targets for therapy, its beneficial effects on normal skeletal physiology are largely unknown due to the absence of suitable animal models. In this research project, conditional gene targeting was applied in mouse as an experimental model system in order to address the role of canonical NF- κ B in the cartilage. Tissue-restricted inhibition of the canonical NF- κ B pathway in cartilage was achieved by chondrocyte-specific deletion of the inhibitory κ B kinase γ gene (IKK γ) encoding NF- κ B essential modulator (NEMO), a key regulator of the NF- κ B canonical pathway. NEMO is a regulatory subunit of the kinase responsible for deactivation of the inhibitor of NF- κ B, therefore, NEMO deficiency leads to the lack of NF- κ B activation. Analyzing such mouse model, we are able to broaden our understanding of NF- κ B-mediated processes on the regulation of normal and pathological cartilage functions.

1.2. Clinical relevance of cartilage disorders

Primary disorders of cartilage such as osteochondrodysplasias and osteoarthritis (OA) are widely distributed clinical problems in our society. Osteochondrodysplasia refers to a heritable disease occurred from genetic mutations

that can affect the development of cartilage and/or bone. There are more than 400 osteochondrodysplasias that are classified. Although each type of osteochondrodysplasia is relatively rare, the summed prevalence of the disease group has raised as much as from 760 per 1 million births (Andersen and Hauge, 1989; Barbosa-Buck et al., 2012; Orioli et al., 1986; Rasmussen et al., 1996). Osteochondrodysplasia can be accompanied with various complications that affect auditory, cardiac, neurologic orthopedic, pulmonary and renal functions. Dwarfism is the most common symptom of osteochondrodysplasia. Some of them cause short-limbed dwarfism, while the others cause short trunk dwarfism. Achondrodysplasia is one of the most common non-lethal osteochondro-dysplasia (frequency 1/20000) that causes disproportioned dwarfism with an average adult height of 130 cm for men and of 125 cm for women (Krakow and Rimoin, 2010). It is resulted from a mutation of the fibroblast growth factor receptor-3 (FGFR-3) gene, an important regulator of bone growth. Due to the genetic dominance, one mutant copy of FGFR-3 gene is able to induce achondrodysplasia. It is either inherited from parents or arises from spontaneous gene mutation (Richette et al., 2008).

Osteoarthritis (OA), a debilitating disorder of the articular cartilage is widely distributed on the world. Overall, approximately 3.6 percent of the global population (250 million people) is suffered from knee osteoarthritis, one of the most prevalent forms of this disease (Vos et al., 2012). The limb OA predominantly occurs at the knee joint that accounts for 41% of all cases. Hands (30%) and hips (19%) are the secondary vulnerable joints for OA (Cushnaghan and Dieppe, 1991). Global analysis for the incidence has shown that OA is one of the most common musculoskeletal diseases (Millennium, 2003; Wieland et al., 2005). In Europe, a joint replacement is performed every 1.5 minutes due to OA. In Germany, osteoarthritis accounts for about 8 % of all orthopedic treatment (Merx et al., 2007). In the United States, the OA patients represented 25% of the total number of seeking medical helps and were responsible for half of non-steroid anti-inflammatory drugs (NSAIDs) prescriptions. It is estimated that approximately 500,000 joint replacements are performed per annum. In 2011, there were 964,000 patients hospitalized for OA treatment. The total cost of OA medication was approximately 1.48 billion (15400 per stay), which was the second-highest Medicare spending after septicemia (Pfundner et al., 2006).

Generally, the articular cartilage lesions are poorly self-repaired. Partially healed phenomenon only appears in certain biological conditions. Articular cartilage lesions usually cause disability and pain symptoms, such as joint pain, locking phenomenon, reduce physical activity and function. In addition, articular cartilage lesions are usually considered to develop into a serious OA (Gilbert, 1998; Messner and Gillquist, 1996). According to previous studies, risk factors of OA have been verified (Riyazi et al., 2008; Zhang and Jordan, 2010). These factors include: (1) arthritis of finger joints and knee, especially in women (Gunther et al., 1998; Zhang and Jordan, 2008); (2) deformity of hip or femoracetabular impingements (Heliovaara et al., 1993); (3) race and gender (Felson et al., 2000; Zhang and Jordan, 2008); (4) obesity or metabolic disorders; sport injuries (Kujala et al., 1994); and (5) employment factors such as weighty physical work load. The incidence of lower limb OA reaches to the peak in 70-79-age bracket. In female population, the occurrence per 100000 person per years increases from 350 in 50-59 age bracket to 1700 in 70-79 age bracket; in male population, the incidence rises from 280 in 50-59 age bracket to 1280 in 70-79 age bracket (Zhang and Jordan, 2008). The worldwide incidence and prevalence of OA are different, but in general are very high. Due to demographic changes and extension the human lifespan, it is estimated that the number of OA patients will continually increase. In the United States, it is predicted that additional 19 million people will be affected by OA yearly between 1995 and 2020 (Iorio et al., 2008). However, drug development of OA also advances side by side. Optimistically speaking, it is believed that effective therapeutic strategies for OA will be developed in the future. In general, chronic painful cartilage disorders are common invalidating conditions for athletes, occupational and aging population. Osteoarthritis not only influences patients' life quality but also raises considerable medical expenses to the worldwide healthcare system. Therefore, it is pivotal to identify the key factors involved in the onset and progression of OA, and improve our understanding of its basic biology in order to develop effective therapeutical solutions for cartilage disorders.

1.3. Structure of articular cartilage

Typically, the articular cartilage can be divided into four layers (Figure 1). Each layer has a different composition of the extracellular matrix (ECM). The superficial layer (also known as tangential layer) covers the surface of the joint. The ECM in this layer contains fine fibrils running parallel of the surface and only little amount of proteoglycans. The elongated cells within this layer are mostly inactive, but still contain the endoplasmic reticulum, Golgi membranes and mitochondria. Below the superficial zone is the transition zone. There are active chondrocytes with endoplasmic reticulum, Golgi membranes, mitochondria, glycogen, and intracytoplasmic filaments. Besides, the collagen fibrils in transition zone are larger than those of the superficial zone, and they orientation is arcade-like. Chondrocytes in the deep zone (also known as radial layer) are similar to those in the transition zone. However, the cartilage cells are organized into a columns perpendicular to the surface. These cells still contain a large number of intermediate filaments and glycogen granules. This zone contains the largest collagen fibrils of articular cartilage running perpendicular of the surface and a huge amount of proteoglycans. The content of proteoglycans increases from the superficial to the deep zone, while the content of water decreases. The cartilage in the calcified layer is just above the subchondral bone and separated from the radial layer by the tidemark. Chondrocytes in the calcified zone have almost no cytoplasm and endoplasmic reticulum.

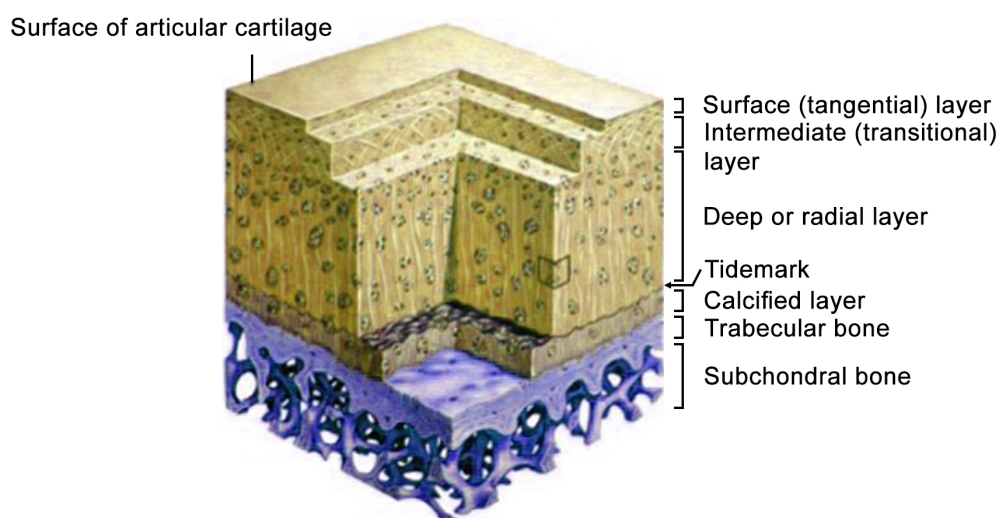


Figure 1. Structure of the articular cartilage. The articular cartilage is organized into various vertical zones and represents a typical anisotropic tissue architecture. From the surface of articular cartilage to the subchondral bone, cartilage is composed of tangential, transitional, radial and calcified layers. Tidemark is located at the surface between the radial and calcified layers. Figure is adapted and modified from (Landínez-Parra et al., 2012).

1.4. Composition of articular cartilage

1.4.1. Chondrocyte

In cartilage tissue, chondrocyte is the only cell type which responsible for cartilage formation and functions. Chondrocytes originated from skeletalgenic mesenchymal stem cells (MSC) during embryonic development. At the site of future chondrogenic elements, mesenchymal stem cells proliferate and aggregate to form condensations in which MSCs differentiated into chondroblasts. Chondroblasts secrete a typical cartilage ECM including collagen fibers, glycosaminoglycans and proteoglycans. The chondroblasts are trapped in cavities known as cartilage lacunae, which is enriched in interstitial fluid (Figure 2). The chondroblasts later become mature chondrocytes that usually stay inactive but are able to secrete and degrade the ECM.

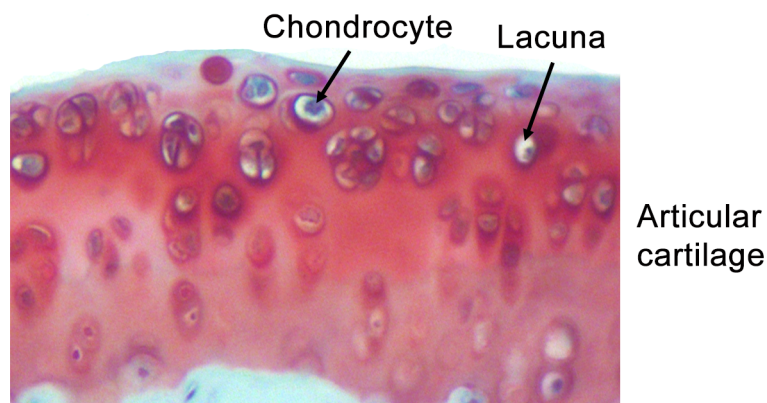


Figure 2. Safranin-orange stained section of the articular cartilage. The chondrocytes are trapped into lacuna of the cartilage matrix.

1.4.2. Water

The water content of cartilage is approximately 80% of wet weight. A small portion of the water is encased within the chondrocytes, but the bulk of water is presented in the pores of the matrix and intrafibrillar space (Maroudas et al., 1991; Torzilli, 1985). The content of water concentration reduces from 80% through the superficial and deep zones. The tissue fluid is enriched with Ca^{2+} , Cl^- , K^+ and Na^+ ions (Lai et al., 1991; Linn and Sokoloff, 1965). Water in the cartilage layers not only

functions as lubricating fluid but also facilitate the distribution of nutrients to chondrocytes.

Principally, water within interfibrillar space is served as a gel. Through compression or applying a pressure gradient across the tissue, most of the water passes through the cartilage ECM. Owing to the high friction resistance of cartilage against water flow, cartilage permeability is very low. The friction resistance and the pressurization of water in cartilage ECM form the basic mechanisms supporting articular cartilage to withstand constant or repeated loads caused by body weight and movement of the skeleton.

1.4.3. Collagens

To date, there are 28 members of collagens discovered and expressed in various tissues. Every member in the collagen family contains triple helix structure from 3 polypeptide chains (α -chains). The polypeptide chains mostly consist of glycine and proline with occasional hydroxyproline, which stabilize the structure of collagen (James and Uhl, 2001).

Collagens are the most abundant structural ECM molecules in cartilage and account for 60% of the dry weight (Sophia Fox et al., 2009). Among all collagens in the cartilage ECM, 90% to 95% of collagens is type collagen II. Collagen II constitutes fibers that entrap with proteoglycan aggregates. Collagen types I, IV, V, VI, IX, and XI account for the remained 5%-10% in the articular cartilage. The cartilage fibrils besides collagen II, contain collagen IX and XI as minor components. In mammalian articular cartilage, proportion of collagen II, IX, and XI in cartilage fibrils does not alter substantially between zones. However, changes in composition of cartilage fibrils were observed in young versus adult articular cartilages (collagen IX: 10% vs. 1%, collagen XI: 10% vs. 3% and collagen II: 80% vs. 95%, respectively) (Eyre, 2002). The triple helix structure of fibrillar collagens accounts for the tensile and shear properties of articular cartilage and stabilizes the structure ECM.

1.4.4. Proteoglycans

Proteoglycans are widely expressed glycosylated proteins in various types of tissues. Proteoglycans consist of a linear core protein and coupling with multiple negative charged side chains glycosaminoglycan (GAG), which can be composed up to more than 100 monosaccharides (James and Uhl, 2001). Due to charge repulsion, all of the glycosaminoglycans chains in proteoglycan separate from each other. Articular cartilage consists of various proteoglycans such as fibromodulin, biglycan, decorin and aggrecan.

The most abundant and the largest protein in cartilage ECM is aggrecan. Aggrecan core protein is substituted with about 100 chondroitin sulfate and multiple keratan sulfate GAG chains. Aggrecan molecules can bind to hyaluronan (HA) via link protein and subsequently form massive proteoglycan aggregates (Figure 3). Aggrecan is predominantly trapped between the collagen fibrils of cartilage ECM and it plays critical role in resisting of compressive loads due to water binding caused by the negative charged GAG chains.

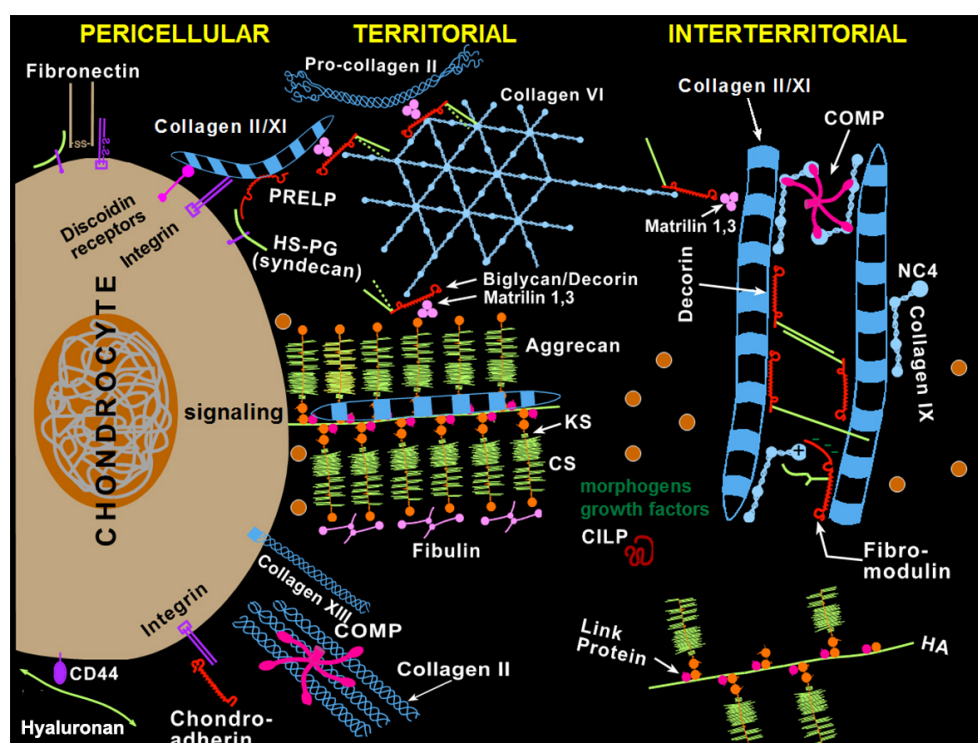


Figure 3: Cartilage extracellular matrix. According to the distance to chondrocyte, cartilage ECM can be divided into pericellular, territorial and interterritorial matrix. The pericellular matrix surrounds a chondrocyte and binds to the membrane receptors of ECM components; the territorial matrix locates between pericellular matrix and interterritorial matrix; the interterritorial matrix is the farthest matrix compartment from the chondrocytes. Each area is formed by macromolecular assemblies (e.g. collagen network and proteoglycan aggregates) which are modulated via numerous regulatory and adaptor proteins. Figure is adapted and modified from (Heinegard and Saxne, 2011).

The major function of non-aggregating proteoglycans is the interaction with collagens. Non-aggregating proteoglycans in articular cartilage such as decorin, biglycan and fibromodulin are much smaller than aggrecan. Although these proteoglycans have similar structure, they can be distinguished by the attached glycosaminoglycan chain. Biglycan predominantly distributes on the periphery of chondrocytes and contains a dermatan sulfate chain which is likely attached to collagen VI (Sophia Fox et al., 2009). Decorin and fibromodulin contain dermatan sulfate and keratan sulfate chains, respectively. They interact with collagen II fibrils and participate in interfibrillar stabilization and fibrillogenesis (James and Uhl, 2001).

1.4.5. Noncollagenous glycoproteins

In addition to proteoglycans, there are numbers of non-collagenous glycoproteins found within the articular cartilage (Neame et al., 1999). Some of these proteins are participated in the structure organization and maintenance of cartilage ECM by interacting with collagens and/or proteoglycans. Thrombospondin-5/cartilage oligomeric matrix protein (COMP), proline- and arginine-rich end leucine-rich repeat protein (PRELP), matrilin-1, matrilin- 3 and fibronectin are know to stabilize the supermolecular assembly of the cartilage ECM (Bengtsson et al., 2000; Briggs et al., 1995; Jenkins et al., 1990; Mann et al., 2004; Romberger, 1997; Wiberg et al., 2003). There are also proteins which play regulatory role in cell proliferation and chondrocyte metabolism such as glycoprotein-39 (gp-39), matrix gla protein (MGP), chondromodulins, cartilage-derived retinoic acid responsive protein (CD-RAP) and various growth factors (Roughley, 2001).

By utilizing transcriptomic, proteomic and mass spectrometry techniques, proteins in cartilage ECM have been broadly characterized. However, the precise biological function of noncollagenous glycoproteins is still not completely understood.

1.5. Function of articular cartilage

Articular cartilage works as shock absorber to distribute the compressive loads, minimize peak stresses on subchondral bone. It efficiently reduces friction resistance and provides weight-bearing surface. Owing to the remarkably elasticity of articular cartilage, it can be deformed and recover its original shape. Articular cartilage has been well characterized with a low level of mitotic and metabolic activities, lacks blood vessels, lymphatic vessels, and nerves compares to other soft tissues. Essentially, articular cartilage functions and stands alone. Structure of cartilage is highly complexed and ordered. Unless affected by diseases or injuries, the structure of articular cartilage remains stable and unchanged (James and Uhl, 2001).

1.5.1. Biomechanical function

The biomechanical behavior of articular cartilage has been well studied. Articular cartilage contains solid ECM and a fluid phase with water and inorganic ions (e.g. sodium, calcium, chloride, and potassium), which represents 20% and 80% of wet weight of articular, respectively. Due to the proteoglycan aggregates and interstitial fluid, negative electrostatic repulsion forces is created and provides compressive resilience to articular cartilage (Mankin et al., 1994; Maroudas, 1979; Mow and Ratcliffe, 1997).

When compressive load is applied to joint, the interstitial fluid pressure raises rapidly. Due to the local increase of fluid pressure, the interstitial fluid flows out of the ECM and generates large friction in the ECM (Frank and Grodzinsky, 1987; Maroudas and Bullough, 1968; Mow et al., 1984). The interstitial fluid flows back into ECM soon after the compressive load is removed. The low permeability efficiently prevents the interstitial fluid from rapidly flowing out of ECM in respond to compressive load. The covered cartilage layer on the both end of bones (e.g. femur and tibia) forms the joint with limited mechanical movements (James and Uhl, 2001).

Articular cartilage is characterized by its viscoelasticity and demonstrates time-dependent behavior when constant compressive loads or deformations are applied (Woo et al., 1987). Two mechanisms are involved in the viscoelasticity of articular cartilage. (1) Flow-dependent mechanism is based on the interstitial fluid and the friction resistance generated by this flow as mentioned above (Ateshian et al., 1997;

Mow et al., 1984; Mow et al., 1980; Simon et al., 1984). The dragging force from interstitial fluid and friction of ECM provide viscoelastic behavior of articular cartilage (Mow et al., 1980). (2) Flow-independent mechanism is attributed to the intrinsic viscoelastic property of collagen-proteoglycan supermolecular assemblies (Hayes and Bodine, 1978). Relying on the flow-dependent mechanism, the pressure of interstitial fluid counteracts the majority of total compressive load. The stress acts directly to solid matrix is largely reduced, viscoelastic property of solid matrix then covers the rest of the total load.

Creep and stress-relaxation reaction in the articular cartilage also play important roles in response to compressive loads. The deformation of articular cartilage shows and increases with time when a constant compressive load is applied (Mow et al., 1984). The zonal organization of cartilage remarkably enhances the resistance against shear stress. Collagen fibrils within the cartilage stretch in response to shear stress (Hayes and Mockros, 1971; Setton et al., 1995) (Figure 4). The molecular composition and inter/intra-molecular interactions of collagen fibrils ensure the cartilage with moderate level of tensile responses (Figure 5).

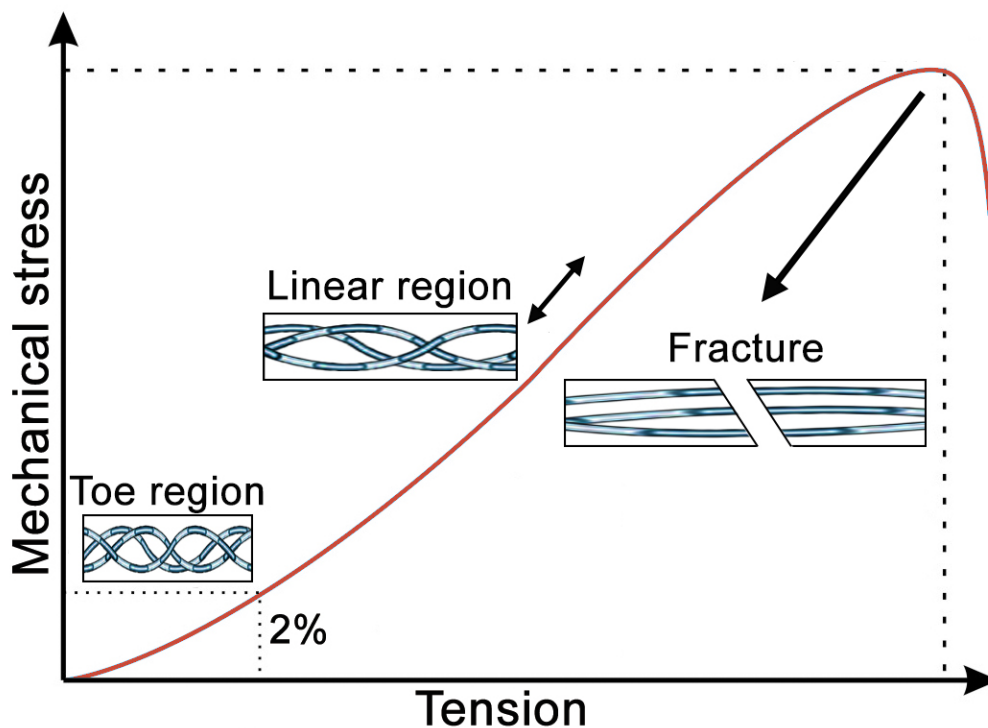


Figure 4: Strain curve of articular cartilage. The curve is consisted of 3 parts: toe region, linear region and fracture. Toe region is considered as relaxed state of collagen fibrils. The collagen fibrils linearly respond to the mechanical stress in toe and linear regions. With the increase of mechanical stress, excessive stress eventually results in cartilage fracture. Figure is adapted and modified from (Robi et al., 2013).

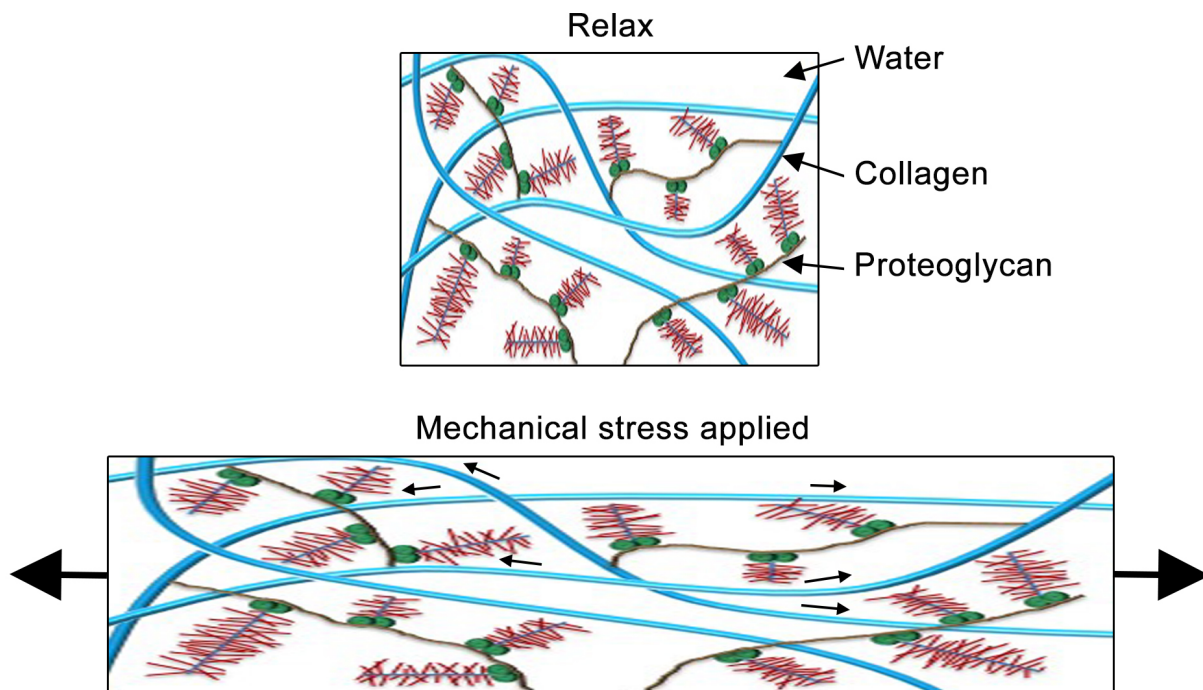


Figure 5: Deformation of cartilage ECM under tensile force. When mechanical stress is loaded, the collagen fibrils are stretched towards both ends. Figure is adapted and modified from (James and Uhl, 2001).

1.6. Metabolism within the cartilage

Articular cartilage receives nutrients from the synovial fluid due to the lack of penetrating blood vessels in the cartilage. Nutrients from synovial fluids diffuse into pores of cartilage ECM that are averagely 6 nm wide (Linn and Sokoloff, 1965; Mow et al., 1992). Thus, the metabolism of chondrocytes is mainly anaerobic.

Chondrocytes play essential role in ECM deposition, maintenance and repair. Various chemical and biomechanical factors from peripheral microenvironment can mediate the metabolism of chondrocytes (James and Uhl, 2001). Cytokines (e.g. TNF- α and IL-1), regulator peptides (e.g. parathyroid hormone-related peptide, PTHrP), growth factors (e.g. IGFs, FGFs), and physiological loadings provide chemical and mechanical signal, respectively, which balance anabolic and catabolic cascades important for the homeostasis and remodeling of the articular cartilage. Controlled synthesis and degradation of cartilage macromolecules (like proteoglycans and collagens) are essential for the proper function of the cartilage.

ECM surrounding the chondrocytes protects the potential damage from biomechanical forces. Cartilage ECM remains homeostatic by newly synthesized

macromolecules such as proteoglycans and collagens. The turnover rate of proteoglycan is ranged from hours to years (Masuda et al., 2003) whereas the turnover rate of collagens is over hundred years (Eyre et al., 2006).

Turnover and degradation of cartilage are mainly accomplished by metalloproteinases including matrix metalloproteinases (MMPs), a disintegrin and metalloproteinase with thrombospondin motifs proteinases (ADAMTSs) and cathepsins. Metalloproteinases are synthesized as proenzymes, which need extracellular cleavage to be fully activated. Collagenases (MMP-1 and MMP-13) and gelatinases (MMP-2 and MMP-9) are responsible to disassemble fibrils of collagens and degradation of elastin and fibronectin, whereas stromlysin-1 (MMP-3), ADAMTS-4 and ADAMTS-5 participate in core protein degradation of aggrecan (Poole et al., 1987). Cathepsins are involved in aggrecan degradation (James and Uhl, 2001).

The physiological architecture and function of articular cartilage is mainly maintained by joint motion and normal mechanical load. Lack of joint activity has been reported to cause cartilage degradation (Buckwalter and Mankin, 1998). Abnormal change of cartilage metabolism is often associated with inflammatory conditions accompanying osteoarthritis, which usually takes place when catabolism and anabolism of chondrocytes are imbalanced (Torzilli et al., 1999).

1.7. The development of bone

The development of bone is defined as bone formation and growth. Intramembranous ossification and endochondral ossification are responsible for the formation of all bone tissue from mesenchymal condensation. Intramembranous ossification is a mechanism that predominately occurs in bones of the skull through the linch differentiation or bone-produced osteoblasts from skullgenic MSCs. Endochondral ossification is the other bone producing mechanism that transforms mesenchymal tissue into cartilage and sequentially into bone tissue. Endochondral bones grow in length at the epiphyseal growth plate mediated by a process, which is similar to endochondral ossification. This process continues throughout entire childhood and the adolescent years. When the growth of cartilage slows down and stops eventually, the growth plate is completely ossified and remains as an epiphyseal line. Even after adult stature is attained, bone development continues

throughout adulthood for increase of thickness or diameter, repair of fractures and remodeling of bone to meet change of lifestyle.

1.7.1. Cartilage differentiation during endochondral bone formation

Early skeletal development of endochondral bone contains two consecutive phases of morphogenesis and growth. In the former phase, the cartilaginous templates of skeletal elements are laying down from the mesenchyme, while in the latter phase the cartilage anlage grows into the mature skeleton. The longitudinal bone growth accounts for the size of organism. The skeletal development initiates from condensation of mesenchymal stem cells, which differentiates into chondroblasts (Figure 6) (Hall and Miyake, 2000; Morriss-Kay, 2001). After an intensive proliferation phase, chondroblasts differentiate into chondrocytes and secrete cartilage ECM that served as a template for the future bones. The typical cartilage ECM of endochondral bones contain a variety of collagens (II, IX, and XI), proteoglycans (aggrecan) and matrix proteins such as matrilins and cartilage oligomeric matrix protein (Morris, 2002). During human embryogenesis, condensation of mesenchymal stem cells can be observed at 6.5 weeks of the pregnancy. Chondrocytes differentiated from mesenchymal stem cells form the bone template (also known as cartilage anlagen), which can be observed from the 16th week of pregnancy (Uthoff, 1988). The development of similar cartilaginous structures can be observed in mouse in between embryonic days E11.5 and E13.5 of the pregnancy (Kaufman, 1992). The transcription factors of SOX family play an important role in the initiation of chondrogenic differentiation (de Crombrughe et al., 2001). SOX-9 participates in the early stage of differentiation and induces the expression of the transcriptions factors SOX-5 and SOX-6, which are important for the differentiation of chondrocytes (Bi et al., 1999; Lefebvre et al., 2001). Moreover, SOX-9 can activate genes of cartilage ECM proteins including collagen II and XI (de Crombrughe et al., 2001). Growth factors such as bone morphogenetic proteins (BMPs), fibroblast growth factors (FGFs), and morphogens like Indian hedgehog (Ihh) also contribute to the cartilage formation, chondrocyte proliferation and differentiation (de Crombrughe et al., 2001).

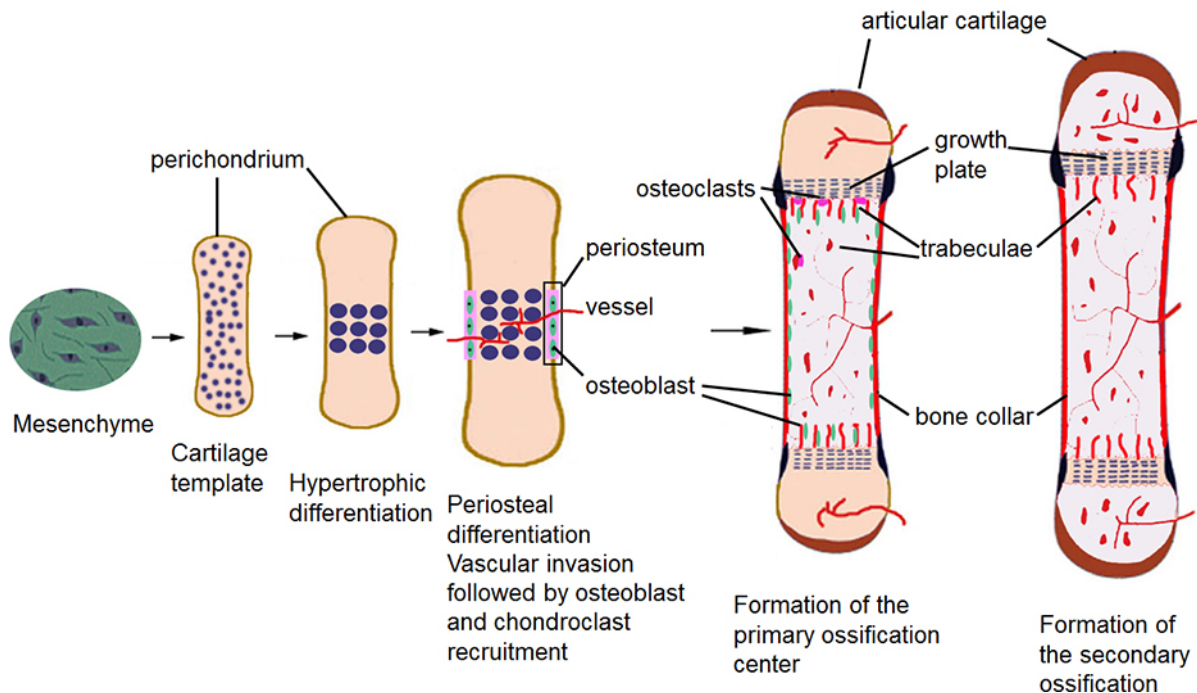


Figure 6: Endochondral bone formation. The mesenchymal stem cells condense and form the cartilaginous anlage surrounded by the perichondrium. Chondrocytes in the center of cartilage template initiate hypertrophic differentiation. The periosteal cells next to hypertrophic chondrocytes become osteoblasts (bone collar) followed by vascular invasion. Mature hypertrophic chondrocytes secrete calcified matrix and undergo apoptosis or transdifferentiate into osteoblasts. Chondroclasts following the invaded blood vessels degrade the calcified matrix, while osteoblasts produce the trabecular bone of the primary ossification center. The secondary ossification centers form at both ends of the long bones. The chondrocytes between primary and secondary ossification region form the cartilaginous growth plate, which is responsible for the longitudinal growth of bone. The groove of Ranvier is involved in the circumferential growth of the bone.

1.7.2. Intramembranous ossification

Intramembranous ossification is the other indispensable process that forms rudimentary bones during embryonic development. It is also known to be an important process in the recovery of bone fractures (Brighton and Hunt, 1991) and in the skull formation. Otherwise from endochondral ossification, no cartilage is created during intramembranous ossification.

1.7.3. Endochondral ossification

Endochondral ossification is an essential process to create bone tissue from cartilaginous templates during development of the mammalian skeletal system. It plays important role in longitudinal growth of the skeletal elements (Brighton and Hunt, 1986). In long bones, endochondral ossification begins at the middle of anlage

called the diaphysis (Figure 6). The perichondrium covering the cartilage templates differentiates into the periosteum at the level of diaphysis. A layer of undifferentiated cells (osteoprogenitor cells) within periosteum soon differentiate to be osteoblasts that are responsible for production and secretion of bone matrix.

At the same time, diaphyseal chondrocytes enlarge and become hypertrophic in the center of primary ossification and secrete mineralized matrix. The remaining calcified ECM is taken as a scaffold and consequently turns into bone trabecula by osteoprogenitor cells, which enter through the periosteal bud (Horton, 2003). Afterwards, trabecular bones are digested by osteoclasts and release an empty cavity known as bone marrow.

1.7.4. Growth plate

The growth plate (known as epiphyseal plate or physis) is a discoidal area that located between the epiphysis and diaphysis of long bones. It is formed during endochondral ossification and mediates a process that largely transforms the preexisting cartilaginous template into bone. The growth plate is responsible for longitudinal and lateral growth of bones and composed of three anatomically distinct but functionally interacting areas: 1) the cartilaginous growth plate, (2) the bony metaphysis and (3) the peripheral ossification groove of Ranvier (Ballock and O'Keefe, 2003; Brighton, 1978).

1.7.4.1. Structure and function of the cartilaginous growth plate

The cartilaginous growth plate is a hierarchically structured, anisotropic tissue which is responsible for longitudinal growth of endochondral bones during embryonic and early postnatal development. Chondrocytes within the growth plate are arranged into horizontal zones of resting, proliferating, prehypertrophic (a transition zone between the proliferative and hypertrophic zones) and hypertrophic. Vertically, cells organized into longitudinal columns from the proliferative zone (Figure 7). The structure and composition of these zones and columns in the cartilaginous growth plate are slightly different from species to species. In avians, the cartilaginous growth plate is characterized as less column structure with high cellularity and less matrix

production. Thus, the size of proliferation zone is the primary growth rate-determining factor for avians (Farquharson and Jefferies, 2000; Howlett, 1979; Kember et al., 1990). The columns in the cartilaginous growth plate of mammals are more distinct owing to the extensive cartilage matrix synthesis. The change of hypertrophic chondrocyte volume, besides chondrocyte proliferation and matrix production, is the most critical factor regulating longitudinal growth in vertebrates (Breur et al., 1991; Hunziker, 1994). Due to the balance between growth and resorption at the cartilage-osseous junction of the metaphysis, the thickness of growth plate remains almost constant during development.

The resting (or reserve) zone consists of small and rounded chondrocytes within the cartilage matrix. Nucleoside analog incorporation experiments show that chondrocytes in resting zone have slow cell cycle and rarely proliferate (Candela et al., 2014; Kember, 1971; Ohlsson et al., 1992). It was suggested that resting zone is a pool of chondro-precursors for chondrocytes supplying in the proliferating zone. Supporting this hypothesis, the surgical-removed rabbit growth plate was recovered by re-implantation of the resting zone (Abad et al., 2002). The origin of resting progenitors is not clear, but it is suggested that these cells are migrating from the bone marrow or follow penetrating blood vessels of the epiphysis (Candela et al., 2014).

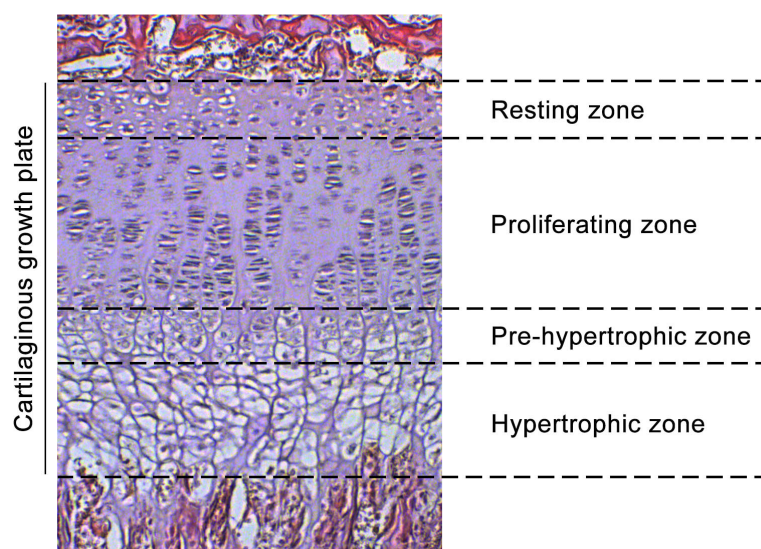


Figure 7: The cartilaginous growth plate. Resting zone is considered as a reservoir of rounded, precursor cells for chondrocytes in the proliferation zone (Kronenberg, 2003). In the proliferating zone, chondrocytes flatten with right angle of the longitudinal direction of the growth, mitotically active and produce cartilage matrix (Ogden and Rosenberg, 1988). In the prehypertrophic zone, the cells start to enlarge in size, and stop to divide as a part of the chondrogenic maturation program. In the

hypertrophic zone, the chondrocytes eventually can be 5–12 times larger in volume compared to cells in the proliferative zone (Ogden and Rosenberg, 1988). Terminally differentiated hypertrophic chondrocytes then either die by apoptosis or transdifferentiate into osteoblasts at the chondro-osseous junction (Pirog and Briggs, 2010).

The proliferating zone consists of flattened chondrocytes which form characteristic, longitudinal columns. Experiments in rodents showed that only chondrocytes in the upper half of the proliferative zone are with mitotic activity. Chondrocytes in the lower half zone merging with the prehypertrophic zone stop proliferating and undergo the process of maturation (Vanky et al., 1998). According to the location of the growth plate, the average cell cycle time is from 24 to 76 hours. (Vanky et al., 1998; Wilsman et al., 1996). From resting zone to proliferation zone, chondrocytes average divide four times and then move into the hypertrophic zone. (Farnum and Wilsman, 1993). Proliferating chondrocytes divide in a specific manner that is different from most of cell types in the body. The general cell biological rules of Hertwig for the orientation of the mitotic spindle and cell division plane describe two prominent features of dividing proliferating chondrocytes: (1) “the axis of the mitotic spindle takes the direction of the greatest protoplasmic masses” and (2) “the plane of division always cuts the axis of the spindle perpendicularly” (Figure 8) (Hertwig, 1893). While these rules explain the oriented cell division observed in the proliferative zone, namely that the division axis is always perpendicular with the direction of the longitudinal growth (e.g. the proximo-distal axis of the bone), the extension of the column is characterized by the classical Dodds model. The behaviors of proliferating chondrocytes in the columns can be summarized as the follow: (1) mitotic chondrocytes lie perpendicular with the proximodistal (longitudinal) and elongate along the mediolateral axis of the bone; (2) cell division plane is parallel to the long axis of the columns; (3) the newly-divided cells initially lie horizontal relative to the longitudinal axis of columns; and (4) by regulating the length and width ratio, the daughter cells eventually move backward to the original vertical axis. This model has a close similarity to the developmental process of convergent extension which leads to tissue narrowing and elongation during organogenesis (Keller et al., 2000). To summarize, chondrocytes in the proliferating zone (1) undergo flattening process; (2) are oriented perpendicularly to the direction of longitudinal growth, and (3) the columns extend along the longitudinal axis.

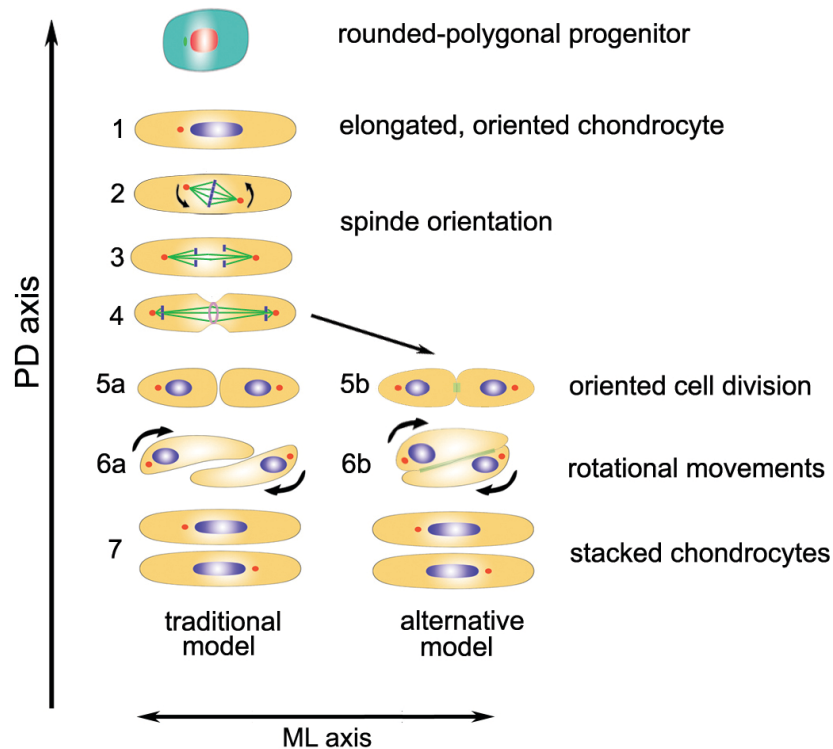


Figure 8: Mechanisms of chondrocyte division and column formation. Chondrocytes in the proliferative zone elongate along the mediolateral (ML) axis with right angle to the longitudinal, proximodistal axis. Following Hertwig's rules, the mitotic spindles form in the long axis of the cell and division plane cut perpendicular to this axis. The horizontally oriented daughter cells then rotate back to the proximodistal (PD) axis by sliding movements mediated by the matrix (classical Dodds model) or by transient cell-cell connections (alternative models). Figure is adapted and modified from (Dodds, 1930).

Numerous growth factors, morphogens and hormones are involved in the regulation of chondrocyte proliferation, maturation and oriented cell division. Besides of the mitotic activity, chondrocytes in the proliferation zone produce the vast amount of typical cartilage matrix components that includes aggrecan and collagen II.

In the prehypertrophic zone, chondrocytes initiate expression of specific marker genes such as Indian hedgehog (Ihh), collagen X and parathyroid hormone/parathyroid hormone-related protein receptor (Ppr1). Most of the chondrocytes in prehypertrophic zone are larger than cells in the proliferation zone and are mitotically inactive.

The chondrocytes in hypertrophic zone are round to polygonal in shape and their cell volume is enlarged 5-10 times compared to the chondrocytes in the proliferating zone (Hunziker, 1994). Hypertrophic chondrocytes predominantly deposit collagen X instead of aggrecan and collagen II. Mature, terminally differentiated hypertrophic chondrocytes either undergo apoptosis or

transdifferentiate into osteoblasts (Park et al., 2015; Yang et al., 2014; Zhou et al., 2014). The hypertrophic chondrocytes near the metaphysis produce vascular endothelial growth factor (VEGF), which facilitates the invasion of blood vessels into the hypertrophic core; and matrix metalloproteinase 13 (MMP-13) which degrade the cartilaginous ECM (Ortega et al., 2004). Chondroclasts and osteoblast precursors, which follow the invasion of the vasculature, carry out the transformation of cartilage into bone.

1.7.4.2. Metaphysis

The vascular invasion starts from the metaphysis where the primary ossification occurs (Ballock and O'Keefe, 2003; Brighton, 1978). The metaphysis contains two regions: (1) primary spongiosa and (2) secondary spongiosa. The initial trabecular network at primary spongiosa is generated from partially degraded intercolumnar area that extends from the hypertrophic zone. Eventually, the primary spongiosa mineralized to form woven bones and secondary spongiosa. At secondary spongiosa area, the primary trabecular network becomes lamellar trabecular bone. Besides its role in cartilage-bone remodeling, metaphysis also support the structural stability of the growth plate.

1.7.4.3. Peripheral ossification groove of Ranvier

The growth plate cartilage laterally is surrounded by a fibro-chondro-osseoustissue, which is composed of the groove of Ranvier and the ossification ring of LaCroix (Brighton, 1978; Langenskiold, 1998). The Ranvier groove is may serve as a storage pool of chondrogenic progenitor cells and contributes to the circumferential growth of bones (Karlsson et al. 2009; Shapiro et al. 1977). The ring of LaCroix help to maintain the structural stability of the growth plate at the chondro-osseous junctions (Rodriguez et al., 1985).

1.8. Chronic cartilage disorders

1.8.1. Aetiology of cartilage lesions

The chondral injuries can be divided into two major types: degenerative and focal lesions. Degenerative lesions commonly result from meniscal injuries, displacement of the joints, osteoarthritis (OA) or joint instability due to weakening of the ligaments. Focal lesions are mainly induced by osteochondritis dissecans, osteonecrosis and trauma (Falah et al., 2010).

Sports injury and accidents represent most prevalent trauma that causes osteochondral lesions or breaking the cartilage-bone interfaces. The shear force may cause cartilage or even subchondral bone fractures. Up to 50% of osteochondral lesions at the knee joint are the consequences of the dislocation of patella (Boden et al., 1997). Osteochondritis dissecans (OD), first described by König in 1988, causes microtrauma in femoral condyles in 60% of OD patients (Bianchi et al., 1999). Osteonecrosis can be primary (also known as spontaneous osteonecrosis) or secondary, as a consequence of, for example, alcoholism, steroid therapy and meniscectomy (Patel et al., 1998). The cartilage lesions after age 40 are mainly caused by OA. In all cases, the appearance of degenerative lesion may diverge from each other. Such cartilage lesion progresses to subchondral bone hardness leading to reduced stress absorption and vulnerable cartilage ECM (Falah et al., 2010). Cartilage lesions and damage of subchondral bone are, in many cases, getting more severe because of weight bearing stress. Ligament (especially the anterior cruciate ligament, ACL) injury causes meniscal and knee instability, which in turn lead to cartilage injury (Stanitski, 1995). Previous studies have showed that about two third of articular cartilage lesions are linked to meniscal tears (Lewandrowski et al., 1997). Owing to its complex etiology, the effect of preventive treatment options of cartilage lesions is still controversial (Falah et al., 2010).

1.8.2. Cartilage injuries among athletes

There is a rising tendency of chondral injuries in professional athletes (Chow et al., 2004). Apart from the prominent occurrence of cartilage damage in high-end

competitive sports, the enhanced incidence of articular cartilage injuries is positively correlated with the increasing participation in leisure sports (e.g. football and basketball) (Arendt and Dick, 1995; Jones et al., 2001; Mithofer et al., 2005). Cartilage damages of the knee joints are reported as one of the most common reasons that accounts for sustained disability of athletes (Drawer and Fuller, 2001; Engstrom et al., 1990). Injuries of the articular cartilage are often associated with osteochondral fractures, patellar dislocations and avulsions of ligaments (Bartz and Laudicina, 2005; Moti and Micheli, 2003; Smith and Tao, 1995). Focal lesions in the femoral condyles are found in approximately 50% of the athletes who receive ACL reconstruction with increasing population of female athletes (Arendt and Dick, 1995; Piasecki et al., 2003). The cartilage injuries often strongly affect athletic performance and progress to early joint degeneration (Felson et al., 2000; Kujala et al., 1995).

Since the cartilage injuries are barely self-repaired, articular cartilage lesions in young and physically active people have been considered as a challenge of treatment (Buckwalter, 1999; Jackson et al., 2001). Newly invented surgical techniques have attempted to address cartilage repair, joint replacement and even the possibility of regeneration (Alford and Cole, 2005a; Alford and Cole, 2005b; Brittberg et al., 1994; Moti and Micheli, 2003; Steadman et al., 2003). Because of the mechanical overload of the joint, articular cartilage injuries in athletes especially require the repair on the surface, which should bear massive impact in highly intensive sports (Jackson et al., 2001). The assessments of articular cartilage repair of athletes are mainly focused on functional scores, mobility and the chance to go back to sports (McAdams et al., 2010).

In the population of athletes, the evaluation of the progression of knee cartilage destruction has been well documented (Drawer and Fuller, 2001; Engstrom et al., 1990; Felson et al., 2000; Lane et al., 2004; Roos, 1998). Healthy, normal articular cartilage is characterized with the best weight-bearing ability depending to the activity. Articular cartilage in teenagers and in people active in sports are thickened, and synthesize more glycosaminoglycans due to the increased weight-bearing impacts of the joint (Roos and Dahlberg, 2005). Generally, articular function is positively correlated to repetitive loading in healthy athletes. However, any athletic activity above the threshold of this linear correlation can cause injuries of articular cartilage (Kiviranta et al., 1992). Massive, non-physiological mechanical stress may

result in chondrocyte apoptosis, activation of degradative enzymes and, consequently, and depletion of cartilage macromolecules such as proteoglycans (Arokoski et al., 1993; Jackson et al., 2001; Lohmander et al., 1994; Pearle et al., 2005). Afterwards, the initial phase of the disease starts caused by cartilage breakdown, increased compressive stress and occurrence of cartilage lesions (McAdams et al., 2010). Meniscal injury, malalignment or ligament instability are known to further enhance articular cartilage degradation, which without medical treatments results in sustained dysfunction of articular cartilage and eventually leads to OA (McAdams et al., 2010).

1.8.3. Osteoarthritis

OA is a multifactorial and highly complex disease of the synovial joints affected by genetic and environmental elements (Buckwalter and Martin, 2006). OA is most prevalent in the joints of hip, knee and hands (Figure 11). Pain and functional impairment (dysfunction and joint stiffness) are the common characteristics of OA. Approximately 80% of the OA patients have movement limitations to certain level that cause imperfect performance in work, sport and everyday life. Importantly, 20% of OA patients aren't able to perform most of the daily activities (Wieland et al., 2005).

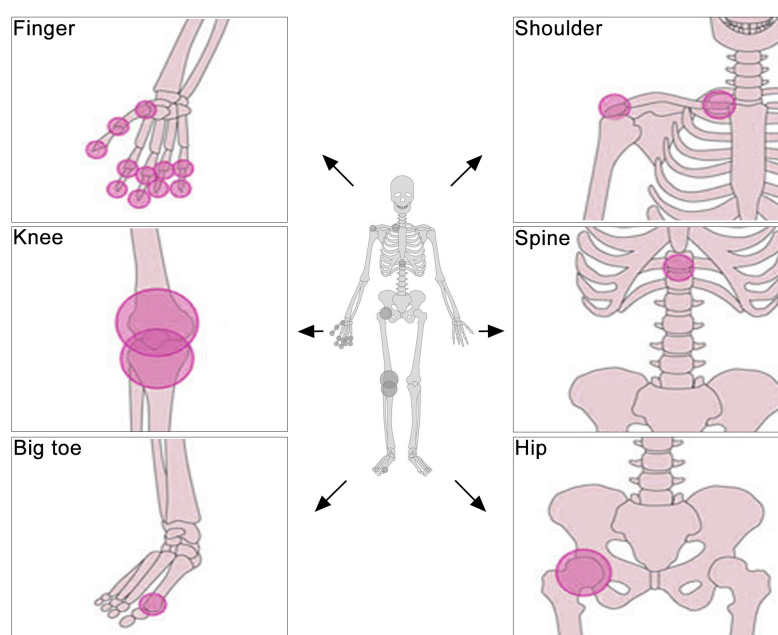


Figure 9: Predominant sites of OA. The common OA-occurring joints such as knee, hip, finger, shoulder and spine are indicated. Figure is adapted and modified from (Wieland et al., 2005).

OA is a slowly developing process of usually single joints that characterized by sustained cartilage destruction associated with occasional signs of synovitis (Figure 12). The occurrence of OA increases with age, eventually affecting half of elderly people over 65 years (Badley and Wang, 1998; Millennium, 2003; Wieland et al., 2005). Rheumatoid arthritis (RA), in contrast to OA, is fast-developing and generalized inflammatory disease driven by autoimmune processes that primarily affects younger people. Although, RA is much less common than that OA (Millennium, 2003; Wieland et al., 2005), RA has tempted more attention than osteoarthritis in the past.

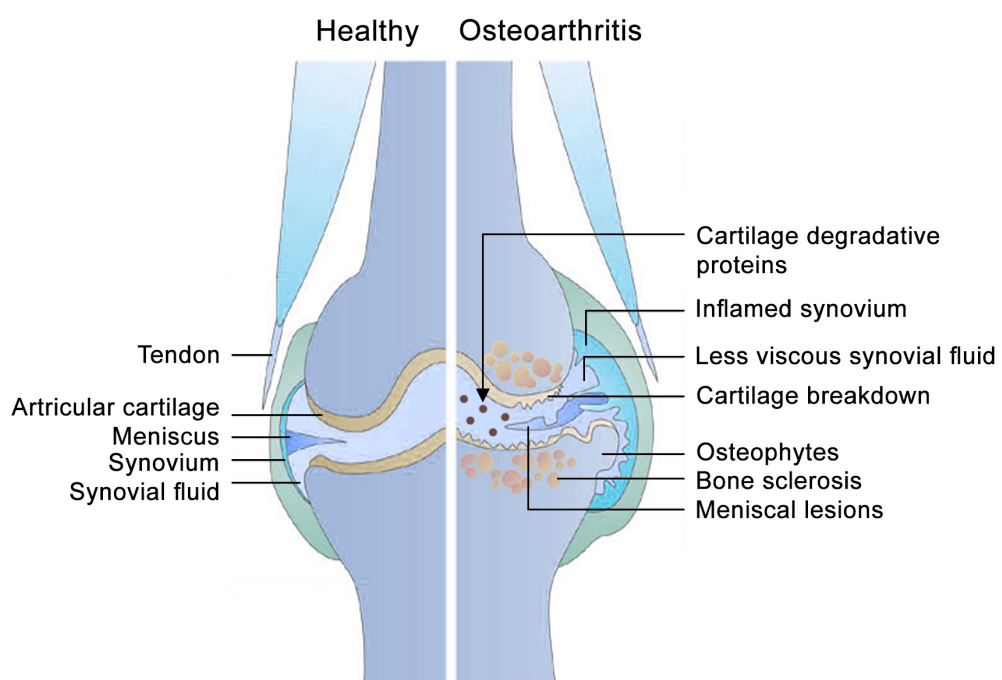


Figure 10: Healthy versus OA-affected knee joint. Compared to healthy knee, OA-affected knee is characterized by cartilage breakdown, meniscal lesions and inflamed synovium. With the progression of OA, osteophytes and bone sclerosis may develop. Figure is adapted and modified from (Wieland et al., 2005).

Multiple biological molecules are involved in cartilage breakdown at the onset and during the progression of OA. These molecules suppress restoration of cartilage and result in imbalance of cartilage metabolism (Figure 13). A shift from anabolic to catabolic processes in chondrocytes plays a pivotal role in the pathology of OA. In primary OA with no clearly identified disease-causing factors, the cartilage ECM production of chondrocytes is impaired due to the disproportion of catabolic and anabolic activities. Excessive catabolic processes in OA chondrocytes result in sustained and advanced damage of the articular cartilage. Secondary OA is defined

as the early-onset degeneration of articular cartilage due to defined factors such as joint malformations (dysplasias), diabetes and mechanical overload.

Remodeling of cartilage ECM involves both proteinases like matrix metalloproteinases (MMPs) and caspases, and proteinase inhibitors such as tissue inhibitors of metalloproteinases (TIMPs). In normal articular cartilage, the activities of these molecules are tightly regulated at multiple levels including cytokine/growth factor signaling pathways, matrix-matrix and cell-matrix interactions (Figure 14). However, the exact nature of the pathways and the potential cross-talks among the different cascades are still partially understood.

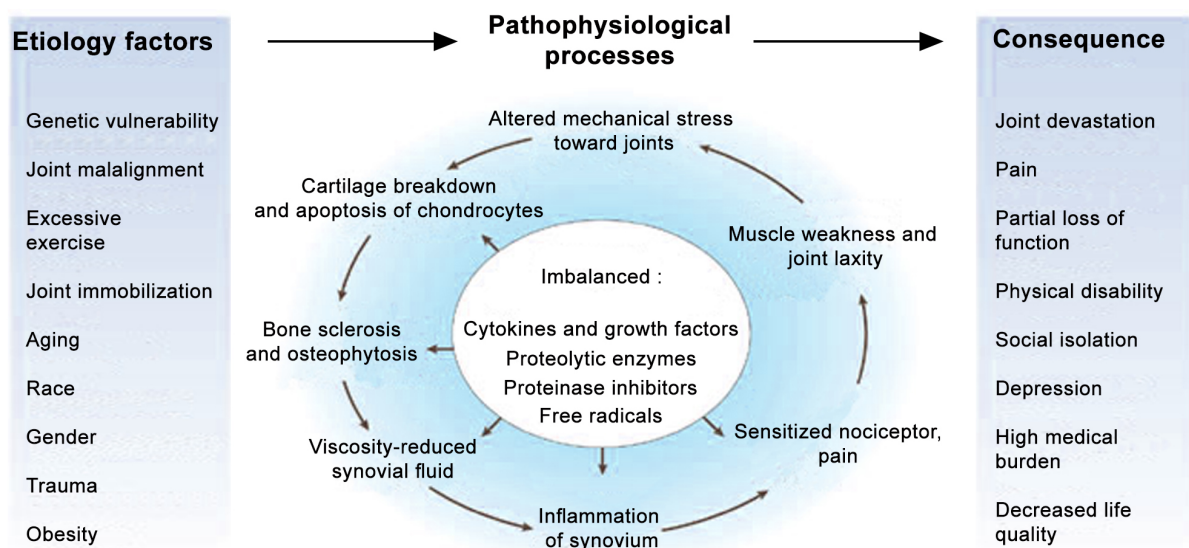


Figure 11: Vicious cycle of osteoarthritis. The connections between etiological factors, pathophysiological events and consequence are demonstrated. The pathophysiological events frequently affect and enhance each other. Figure is adapted and modified from (Wieland et al., 2005).

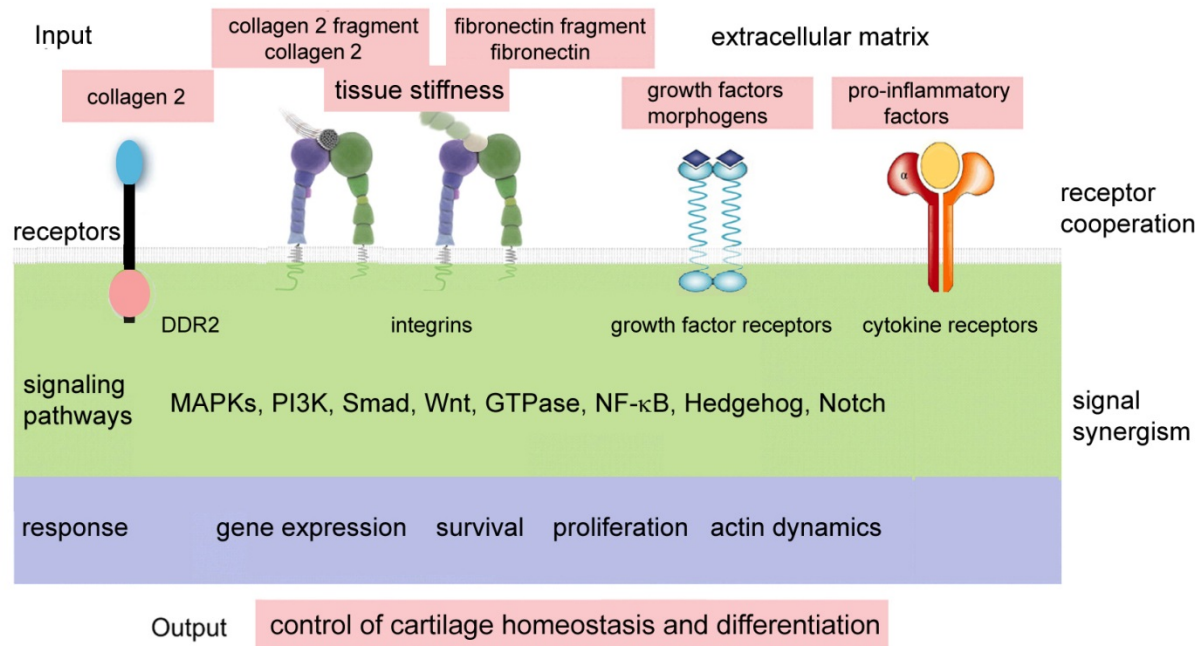


Figure 12: Mechanisms controlling articular cartilage function. Transmembrane receptors such as integrins, growth factor and cytokine receptors, discoidin domain receptor 2 (DDR-2) receive mechanical and chemical signal from the cartilage ECM. The following signal transduction processes are mediated via multiple intracellular signaling cascades involving MAPKs, PI3K, Smad, Wnt, GTPase, NF-κB, Hedgehog and Notch. As net effect, gene expression, cell survival, proliferation and actin dynamics are regulated to maintain cartilage homeostasis and differentiation. Figure is adapted and modified from (Legate et al., 2009).

Cartilage resident matrix proteins interact with each other in a complex manner to define the physical framework for cells and to control the availability, activity and cell surface presentation of bioactive molecules. Almost all ECM proteins, directly or indirectly, bind to and activate cellular receptors such as integrins, which in turn stimulate intracellular signaling pathways regulating cellular behavior such as gene expression, proliferation, survival and cytoskeletal reorganization (Legate et al., 2009). The pericellular matrix (PCM) – surface receptors interactions are suggested to play critical role in transmitting signals from cartilage ECM into chondrocytes, which maintain homeostasis of matrix metabolism (Knudson and Loeser, 2002). Alterations of cartilage ECM such as injury, proteolytic degradation and chronic stress, which interfere matrix-cell signaling, largely increase the risk of OA incidence (Roos and Dahlberg, 2005).

1.8.4. Current, non-surgical treatment options for cartilage injury

According to age, daily activities, and the deterioration level of the lesion, current treatment options include open or arthroscopic surgery and conservative therapy.

A conservative treatment aims for easing the symptoms rather than healing cartilage damage. Surgery is not recommended to apply for mild cartilage injuries or small lesions because it may do more secondary damage (Falah et al., 2010). Thus, clinicians may suggest several alternative treatments that are non-surgical and specific for patient's condition (Fritz et al., 2006). One of the most common treatments is medication such as hormones, analgesics and non-steroidal anti-inflammatory drugs (NSAIDs). Other common treatments consist of physical therapy, weight control and the use of bracing combined with food nutrients with possible chondroprotective effect (e.g. chondroitin phosphate, glucosamine, ascorbic acid).

Acetaminophen is commonly used for pain ease and is the first-line oral medication for osteoarthritis even though the detail mechanism is remained unclear. The effect of pain relief is nearly as good as NSAIDs (Jordan et al., 2003). However, the following clinical studies implied that NSAIDs and COX-2 inhibitors are with better efficacy than acetaminophen (Lee et al., 2004a; Neame et al., 2004; Wieland et al., 2005; Zhang et al., 2004).

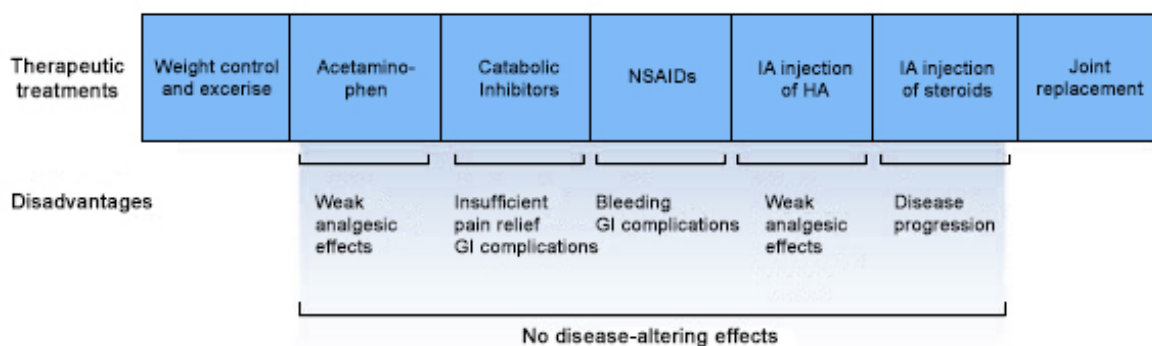


Figure 13: Current treatments for OA. Various therapeutic strategies, according to different level of OA, are used to prevent joint degradation. Figure is adapted and modified from (Wieland et al., 2005).

NSAIDs are usually applied to the OA patients that are poorly respond to acetaminophen (Figure 15) (Jordan et al., 2003). NSAIDs exert its anti-inflammation by blocking cyclooxygenase COX-1 and COX-2. Previous study indicates that COX-2 is induced at the inflammatory site (Vane et al., 1998). The effects of anti-inflammatory and pain relief from NSAIDs are associated with inhibition of

prostaglandin and with direct influence on the nervous system (Samad et al., 2001). Several reviews have showed the effect of distinct NSAIDs given to knee OA patients is comparably similar (Warner et al., 1999; Watson et al., 2006). Application of the NSAIDs should always consider patient acceptance, safety and costs (Watson et al., 2006; Wieland et al., 2005). COX-2 selective inhibitors were first described in 1999. Compared to non-selective COX-2 inhibitors, such selective COX-2 inhibitors have lower side effect, e.g. lower gastrointestinal complications (Warner et al., 1999). With regards to pain relief and improvement of OA patients, effect of selective COX-2 inhibitors is similar to NSAIDs (Bensen et al., 1999; Day et al., 2000). In the cases of patients which barely respond to NSAIDs and selective COX-2 inhibitors, opioid analgesics are also considered.

Chondroprotective nutrients such as glucosamine and chondroitin sulfate are common health care products that used worldwide and approved by European League Against Rheumatism (EULAR) (Jordan et al., 2003). However, the effects of such chondroprotective agents are still dubious and so far no clear indications that they would effectively stop or reverse the progression of OA (Chard and Dieppe, 2001; McAlindon et al., 2000; Zerkak and Dougados, 2004).

Administration of topical medications is noticed with lower systemic side effects than systemically applied drugs. Short-term, local administrated NSAIDs has proved to reduce knee OA (Lin et al., 2004). The effect of long-term local administration still remains unclear. Apart from NSAIDs, studies showed that topical application of capsaicin and salicylates also reduce knee OA but less effective than NSAIDs (Mason et al., 2004).

Intra-articular injection is another way to apply topical administration in OA patients. Injection of long-lasting corticosteroids is considered as ideal treatment against knee pain (Jordan et al., 2003). The effect of intra-articular injection can reach to the peak within a week and gradually wear off until the 4th weeks (Ayril, 2001; Gossec and Dougados, 2004). It is still unclear if multiple injections of steroids might accelerate progression of OA. The efficacy of steroid injection is also agonistic (Creamer, 1999).

In cartilage and the synovial cavity, hyaluronic acid (HA) is one of the most common matrix components. HA is associated with multiple tasks such as cell-cell

interactions, inhibition of prostaglandin E2 (PGE2) synthesis and lubrication (Brandt et al., 2000; Lohmander et al., 1996). The level of HA is usually decreases in OA joint. To compensate the loss of HA; intra-articular injection of HA can be applied (Brandt et al., 2000). Compared to placebo injection, however, HA injection shows only slight improvement of knee OA. Thus, re-evaluation and further analysis of HA application are required to determine its beneficial effect (Jordan et al., 2003; Lo et al., 2003).

1.8.5. Inhibition of NF- κ B pathway by pharmacologic agents

To date, there are more and more NF- κ B inhibitors discovered. For example, glucocorticoids can effectively inhibit NF- κ B pathway via modulating various intracellular signaling pathways (De Bosscher et al., 2000a; Garg and Aggarwal, 2002; Payne and Adcock, 2001; Yamamoto and Gaynor, 2001). It is known that glucocorticoids increase expression of I κ B, which enhances cytosolic preservation of NF- κ B (Auphan et al., 1995; Scheinman et al., 1995). Glucocorticoids are also suggested to mask the DNA-binding ability of NF- κ B by interacting with glucocorticoid receptor and NF- κ B binding components (De Bosscher et al., 2000b). In some cell types, the activated glucocorticoid receptor can inhibit the activation of NF- κ B by direct binding (De Bosscher et al., 1997). Some of NSAIDs (aspirin, salicylate and sulindac) are able to efficiently inhibit activity of IKK and I κ B phosphorylation, which in turn results in the blockade of NF- κ B activation (Tegeeder et al., 2001). Likewise, sulfasalazine, a medication against RA, is proved to inhibit the phosphorylation of I κ B (Wahl et al., 1998).

Immunosuppressants such as cyclosporin A and tacrolimus can also block NF- κ B activation. In T lymphocytes, macrophages and lymphoma cells, Cyclosporin A is found to inhibit degradation of I κ B α via lowering proteasome activity (Frantz et al., 1994; Meyer et al., 1997). Tacrolimus sequesters c-Rel in the cytoplasm of certain cell types (Jurkat cells, B- and T-lymphocytes), which consequentially blocks the activation of NF- κ B pathway (Su and Semerjian, 1991; Venkataraman et al., 1995). Agents such as curcumin, flavonoids (Bremner and Heinrich, 2002), diacehrein (Mendes et al., 2002), glucosamine (Largo et al., 2003), lactacystin (Cuschieri et al., 2004), leflunomide (Manna et al., 2000), pyrrolidine dithiocarbamate (Cuzzocrea et al., 2002), thalidomide (Meierhofer and Wiedermann, 2003), vitamin C (Carcamo et

al., 2002) and vitamin E (Calfée-Mason et al., 2004), are reported to suppress NF- κ B activation.

In recent years, new therapeutic strategies have been innovated for specific suppression of essential components activating NF- κ B pathway (Bacher and Schmitz, 2004; Feldmann et al., 2002; Firestein, 2004; Lewis and Manning, 1999; Smolen and Steiner, 2003). Decoy oligonucleotides (ODN), peptides specifically masking NLS of NF- κ B, and proteasome inhibitors are applied to block NF- κ B activation in animal models (Elliott et al., 2003; Epinat and Gilmore, 1999). Daily intake of bortezomib, a Food and Drug Administration (FDA)-approved proteasome inhibitor, can effectively reduce activity of NF- κ B in streptococcal cell wall (SCW)-induced arthritis in a rat model (Roman-Blas and Jimenez, 2006). The decline of NF- κ B activity is related to metabolism of nitric oxide (NO), and decreased levels of IL-1 and IL-6 in the serum (Kawakami et al., 1999). In a collagen II induced rheumatoid arthritis rat model, intra-articular injection of ODN can directly bind to NF- κ B and therefore block its activity by masking the DNA-binding sequence of NF- κ B. ODN significantly eases the paw-swelling accompanied with reduced IL-1 β and TNF- α in the inflammatory synovium, which suppressing the destruction of joint (Tomita et al., 1999). Similarly, injecting NF- κ B decoy ODN into the knee joints of an animal OA model induced by ACL transection, ODN significantly ameliorated knee OA owing to the largely decreased IL-1 β and TNF- α in cartilage and synovial (Fujihara et al., 2000).

Novel therapeutic strategies using antisense oligonucleotides and RNA interference also aim for specific inhibition of NF- κ B components. Lock nucleic acid (LNA), a type of modified nucleotides with better DNA and RNA binding affinity and specificity, was first introduced in 1997 (Jepsen and Wengel, 2004). Morpholino oligomers, which contain an ODN structure, are nucleic acid analogs that used to modify expression of gene (Jepsen and Wengel, 2004; Kawai et al., 2005). RNA interference, including micro RNA (miRNA) and small interfering RNA (siRNA), is defined as a post-transcriptional process of gene silencing. The target mRNA is specifically cleaved by siRNA-induced ribonucleoprotein complex and sent for degradation (Huppi et al., 2005; McManus and Sharp, 2002; Pinkenburg et al., 2004). It has shown a great inhibition efficacy of NF- κ B by siRNA, witnessed by the eliminations of downstream signaling factors such as COX-2, iNOS and MMP-9 in IL1 β - and TNF α -treated rat chondrocytes (Lianxu et al., 2006).

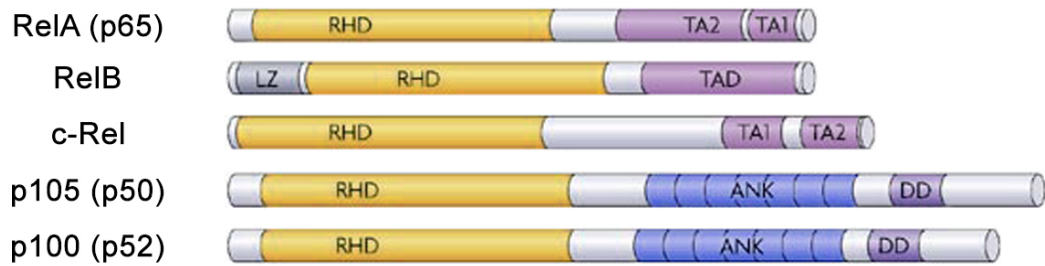
1.8.6. Operative treatment options

The idea of surgical intervention is to repair the damage and facilitate the regeneration of injured cartilage to its original state. However, regenerated tissue is mainly fibrocartilage with small HA level after surgery (Odenbring et al., 1992). Ideally, surgical treatments should orient to patients with considerations of repair associated problems before the operation (Falah et al., 2010; Fritz et al., 2006). Arthroscopy is minimally-invasive and the most common surgical procedure, which can repair cartilage function, relieves pain and reduces the risk and progression of OA. Under certain circumstances such as infection, misaligned joint and obesity, surgical intervention for cartilage lesions should not be performed (Falah et al., 2010).

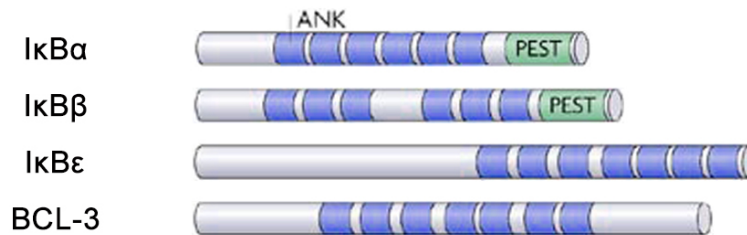
1.9. The NF- κ B/Rel family of transcription factors

The mammalian NF- κ B family of ubiquitously expressed transcription factors consists of five members: NF- κ B1 (p50 and its precursor p105, NF- κ B2 (p52 and its precursor p100), RelB, c-Rel and RelA/p65 (Ghosh and Karin, 2002). NF- κ B members are able to form homo- and heterodimers that in various cell types are cytoplasmatically-sequestered by inhibitors of NF- κ B (I κ Bs) (Figure 9). Phosphorylation of I κ B by I κ B kinase (IKK) complex leads to degradation of I κ B, which in turn can release active NF- κ B dimers and allow them to translocate into nucleus for the control of gene regulation (Hayden and Ghosh, 2004; Perkins, 2007).

A. Members of NF- κ B family



B. Members of I κ B family



C. Members of IKK family

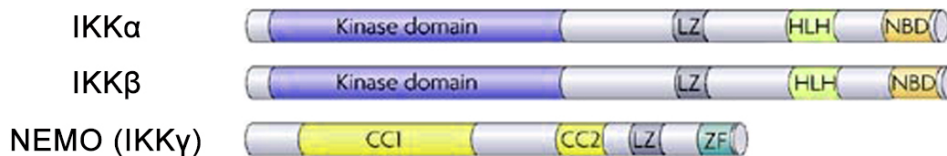


Figure 14: The members of NF- κ B, I κ B and IKK families. (A) The NF- κ B family contains five subunits: RelA (p65), RelB, c-Rel, p50/p105 (NF- κ B1) and p52/p100 (NF- κ B2). NF- κ B1 and NF- κ B2 are processed and become fully-activated p50 and p52, respectively. All members of NF- κ B family possess a N-terminal RHD (Rel-homology) domain, which is responsible for dimerization, nuclear localization and DNA binding. The Rel subunits are characterized with C-terminal transcriptional activation domains (TADs). (B) The I κ B family is composed of I κ B α , I κ B β , I κ B ϵ and BCL-3. The I κ B subunits contain ankyrin-repeat motifs (ANK). (c) The IKK family contains 3 members: IKK α , IKK β and IKK γ , which later one also known as NF- κ B essential modifier (NEMO). These three IKK subunits together form the IKK complex. LZ, RelB-transactivation-domain containing a putative leucine-zipper-like motif; PEST, domain rich in proline (P), glutamate (E), serine (S) and threonine (T); ZF, zinc-finger domain; HLH, helix-loop-helix; NBD, NEMO-binding domain. Figure is adapted and modified from (Perkins, 2007).

All members of the NF- κ B family contain a Rel-homology domain (RHD) at the N-terminus, which is involved in dimerization and DNA binding. The Rel subfamily members are also characterized by the presence of one or two C-terminal transcriptional activation domains (TADs) (Figure 9). Apart from the similar structure and the DNA binding capability, NF- κ B members are reported to have different functions (Gerondakis et al., 1999; Hoffmann et al., 2003).

In unstimulated healthy mammalian cells, members of Rel family are mainly restricted in the cytoplasm together with the I κ B proteins (Hayden and Ghosh, 2004). The I κ Bs are known to sequester NF- κ B subunits and prevent their translocation into the nucleus by masking the nuclear localization signal (NLS) in the RHD. Due to the partial masking effect of I κ B α , NF- κ B/I κ B α complexes are able to translocate into nucleus without any stimulation. Owing to the nuclear export sequence (NES) on I κ B α , the complexes are soon exported back to cytoplasm (Hayden and Ghosh, 2004; Perkins, 2007).

Ankyrin-repeat motifs are characteristic for the NF- κ B subunits p105 and p100, and can be found in I κ B proteins as well (Figure 9). The function of p100 and p105 is similar to I κ B proteins because they help the cytoplasmic sequestration of NF- κ B-subunit dimers (Hayden and Ghosh, 2004; Perkins, 2007). There are several mechanisms to process of p100 and p105, which are necessary for the activation of p50 and p52. The homodimers of p50 and p52 are able to interact with BCL-3 in the nucleus. In contrast to I κ Bs, BCL-3 is working as a transcriptional coactivator (Hayden and Ghosh, 2004; Perkins, 2007). Due to the ability to avoid I κ Bs regulation, p50 and p52 homodimers stay constitutively in the nucleus. When members of Rel subfamily form heterodimers with p50 or p52, they are no longer able to escape the regulation of I κ Bs (Hayden and Ghosh, 2004; Perkins, 2007). The p52–RelB complex is the only exception that evades the regulation due to its low affinity for I κ B α (Dobrzanski et al., 1994).

1.9.1. The NF- κ B signaling pathways

There are three NF- κ B activation pathways. The most common one is the canonical, classical pathway (Figure 10), which is triggered by a range of inflammatory stimuli such as interleukin-1 (IL-1), tumour necrosis factor- α (TNF α), engagement of the T-cell receptor (TCR) and lipopolysaccharide (LPS) (Hayden and Ghosh, 2004). The activation of canonical pathway is characterized by the serine phosphorylation of I κ B α at the amino acid positions 32 and 36, followed with its proteosomal degradation (Hayden and Ghosh, 2004; Perkins, 2007). In various types of cell, I κ B β and I κ B ϵ are phosphorylated and degraded slower than I κ B α (Hayden and Ghosh, 2004; Perkins, 2006; Perkins, 2007).

In the NF- κ B canonical pathway, phosphorylation of I κ B is the consequence of IKK-complex activation (Hayden and Ghosh, 2004). There are three components in the IKK complex, IKK α (IKK1), IKK β (IKK2) and NF- κ B essential modifier (NEMO, also known as IKK γ) (Hayden and Ghosh, 2004). IKK β has been proved as the major I κ B kinase in NF- κ B canonical pathway (Bonizzi and Karin, 2004; Pasparakis et al., 2006).

The non-canonical or alterative pathway can be induced by stimuli such as LPS, CD40, B-cell-activating factor of the TNF family, and the latent membrane protein-1 (LMP1) of Epstein–Barr virus (Bonizzi and Karin, 2004; Perkins, 2003). The activation of IKK complex, which lack Nemo, by the NF- κ B-inducing kinase (NIK) processes p100 into p52 (Bonizzi and Karin, 2004; Perkins, 2006). Afterwards, the p52 complex shuttles into the nucleus for gene regulation. p52-RelB dimers have higher affinity for a subset of κ B elements and regulate certain NF- κ B target genes (Figure 10). The non-canonical pathway has been suggested to be regulated by IKK α homodimers instead of the larger IKK complex (Bonizzi and Karin, 2004; Perkins, 2006).

Certain stimuli such as hypoxia, reoxygenation and hydrogen peroxide cause Tyr42 phosphorylation of I κ B α , which is subsequently degraded or dissociated from the NF- κ B complex (Perkins, 2006; Perkins and Gilmore, 2006). Exposure to ultraviolet (UV) light or constitutively activation of HER2 in breast cancer cells also triggers PEST domain phosphorylation of I κ B α by casein kinase-II (CK2) (Perkins, 2006). Both phenonmenons are IKK-independent and lead to NF- κ B activation which is classified as atypical NF- κ B pathway.

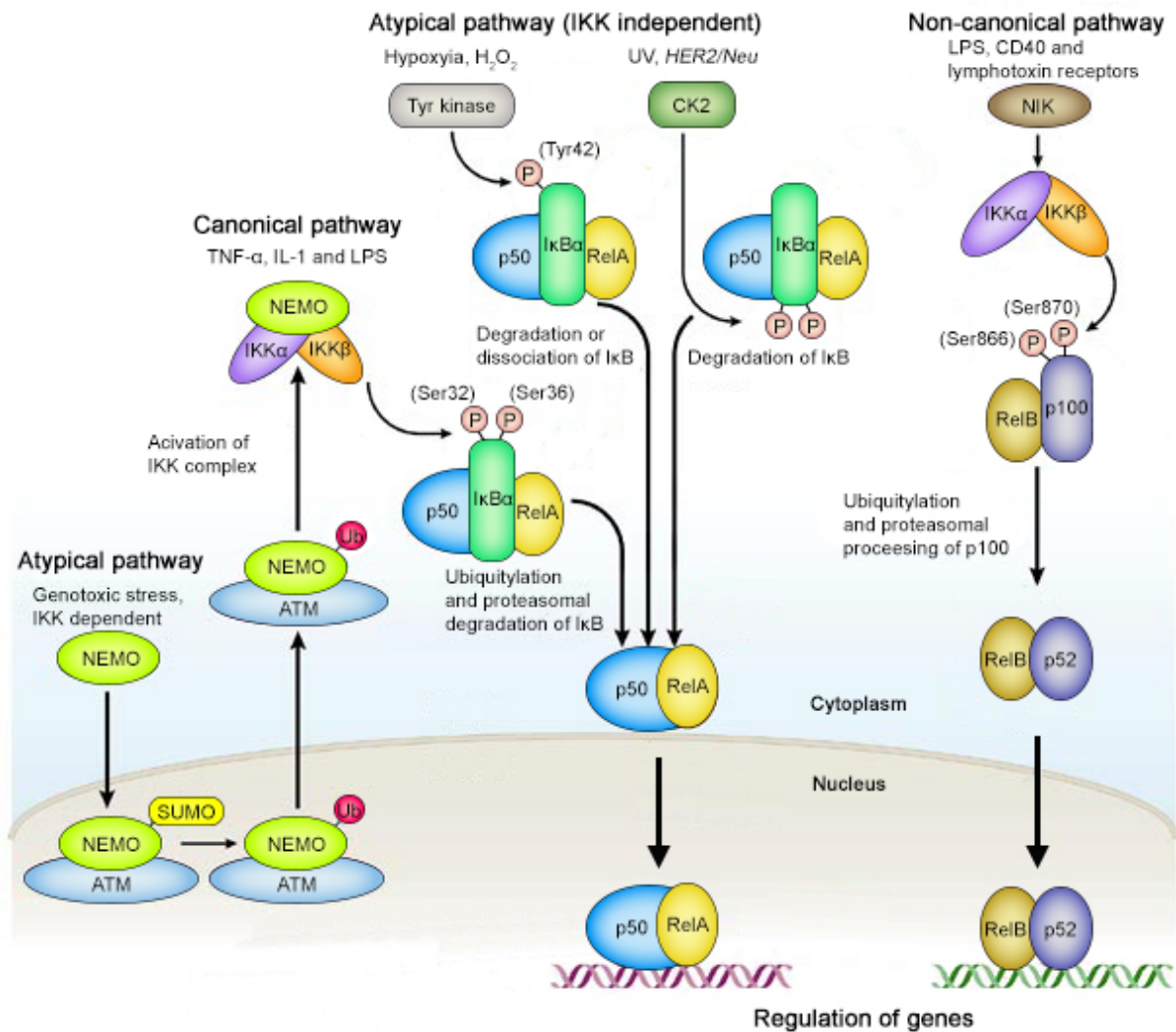


Figure 15: Activation of NF- κ B pathways. The canonical pathway is depended on IKK β activation and induced by many stimuli (e.g. IL-1 and TNF α). The IKK complex is activated by Ser32 and Ser36 phosphorylation of I κ B α , which is subsequently degraded. Later, p50/RelA dimer is released and translocated into the nucleus. In certain situation such as genotoxic stress, NF- κ B essential modifier (NEMO) is processed by ataxia telangiectasia mutated (ATM) checkpoint kinase in nucleus and enters the cytoplasm for the activation of IKK complex afterwards. Tyrosine kinases and casein kinase-II (CK2) are known to mediate the activation of atypical NF- κ B signaling. The non-canonical NF- κ B pathway is regulated by NF- κ B-inducing kinase (NIK), which activates IKK α and the following modification of p100. The active p52/RelB dimer (non-canonical) regulates distinct genes comparing to canonical/atypical NF- κ B signaling. Figure is adapted and modified from (Perkins, 2007).

1.9.2. Activation of the IKK complex

The NF- κ B canonical pathway activation can be induced by numbers of external stimuli, which usually trigger membrane receptors and/or inner signaling pathways (Chen, 2005; Hayden and Ghosh, 2004; Kawai and Akira, 2006; Krappmann and Scheidereit, 2005; Perkins, 2006). The regulatory subunit NEMO is elementary for IKK complex activation. NF- κ B activating stimuli cause Lys63-linked

ubiquitylation of NEMO (Burns and Martinon, 2004; Chen, 2005; Krappmann and Scheidereit, 2005; Perkins, 2006). The Lys63-linked ubiquitylation is known to promote interactions between proteins with ubiquitin-binding domains (Burns and Martinon, 2004; Chen, 2005; Krappmann and Scheidereit, 2005; Perkins, 2006). Transforming growth factor-beta (TGF β)-activated kinase-1 (TAK1) is recruited after ubiquitylation of NEMO and phosphorylates IKK β at Ser177 and Ser181 (Burns and Martinon, 2004; Chen, 2005; Krappmann and Scheidereit, 2005; Perkins, 2006).

Among NF- κ B activating stimuli, genotoxic stimuli are also known to initiate NEMO-dependent IKK β activation in NF- κ B canonical pathway (Figure 10) (Janssens and Tschopp, 2006). Under certain circumstances, NEMO interacts with ataxia telangiectasia mutated (ATM) and translocates into nucleus for following sumoylation and phosphorylation (Wu et al., 2006). The mono-ubiquitylation is then substituted for the sumoylation of NEMO-ATM complex, which is exported back to cytoplasm and activates the IKK complex.

1.9.3. NF- κ B pathway in skeletal development and arthritis

Previous studies using genetic-engineered mice have gained us valuable information of NF- κ B pathway during skeletal development. p50/p52 double knockout mice displayed an arrest of osteoclast maturation, which results in imbalance of bone production/resorption and sequentially causes osteopetrosis. The mutant phenotype is cured by bone marrow transplantation, which indicates the components of hematopoietic system are also affected (Iotsova et al., 1997). The IKK1 knockout mice die shortly after birth and show impaired skeletal development and epidermal differentiation (Li et al., 1999a). Overexpressing wild type IKK1 in epidermal cells of IKK1-null mice rescues the skin as well as the skeletal phenotype. The appropriated morphogenesis of skeletal components originated from mesoderm likely requires epidermal-mesenchymal interactions (Sil et al., 2004). Owing to the normal development of cartilage and bone in rescued mice, IKK1 seems to be replaceable in skeletal development. The p65-null, NEMO-null and IKK2-null mice die in early- or mid-embryonic stage due to liver degeneration and massive hepatic apoptosis (Beg et al., 1995; Li et al., 1999b; Rudolph et al., 2000). The heterozygous NEMO-deficient (+/-) female mice display skin lesions similar to the human genetic disorder incontinentia pigmenti (Schmidt-Supprian et al., 2000).

Studies of human cell culture, tissue explant cultures and patient samples have indicated the involvement of NF- κ B activation in rheumatatic disorders such as RA, OA, juvenile RA, psoriatic and septic arthritis (Roman-Blas and Jimenez, 2006). IKKs, p65 and p50 are involved in synovitis and are abundant in OA and RA. IKK2 activation has been suggested to be a critical step in NF- κ B-mediated cytokine and collagenase upregulation in synoviocytes in response to TNF- α and IL-1 β stimulation (Aupperle et al., 2001). In the inflammatory arthritis animal models such as collagen type II or rat adjuvant induced arthritis, activation of NF- κ B is one of the earliest events in disease progression and associated with the level of MMP-13 and MMP-3 (Makarov, 2001; Mor et al., 2005). The intra-articular injection of adenoviral construct carrying IKK2 gene results in severe arthritis coupling with synovial swelling, indicating the essential role of IKK2 in synovial inflammation (Tak et al., 2001). In RA rat model, inhibition of IKK2 has proved to ease damage to cartilage and bone (Schopf et al., 2006). Similar to synoviocytes, NF- κ B appears to be pivotal in mediating inflammatory and catabolic processes in articular chondrocytes: 1) NF- κ B is activated in articular cartilage chondrocytes upon stimulation with TNF- α and IL-1 β ; 2) it regulates the expression of MMP-1, -3 and -13 in response to proinflammatory cytokines (Roman-Blas and Jimenez, 2006); 3) chemical inhibition of IKK in IL-1-treated cartilage explants blocked collagen II and aggrecan degradation by suppressing the expression of collagenases and ADAMTS-5 (Pattoli et al., 2005); 4) NF- κ B is rapidly activated by physical trauma induced by articular cartilage explantation and cutting (Gruber et al., 2004); 5) proteolytic cleavage fragments of collagen II and fibronectin (Fn) have NF- κ B-dependent cartilage destructive activities (Ding et al., 2009); 6) elimination of IKK1 and IKK2 by shRNAs in osteoarthritic chondrocytes has showed the protective potential to increase cartilage ECM production (Olivotto et al., 2008). These scientific evidences imply that blockade of the NF- κ B pathway through pharmacological or gene therapeutic inhibition is a potential strategy against OA and RA. However, since NF- κ B is believed to exert positive physiological functions such as its anti-apoptotic effect on CD95-induced apoptosis (Kuhn et al., 2000), further in vivo studies are needed to clarify the natural roles of NF- κ B signaling in the skeletal system in order to develop effective therapy for joint diseases. This is especially relevant in cartilage, as chondrocyte apoptosis is considered to be an important early event in induction of disease.

1.10. Model to study NF- κ B canonical pathway in cartilage development

Although numerous animal species are used for studying the development and function of skeletal tissues, mouse (*Mus musculus*) is one of the most common genetic model organisms owing to its easily-manipulated genome. Mouse strains with engineered gene mutations have been increasingly used to understand the complex interaction between ECM, cytokines, receptors, signaling molecules and transcription factors during OA (Aszodi et al., 2006; Raducanu and Aszodi, 2008). Because the skeletal development and the genome are very similar between human and mouse, genetically-modified mice have shown precious insights of the differentiation and function of the mammalian cartilaginous skeleton.

Transgenic and gene knock-out experiments have significantly contributed to the clarification of the physiological functions of NF- κ B signaling pathways (Pasparakis et al., 2006). Inhibition of the canonical NF- κ B pathway by ablating the genes coding for p65/RelA, NEMO or IKK2 by conventional knockout (constitutive null mutation) results in early to mid-embryonic lethality owing to hepatic apoptosis and liver degeneration (Beg et al., 1995; Li et al., 1999a; Rudolph et al., 2000). Owing to the early lethal phenotype of mice with constitutive deletion of genes, conditional gene targeting strategies utilizing the Cre/LoxP recombination system (Rajewsky et al., 1996) have been developed to dissect the function of NF- κ B pathways in an inducible and/or tissue-specific manner. Inhibition or forced activation of NF- κ B in these mice as well as the classical transgenic mice overexpressing constitutively active or dominant-negative proteins have revealed the critical role of NF- κ B/Rel proteins in various cells and tissues including lymphocytes, myeloid and epithelial cells, neurons and skeletal muscle (Pasparakis et al., 2006). By utilizing the NEMO conditional knockout mice, we are able to analyze the role of canonical NF- κ B-mediated processes in the regulation of normal and pathological cartilage functions.

2. Aim and milestones of the thesis

The NF- κ B transcription factors are believed to be important for articular cartilage destruction during osteoarthritis and rheumatoid arthritis through their capacity to mediate protease induction by pro-inflammatory cytokines such as IL-1 and TNF α , cartilage injury directly, or articular cartilage degradation products such as fibronectin fragments. Consequently, numerous studies have been devoted to develop therapeutic strategies aiming to treat these debilitating rheumatoid conditions by inhibition the canonical NF- κ B signaling pathway. However, the exact role of NF- κ B in cartilage physiology is unclear, hampering the discovery of effective strategies that consider both the beneficial and deleterious effects of NF- κ B activation on cartilage pathology.

The hypothesis of this study is that a suitable mouse model with inhibited canonical NF- κ B signaling in chondrocytes could significantly contribute to our knowledge about the function of NF- κ B in cartilaginous tissues. The main objective of the proposed research is the analyses of the *NEMO-Col2a1cre* conditional knockout mice, in which the canonical NF- κ B pathway is inhibited genetically in chondrocytes, to promote our understanding of NF- κ B-mediated processes on the regulation of normal and pathological cartilage functions.

The following milestones are defined:

1. Understand the impact of NEMO-deficiency on endochondral bone formation.
2. Clarifying the role of canonical NF- κ B pathway in cartilage metabolism using hip explant culture.
3. Investigate the role of canonical NF- κ B pathway in cartilage responses upon ex vivo-induced hip injury.
4. The involvement of canonical NF- κ B pathway in the development of spontaneous osteoarthritis with aging.

3. Materials and Methods

3.1. Animal

3.1.1. Mouse housing and breeding

The floxed $NEMO^{fl/fl}$ female mice were generated from C57BL/6J background (Schmidt-Supprian et al., 2000, generously provided by Dr. Marc Schmidt-Supprian, Max Planck Institute for Biochemistry, Martinsried, Germany). Due to NEMO gene is located on X-chromosome, intercrosses between $NEMO^{fl/fl}$ females and wild-type C57BL/6J male resulted in a ratio of 50% heterozygous $NEMO^{fl/+}$ females and 50% $NEMO^{fl/Y}$ males. Next, homozygous $NEMO^{fl/fl}$ females and $NEMO^{fl/Y}$ males were obtained from inbreeding of homozygous $NEMO^{fl/fl}$ females with $NEMO^{fl/Y}$ males. $NEMO^{fl/Y}COL2a1Cre$ males were generated from intercrosses of $NEMO^{fl/fl}$ female with $Col2a1Cre$ male (Sakai et al., 2001). In this study, we used $NEMO^{fl/Y}$ male as control group to compare difference with $NEMO^{fl/Y}Col2a1Cre$ male.

All mice were housed under standard laboratory conditions with controlled temperature and ventilation, under a 12:12 h light/dark cycle and fed *ad libitum*. Mice were sacrificed via cervical dislocation and tissues dissection was done *post mortem*.

3.1.2. Mouse genotyping

Genomic DNA (gDNA) was isolated from 2-3 mm length mouse tail were lysed overnight (O/N) at 55°C in 0.2 ml lysis buffer. The digestion was neutralized at 95°C for 10 minutes. After centrifugation to spin down non-digested tissue, the solution was placed on ice and used directly for PCR reaction. The PCR products were visualized by agarose gel electrophoresis in 1x TAE solution with 0.05 µl/ml ethidium bromide on the UV imager. Instruments, chemicals, buffers and PCR condition were listed in table 1 and 2.

Table 1. Instruments, chemicals and buffers for mouse genotyping

Instruments

PTC-2000 Thermo Cycler	BioRad, USA
PowerPac Basic Power Supply	BioRad, USA
Serial N Gel Documentation System	Vilber Lourmat, Germany

Chemicals

Tris-HCl	Merck, Germany
Magnesium chloride (MgCl ₂)	Merck, Germany
Potassium chloride (KCl)	Merck, Germany
Protease K	Merck, Germany
10x PCR buffer	Qiagen, Netherlands
Desoxynucleotides (dNTPs)	Qiagen, Netherlands
PCR grade water	Qiagen, Netherlands
Taq DNA polymerase	Qiagen, Netherlands
Oligonucleotides (primers)	Metabion, Germany
Ethidium bromide	Sigma-Aldrich, USA
GeneRuler 100bp Plus DNA Ladder	Thermo Scientific, USA
Ethylenediaminetetraacetic acid (EDTA)	Merck, Germany
Tris base	Merck, Germany
Acetic acid	Merck, Germany

Buffers

Lysis buffer	10 mM Tris-HCl 1.5 mM MgCl ₂ 50 mM KCl 100 ug/ml Protease K
1x TAE buffer (pH 8)	1 mM EDTA 40 mM Tris base 20 mM Acetic acid

Table 2. PCR primers and condition for mouse genotyping

Genes		Primer sequence (5'-3')	Temperature	Size (bps)
<i>NEMO</i>	Fwd 1	GCCTTGGTGCTCCCTAACTCT	55°C	432 (wt)
	Fwd 2	ATGAACAAGCACCCCTGGAAG		
	Rev	TCACATC ACATCGTTATCCTT		842 (mt)
<i>Cre</i>	Fwd	AACATGCTTCATCGTCCG	55°C	419
	Rev	TTCGGATCATCAGCTACACC		
PCR condition			Temperature	Time
	Pre-heating		95°C	5 min
Thermo cycle (35)		Denaturation	95°C	30 sec
		Annealing	55°C	30 sec
		Elongation	72°C	1 min
	Final extension		72°C	10 min
	Storage		4°C	∞

3.2. Primary chondrocyte isolation

Primary mouse chondrocytes were isolated from rib cage. Pups were sacrificed soon after birth and briefly disinfected with 70% ethanol. From this point on, all the procedures were carried out in sterile conditions in a primary cell culture laminar flow hood (Heraeus Instruments, Jena, Germany). Isolated rib cages were placed in Dulbecco's Modified Eagle Medium: Nutrient Mixture F-12 Ham 1:1 (DMEM/F12) (Thermo Fisher Scientific, USA) media, adherent tissues were removed with sterile surgical forceps. The pre-cleaned ribs were put into DMEM/F12 media containing 2 mg/ml type II collagenase (Worthington, USA) at 37°C for 30 minutes. The partially digested perichondrium around ribs was again carefully removed with dissecting forceps and scissors (DUMONT, Switzerland). Afterwards, cleaned ribs were replaced to fresh DMEM/F12 media containing type II collagenase in a humidified atmosphere (5% CO₂, 95% air and 37°C) for 3 h. After enzymatic digestion, the cell suspension was centrifuged at 500g for 5 minutes. The supernatant was discarded and pelleted cells were resuspended in fresh DMEM/F12 media supplemented with 10% fetal bovine serum (FBS) (Thermo Fisher Scientific, USA) and 1%

penicillin/streptomycin (Pen/Strep) mixture (Biochrom, UK). Primary chondrocytes were counted and plated as passage 0.

3.3. Cell culture

3.3.1. Primary cells and culture media

Primary chondrocytes were isolated from the rib cages of *NEMO* knockout mice and their wild-type littermate as described above. Since primary cells were rapidly loss of characteristics *in vitro*, all experiments were performed at low passage number (no more than passage 4). Primary chondrocytes were cultured in complete DMEM/F12 enriched with 10% FBS, and 1% Pen/Strep mixture.

3.3.2. Passaging and counting cells

Chondrocyte monolayer was washed with 1x PBS (Biochrom, UK) and then detached by covering with 1x Trypsin/EDTA (Biochrom, UK) for 5 min at 37°C. A double volume of complete DMEM/F12 media was added to neutralize the effect of trypsin. Cells were pelleted by centrifugation at 500g for 5 minutes. The supernatant was removed and cells were resuspended thoroughly with complete DMEM/F12. 100 µl cell suspension was transferred and mixed with equal amount of Trypane blue (Thermo Fisher Scientific, USA), an aliquote of 10 µl mixture was injected into a Neubauer chamber (Brand, Grafrath, Germany) for counting. Cells were counted in the four quadrants and the total number of cells per ml was determined. Cells were then plated into new culture flasks (Thermo Fisher Scientific, USA) and incubated in Water Jacketed CO₂ Incubator TC 230 (Thermo Scientific, USA) under constant conditions of 37°C and 5% CO₂. Cells were maintained at a maximum of 80% confluence and media-renewed every third day.

3.3.3. Cryopreservation and thawing of cells

To cryopreserve the primary murine chondrocytes, freezing medium consisting of 70% of DMEM/F12 media, 20% of FBS and 10% of dimethylsulfoxide (DMSO)

(Sigma-Aldrich, USA) was used. After trypsinization, cells were pelleted by centrifugation at 500g for 5 min. The supernatant was removed and cells were resuspended in pre-cooled freezing media and aliquoted into cryovials (Thermo Scientific, USA), which were then placed in freezing container (Sigma-Aldrich, USA) stored at -80°C freezer or liquid nitrogen tank (Thermo Scientific, USA). To thaw cells, cryovials were placed in a water bath at 37°C until suspension melted. Afterwards, cells were mixed with fresh media into a 15 ml Falcon tube and spinned down for 5 min at 500g. Next, the supernatant was aspirated and the cells were resuspended in fresh and pre-warmed complete DMEM/F12 media and finally transferred into culture flask T-75 (Thermo Fisher Scientific, USA). Complete DMEM/F12 media was changed after 24h in order to remove non-attached/dead cells.

3.4. Tissue culture techniques

3.4.1. Femoral head explant culture

Femoral heads were harvested from euthanized 4-week-old control and *NEMO^{fl/y}Col2a1Cre* mice. The experimental procedures were briefly describes as followed: (1) the euthanized mouse was placed in dorsal recumbency and sprayed with 70% ethanol; (2) the dissecting scissors were used to cut skin open at the mid-abdomen of mouse; (3) grasp the skin with hands and gently pull toward the feet to expose the underlying hind limb; (4) the little dissecting scissors were used to cut muscle around hip joint; (5) tissue forceps were used to grasp the mid of femur and carefully disarticulate the hip joint (Figure 16) (Stanton et al., 2011). The femoral head was then exposed and collected from cutting the femoral neck and cultured in 300 μ l of serum-free DMEM/F12 media supplemented with streptomycin-penicillin in a 48-well cell culture plate (Thermo Fisher Scientific, USA) for 4 days. The femoral heads were treated with 100 ng/ml TNF- α (R&D, USA) or 10 ng/ml IL-1 (R&D, USA) from the first and third day of the culture. At the end of the experiment, femoral heads were fixed in 4% paraformaldehyde (PFA) (Merck, Germany)/PBS solution.

3.4.2. Mechanically-induced hip injury

Articular cartilage of femoral head was harvested from euthanized 4-week-old control and *NEMO^{fl/y}Col2a1Cre* mice. The isolation procedures are mostly the same as described in 3.4.1. To mimic mechanical injury, the articular cartilage of femoral head was carefully pilled off by tissue forceps (Figure 16) and frozen in isopropanol chamber in liquid nitrogen. Half of harvested femoral head articular cartilage was frozen immediately. To observe the genes responding to mechanical injury, the other half of the articular cartilage of femoral head was cultured at 37°C for 4 hours in DMEM/F12 media and frozen down afterwards. Frozen samples were then subjected to Taqmen Low-Density Array (TLDA) experiment that carried out in Tonia Vincent's lab (Kennedy Institute of Rheumatology, UK)

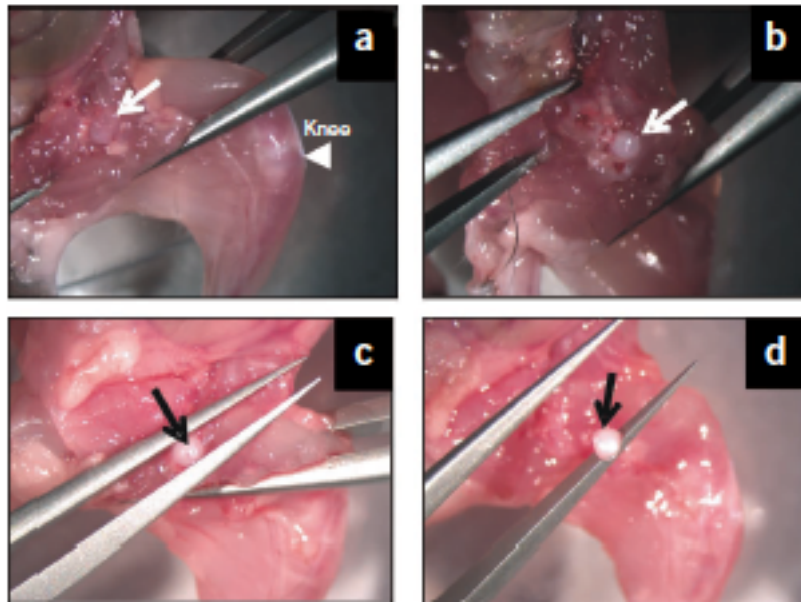


Figure 16: Isolation of articular cartilage of femoral head. a: the underlying leg was exposed after pulling skin toward the mouse feet. b: the femoral head was disarticulated by tissue forceps and visible. c: tissue forceps pinched the neck of femoral head. d: applied pressure to tissue forceps caused breakage at femoral physis and the articular cartilage of femoral head was released (Stanton et al., 2011).

3.4.3. Metatarsal explant culture

Embryos were harvested from pregnant female mice of wild-type or *NEMO^{fl/y}Col2a1Cre* at E15.5 postcoitum. Tissue forceps were used to remove surrounding tissue and release metatarsals (Figure 17). The 2nd, 3rd and 4th metatarsals were selected for explant culture and incubated in 48-well cell culture

plates. Metatarsal explants were cultured in BGjb media (Thermo Scientific, USA) supplemented 1% streptomycin/penicillin with or without 100 ng/ml BMP-2 (R&D, USA), 100 ng/ml FGF-2 (R&D, USA), 100 ng/ml TGF β -1 (R&D, USA) or 10 ng/ml IGF-1 (R&D, USA) for 5 days. The metatarsals were fixed in 4% PFA/PBS solution, paraffin-embedded and sectioned as 7 μ m thick.

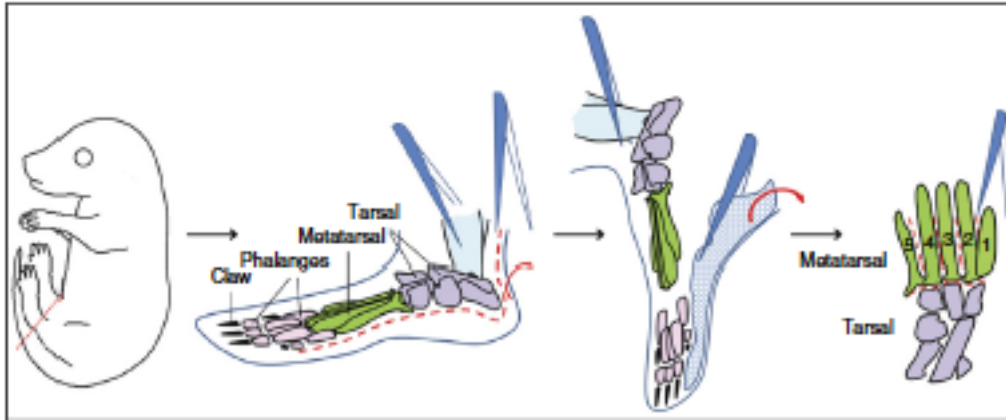


Figure 17: Dissection procedure of metatarsal isolation. The euthanized E15.5 mouse embryo was surface-sterilized with 70% ethanol. By holding tibia with one pair of tissue forceps, used the other pair of forceps carefully remove the surrounding tissue underneath metatarsals. Metatarsals were pulled away with tarsal and separated each other with tweezers (Song et al., 2015).

3.5. mRNA analysis

3.5.1. Total RNA isolation

Isolation of total RNA from primary chondrocytes was performed with the Qiagen RNeasy Mini kit (Qiagen, Netherlands) according to the manufacturer's instruction. Briefly, Cells were lysed in Buffer RLT supplemented with 1% β -mercaptoethanol and homogenized by passing through a QIAshredder spin column (Qiagen, Netherlands). 1 ml of 70% ethanol was add to the homogenized lysatem and mixed by pipetting. Afterwards, samples were loaded into RNeasy Mini Spin Column and subjected to an on-column genomic DNA digestion with 10 U of DNase (Qiagen, Netherlands). Column was washed twice with Buffer RPE and dried by centrifugation at maximum speed. Finally total RNA was eluted in RNase-free water and measured with NanoDrop 1000 (Thermo Scientific, USA) at A260 and at A260/A280, respectively for the evaluation of the RNA concentration and purity.

3.5.2. Complementary DNA (cDNA) synthesis

cDNA synthesis was performed with the Transcriptor First-Strand cDNA Synthesis Kit (Roche, Switzerland). Briefly, 1 µg of total RNA, hexamer-random primers (50 ng/µl) and 10mM dNTPs were heated for 5 min at 65°C. The denatured RNA was then added to a mixture of PCR buffer, 40U of RNase inhibitor, 0.1M dithiothreitol (DTT) and 15U of reverse transcriptase for 1 hour at 50°C. The newly synthesized cDNA was tested for the expression of a housekeeping gene glyceraldehyde-3-phosphate dehydrogenase (GAPDH) to evaluate the synthesis quality and to normalize the input of different samples.

3.5.3. Polymerase chain reaction (PCR)

Semi-quantitative RT-PCR for the genes of interest were performed adding a normalized amount (determined by the expression of GAPDH) of cDNA to a master mix containing PCR buffer, 1.5 mM MgCl₂, 0.2 mM dNTPs, 0.25 pmol gene-specific primers and 1 U Taq DNA polymerase (Roche, Switzerland) in the PCR thermal cyclor. Instruments and chemicals were the same as used in mouse genotyping (Table 1). Sequence of primers, PCR condition and size of PCR products were showed in table 3.

Table 3. PCR primers and condition for RT-PCR

Genes		Primer sequence (5'-3')	Temperature	Size (bps)
<i>NEMO</i>	Fwd	ATGAACAAGCACCCCTGGAAG	55°C	486 (wt)
	Rev	CTTCCCTCTAAAGCTTGCCGA		301 (mt)
<i>Cyclin D1</i>	Fwd	CTGGCCATGAACTACCTGGA	55°C	278
	Rev	ATCCGCCTCTGGCAT TTTGG		
<i>p16</i>	Fwd	CAACGCACCGAATAGTTACG	57°C	423
	Rev	AGCACCACCAGCGTGTC		
<i>p53</i>	Fwd	AAGGAAATTTGCGTGTGGAG	58°C	702
	Rev	TTCTGACGCACACCTATTGC		
<i>GADPH</i>	Fwd	CAACTACATGGTTTACATGTTC	50°C	181
	Rev	GCCAGTGGACTCCACGAC		

PCR condition		Temperature	Time
Pre-heating		95°C	5 min
Thermo cycle (35)	Denaturation	95°C	30 sec
	Annealing	differ from primers	30 sec
	Elongation	72°C	1 min
Final extension		72°C	10 min
Storage		4°C	∞

3.6. Western blotting

3.6.1. Protein extraction from monolayer culture

Cells were washed 2 times in PBS and lysed with radioimmunoprecipitation assay buffer (RIPA) containing protease inhibitor cocktail (PIC). Chemicals and buffer were showed in table 4. Cell scrapers (Sigma-Aldrich, USA) were used to collect cell lysates. After centrifugation at 14000 rpm, 4°C for 30 minutes, the supernatants were transferred to new eppendorf and stored at -20°C.

Table 4. Chemicals and buffer for protein extraction

Chemicals

Protease inhibitor cocktail	Roche, Switzerland
Sodium chloride (NaCl)	Merck, Germany
Triton X-100	Sigma-Aldrich, USA
Sodium deoxycholate	Merck, Germany
Sodium dodecyl sulphate (SDS)	Sigma-Aldrich, USA
Tris-HCl	Merck, Germany

Buffer

RIPA buffer	150 mM NaCl 1% Triton X-100 0.5% Sodium deoxycholate 0.1% SDS 50 mM Tris-HCl pH8.0
-------------	--

3.6.2. Protein quantification

The total protein concentration was measured using the bicinchoninic acid (BCA) protein assay kit (Thermo Fisher Scientific, USA). Briefly, the protein concentration was determined based on a chemical reaction where BCA interact with the cuprous cations that are reduced by the proteins in an alkaline media. As a result an intense purple-colored reaction is observed and the intensity of the color correlates with the protein concentration. The protein amount was calculated using a standard curve that is built by serial bovine serum albumin (BSA) (Thermo Fisher, Scientific USA) dilutions. The optical density measurements were performed at 450 nm on a FC Microplate Reader (Fisher Scientific, USA).

3.6.3. SDS-Polyacrylamide gel electrophoresis (PAGE)

Protein extracts (ca. 20 µg) were mixed with 4x Laemmli buffer and boiled for 5 min at 99°C. The protein mixtures were spun down and loaded on 12% acrylamide gels. The electrophoresis was performed in 1x running buffer composed

of 0.25 M Tris-base pH 8.3, 1% SDS and 1.92 M glycine. As molecular weight standard, PageRuler Plus prestained protein ladder (Thermo Scientific, USA) was used. The electrophoresis was run at constant 60 mA in an electrophoresis tank (BioRad, USA). Information of instruments, chemicals and buffers were listed in table 5.

Table 5. Instruments, chemicals and buffers for SDS-PAGE**Instruments**

Tetra Vertical Electrophoresis Cell	BioRad, USA
Electrophoresis power supply	Gentaur, Germany

Chemicals

Tris-HCl pH 6.8	Merck, Germany
Glycerol	Merck, Germany
SDS	Sigma-Aldrich, USA
2-mercaptoethanol	Merck, Germany
Bromphenolblue	Sigma-Aldrich, USA
Dithiothreitol (DTT)	Merck, Germany
Tris base	Merck, Germany
SDS	Sigma-Aldrich, USA
Glycine	Merck, Germany
PageRuler Prestained Protein Ladder	Thermo Scientific, USA

Buffers

4x Laemmli buffer	200 mM Tris-HCl pH 6.8 40% Glycerol 10% SDS 30% 2-mercaptoethanol 0.02% Bromphenolblue 0.2 M DTT
1x Running buffer	0.25 M Tris base pH 8.3 1% SDS 1.92 M glycine

3.6.4. Protein transfer

The protein transfer was performed by applying the vertical wet transfer method. Briefly, the gel loaded with proteins was equilibrated for 15 min in 1x blotting buffer. Meanwhile, the polyvinylidene fluoride (PVDF) membrane was activated by soaking into methanol for few seconds, rinsed in water and placed in 1x blotting buffer. The western blot “sandwich” was then assembled and the protein transfer was performed in a trans-blot system (Bio-Rad), O/N at 4°C with a constant voltage of 30 V. Afterwards, membranes were proceed for immunodetection or stored in a 0.1% PBS/Tween-20 (PBST) washing solution at 4°C until use. The instruments, chemicals and buffers were listed in table 6.

Table 6. Instruments, chemicals and buffers for protein transfer

Instruments

Trans-Blot Cell tank	BioRad, USA
Colored-coded cassettes	BioRad, USA
Cooling unit	BioRad, USA
PVDF membrane	Roche, Switzerland
Electrophoresis power supply	Gentaur, Germany

Chemicals

Tris-HCl	Merck, Germany
Glycine	Merck, Germany
Methanol	Merck, Germany
Tween-20	Thermo Scientific, USA

Buffers

1x Blotting buffer (pH 8.3)	2.5 mM Tris-HCl 192 mM Glycine 10% methanol
PBST buffer	1x PBS 0.1% Tween-20

3.6.5. Protein immunodetection

For immunodetection, PVDF membranes were blocked with 5% skimmed milk (Merck, Germany) in 0.1% PBST buffer for 1 hour at room temperature (RT) under gently shaking. Afterwards, PVDF membranes were incubated O/N with appropriate dilutions of primary antibody in blocking buffer at 4°C. The membrane was washed 10 min for 3 times with 0.1% PBST solution and incubated with diluted, corresponding horseradish peroxidase (HRP)-conjugated secondary antibody in the blocking solution at RT for 1 hour. Finally, the membrane was washed 10 min for 3 times with 0.1% PBST buffer. Proteins on PDVF membrane were visualized by using chemi-luminescent Amersham ECL plus solution and the luminiscent image analyser Image Quant LAS 4000 mini (GE Healthcare, USA). Antibodies used in western blotting were listed in table 7.

Table 7. Antibodies for western blotting

Primary antibodies	
IKK γ /NEMO (Mouse, 1:1000)	MBL international, USA
Phospho-NF κ B p65 (Rabbit, 1:1000)	Cell Signaling, USA
NF κ B p65 (Rabbit, 1:1000)	Cell Signaling, USA
I κ B α (Rabbit, 1:1000)	Cell Signaling, USA
β -actin (Mouse, 1:10000)	Santa Cruz, USA
Secondary antibodies	
Goat anti-mouse IgG-HRP (1:5000)	Santa Cruz, USA
Goat anti-rabbit IgG-HRP (1:4000)	Santa Cruz, USA

3.6.6. Gelatin/collagen Zymography

Cultured media from femoral head explant (see 3.4.1) were centrifuged at maximum speed at 4°C to remove cell debris and subjected to Gelatin Novex Zymogram Gels (Thermo Fisher Scientific, USA) and collagen I SDS-polyacrylamine gel. The electrophoresis was performed in 1x running buffer and coupled with PageRuler Plus prestained protein ladder (see table 5). The electrophoresis was run at constant 60 mA in an electrophoresis tank (see table 5). After electrophoresis, the

gels were incubated in 1x Novex Zymogram Renaturing Buffer (Thermo Fisher Scientific, USA) for 30 min at room temperature with gentle agitation. The gels were incubated in 1x Novex Zymogram Developing Buffer (Thermo Fisher Scientific, USA) for 30 min with gentle agitation and fresh 1x Novex Zymogram Developing Buffer at 37°C O/N. Afterwards, the gels were stained with coomassie staining solution, destained with destain solution and dried by using DryEase Mini-Gel Drying System (Thermo Fisher Scientific, USA). Instruments, chemicals and buffers for zymography are listed in table 8.

Table 8. Instruments, chemicals and buffers for zymography**Instruments**

Tetra Vertical Electrophoresis Cell	BioRad, USA
Electrophoresis power supply	Gentaur, Germany
DryEase Gel Drying Frame	Thermo Fisher Scientific, USA
DryEase Gel Drying Base	Thermo Fisher Scientific, USA

Chemicals

Collagen I	R&D, USA
Coomassie Brilliant Blue R-250	Sigma-Aldrich, USA
Acetic acid	Merck, Germany
Ethanol	Merck, Germany
Deionized water	Thermo Scientific, USA

Buffers

Coomassie staining solution	0.1% Coomassie Blue 40% ethanol 10% acetic acid 50% dH ₂ O
Destain solution	10% ethanol 7.5% acetic acid 82.5% dH ₂ O

3.7. NF- κ B reporter assay

3.7.1. Transfection

Cignal NF- κ B reporter assay kit (Qiagen, Netherlands) was utilized to monitor NF- κ B activity in *NEMO^{fl/y}Col2a1cre* chondrocytes. Experimental procedure was followed the handbook of the kit. 1×10^4 Primary wild-type/*NEMO^{fl/y}Col2a1cre* chondrocytes were trypsinized and resuspended in reduced serum medium modification of minimal essential media (Opti-MEM) (Thermo Scientific, USA). Transient transfection of Cignal reporter was carried out in 4D-Nucleofector Core Unit (Lonza, Switzerland). 1×10^3 transfected cells were then seeded into 96-well cell culture plate and incubated for 24 hours. After 24 hours incubation, media were replaced with complete DMEM/F12 media.

3.7.2. Dual-Luciferase assay

The luciferase assay was performed by using a dual-luciferase reporter assay system (Promega, USA) according to manufacturer's instructions. The cells were washed with PBS twice and mixed with 20 μ l passive lysis buffer after 10 ng/ml IL-1 treatment for one hour. After gently shaking at room temperature for 15 minutes, the lysate was transferred to new 96-well cell culture plate with 100 μ l luciferase assay reagent. SAFIRE₂ Microplate Reader (Thermo Fisher Scientific, USA) was used to measure firefly luciferase activity. 100 μ l Stop&Glo[®] Reagent was add into each well to measure *Renilla* luciferase activity that normalized for cell death caused by the treatment.

3.8. Time-lapse migration and adhesion assay

2×10^4 primary chondrocytes were seeded sparsely in 6-well cell culture plate. The cell culture plate was then put into environment control chamber with heating unit, CO₂ controller (Pecon, Germany). The system included a stage top environmental control chamber (Pecon, Germany) and an automated XY stage controller (Proscan, Canada). AxioCam MRc (Carl Zeiss, Germany) and Axiovision

Rel. 4.8 (Carl Zeiss, Germany) were used for automated image acquisition. Images were acquired with a 10X UPLANFL Ph1/0.30 objective in bright field mode and using a defined time interval. The observation of cell adhesion, spreading and migration was lasted for 48 hours and analyzed by ImageJ.

3.9. Cell attachment assay

96-well cell culture plate was pre-coated with 10 µg/ml fibronectin (R&D, USA), 10 µg/ml vitronectin (R&D, USA), 10 µg/ml laminin (R&D, USA), 10µg/ml collagen type I (R&D, USA), 10 µg/ml collagen type II (R&D, USA), 10% FBS and 1% BSA for 1 hour at 37°C. Pre-coating solution was replaced with 1% BSA to block non-specific binding sites for 1 hour at 37°C. After washing with PBS, 1×10^5 wild-type and *NEMO^{fl/y}Col2a1cre* chondrocytes were seeded into the plate and incubated for 1 hour. Afterwards, cells were washed with PBS, fixed with 96% ethanol for 10 minutes, stained with 0.1% crystal violet/H₂O for 30 minutes at room temperature and lysed with 0.1% Triton X-100/H₂O. The optical measurement was performed at 595 nm on a microtiter-plate reader (Thermo Scientific, USA).

3.10. Immunofluorescence staining

Primary chondrocytes

Primary wild-type and *NEMO^{fl/y}Col2a1Cre* chondrocytes (1×10^4 cells/cm²) were grown in presence of complete DMEM/F12 media on chamber slides (Thermo Scientific, USA) for at least two or three days under normal culture conditions. Afterwards, cells were rinsed in PBS and fixed with 4% PFA for 20 min at room temperature (RT).

For immunodetection, fixed cells were rehydrated in PBS (3x5 min at RT) and permeabilized with 0.2% Triton X-100/PBS for 15 min. Image-iT FX Signal Enhancer (Invitrogen, USA), a solution which reduces the unspecific binding of secondary antibodies, was applied for 30 min. Slides were placed in 2% BSA/PBS solution for one hours at RT and then incubated with primary antibodies (Table 9) O/N at 4°C. After PBS washing (5 minutes for 3 times), corresponding secondary antibodies conjugated with fluorescence were applied to slides for 1 hour at RT. Finally, slides

were washed with PBS (3 times for 5 minutes at RT) and a nuclear counterstaining was performed with 4', 6-diamidino-2-phenylindole (DAPI) for 5 min. After PBS washing (3 times for 5 minutes), slides were mounted with Fluoromont Anti-Fading Mounting Media (Sigma- Aldrich, USA). Negative controls for antibody were carried out on the same slide by omitting the primary antibody. Primary, secondary antibodies and dyes were listed in table 10. Photomicrographs were taken with Axiocam MRm camera mounted on Axio Observer Z1 Microscope (Carl Zeiss, Germany).

Knee sections

Knee sections of 2-week-old mice were dewaxed, rehydrated, peroxidase-blocked, hyaluronidase-treated and incubated in 1% BSA/PBS solution. Sections were then incubated with anti-NEMO antibody (1:1000, Table 9) O/N at 4°C. After washing with PBS for 3 times, sections were incubated with Alexa Fluor 488-conjugated Phalloidin and Alexa Fluor 546 Dye for 1 hour at room temperature. Finally, sections were PBS-washed, counterstained with DAPI for 5 min and mounted with Fluoromont Anti-Fading Mounting Media. Photomicrographs were taken with Axiocam MRm camera mounted on Axio Observer Z1 Microscope.

Table 9. Primary antibodies and fluorescence-conjugated secondary antibodies or chemicals for immunofluorescence staining

Primary antibodies	
NFκB p65 (Rabbit, 1:1000)	Cell Signaling, USA
Secondary antibodies	
Alexa Fluor 488-conjugated Phalloidin (1:300)	Invitrogen, USA
Donkey anti-rabbit Alexa Fluor 546 (1:300)	Invitrogen, USA
Chemicals	
4', 6-diamidino-2-phenylindole (DAPI) (1:10000)	Invitrogen, USA

3.11. Whole-mount skeletal staining

The gross morphology of the whole skeleton was analyzed by Alizarin blue/Alizarin red staining of E13.5 – E16.5 and newborn. Euthanized embryo and newborn specimens were deskinning and eviscerated, fixed in 95% ethanol for 3 days and then transferred into acetone for 1 day. Staining was performed in the alizarin red/alizarin blue solution for 3 days at 37°C. Samples were rinsed in water and cleared for 3 days in 1% potassium hydroxide (Merck, Germany) followed by clearing in KOH/glycerol (0.8% and 20%, respectively) solution for 1 week. Samples were then transferred into 0.5%/50%, 0.3%/80% KOH/glycerol solution and finally 100% glycerol for long-term storage. The humerus, femur, and tibia were dissected from ten control and ten double *NEMO^{fl/y}Col2a1Cre* mice and measured longitudinally using a fine calibrated ruler. Chemicals and buffers used were listed in table 10.

Table 10. Chemicals and buffers for whole-mount skeletal staining

Chemicals

Ethanol	Merck, Germany
Acetic acid	Merck, Germany
Alizarin red S	Sigma-Aldrich, USA
Alcian blue 8GS	Sigma-Aldrich, USA
Potassium hydroxide (KOH)	Merck, Germany
Glycerol	Merck, Germany

Buffers

Alizarin red/alcian blue solution	90% Ethanol 5% Acetic acid 0.005% Alizarin red S 0.015% Alcian blue 8GS 4.985% H ₂ O
20% KOH/glycerol solution	0.8% KOH 20% Glycerol 79.2% H ₂ O
50% KOH/glycerol solution	0.5% KOH 50% Glycerol 49.5% H ₂ O
80% KOH/glycerol solution	0.3% KOH 80% Glycerol 19.7% H ₂ O

3.12. Histology

3.12.1. Fixation

Hind limbs of euthanized mouse were de-skinned, the muscles around knee joints removed and rinsed in PBS. Knee joints were fixed in pre-cooled 4% PFA O/N,

fixed samples were washed 15 min in PBS for 3 times with slow shaking at room temperature.

3.12.2. Decalcification

Decalcification of bony tissues was achieved by incubating PFA-fixed samples in a 20% EDTA/PBS solution (pH 8) for approximately 4 weeks. Chelating agents such as EDTA captured the calcium ions and soften bones. 20% EDTA/PBS solution was renewed twice per week.

3.12.3. Embedding

Decalcified samples were ready either for cryo or paraffin embedding. For frozen sectioning, specimens were firstly rinsed 15 min in PBS for 3 times and were then placed in an ascending solution of sucrose/PBS: 10 and 15% for 2 hour each and 20% O/N at 4°C. The next day, specimens were embedded in FSC 22 Frozen Media (Leica, Germany) in plastic base mould disposable cassettes (Leica, Germany) placed on a copper plate on dry ice. Samples were stored wrapped in parafilm (Sigma-Aldrich, USA) at 20°C until use.

For paraffin sectioning, specimens (placed in embedding cassettes (Proscitech, Australia)) were firstly rinsed 15 min in PBS for 3 times and then passed through ascending row of ethanol solution (50, 70, 80, 90 and 2x100 %, one hour for each step), xylol (5 min for 2 times) and melted Paraplast Paraffin Tissue Embedding Media (60°C, 1 hour for 3 times) (Leica, Germany). Afterwards, specimens were embedded in paraffin tissue embedding media in stainless steel base embedding cassettes (Leica, Germany) on Tissue Embedding Center (IMEB, USA).

3.12.4. Sectioning

Cryosectioning was performed with a Cryotome Microm HM500 (Thermo Scientific, USA) and slices of 10 µm thickness were collected on SuperFrost glass slides (Thermo Scientific, USA) and stored at -20°C.

Paraffin block specimens were cut with a Rotary Microtome HM360 (Thermo Scientific, USA) and slices of 8 μm were collected on SuperFrost glass slides. Slides were kept O/N at 37°C and then stored at room temperature.

3.12.5. Hematoxylin and eosin (H&E) staining

For a first screening of the general tissue morphology H&E staining was performed. Paraffin sections of 8 μm thickness were rehydrated through a descendent ethanol row (100, 90, 80 and 70% for 5 min each) and a final step in dH₂O. 0.1% Mayer's Hematoxylin Solution (Merck, Germany) was applied for 5 min, followed by intense washing with tap water. Next, slides were rinsed in dH₂O and incubated in 0.1% eosin (Sigma-Aldrich, USA) solution for 5 min. After rinsing in dH₂O, slides were dehydrated in an ascending ethanol row (70, 80, 90, 100 and 100% for 5 min each) and cleared by two steps in xylol for 5 min each. Finally, slides were mounted with DPX mounting media (Sigma-Aldrich, USA). Pictures were taken on an Axiovert 100 microscope using AxioCam ICc3 colour camera (Carl Zeiss).

3.12.6. Safranin orange staining

After dewaxing in xylene and stepwise rehydration in ethanol (100, 90, 80 and 70% for 5 min each), and distilled water (dH₂O), the sections were stained with 0.1% Safranin-O (Sigma-Aldrich, USA) for 3 min. Afterwards, sections quickly went through 95%, 100% ethanol, xylene and mounted with DPX mounting media.

3.12.7. Von Kossa staining

Sections of E16.5 embryo were dewaxed, rehydrated and exposed to bright light with Silver nitrate (Merck, Germany) for 30 min. Sections were washed with distilled water and incubated with 2.5% sodium thiosulphate (Merck, Germany) for 5 min. After washing with dH₂O, sections were counterstained with safranin orange for 3 min and quickly went through 95%, 100% ethanol, xylene and mounted with DPX mounting media.

3.12.8. Toluidin blue staining

Sections were rehydrated (described above) and stained with 0.1% Toluidine blue in toluidine buffer pH 2.5 (0.1M K_2HPO_4 and 0.1M HCl (Merck, Germany)) for 10 mins, followed by staining with 2% $K_3Fe(CN)_6$ for 3 min, excessive staining reagents were removed by WATTMAN paper (Sigma-Aldrich, USA). Sections were finally air-dried, mounted with DPX mounting media.

3.12.9. Tartrate-resistant acid phosphatase staining (TRAP)

Acid Phosphatase, Leukocyte (TRAP) Kit (Sigma-Aldrich, USA) was used to perform the TRAP staining on E15.5 sections. According to manufacturer's instruction, paraffin-fixed sections were rehydrated and incubated in pre-warmed staining solution (37°C) containing 0.5 ml Fast Garnet GBC Base solution (Sigma-Aldrich, USA), 0.5 ml Sodium Nitrite Solution (Sigma-Aldrich, USA), 0.5 ml Naphthol AS-BI Phosphate Solution (Sigma-Aldrich, USA), 2 ml Acetate Solution (Sigma-Aldrich, USA), 1 ml Tartrate Solution (Sigma-Aldrich, USA) and 45ml Deionized water (Thermo Scientific, USA) at 37°C for 1 hour. Afterwards, sections were rinsed in deionized water and counterstained in Hematoxylin solution, Gill No 3 (Sigma-Aldrich, USA) for 2 min followed by tap water washing for 5 min. Sections were then air-dried and mounted with DPX mounting media.

3.12.10. Immunohistochemistry staining (IHC)

After dewaxing and rehydration, specimens were placed in 0.01% hydrogen peroxide (H_2O_2) (Merck, Germany)/methanol (Merck, Germany) solution for 20 min at room temperature to block endogenous peroxidase activity. After washing with PBS, antigen retrieval was achieved by incubating specimens with 0.2% Bovine Testicular Hyaluronidase (Sigma-Aldrich, USA)/PBS solution for 30 min at 37°C. Specimens were then washed with PBS and blocked with 1% BSA/PBS solution for 1 hour and incubated with primary antibody/blocking solution O/N at 4°C. Primary antibodies used in IHC staining were listed in table 11. Afterwards, the specimens were washed by PBS and incubated with Biotinylated Anti-mouse IgG Reagent from Mouse on Mouse (M.O.M. Kit) (Vector Laboratories, USA) for 1 hour. The specimens were then

wash by PBS and incubated with Vectastain ABC solution from Vectastain Elite ABC Kit (Vector Laboratories, USA) for 30 min at room temperature. For color detection, specimens were placed in 3,3'-diaminobenzidine (DAB) solution (pH7.2) containing 0.05% DAB (Sigma-Aldrich, USA) and 0.015% H₂O₂ in PBS for 7 min in dark. After color detection, specimens were washed in dH₂O, counterstained in Mayer's Hematoxylin Solution, dehydrated and mounted with DPX mounting media.

Table 11. Antibodies for IHC stainingPrimary antibodies

Aggrecan (1:1000)	Abcam, UK
BrdU (1:100)	Roche, Switzerland
TEGE (1:500)	Arcis, Germany
VIDIPEN (1:4000)	from Dr. Amanda Fosang
MMP-2 (1:400)	Millipore, USA
MMP-3 (1:250)	Sigma-Aldrich, USA
MMP-9 (1:400)	Millipore, USA,
MMP-13 (1:400)	GeneTex, USA

3.12.11. Measurement of growth plate

H&E stained knee sections of 2-week-old and 4-week-old mice were pictured and analyzed in Adobe Photoshop CS2 (Adobe, USA). All measurements were performed in the central two-thirds of growth plate sections. The area of total growth plate (TGP) was defined from the top of resting zone (RZ) through proliferating zone (PZ) to the bottom of hypertrophic zone (HZ). The height of TGP, RZ+PZ and HZ were presented as mean \pm standard deviation (SD).

3.12.12. Analysis of proliferating columns in growth plate

All measurements were performed in the central two-thirds of growth plate sections. Using Photoshop CS2, the axis of proliferating columns in growth plate and the horizontal angle were measured. The shape of columns was determined by ratio of horizontal axis / vertical axis. It was generally accepted that proliferating column

were supposed to be oval shape and ratio below 0.7. Columns with ratio over 0.7 were more round-liked in shape. The horizontal angle of vertical axis were also measured (Figure 18), most of the columns were perpendicular to the growth plate under normal development.

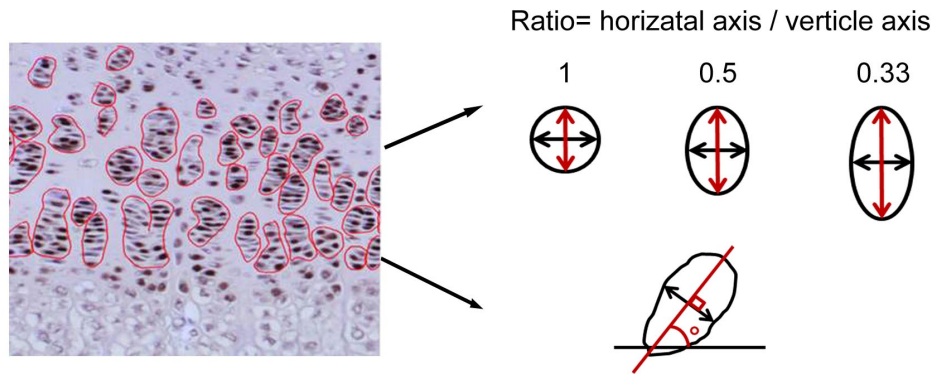


Figure 18: Schematic representation of methods to analyze shape and angle of columns. Shape was determined by the ratio defined as horizontal axis of column / vertical axis of column (e.g. 0.1 represented slit-shaped columns, 1 represent round-liked column). Horizontal angle (angle between vertical axis and horizontal line) of proliferating columns was measured.

3.13. Non-radioactive *in situ* hybridization

Plasmid linearization and generation of RNA probes

DNA templates were linearized with restriction enzymes for RNA *in vitro* transcription (Table 12). 10 µg of plasmid DNA were linearized with restriction endonucleases and buffers according to manufacturer's instruction (restriction endonucleases and buffers were all from New England BioLab, USA). Linearized DNA were purified through Nucleospin column (Macherey-Nagel, Germany) and *in vitro* transcribed with T3 RNA polymerase in 10x transcription buffer with digoxigenin (DIG) labeled ribonucleotides (Roche, Switzerland) for 2 hour at 37°C. Afterwards, transcription was examined by electrophoresis in 2% agarose gel. The transcribed RNA was purified after DNA digestion with G-50 spin columns (GE Healthcare Life Science, USA), suspended in RNase-free water and restored in -80°C.

Table 12. Restriction enzymes and polymerase for DNA plasmid linearization

Nucleotides	Restriction enzymes	Polymerase
<i>Collagen I</i>	EcoRI	T3
<i>Collagen II</i>	EcoRI	T3
<i>Collagen X</i>	Clal	T3

Unfixed, cryo-embedded sections of newborn limb were fixed in 4% PFA/Diethyl pyrocarbonate (DEPC)-PBS (pH 9.5) solution for 1 hour and rinsed in DEPC-PBS (pH 9.5). The sections were placed in 1% Triton X-100/DEPC-PBS (pH 9.5) solution for 20 min, then 5x saline-sodium citrate (SSC)/50% formamid solution for 15 min and pre-heat (80°C) hybridization solution with 2 µl RNA probe (approximately 200 ng) at 95°C for 2 min. Afterwards, the sections were covered with parafilm and placed in humid chamber soaked with 2x SSC/50% formamid at 55°C O/N followed by washing with pre-heat washing solution I and II at 55°C for 30 min. After washing with 0.2x SSC for 5 min and PBS (pH 7.4) for 3 times at room temperature, the sections were then incubated with an alkaline phosphatase-coupled antibody against DIG (Roche, Switzerland) diluted (1:500) in PBS (pH 7.4) containing 10% FBS for 1 hour at room temperature. The sections were then rinsed in PBS (pH 7.4) 5 min for 3 times, incubated with DIG III solution for 10 min and placed in staining solution for color development. After sufficient color reaction, sections were mounted with Aqua mounting media (Sigma-Aldrich, USA). Chemicals and buffers for *in situ* hybridization were described in table 13.

Table 13. Chemicals and buffers for *in situ* hybridization

Chemicals

50x Denhardt's solution	Sigma-Aldrich, USA
Anti-DIG-AP, Fab fragments	Sigma-Aldrich, USA
Salmon sperm DNA (SS-DNA)	Sigma-Aldrich, USA
NBT/BCIP stock solution	Sigma-Aldrich, USA
tRNA from baker's yeast	Sigma-Aldrich, USA
Levamisol	Sigma-Aldrich, USA
Deionized formamid	Merck, Germany
DEPC	Sigma-Aldrich, USA

Buffers

20x SSC buffer	3M NaCl 300 mM Sodium citrate DEPC-H ₂ O
Hybridization solution	10% 50x Denhardt's solution 10 mg baker's yeast 2% SS-DNA 25% 20x SSC buffer 50% Deionized formamid 13% dH ₂ O
Washing solution I	10% 20x SSC buffer 50% Deionized formamid 40% DEPC-H ₂ O
Washing solution II	1% 20x SSC buffer 50% Deionized formamid 49% DEPC-H ₂ O
DIG III solution	10% 1M Tris-HCl pH 9.5 2% 5M NaCl 5% 1M MgCl ₂ 83% dH ₂ O
Staining solution	0.1% 0.24 g/ml Levamisol solution 2% NBT/BCIP stock solution 97.9% DIG III solution

3.14. Sulphated glycosaminoglycan (sGAG) assay

The sGAG in conditioned DMEM/F12 media of hip explant was examined by sGAG assay kit (Biocolor, UK). The assay was performed as manufacturer's instruction. Briefly, Conditioned DMEM/F12 media were centrifuged at 10000g for 10 minutes to remove cell debris and assay the supernatant. 10µl conditioned media from each group were added into 1ml 1x Blyscan Dye Reagent (Biocolor, UK) and incubated for 30 minutes. After centrifuging 10000g for 10 minutes and removing supernatant, insoluble sGAG-dye complex was seen at the bottom of the tube. 500 µl Dissociation Reagent (Biocolor) was added to resolve the GAG-dye complex. Transfer 200 µl well-mixed samples into 96-well plate and measure absorbance in microtiter-plate reader (Thermo Scientific, USA) at 656 nm. The data was exported to Office Excel 2003 (Microsoft, USA) for statistical analysis.

3.15. Pathological Scoring System of Articular Cartilage

The *NEMO^{fl/y}Col2a1Cre* and wild-type mice were euthanized and knees were harvested at various time points. The samples were fixed in 4% PFA/PBS solution, decalcified in 20% EDTA/PBS and processed to paraffin embedding. Approximately 250 serial, 7-µm-thick sections were collected from 1 specimen. Every 10th slide was chosen to stain with hematoxylin-eosin for general H&E or SO to view proteoglycans (PGs) depletion. About 8-10 serial sections representing the entire knee were evaluated from every mouse of age and genotype. Based on previous study of our laboratory, to assess pathological changes of the articular cartilage (Raducanu et. al., 2009), we used a scoring system as follows: I, cartilage erosion (0–5; 0, smooth cartilage surface; 1, surface irregularities; 2, cleft to transition zone; 3, cleft to radial zone; 4, cleft to calcified zone; 5, exposure of subchondral bone); II, cellularity (0–3; 0, normal; 1, hypercellularity; 2, clustering; 3, hypocellularity); III, tidemark integrity (0–1; 0, normal; 1, loss of tidemark); IV, GAG content in the pericellular matrix (PM) (0–2; 0, normal SO staining intensity; 1, focally increased intensity; 2, increased intensity throughout the cartilage); V, GAG content in the interterritorial matrix (ITM) (0–3; 0, normal SO staining intensity; 1, reduced staining; 2, focal patchy loss of staining; 3, 50% of cartilage without staining); VI, osteophyte formation (0–2; 0, none; 1, formation of cartilage; 2, formation of bone). Total scale (0–16) and OA

severity were as follows: 0–1, normal; 2–5, mild OA; 6–11, moderate OA; 12–16, severe OA (Raducanu et al., 2009).

X-ray imaging

1-year and 1.5-year-old *NEMO^{fl/Y}COL2a1Cre* and control mice were euthanized and radiographs were taken with a sealed x-ray cabinet 43855A (Faxitron, USA) at 35 kV, 2 mA and 2 sec of exposure time.

3.16. Proliferation and Apoptosis Assays

Proliferation of chondrocytes *in vivo* was monitored by incorporation of bromodeoxyuridine (BrdU) (Sigma-Aldrich, USA) into 2- and 4-week-old wild-type and *NEMO^{fl/Y}COL2a1Cre* mice. 5 mg/ml BrdU/PBS solution was injected intraperitoneally and the injected amount was approximately 50 µg/g per body weight. Mice were euthanized 2 hours after injection, isolated knee joints were fixed, paraffin embedded, sectioned (7µm), stained with primary BrdU antibody (Table 11) and counterstained with hematoxylin. The number of labeled cells and total cell number were scored and analyzed by Photoshop CS2 and Office Excel 2003.

To investigate primary chondrocyte proliferation *in vitro*, a Cell Proliferation Enzyme-Linked Immunosorbent (ELISA) Assay Kit (colorimetric) (Roche, Switzerland) was utilized to analyze the incorporation of BrdU during DNA synthesis following the manufacturer's protocols. Briefly, 1×10^4 cells were seeded in 96 well culture plate and incubated with DEME/F12 media containing BrdU labeling Solution (working concentration of BrdU: 10 µM) (Roche, Switzerland) for 2 hours. Labeled cells were air-dried for 15 min and incubated with FixDenat Solution (Sigma-Aldrich, USA) for 30 min at room temperature. After removing the FixDenat Solution, 100 µl anti-BrdU-POD solution (Sigma-Aldrich, USA) was added to each well and incubated for 90 min at room temperature followed by washing 3 times with Washing Solution (Sigma-Aldrich, USA). 100 µl Substrate Solution (Sigma-Aldrich, USA) was then added to each well and incubated for 20 min at room temperature. The absorbance of the samples was measured in microtiter-plate reader (Thermo Scientific, USA) at 370 nm.

To detect apoptotic and necrotic cells *in vitro*, an Apoptotic/Necrotic/healthy Cells Detection Kit (PromoKine, Germany) was used. Primary chondrocytes of wild-type or *NEMO^{fl/y}Col2a1Cre* were treated with or without 100 ng/ml TNF- α for 24 hours and proceeded as manufacturer's instruction. The cells were washed twice with 1x Binding Buffer (PromoKine, Germany) and stained with solution containing 5 μ l fluorescein isothiocyanate (FITC)-AnnexinV (PromoKine, Germany), 5 μ l ethidium homodimer III (PromoKine, Germany) and 5 μ l Hoechst 33342 (PromoKine, Germany) for 15 min at room temperature in dark. Stained cells were washed twice and mounted with Binding Solution. Afterwards, sections were pictured using AxioCam MRm camera (Carl Zeiss, Germany) mounted on Axio Observer Z1 Microscope (Carl Zeiss, Germany) with 10x objective.

3.17. Atomic force microscopy (AFM)

All AFM measurements were carried out using a NanoWizard AFM instrument (JPK Instruments, Berlin, Germany) mounted on a modified microscope stage of an inverted optical microscope (Axiovert 200, Zeiss). The optical microscope with a 40x magnification was used to ensure the right positioning of the cantilever tip on the proliferating zone of growth plate. The AFM had a maximum horizontal scanning range of 100 x 100 μ m² and a vertical range of 15 μ m. Prior to each measurement, the force constants of all cantilevers were determined individually using the thermal noise method (Butt, 1995). Calibrations were performed in PBS. In order to obtain an accurate calibration, three independent measurements were performed and the mean value was used for the experiment. All analyses were processed with the JPK Data processing software 4.0.23 (JPK instruments). The AFM observation was performed in collaboration with Carina Preis, under supervision of Prof. Hauke Clausen-Schaumann (Hochschule Munich, Germany).

3.18. Taqman Low-Density Array (TLDA) microfluidic cards

Prof. Tonia L. Vincent (Kennedy Institute of Rheumatology, UK) and her group carried out this experiment and the following data analysis as described (Burleigh et al., 2012). Briefly, complementary DNA (cDNA) was generated from articular cartilage RNA using a Promega Reverse Transcription system. TLDA microfluidic

cards were custom designed for a set of 47 pre-determined genes that known to be strongly regulated following injury. All thermo cycles were carried out on a 7900HT system (Thermo Scientific, USA). The 47 pre-determined genes were list in table 14.

Table 14. 47 pre-determined genes for TLDA

ECM and ECM associated proteins

Aggrecan (ACAN)

Collagen type II alpha 1 (COL2 α 1)

Collagen type XI alpha 2 (COL6 α 2)

Collagen type X alpha 1 (COL10 α 1)

Connective tissue growth factor (CTGF)

heparan sulfate proteoglycan 2 (HSPG-2)

Inflammatory associated proteins

Cluster of Differentiation 68 (CD-68)

Interleukin 18 binding protein (IL18BP)

Interleukin 18 receptor accessory protein (IL18RAP)

Tumor necrosis factor alpha induced protein 6 (TNFaIP-6)

Tumor necrosis factor superfamily, member 11 (TNFSF-11, RANKL)

Inflammatory cytokines

Chemokine (C-C motif) ligand 2 (CCL-2)

Interleukin 1 alpha (IL-1 α)

Interleukin 1 beta (IL-1 β)

Interleukin 6 (IL-6)

Interleukin 18 (IL-18)

Interleukin 33 (IL-33)

Proteinases and proteinase inhibitor

A disintegrin and metalloproteinase with thrombospondin motifs 1 (ADAMTS-1)

A disintegrin and metalloproteinase with thrombospondin motifs 4 (ADAMTS-4)

A disintegrin and metalloproteinase with thrombospondin motifs 5 (ADAMTS-5)

A disintegrin and metalloproteinase with thrombospondin motifs 15 (ADAMTS-15)

Inhibin beta-A (INH β A)

Matrix metalloproteinase 3 (MMP-3)

Matrix metalloproteinase 9 (MMP-9)

Matrix metalloproteinase 13 (MMP-13)

Tissue inhibitor of metalloproteinase 1 (TIMP-1)

Table 14. 47 pre-determined genes for TLDA (continued)**Receptor proteins**

Antrogon receptor (AR)

Chemokine (C-C motif) receptor 2 (CCR-2)

Estrogen receptor 1 (ESR-1)

Fibroblast growth factor receptor 1 (FGFR-1)

Fibroblast growth factor receptor 2 (FGFR-2)

Fibroblast growth factor receptor 3 (FGFR-3)

Interleukin 1 receptor 1 (IL1R-1)

Interleukin 1 receptor-like 1 (IL1RL-1)

Interleukin 18 receptor 1 (IL18R-1)

Tumor necrosis factor alpha receptor superfamily member 11A (TNFaRSF-11A)

Tumor necrosis factor alpha receptor superfamily member 12A (TNFaRSF-12A)

Synthases

Hyaluronan synthase 1 (HAS-1)

Hyaluronan synthase 2 (HAS-2)

Nitric oxide synthase 2 (NOS-2)

Prostaglandin-endoperoxide synthase 2 (PTGS-2)

Diverse proteins

Arginase I (ARG-1)

Runt-related transcription factor 2 (RUNX-2)

Secreted frizzled-related protein 2 (SFRP-2)

WNT1-inducible-signaling pathway protein 2 (WISP-2)

Wnt family member 16 (WNT-16)

3.19. Microscopy

The microscopes and cameras used in this thesis were purchased from Carl Zeiss MicroImaging (Germany). Phase-contrast pictures of tissue histology staining were imaged using the AxioCam ICc3 colour camera (Carl Zeiss, Germany) mounted on AxioVert S100 Inverted Microscope (Carl Zeiss, Germany) with 10x objective.

3.20. Computer software and statistical analysis

In this doctoral thesis a number of programs for processing and analyzing data were used. Primers sequences were designed using Clone Manager 9 (Sci-Ed software, USA). Photomicrographs were processed with AxioVision LE software (Carl Zeiss, Germany). Quantitative data, various graphs and charts were evaluated and created by using Microsoft Office Excel 2003 and GraphPad Prism 5 (GraphPad, USA). The student *t*-test was performed to compare two normal distributed sets of samples. Non-parametric Mann-Whitney U test was applied to compare sets of non-normal distributed data. All data was presented as the mean \pm SD. *p* value less than or equal to 0.05 was considered as statistically significance and symbolized as 1 star (*). *p* value less than or equal to 0.01 or 0.001 was symbolized as 2 (**) or 3 stars (***), respectively. Analysis of stained cells, cell number, bone length and metaphysis measurement were performed with Adobe Photoshop CS2. Morphometric analysis was performed with ImageJ 1.41o. Bibliography of this thesis was managed with EndNote X7.5.3 (Thomson Reuters, USA).

4. Results

4.1. Characterization of $NEMO^{fl/Y} Col2a1Cre$ mice

To study the function of the canonical NF- κ B pathway in endochondral bone formation and articular cartilage, we have used the floxed (fl) $NEMO$ mice (Schmidt-Supprian et al., 2000, generously provided by Dr. Marc Schmidt-Supprian, Max Planck Institute for Biochemistry, Martinsried, Germany) and the $Col2a1-Cre$ transgenic mouse line generated in the Aszodi lab (Sakai et al., 2001). The murine gene encoding $NEMO$ is X chromosome localized, whereas in $Col2a1-Cre$ mice cre is driven by the type II collagen regulatory regions, and efficiently deletes floxed genes in differentiated chondrocytes. To obtain mice lacking $NEMO$ in cartilage, $NEMO^{fl/fl}$ females were crossed with $Col2a1-Cre$ males. From such a cross, $NEMO^{fl/Y}-Col2a1Cre$ males were generated that lack $NEMO$ expression in chondrocytes (Figure 19).

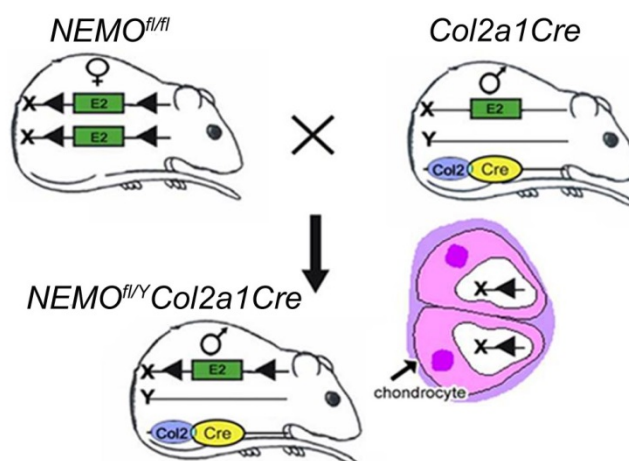


Figure 19: Schematic representation of the generation of $NEMO^{fl/Y} Col2a1Cre$ mice. The X chromosome-localized $NEMO$ gene was floxed (fl) using the LoxP sites. The chromosome recombinase (Cre) was controlled by $Col2a1$ promoter, which was specifically active in differentiating chondrocytes. To achieve chondrocyte-specific deletion, floxed $NEMO$ females were then crossed with males carrying the $Col2a1cre$ transgene males.

4.1.1. RNA and protein expression of NEMO in *NEMO^{fl/y}Col2a1Cre* chondrocytes were completely inhibited

The offspring carrying floxed *NEMO* gene and *Col2a1Cre* transgene expressed abnormal *NEMO* mRNA with disrupted exon 2. Deletion of exon 2 of *NEMO* was examined by PCR primers designed for fragment from exon 1 to exon 3 of *NEMO* gene (Figure 20A). The exon 1 to exon 3 in wild-type chondrocytes from PCR amplification gave 489 base pairs (bps) products. Due to the disruption of exon 2 of *NEMO* gene in mutant chondrocytes, the size of PCR product was 301 bps. The exon 2 of *NEMO* gene was completely deleted in mutant chondrocytes, and, incomplete *NEMO* mRNA was suggested to translate abnormal NEMO protein. The NEMO protein was not detected in primary mutant chondrocytes (Figure 20B). Misfolded NEMO protein in mutant chondrocytes was likely degraded by 26S proteasome or existed as inclusion bodies within the cell.

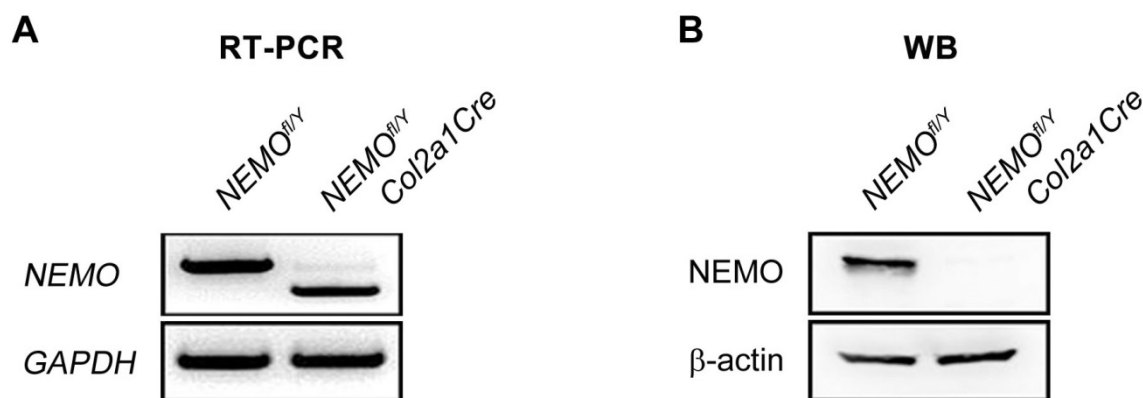


Figure 20: RT-PCR and WB results of wild-type (WT) and mutant (MT) chondrocytes. (A) Fragment from exon 1 to 3 of *NEMO* gene was amplified by RT-PCR. In wild-type chondrocytes, a 489 bps product was observed that represented the length of exon 1 to 3. Owing to the deletion of exon 2 of *NEMO* gene, a shorter PCR product (301 bps) was showed. (B) NEMO protein expression was clarified by western blotting (WB). No signal of NEMO protein was detected in mutant chondrocytes. The lack of full-length *NEMO* mRNA might lead to misfolding of protein structure or formation of aggregates known as inclusion bodies.

4.1.2. Activation of NF- κ B canonical pathway was diminished in *NEMO^{fl/Y}Col2a1Cre* chondrocytes

To examine the activation of NF- κ B was diminished in NEMO-deficient chondrocytes, NF- κ B reporter assay was applied to monitor the activity of NF κ B-regulated signal transduction pathways. The pro-inflammatory cytokines interleukin-1 (IL-1 β) was known to elevate chondrocyte catabolism and block chondrocyte anabolism partially via through the canonical NF- κ B signaling. IL-1 β was applied to induce NF- κ B activation in wild-type and mutant chondrocytes (Figure 21). In response to IL-1 β , wild-type chondrocytes showed a significantly increase of NF- κ B activation comparing to mutant chondrocytes. Due to the critical role that NEMO played in regulation of NF- κ B canonical activation, we suggested that the canonical signaling of NF- κ B in mutant chondrocytes was successfully blocked. A light NF- κ B activation was detected in mutant chondrocytes toward IL-1 β . It was possibly caused by contamination of normal NEMO-expressed cell types in the population of mutant chondrocytes.

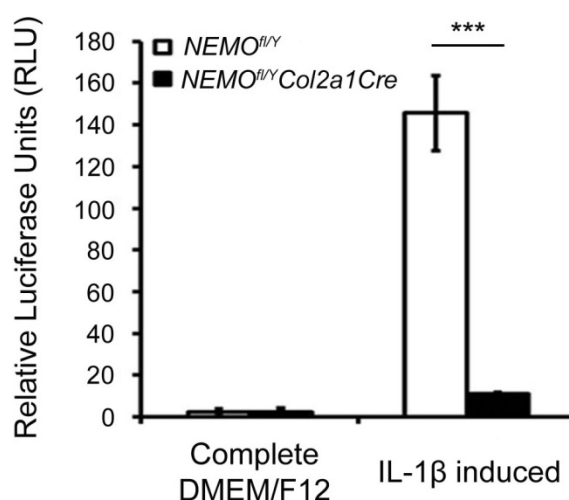


Figure 21: NF- κ B reporter assay of wild-type and mutant chondrocytes. Primary chondrocytes were transiently transfected with NF- κ B-responsive firefly luciferase construct and constitutively expressing *Renilla* luciferase construct (served as internal control for transfection efficiency). 24 hours after transfection, chondrocytes were incubated with complete DMEM/F12 (with 10% FBS and 1% pen/strep mix) or DMEM/F12 with 10ng/ml IL-1 β for 24 hours. Dual Luciferase assay was performed 48 hours after the transfection. By measuring the absorbance using an ELISA reader, promoter activity values are expressed as arbitrary units using a *Renilla* reporter for internal normalization. In response to IL-1 β , activation of NF- κ B arose to 140 folds of RLU compared to non-stimulate states. Owing to the lack of NEMO protein, NF- κ B activation was largely reduced in mutant chondrocytes. As the essential role of NEMO in regulating NF- κ B canonical signaling, we suggested that NF- κ B canonical activation was shot down in mutant chondrocytes. The minor activation of NF- κ B in mutant group was possibly from normally-NEMO-expressing cells in the population. Values were presented as mean \pm SD, ***: $p < 0.001$.

4.1.3. I κ B α sequestered p65 dimers in cytoplasm of *NEMO^{fl/y}Col2a1Cre* chondrocytes

I κ B α was functioned to inhibit the NF- κ B transcription factor. By masking the nuclear localization signals (NLS) of NF- κ B proteins, I κ B α kept NF- κ B homo- or heterodimers sequestered in an inactive state in the cytoplasm (Jacobs and Harrison, 1998). Among NF- κ B activation, I κ B α was phosphorylated and degraded through an ubiquitin-dependent process. Thus, degradation of I κ B α was generally regarded as a marker of NF- κ B canonical pathway activation. To test the phosphorylation of p65 and degradation of I κ B α followed by canonical NF- κ B activation, primary wild-type and mutant chondrocytes were treated with IL-1 and incubated for different time periods (0, 5, 10, 15 and 20 minutes). A rapid phosphorylation of p65 and I κ B α degradation were observed in wild-type chondrocytes upon 5 minutes IL-1 treatment. As we expected, neither phosphorylation of p65 nor degradation of I κ B α was detected in mutant chondrocytes toward IL-1 β stimulation (Figure 22).

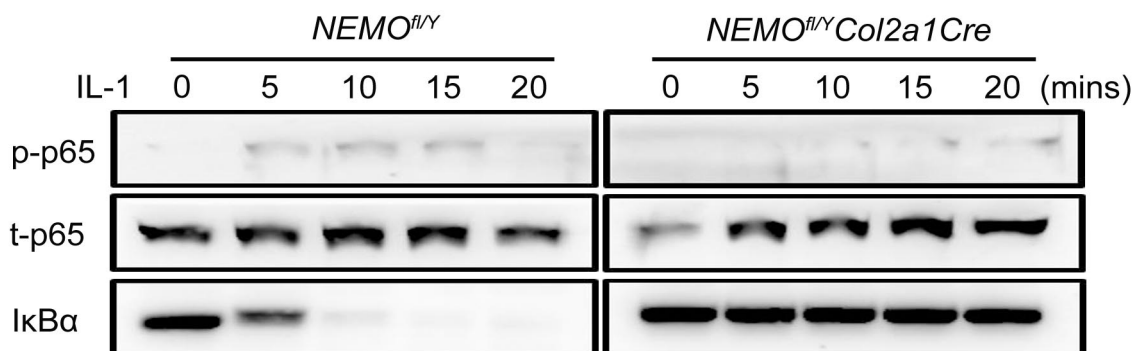


Figure 22: WB of wild-type and mutant chondrocytes in response to IL-1 β induction from different time points. Primary chondrocytes were treated with 10 ng/ml IL-1 β for several time periods (0, 5, 10, 15 and 20 minutes). Degradation of I κ B α was considered as a marker of NF- κ B canonical activation. I κ B α degradation and p65 phosphorylation, which represented activation of NF- κ B canonical pathway, were showed at 5 minutes of IL-1 treatment in wild-type chondrocytes. However, I κ B α degradation and p65 phosphorylation was mostly suppressed in mutant chondrocytes.

4.1.4. p65 in *NEMO^{fl/y}Col2a1Cre* chondrocyte failed to relocate into nucleus

In the activation of NF- κ B canonical pathway, the NF- κ B/Rel complexes were further activated by post-translational modifications (phosphorylation, acetylation, glycosylation) and translocate to the nucleus. Primary wild-type and mutant chondrocytes were treated with or without proinflammatory cytokines TNF- α and IL-1 to induce NF- κ B activation and the following nuclear relocation. The p65 dimers were relocated by its N-terminal nuclear localization signal (NLS) sequence due to the

proinflammatory stimuli (Figure 23, upper). On the contrary to wild-type chondrocytes, p65 in mutant chondrocytes were failed to translocate into nuclei. NF- κ B component p65 was kept inactive, NLS-masked and sequestered in cytoplasm of mutant chondrocytes due to NEMO-deficiency (Figure 23, lower).

p65 immunofluorescence staining

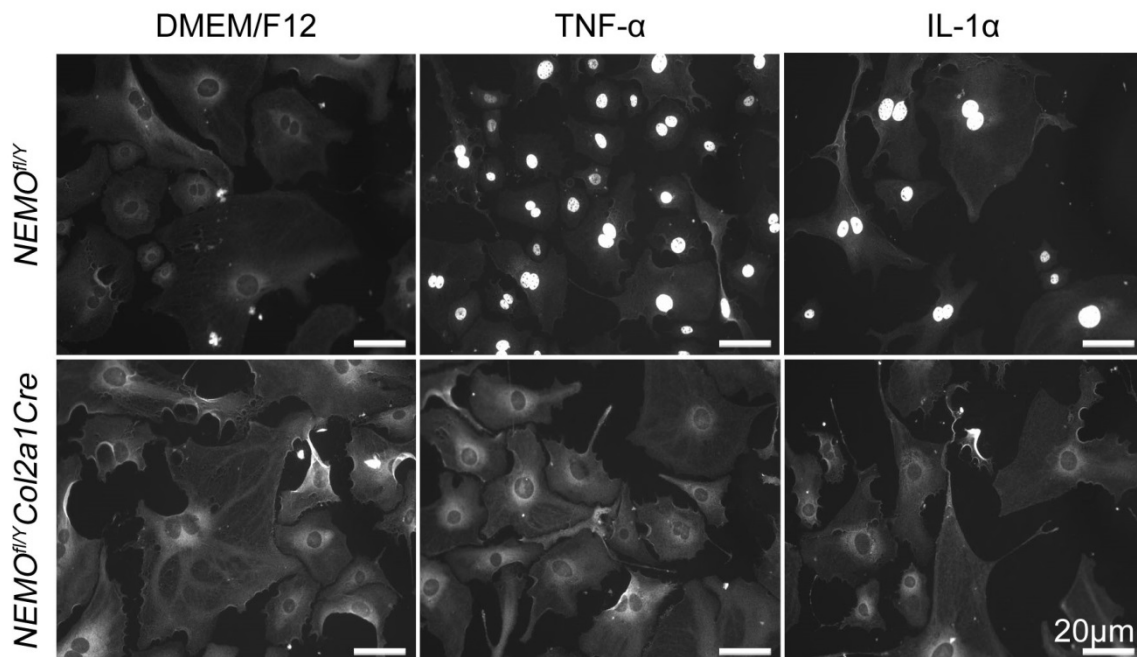


Figure 23: Immunofluorescence staining of p65 in primary chondrocytes. Chondrocytes were pre-treated with TNF- α (20 ng/ml, 10 minutes) or IL-1 (10 ng/ml, 10 minutes) or complete media only. With treatment of TNF- α and IL-1 β shortly before staining, p65 home- or heterodimer complexes were translocated into nucleus of wild-type chondrocytes. The lack of p65 nuclear translocation in mutant chondrocytes was found. The NLS sequence was still remain masked in mutant chondrocytes.

4.1.5. Expression of NEMO was specifically prohibited in cartilage tissue of *NEMO^{fl/y} Col2a1Cre* mice

To clarify NEMO expression *in vivo*, immunofluorescence staining was applied to sections of hindlimb of newborn. Sections of knee joints were processed and stained with NEMO antibody. In wild-type mouse, NEMO expressed widely in muscles and cartilage (Figure 24, upper). No signal of NEMO was observed in sections of mutant knee, whereas other tissue in mutant mouse such as the muscle still expressed NEMO independently of the genotype (Figure 24, lower). Taken together, the NEMO conditional knockout mouse model was therefore successfully established, which characterized by specific prohibition of NF- κ B canonical pathway activation in chondrocytes.

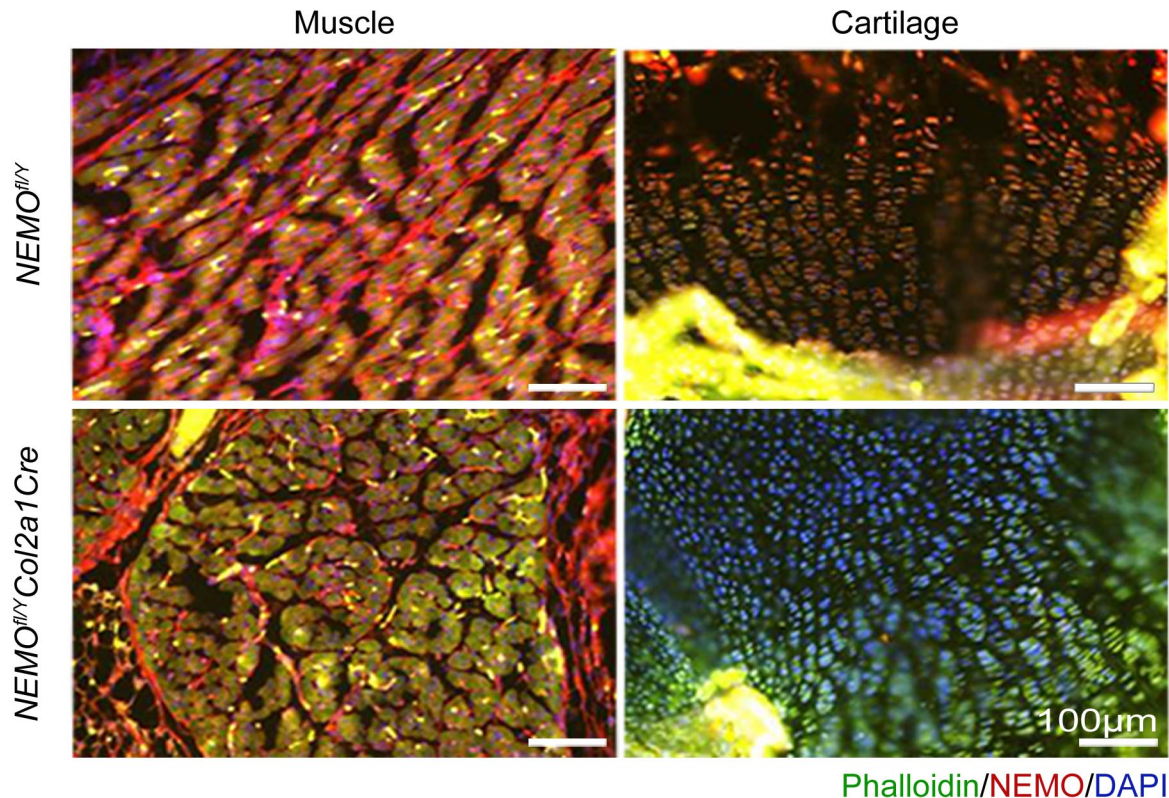


Figure 24: Immunohistochemistry using a NEMO-specific antibody on newborn limb section. NEMO was silenced in cartilage tissue of $NEMO^{fl/y} Col2a1Cre$ mice. Conditional knockout strategy worked successfully in $NEMO^{fl/y} Col2a1Cre$ mice.

4.2. The influence of *NEMO*-deficiency on the skeleton development of the embryonic stage

4.2.1. $NEMO^{fl/y} Col2a1Cre$ mice displayed similar skeleton development at embryonic stage

Cartilaginous tissue development of mouse began approximately from embryonic day 13.5. To determine the role of NF- κ B canonical pathway in development of cartilaginous skeleton, embryos at days 13.5-16.5 and newborns were selected for skeletal staining. All skeletal elements formed normally in $NEMO^{fl/y} Col2a1Cre$ embryos and no obvious difference in the lengths of long bones was found compared with wild-type at these stages (Figure 25, data of E13.5 and E14.5 not shown). Despite of the individual difference between every embryo during embryonic stage, the average size and skeleton were no statistically different. Interestingly, a trend of decreased size showed in neonatal mutants. Although the

explore the influence of NEMO ablation in embryonic skeleton development, ossification region of forelimbs and hindlimbs was carefully measured (Figure 24, lower). Similar to length of long bones, ossified region of long bones in newborn $NEMO^{fl/Y}Col2a1Cre$ mice presented the same pattern, even though there was no difference of ossification region at embryonic stage.

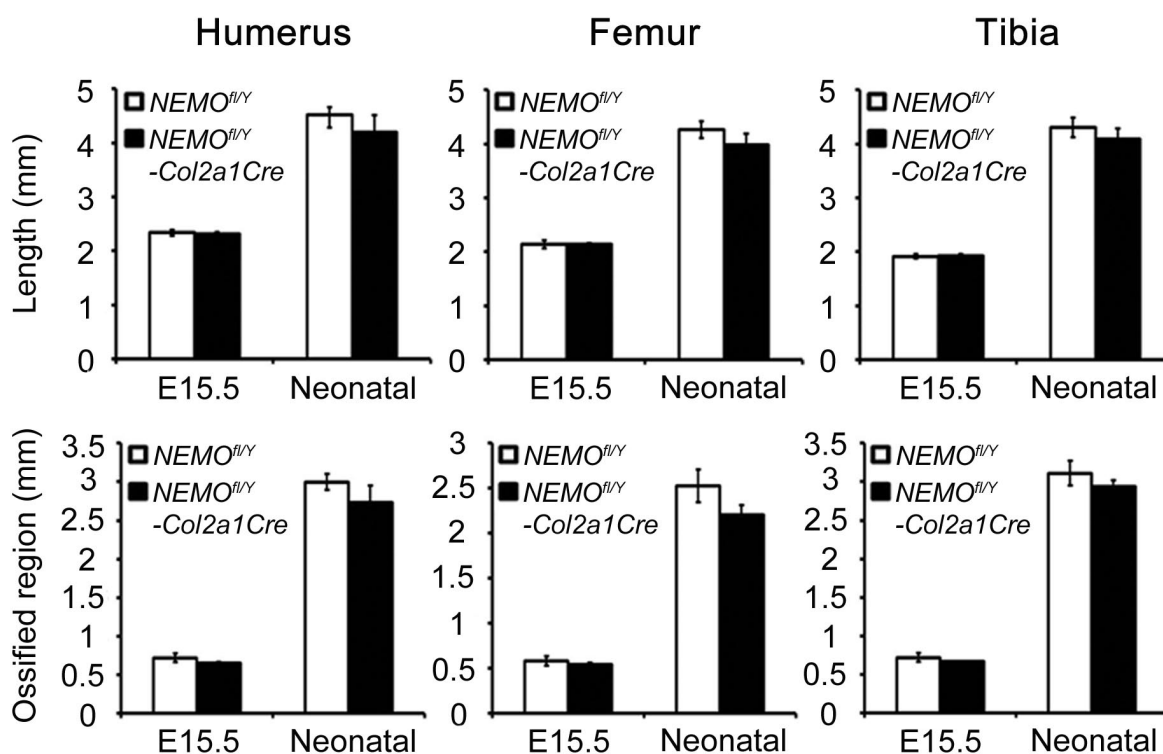


Figure 26: Quantification of length and ossified region of long bones. The length and ossified region from humerus, femur and tibia from E15.5 and neonatal mice were measured. During embryonic development, length of long bones and ossified region from mutants were consistent with wild-type (data of E14.5 and E16.5 not shown). Note the reduced pattern of length and ossified region at newborn stage, length and ossification region of long bones from mutant were slightly shorter compared to wild-type. However, the difference was not significant. Values were presented as mean \pm SD,

4.2.3. Skeleton differentiation in $NEMO^{fl/Y}Col2a1Cre$ mice during embryo stage were fairly the same as wild-type

Due to the important role of NF- κ B pathway in chondrogenic differentiation, markers for osteogenic and chondrogenic differentiation were examined via *in situ* hybridization. Since the phenotype of NEMO-deficiency was likely showed after birth, the riboprobes that specific for cartilaginous markers such as Collagen II (cartilage marker) and X (hypertrophic cartilage marker), for skeletal development markers such as collagen type I (bone marker) were applied to the hindlimb sections of

newborns (Figure 27). Cartilage and bone differentiation markers expressed and distributed correctly in mutant epiphysis of tibia. The expression patterns in both wild-type and mutant was the same. *Col I* was regarded as a bone differentiation marker that predominately expressed in bone tissue. The expression of *Col I* in mutant epiphysis was consistently distributed in bone tissue as wild-type (Figure 27, upper). *Col II* and *Col X* were markers for proliferating and hypertrophic chondrocytes, respectively. The expression and distribution of *Col II* and *Col X* were comparable to wild-type as well (Figure 27, lower).

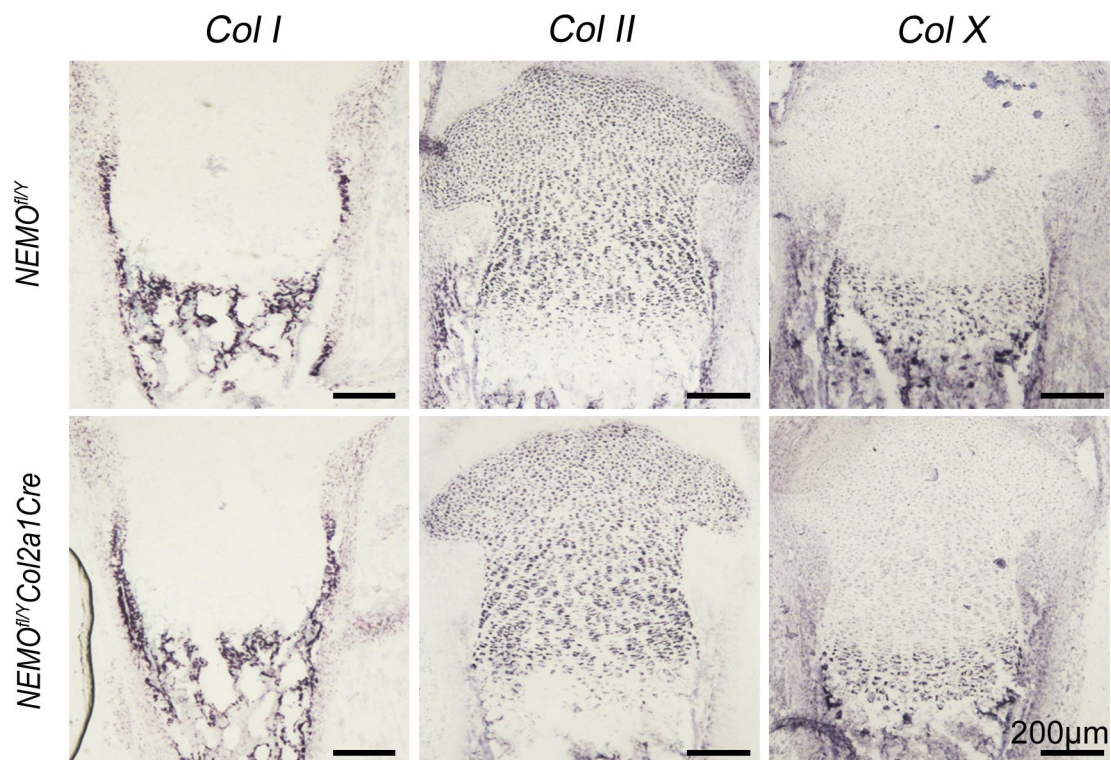


Figure 27: *in situ* hybridization on paraformaldehyde (PFA)-fixed sections of tibia epiphyseal cartilage from new born mice using DIG-labelled riboprobes specific for *Col I*, *Col II* and *Col X*. *Col I*, *Col II* and *Col X* were expressed comparably in wild-type and *NEMO^{fl/Y}Col2a1Cre* mice.

4.2.4. No difference was noticed in long bone morphology and proliferation

To check the morphology of developed long bones, hematoxylin-eosin staining was performed to hindlimb sections of E15.5 and newborn mice (Figure 28). In gross observation of H&E stained sections, *NEMO^{fl/Y}Col2a1Cre* mice displayed normal structure of tibia epiphysis as wild-type. Due to the delayed growth of long bones and endochondral ossification we previously revealed, a BrdU incorporation experiment was performed to clarify the underlying reason that lead to the delay growth and

endochondral ossification (Figure 29). To our expectation, numbers of proliferating cells in tibia epiphysis were comparable during embryonic stage, whereas slightly less proliferation was detected in mutant epiphysis. Nevertheless, proliferation in mutant epiphysis was not significantly reduced as well.

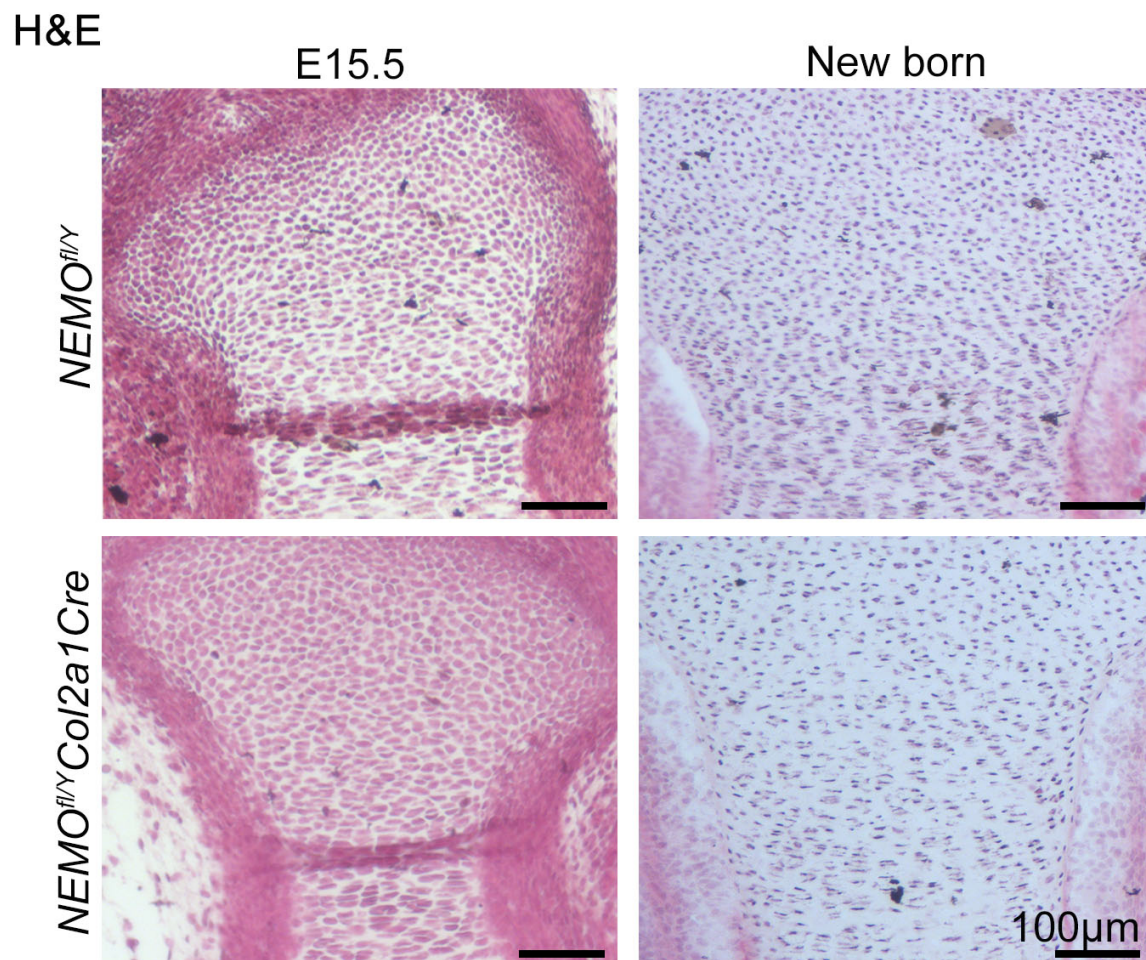


Figure 28: Hematoxylin-Eosin (H&E) staining of tibia epiphysis from E15.5 and newborn mice. Sections of E15.5 and newborn epiphyseal cartilage were processed and stained with H&E. Development and structure of mutant epiphysis at neonatal stage were more or less normal as wild-type.

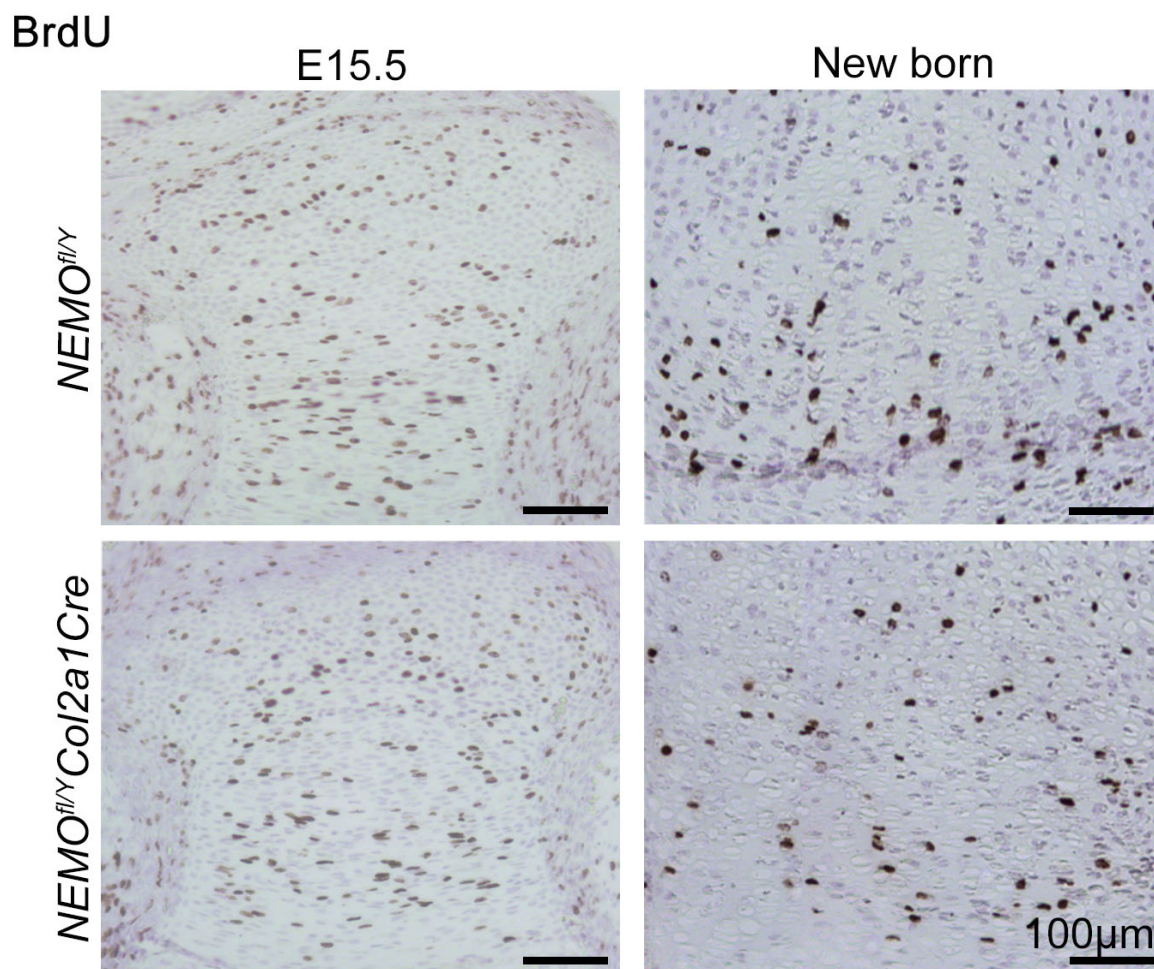


Figure 29: BrdU incorporation assay in tibia epiphysis from E15.5 and newborn stage. Sections of E15.5 and newborn epiphyseal cartilage incorporated with BrdU and stained with anti-BrdU antibody. Proliferating chondrocytes were presented as BrdU-positive cells (brown). The numbers of BrdU-positive cells were comparable to wild-type during embryonic stage. However, reduced proliferating activity was observed in mutant at newborn stage as reduced bone length and ossification we previous found.

4.2.5. Vascular invasion and intramembranous ossification of NEMO-deficient skeleton were comparable to wild-type

At day 14 of embryo development, chondrocytes in the center of the cartilage model mature to hypertrophy. One day later, the hypertrophic cartilage begins to be invaded by sprouting blood vessels, osteoclastic cells, and hematopoietic precursors; in the perichondrium, a bone collar is forming. To examine the impact of NF- κ B canonical pathway in vascular invasion and bone formation, the invading vasculature was examined by histochemical staining for tartrate resistant acid phosphate (TRAP) activity (Figure 30, left). Ossification level was identified by SO-von Kassa staining

(Figure 30, right). The level of vascular invasion and ossification were fairly the same in wild-type and *NEMO^{fl/y}Col2a1Cre* mice.

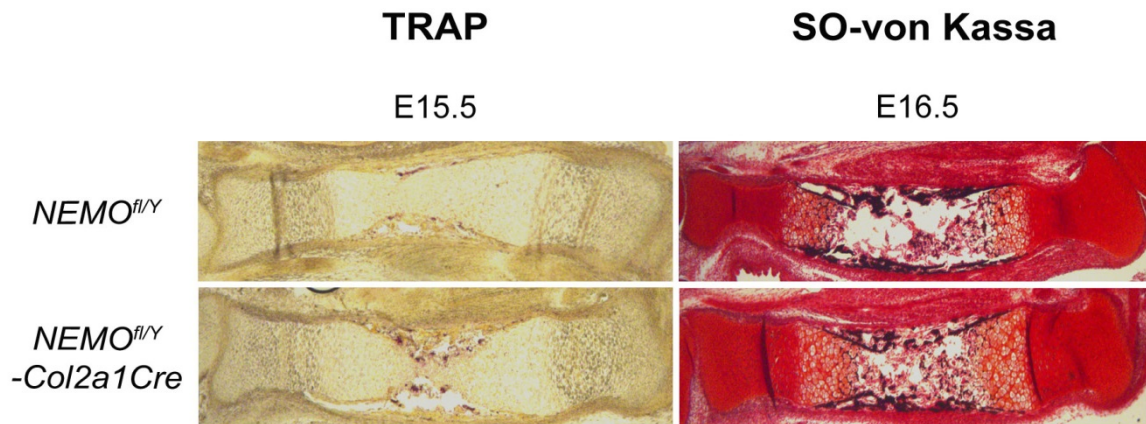


Figure 30: TRAP and SO-von Kassa stained tibia of wild-type and mutant. TRAP staining and SO-von Kassa were performed to PFA-fixed E15.5 and E16.5 sections, respectively. Vascular invasion was showed as purple dots, and ossified matrix was stained as deep purple. The level of vascular invasion and ossified bone in embryonic development were mostly similar between wild-type and mutant.

4.2.6. In cytokine-induced growth, NEMO-deficient metatarsals demonstrated comparable growth pattern as wild-type

To test the response of cytokine-induced growth, the metatarsal culture experiment was performed with cytokines such as BMP-2 and IGF-1 that were known to be partially regulated by NF- κ B canonical pathway and play important role in skeleton development (Wu et al., 2008; Wu et al., 2011). The metatarsals were cultured for 5 days with BMP-2 or IGF-1 or BGjb media only (Figure 31A). The growth of metatarsal rudiments was not altered in *NEMO^{fl/y}Col2a1Cre* mice upon BMP-2 or IGF-1 stimulation. Quantified charts confirmed again that there was no significant change of metatarsal growth between wild-type and mutant (Figure 31B).

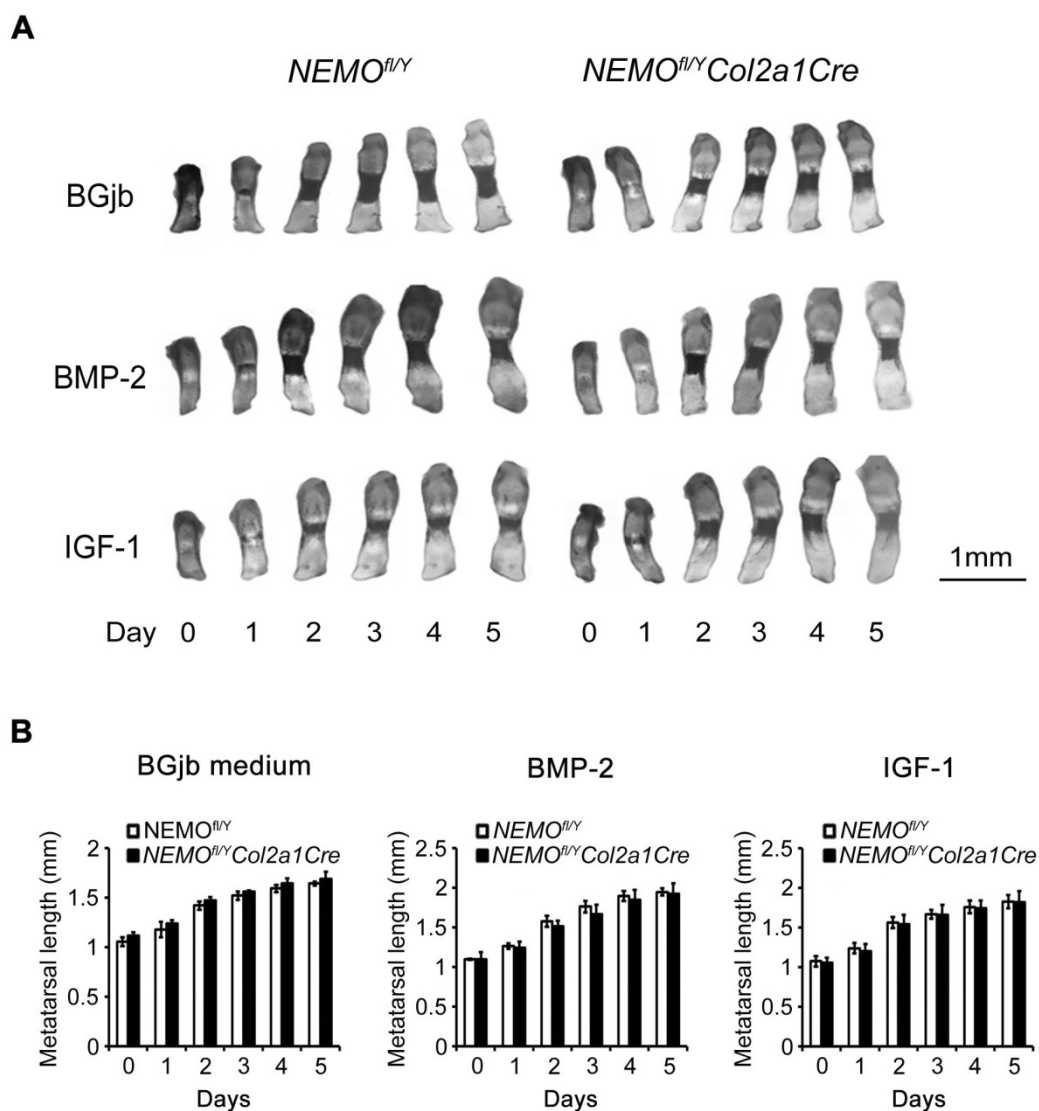


Figure 31: Cytokines induced metatarsal growth. (A) Metatarsals isolated from E15.5 embryo were incubated with BGjb or BMP-2 or IGF-1 for 5 days. The second, third and fourth metatarsal bone rudiments were selected for this experiments. The growth of mutant metatarsal rudiments in BMP-2 and IGF-1 groups was comparable to wild-type. (B) Quantification of metatarsal length confirmed again that cytokine-induced metatarsal growth was comparable between wild-type and mutant.

The impact of NF- κ B canonical pathway to embryonic skeleton development we had studied in various ways such as morphology, length, ossification, vascular invasion, proliferation and cytokine-induced growth. The results indicated that *NEMO*-deficient mutants were with normal skeleton development during embryonic stage. We suggested that NF- κ B canonical pathway was likely optional for skeletal development in embryo stage.

4.3. The impact of NEMO-deficiency to skeleton development at postnatal stage

4.3.1. Post-natal skeletal phenotype of $NEMO^{fl/Y} Col2a1Cre$ mice

To investigate the phenotype of NEMO-deficiency after birth, 2-, 4-week-old and 1-year-old $NEMO^{fl/Y} Col2a1Cre$ mice were collected and compared morphological and skeletal differences. A moderate postnatal dwarfism was showed in $NEMO^{fl/Y} Col2a1Cre$ mice that appeared to be a lifelong defect (Figure 32 left). To understand the impact of NEMO-deficiency in $NEMO^{fl/Y} Col2a1Cre$ mice at post-natal stage, totally skeletons were took as X-ray pictures. Proportionally smaller of skeleton was found in $NEMO^{fl/Y} Col2a1Cre$ mice, whereas all skeleton elements were apparently normal as wild-type (Figure 32, right).

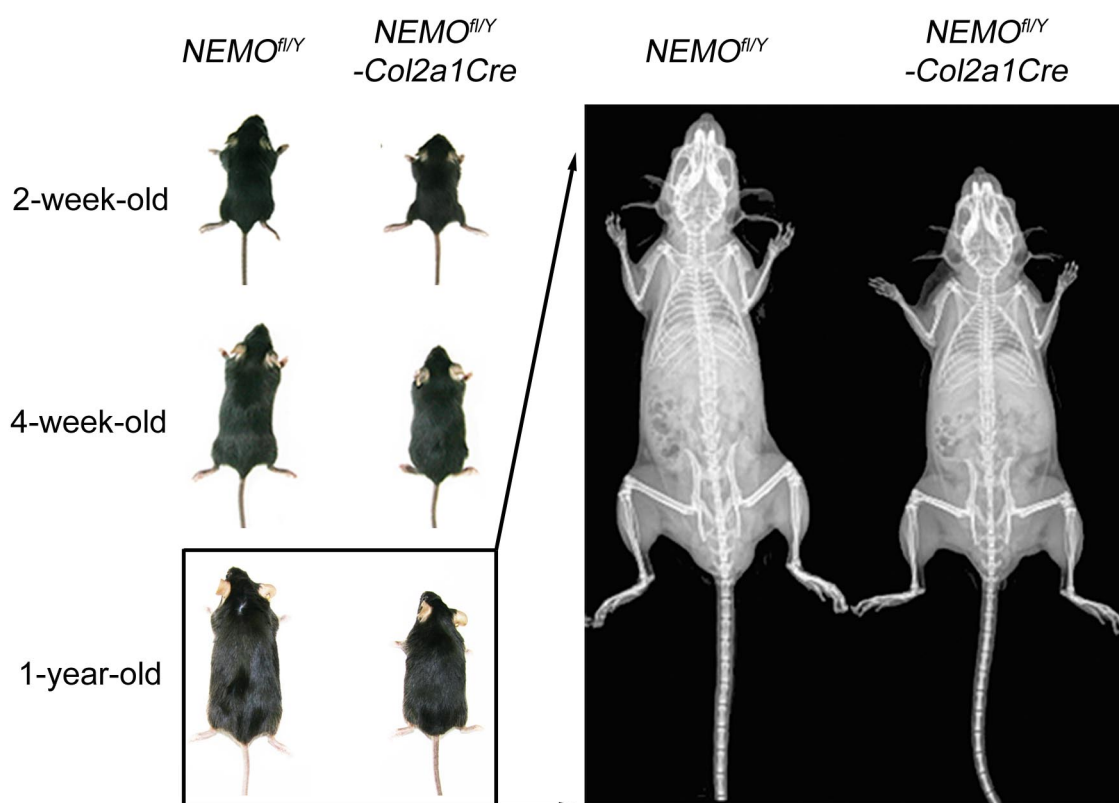


Figure 32: Gross analysis of 2-week-, 4-week- and 1-year-old mice. $NEMO^{fl/Y} Col2a1Cre$ mice displayed dwarfism from age of 2 weeks, 4 weeks and 1 year (left). We suggested that the phenotype of NEMO-deficiency was lifelong that did not catch up. The x-ray picture at age of 1 year showed the proportional reduction of skeleton in mutant mice (right).

4.3.2. Length of NEMO-deficient long bones was significantly shorten

As we found in fig. 30 that proportional smaller skeleton in *NEMO^{fl/Y}Col2a1Cre* mice, length of long bones was then measured. Neonatal, 2-, 4-week-old and 1-year-old mice were selected to measure body weight, length of humerus, femur and tibia (Figure 33). Due to *NEMO^{fl/Y}Col2a1Cre* mice with integrally smaller skeleton, the average body weight of mutant was smaller as expected (Figure 33, left upper). The long bones of *NEMO^{fl/Y}Col2a1Cre* mice such as humerus, femur and tibia were averagely 2-3 mm shorter than wild-type (Figure 33A, B and C). Consistent with the previous results, it was confirmed that ablation of NEMO specifically in chondrocytes resulted in the delayed growth of long bone after birth. We suggested that delay growth of long bones in mutant might be due to impaired secondary endochondral ossification that began at perinatal stage, which was responsible for the following skeleton growth.

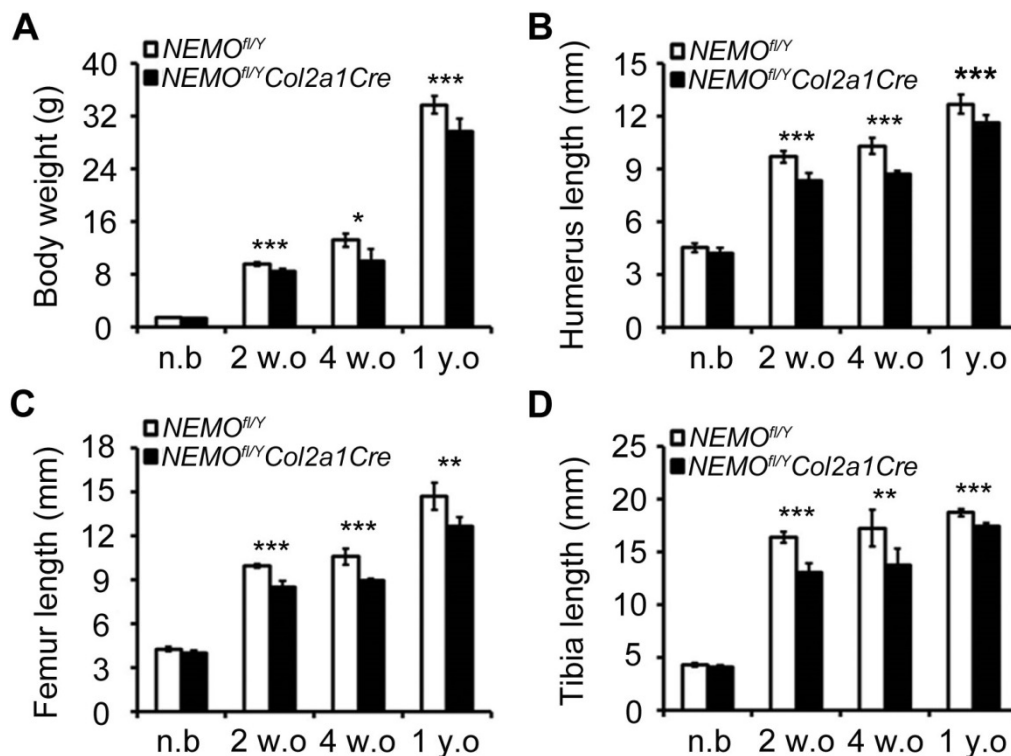


Figure 33: Measurement of body weight and long bone length of wild-type and *NEMO^{fl/Y}Col2a1Cre* mice. (A) The body weight of mutant was significantly smaller that was not surprised since *NEMO^{fl/Y}Col2a1Cre* mice were bearing proportional smaller skeleton. The measurement of long bones such as humerus (B), femur (C) and tibia (D) from *NEMO^{fl/Y}Col2a1Cre* mice was further confirmed that defect of NEMO ablation showed after birth. Averagely, length of humerus, tibia and femur were 2-3 mm shorter compared to wild-type. Values were presented as mean±SD, **: $p < 0.01$, ***: $p < 0.001$.

4.3.3. Metaphysis of NEMO-deficient long bone was characterized with shorten growth plate

The secondary endochondral ossification was essential for skeleton growth during the postnatal and adolescent years. In long bones, the secondary ossification appeared in the epiphysis. The epiphyseal plates (known as growth plate) continuously generated more chondrocytes through mitosis and increase the length of long bones. To know the impact of NEMO deficiency in growth plate, growth plate morphometric analysis was performed at 2 and 4 weeks of age. Total growth plate (TGP) was divided into resting zone (RZ), proliferating zone (PZ) and hypertrophic zone (HZ). Hematoxylin and eosin (HE)-stained sections through the tibiae revealed significantly shortened TGP, RZ+PZ and HZ in mutant growth plates at age of 2 weeks (Figure 34A). At age of 4 weeks, we observed no statistically significant differences in zone lengths between wild-type and *NEMO^{fl/y}Col2a1Cre* mice. Results were further confirmed with quantified measurements of TGP, RZ+PZ and HZ (Figure 34B). At age of 2 weeks, the average length of wild-type total growth plates was approximately 600µm (resting+proliferating zone and hypertrophic zone were 350 and 250µm, respectively). Length of total Growth plate of *NEMO^{fl/y}Col2a1Cre* was 400µm (RZ+PZ and HZ were about 250 and 150µm, respectively). The shorten PZ and HZ in mutant growth plate implied that proliferation of chondrocytes was likely affected. However, no statistically significant differences in zone lengths between wild-type and mutants at 4 weeks of age were found. However, phenomenon of shorten growth plate at age of 2 weeks provided a hint that likely the proliferation of mutant chondrocytes was altered due to ablation of NF-κB canonical pathway.

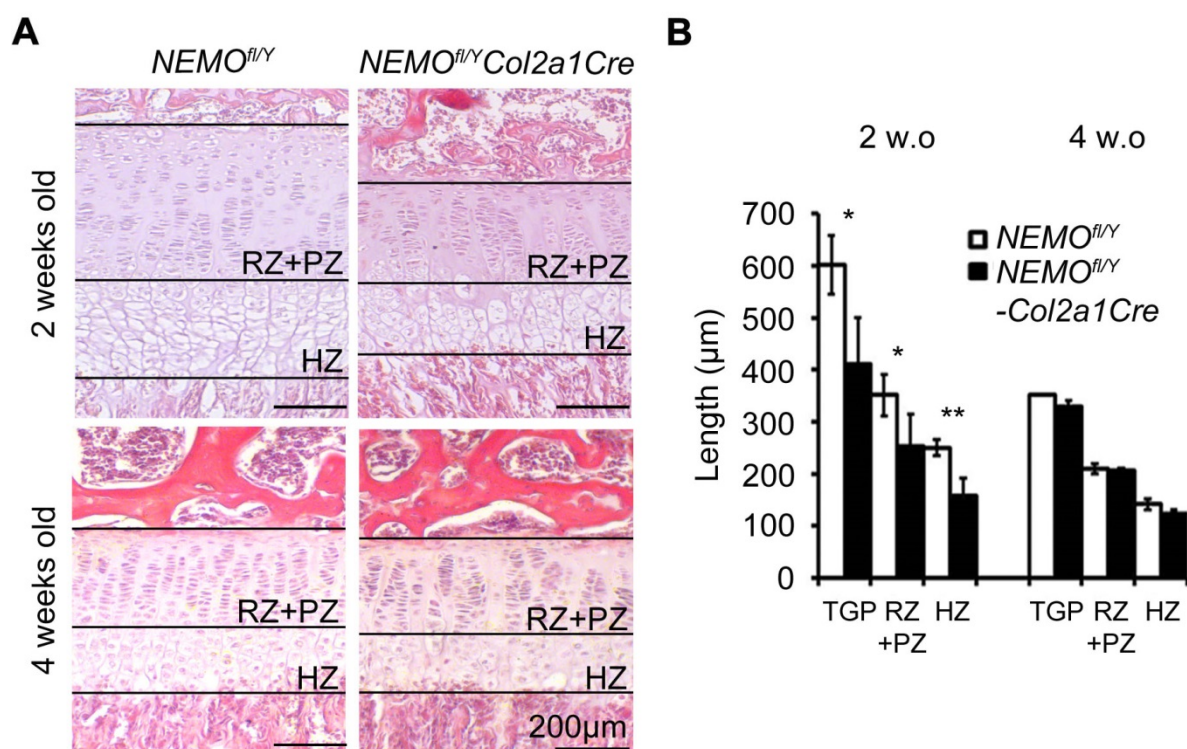


Figure 34: Growth plate morphometric analysis of 2- and 4-week-old mice. (A) Analysis of cartilage development on H&E-stained sections through the tibia in 2 weeks and 4 weeks old mice. The TGP was consisted of RZ+PZ and HZ. (B) Quantified chart showed that the structure and the length of growth plate zones were significantly shorten in *NEMO^{fl/y} Col2a1Cre* mice (TGP, total growth plate; RZ, resting zone; PZ, proliferative zone; HZ, hypertrophic zone). Values were presented as mean \pm SD, *: $p < 0.05$, **: $p < 0.01$.

4.3.4. NEMO-deficient chondrocytes displayed reduced proliferation activity

As previous showed *NEMO^{fl/y} Col2a1Cre* mice were characterized with proportional smaller skeleton. We suggested that proliferation of chondrocytes were likely altered. To test this hypothesis, BrdU incorporation assay was applied to identify chondrocytes in the S phase of the cell cycle in 2 and 4-week-old growth plate sections. Interestingly, at age of 2 and 4 weeks, proliferation activity of mutant chondrocytes was decreased compare to wild-type chondrocytes (Figure 35A). In proliferating zone of growth plate, approximately 25% and 22% of wild-type chondrocytes were actively proliferating at age of 2 and 4 weeks, respectively. Whereas, there were 18% and 7% of NEMO-deficient chondrocytes were BrdU positive at age of 2 and 4 weeks, respectively (Figure 35B). To further confirm the decrease of proliferation, a BrdU ELISA assay was performed in primary chondrocytes (Figure 35C). As expected, proliferation of primary mutant chondrocytes was significantly reduced compared to wild-type. Thereby, impaired

proliferation in mutant chondrocytes was confirmed both *in vivo* and *in vitro*. Our preliminary PCR results showed that blockade of NF- κ B canonical pathway might result in up-regulation of p16 mRNA, cyclin-dependent kinase inhibitor 2A, which prohibited cells entering S phase (Figure 33D).

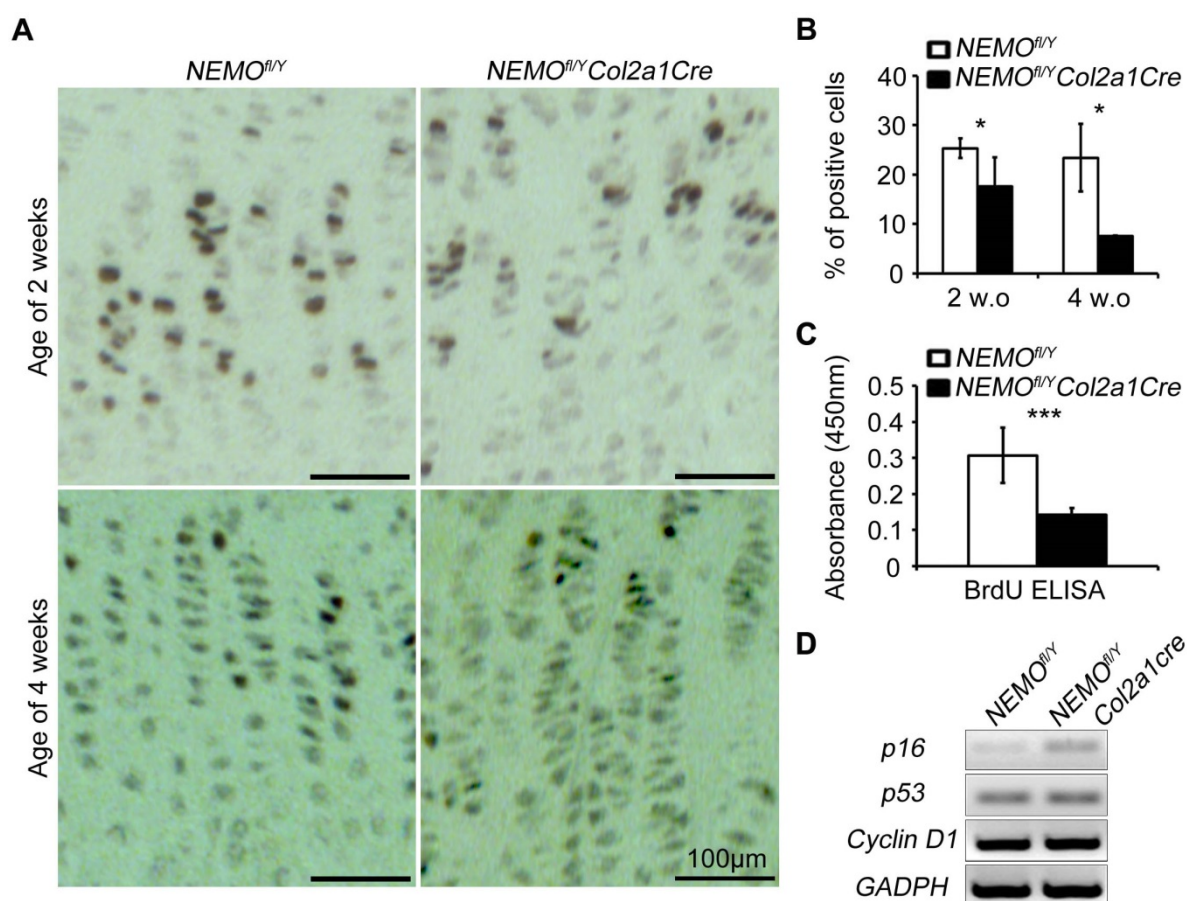


Figure 35: BrdU incorporation assay of PFA-fixed sections from mice knee joint. (A) Under microscope, there were less BrdU-positive cells in growth plate of *NEMO^{fl/y}Col2a1Cre* mice at age of 2 and 4 weeks. (B) Quantified results from A. (C) BrdU ELISA assay was performed to primary chondrocytes. Reduced proliferation of NEMO-deficient chondrocytes was confirmed both *in vivo* and *in vitro*. Values were presented as mean \pm SD, *: $p < 0.05$, **: $p < 0.01$, ***: $p < 0.001$. (D) RT-PCR showed the increased level of p16 mRNA in *NEMO^{fl/y}-Col2a1Cre* chondrocytes.

4.3.5. Apoptotic cells were found in NEMO-deficient growth plate

As previously mentioned that *p65-* or *NEMO-null* mice displayed early embryonic lethality coupling with liver degeneration and enhanced apoptosis. Blockade of NF- κ B canonical pathway might lead to apoptosis of chondrocyte as well. To examine this, TUNEL assay was performed to sections of tibia at age 2- and 4-week-old. Apoptotic cells were found in sections of the growth plate from *NEMO^{fl/y}Col2a1Cre* mice at age of 2 and 4 weeks (Figure 36, arrows). Instead of

massive apoptosis, apoptotic cells in mutant growth plate were showed sporadically. It implied that mutant chondrocytes were more sensitive to apoptosis compared to wild-type. There was no apoptotic cell found in growth plate of wild-type mice.

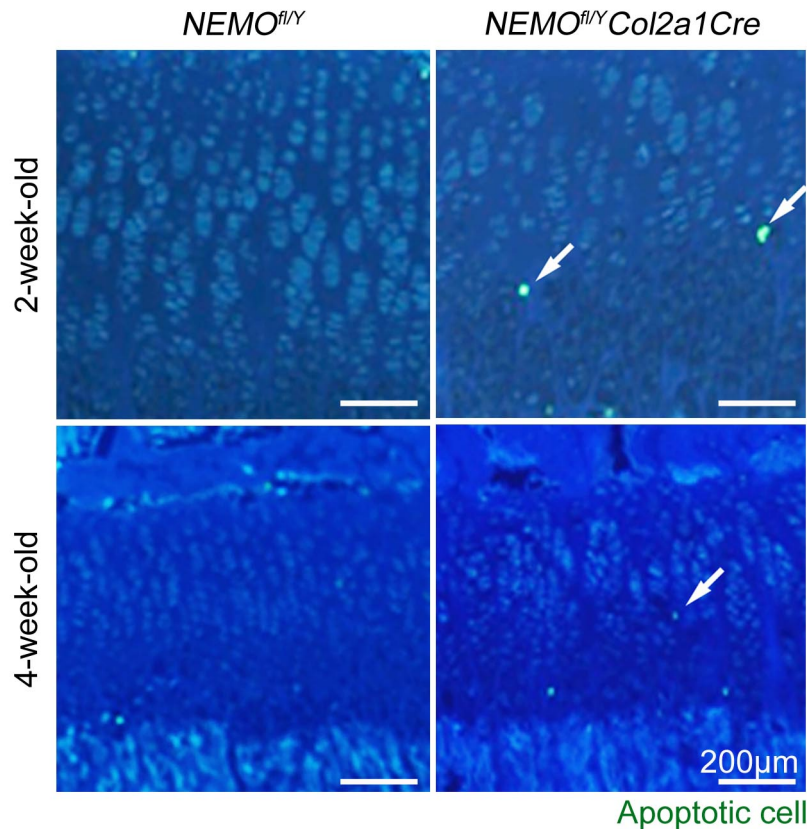


Figure 36: Apoptosis assay in tibia sections of wild-type and mutant. TUNEL assay was performed to sections of 2- and 4-week-old tibia. Notice that apoptotic cell (white arrow) appeared in growth plate of $NEMO^{fl/y} Col2a1Cre$ mice.

4.3.6. In proinflammatory cytokine induced apoptosis, primary *NEMO*-deficient chondrocytes were more sensitive to $TNF-\alpha$ -induced apoptosis

To further confirm this finding, primary chondrocytes were isolated and treated with $TNF-\alpha$ as reported that proinflammatory cytokines could effectively trigger cell apoptosis. Massive apoptosis was showed in wild-type chondrocytes as we expected (Figure 37, left lower). Abundant annexinV and ethidium homodimer signals represented late stage of apoptosis. Signal of ethidium homodimers was predominantly showed in mutant chondrocytes treated with $TNF-\alpha$, whereas very few annexinV was detected. It seemed that apoptosis was triggered in most of *NEMO*-deficient chondrocytes in response to $TNF-\alpha$ prior to wild-type chondrocytes (Figure

37, right lower). It was also possible that NEMO-deficient chondrocytes underwent necrosis.

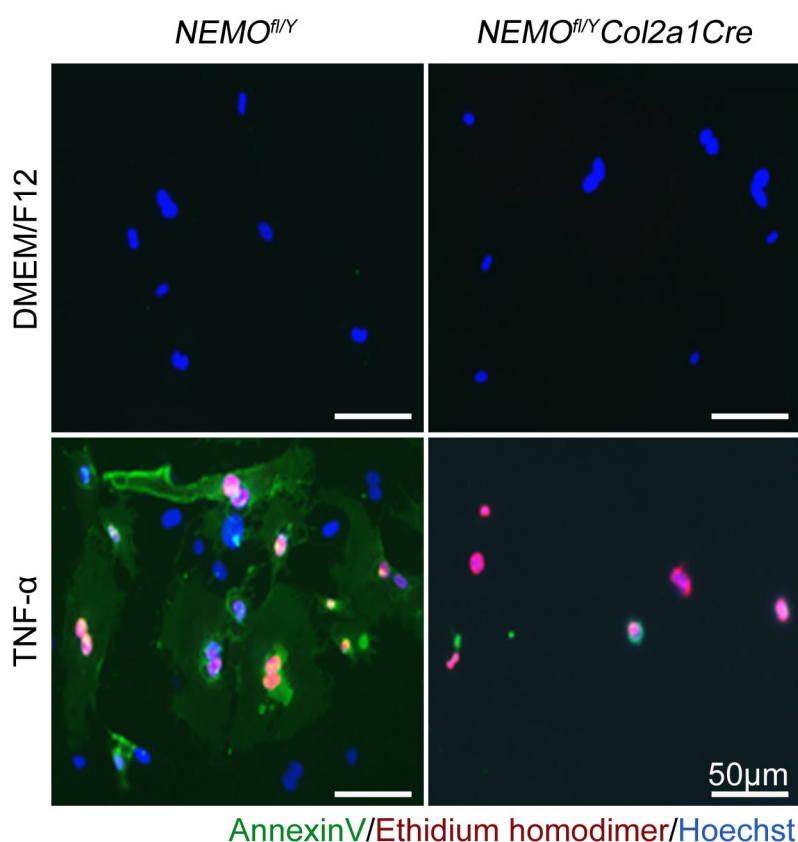


Figure 37: Health/apoptotic/necrotic cells assay in primary chondrocytes with or without pro-inflammatory cytokine stimulation. In response to TNF- α , wild-type chondrocytes displayed massive apoptosis. Further stage of apoptosis was mutant chondrocytes, which implied that apoptosis occurred prior than wild-type. 10 ng/ml TNF- α was 24 hours pre-treated before assay, cells with annexinV (green) and ethidium homodimer (pink) were in late stage of apoptosis. Cells with only ethidium homodimer were likely at the end stage of apoptosis or necrosis.

4.3.7. Disoriented columns in proliferating zone of *NEMO^{fl/Y} Col2a1Cre* mice

In low magnification, fat, oval-shaped columns were found in the mutant growth plate as fig. 32 showed. To study this interesting phenomenon, high magnification pictures were taken for further analysis. It seemed that the PZ of mutant GP was composed of round-shaped proliferating columns whereas linear-shaped column distributed in wild-type GP, in age of 2 and 4 weeks (Figure 38A). When chondrocytes in growth plate proliferated, divided daughter cells were then soon formed a linear-shaped column by compression of surrounding ECM and its own migration ability. The disoriented columns indicated a possibility that migration ability of chondrocyte or ECM stiffness was altered in *NEMO^{fl/Y} Col2a1Cre* mice. To

understand whether cell number within column affected shape of columns, analysis to cell number within each column was performed. Interestingly, mutant at age of 2 weeks, a 20% increase in 16-20 cells subset was found that represent 20% of total columns were consisted of 16-20 chondrocytes (Figure 38B). The formation of disoriented columns in mutant was likely because of over-averaged chondrocytes in a mutant column. At age of 4 weeks, mutant columns were bearing comparable cells within and displayed twisted shape coupling with column-column fusion.

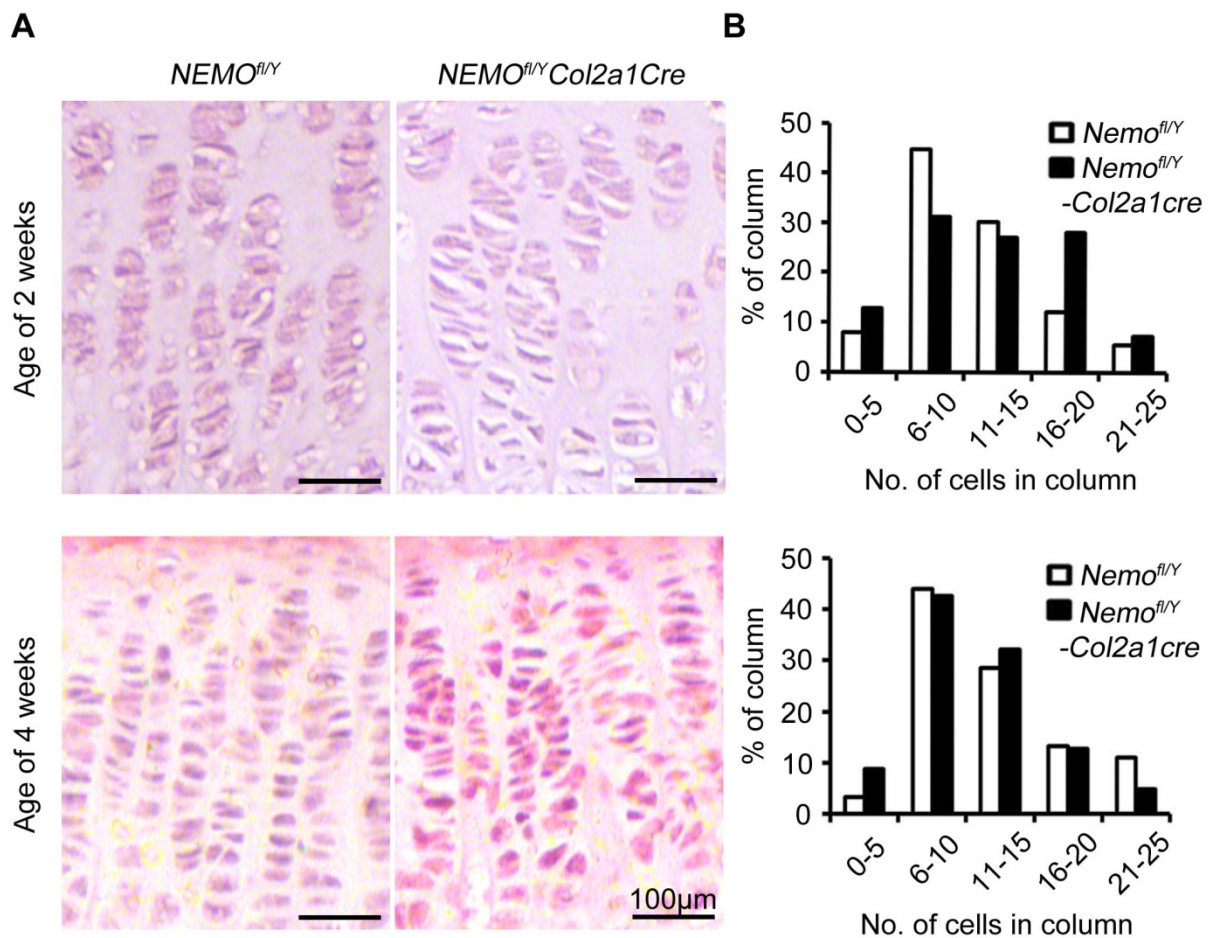


Figure 38: Hematoxylin and eosin (HE) staining of sections of 2- and 4-weeks old growth plate. (A) At high magnification, proliferating columns of mutant were disoriented and formed a fat-oval shape. Under normal circumstance, chondrocytes divided into 2 daughter cells and formed a linear column due to its own migration ability and the compressive stress from surrounded cartilage ECM. The disoriented proliferating columns implied that migration of mutant chondrocytes or stiffness of ECM might be altered. (B) Quantification of cell number in columns. Note a 20% increase of 16-20 subset in mutant columns at age of 2 weeks, which might cause round-shape column formation with 16 to 20 chondrocytes within (upper). Comparable composition of cells in columns was observed in both wild-type and mutant. However, fused and twisted columns were found in mutant growth plate. Abnormal proliferating columns might result in malformation of bone.

4.3.8. Fat-oval-shaped proliferating columns were pronounced in NEMO-deficient growth plate

To further investigate twisted columns in $NEMO^{fl/Y} Col2a1Cre$ mice, we analyzed shape of and horizontal angle of columns. In survey of column shape difference, mutant columns displayed a shifting proportion of horizontal-vertical ratio toward 1 (Figure 39A, upper). In another word, there were more roundish-shaped proliferating columns in mutant growth plate at age of 2 weeks. Similar results were showed in mutant at age of 4 weeks as well (Figure 39A, lower). These disoriented, round-shaped proliferating columns in mutant growth plate might increase the incidence of bone malformation; however, bone malformation was likely imperceptible (no obvious malformation was noticed) and the implication was still remained unclear. As for analysis of horizontal angle of columns, results from wild-type and mutant were fairly comparable (Figure 39B). Most of columns from both groups were more or less perpendicular to the growth plate. These preliminary results indicated $NEMO^{fl/Y} Col2a1Cre$ mice were with more round-shaped columns and more chondrocytes within; however, no bone malformation was observed. More efforts are required to conclude this interesting finding.

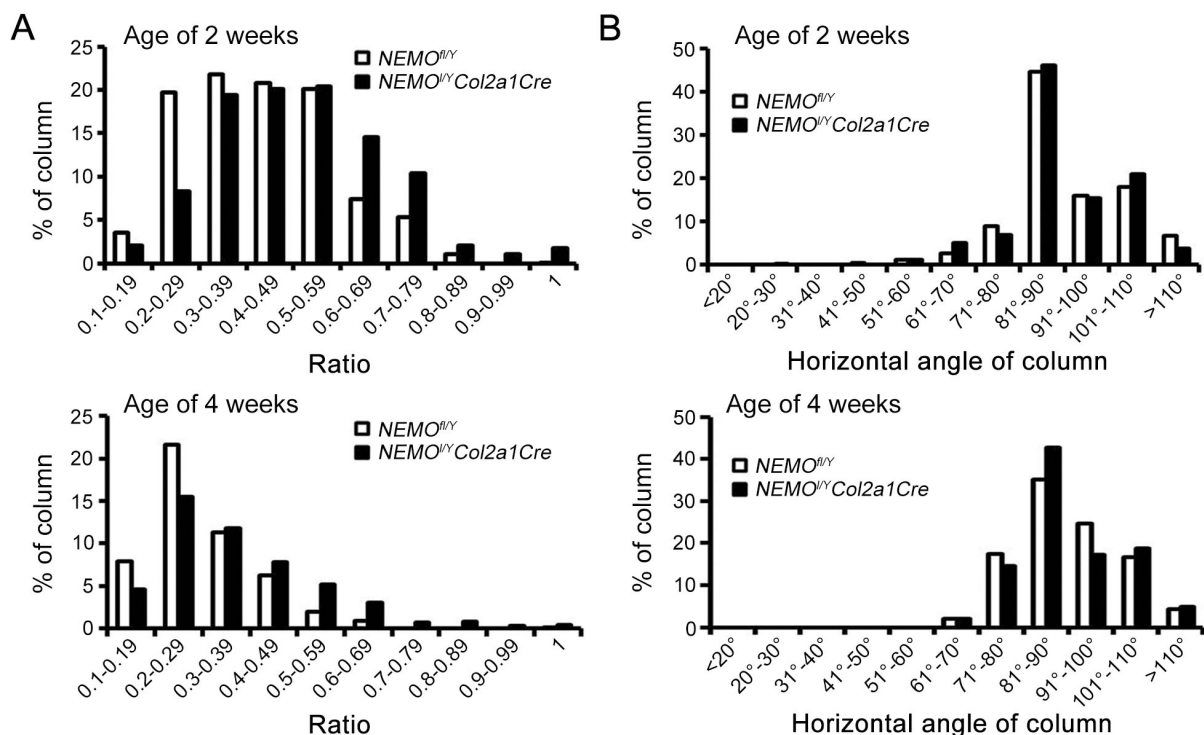


Figure 39: Analysis of proliferating columns in growth plate at age of 2- and 4-week-old mice. (A) Ratio of short-long axis analysis of proliferating columns. At age of 2 weeks, a proportional ratio shift from linear-shaped to round-shaped was observed. Similarly, results of 4-week-old showed the same shifted pattern that indicated mutants were with more round-like columns. (B) Analysis of horizontal angle showed a fairly the same distribution in both wild-type and mutant.

4.3.9. *NEMO*-deficient chondrocytes displayed a reduced migration activity

At metaphyseal side, cartilage cells become aligned into well-defined columns due to compression of matrix and mobility of chondrocytes, known as zone of cellular proliferation (proliferating zone). Failure of these chondrocytes to thrive resulted in abnormal growth of bones. The disoriented columns that we previously discovered indicated a possibility that migration ability of chondrocyte or ECM stiffness was altered in *NEMO^{fl/y}Col2a1Cre* mice. To examine our hypothesis of migration alteration in mutant chondrocytes, migration ability of chondrocytes was tested. A 24-hours random migration assay was performed to check mobility of wild-type and mutant chondrocytes. Wild-type chondrocytes were able to explore averagely 100-200 μm range from origin, whereas the exploring area of mutant chondrocytes was narrowed down to below 100 μm (Figure 40A, left). Quantification of velocity shown mutant chondrocytes were with slower mobility compare to wild-type chondrocytes (Figure 40B, right). Further quantification showed that the average velocity of mutant chondrocytes was 0.2 $\mu\text{m}/\text{min}$, which was half speed of wild-type chondrocytes. Consistent with our hypothesis, migration ability of mutant chondrocytes was impaired.

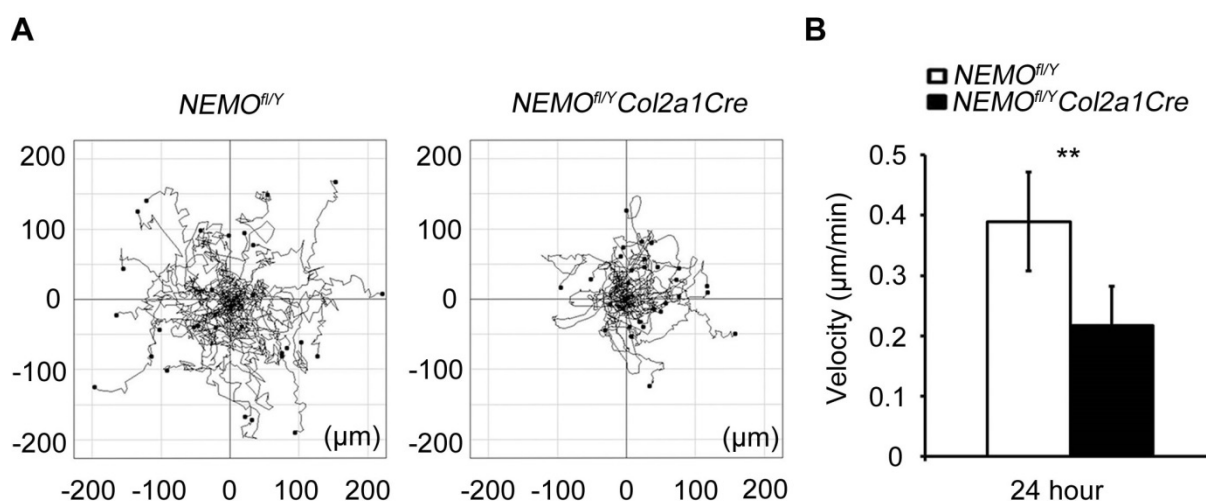


Figure 40: Migration assay of primary chondrocytes. (A) 24-hours random migration assay of chondrocytes. Primary *NEMO^{fl/y}* and *NEMO^{fl/y}Col2a1Cre* chondrocytes from frame by frame analysis of time-lapse was recording during a 20-mins observing period. (B) The migration velocities of the respective cells are indicated (mean \pm SD, **: $p < 0.01$, migration data of over 30 cells). Quantification of cell migration velocity indicated *NEMO^{fl/y}Col2a1Cre* chondrocytes with reduced migration.

4.3.10. *NEMO*-deficient chondrocytes possess higher adhesion to cartilage ECM

Generally, adhesion strength and dynamic could determine migration ability of cells. To clarify whether attachment of mutant chondrocytes to ECM ligands was altered, an adhesion assay was performed. Usual and abundant ECM components such as fibronectin, vitronectin, laminin, collagen I and collagen II were tested. Interestingly, *NEMO*-deficient chondrocytes exhibited higher binding affinity to both cartilaginous (collagen I, fibronectin, laminin) and non-cartilaginous (vitronectin, collagen I) ECM components (Figure 41A). The generally enhanced adhesion of mutant cells to ECM could affect migration ability of mutant chondrocytes, which may involve integrin-associated signaling pathways. In order to test if downstream signaling of integrins was effected by the lack of *NEMO*, primary chondrocytes were analyzed for IL-1-induced activation of mitogen activated protein (MAP) kinases, focal adhesion kinase (FAK) and AKT (or protein kinase B) by western blotting (Figure 41B). Surprisingly, we could not detect any obvious difference in the timely phosphorylation status of FAK, AKT, ERK and p38 between the genotypes implying that integrin-associated signaling cascades are likely not affected in the absence of *NEMO*/canonical NF- κ B pathway in chondrocytes.

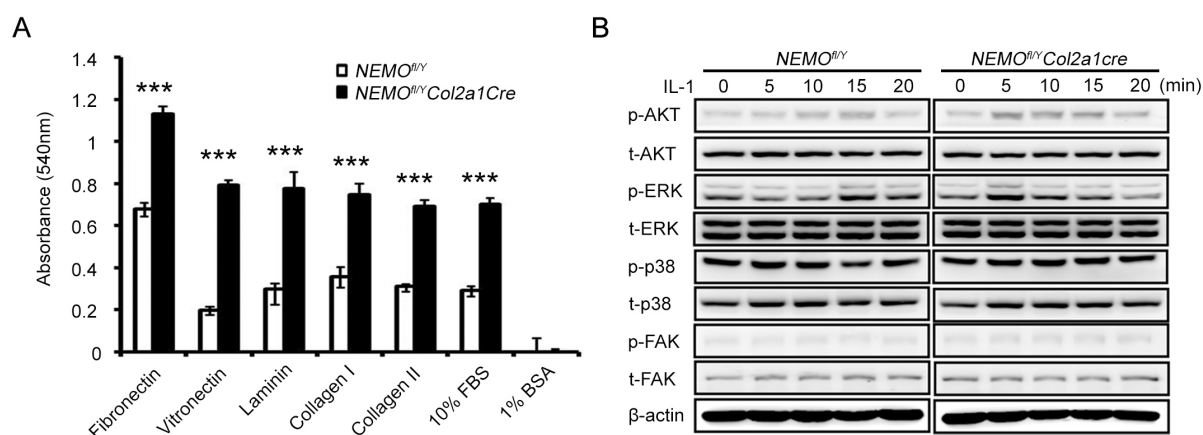


Figure 41: Increased adhesion to ECM ligands is not associated with obvious changes in integrin signaling pathways. (A) Stronger adhesion of *Nemo*-deficient chondrocytes to ECM substrates. Components of ECMs (fibronectin, vitronectin, laminin, collagen I and collagen II) were pre-coated on plastic surface, than wild type and mutant chondrocytes were added and allowed to adhere for one hour. Mutant chondrocytes showed stronger binding affinity than wild type chondrocytes as verified by the increased absorbance at 540 nm after cresyl violet staining. (B) Western blotting of cultured primary chondrocytes with or without IL-1 stimulation shows no significant differences in activation of integrin-linked signaling molecules.

4.3.11. The stiffness of cartilage ECM from *NEMO^{fl/y}Col2a1Cre* mice was fairly the same as wild-type

To verify the last suggestion of possible reasons that resulted in disoriented columns in *NEMO^{fl/y}Col2a1Cre* mice growth plate. The stiffness of ECM in disoriented columns in *NEMO^{fl/y}Col2a1Cre* mice was tested by atomic force microscope (AFM). The vDeflection of wild-type and mutant, which represented the topography of cartilage ECM, were comparable (Figure 42A). The composition of cartilage ECM in *NEMO^{fl/y}Col2a1Cre* mice was fairly comparable to wild-type. The matrix elasticity analysis showed the same cartilage matrix stiffness between wild-type and *NEMO^{fl/y}Col2a1Cre* mice (Figure 42B). The elastic modulus (E) of wild-type and *NEMO^{fl/y}Col2a1Cre* were 49 ± 0.7 kPa and 55.5 ± 1.1 kPa, respectively. The elastic moduli from both were in the range of normal elasticity modulus. Even though the stiffness of mutant cartilage was approximately 5 kPa more than of wild-type, no statistical significance was found.

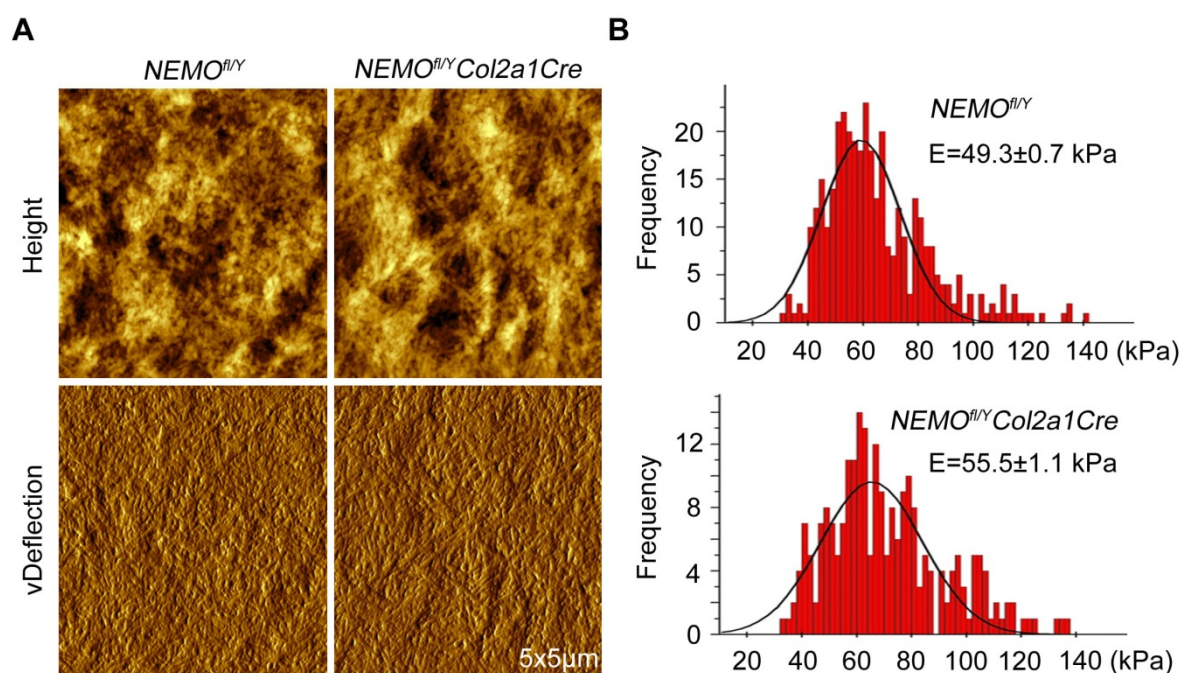


Figure 42: Atomic force microscope (AFM) observed comparable ECM orientation and elasticity. (A) Topology of cartilage ECM surface was presented as height and vDeflection. It showed comparable cartilage ECM surface between wild-type and mutant cartilage. (B) Elastic modulus from both groups was calculated. Similar ECM stiffness was concluded as were 49 ± 0.7 kPa in wild-type and 55.5 ± 1.1 kPa in mutant, respectively. E=elastic modulus (calculation formula not shown).

4.3.12. NEMO-deficient chondrocytes displayed larger spreading area in vitro

During experiment of migration assay, we found that mutant chondrocytes were with larger spreading area (data not show). To confirm this observation, cell-spreading assay was performed. With time after chondrocytes seeding to petri-dish, NEMO-deficient chondrocytes were observed with larger spreading area compared to wild-type chondrocytes (Figure 43A). The average cell spreading area of mutant chondrocytes could reach 6500 μm^2 ; however, the spreading area of wild-type chondrocytes was half of mutant chondrocytes (Figure 43B). The average spreading time was approximately 6.5 hours post seeding, which was comparable between wild-type and NEMO-deficient chondrocytes (Figure 43C). Enlarged cell spreading area might be related to remodeling of actin cytoskeleton or alteration of adhesion molecules. To further investigate the spreading phenotype, we have seeded wild-type and NEMO-deficient chondrocytes on fibronectin-coated glass slides and stained with paxillin to visualize focal adhesion sites, and with phalloidin to detect actin cytoskeletal structures. After 24 hours, we could not observe obvious differences in the appearance and number of focal complexes, and the organization of cytoskeletal elements including actin stress fibers, microfilaments and lamelopodia.

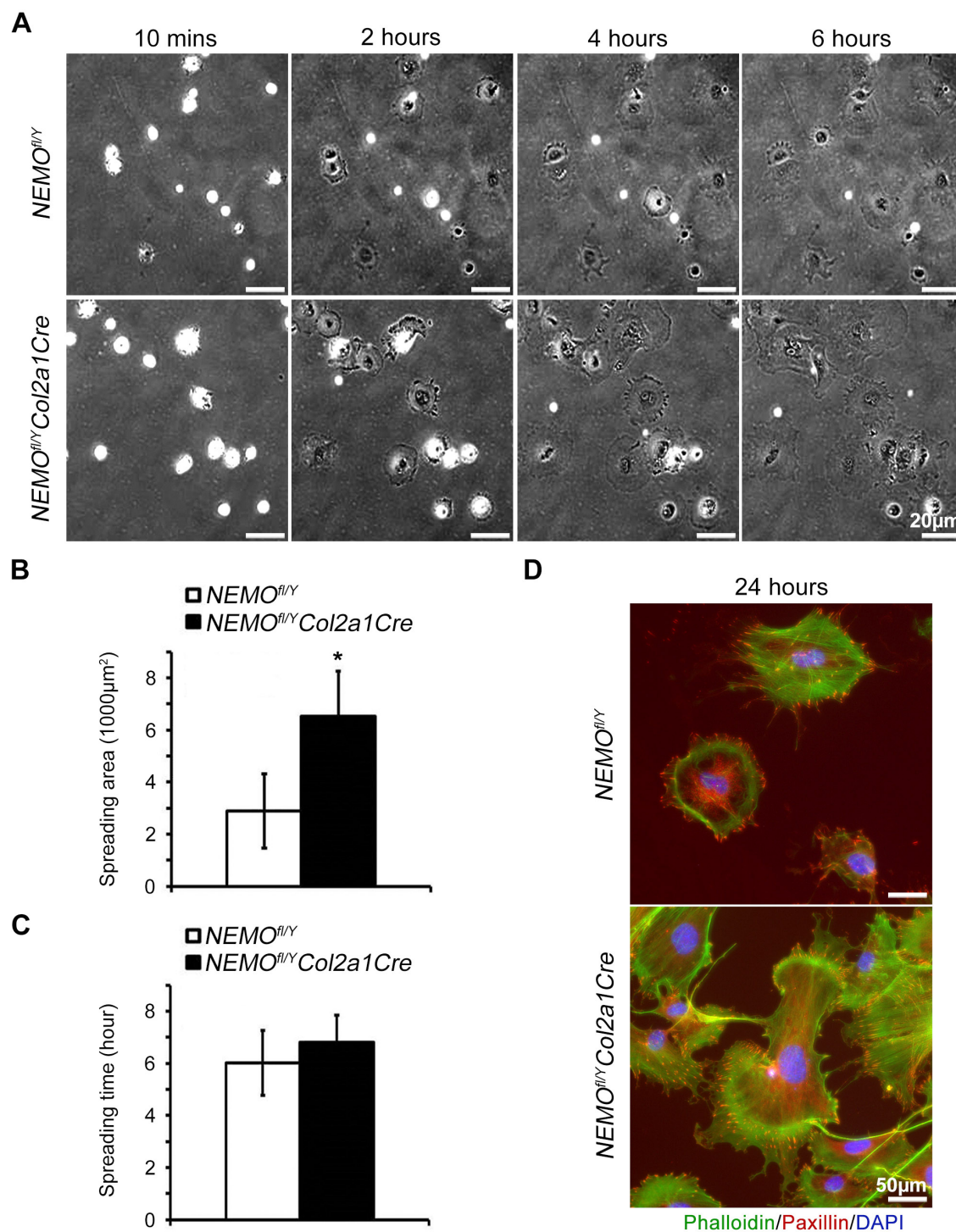
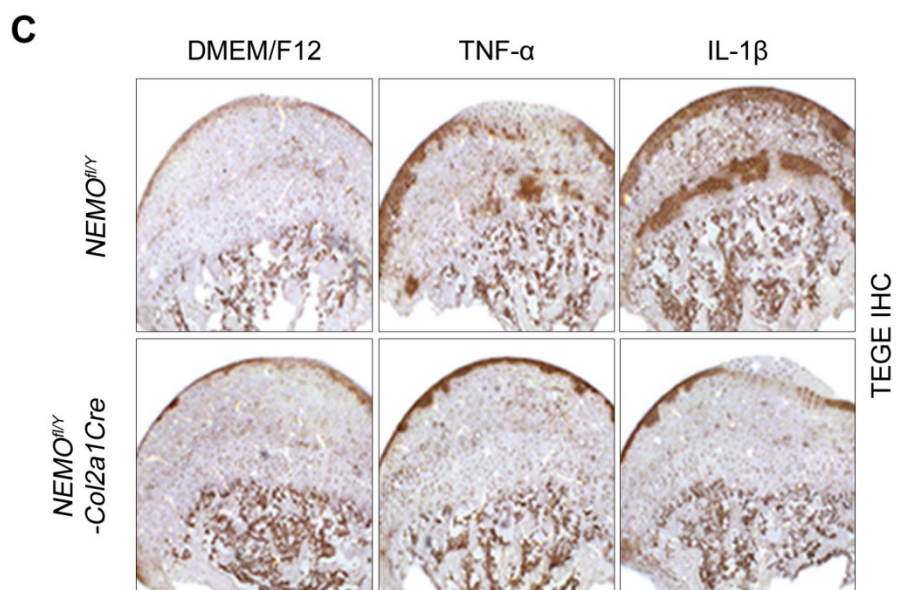
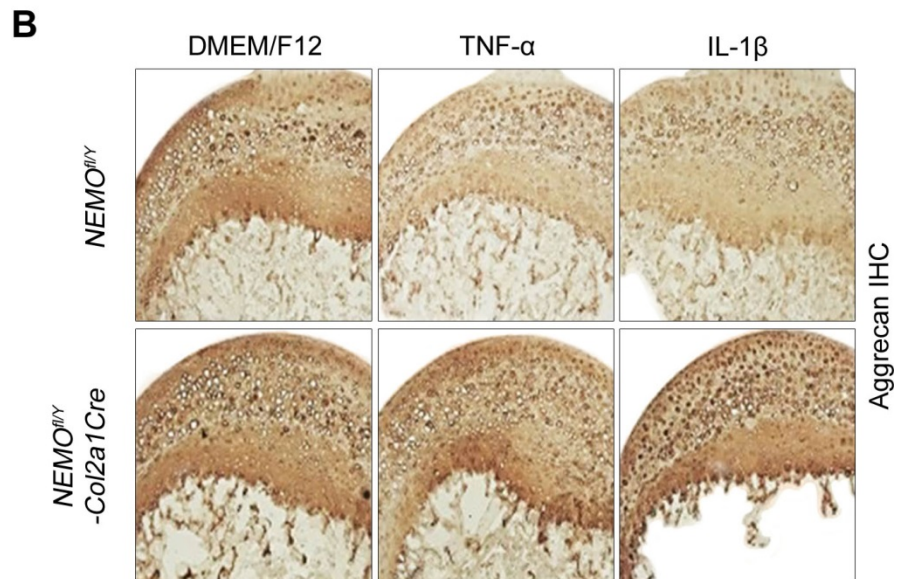
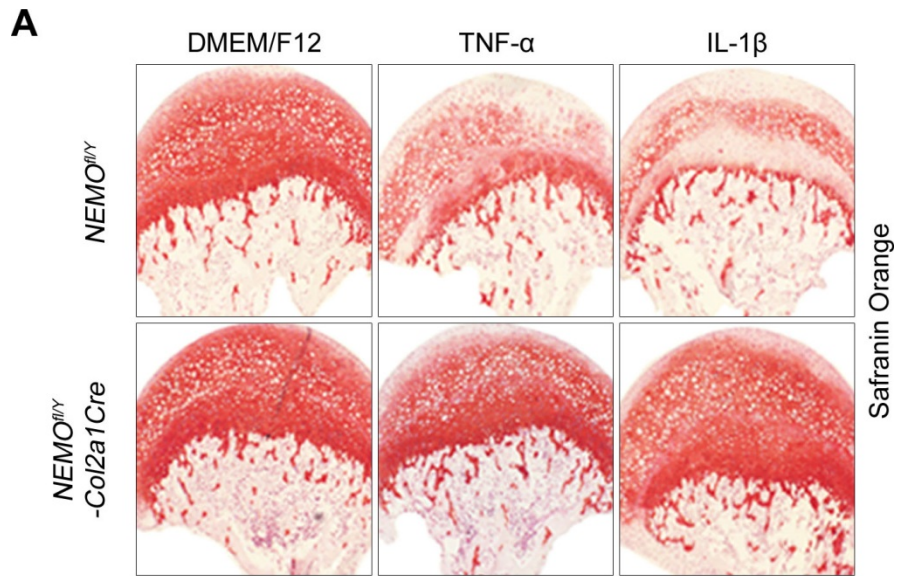


Figure 43: Abnormal spreading behavior of *NEMO^{fl/y} Col2a1cre* chondrocytes. (A) Representative images of time laps recording showing cell spreading through the indicated time points on the plastic surface in the presence of serum. Note that NEMO-deficient chondrocytes spread into larger area than wild-type cells. (B) Quantification of cell spreading area. (C) Quantification of cell spreading time of wild-type and *NEMO^{fl/y} Col2a1Cre* chondrocytes. Average spreading time was comparable between the genotypes. (D) On fibronectin coated glass slide, Nemo-deficient chondrocytes show comparable distribution of focal complexes (demonstrated by paxillin staining) and normal formation of cytoskeletal structures (actin stress fibers, micro-spikes, lamellopodia) compared with wild-type after 24 hours of seeding.

4.4. The role of NF- κ B canonical pathway in cartilage metabolism using hip explant culture

Degradation of proteoglycans and glycosaminoglycans breakdown were partially eased in hip cap of *NEMO^{fl/Y}Col2a1Cre* mice

The proinflammatory cytokines interleukin-1 β (IL-1 β) and tumor necrosis factor α (TNF- α) were known to elevate chondrocyte catabolism and block chondrocyte anabolism partially via through the canonical NF- κ B signaling. To address to role of NF- κ B in cartilage metabolism pathologically, *in vitro* experiments were performed with femoral head cartilage explants isolated from wild type and *NEMO^{fl/Y}Col2a1Cre* mice as described in a previous publication from the Aszodi lab (Raducanu et al., 2009). After 4-days treatment of TNF- α and IL-1 β , the loss of proteoglycans in articular cartilage was observed in wild type femoral head. However, the proteoglycan breakdown in articular cartilage from NEMO-deficient group was largely reduced (Figure 44A and 44B). Signals of aggrecan neoepitope G1-TEGE and VIDIPEN were pronounced at the surface and growth plate of wild-type articular cartilage that indicated where the massive cartilage ECM breakage occurred. As expected, the signals of G1-TEGE and VIDIPEN were much milder in articular cartilage of *NEMO^{fl/Y}Col2a1Cre* mice (Figure 44C and D). Blocking NF- κ B signaling had been merged as very attractive and potential strategy against OA. Our results supported this view as well. However, the experiment time was relatively short compared to spontaneous progression of cartilage ECM breakdown. The protection from blocking NF- κ B canonical signaling might only decelerate progression of ECM breakdown at early stage. More efforts were need to verify the effect of blocking NF- κ B canonical pathway in mid and later stage of cartilage ECM loss.



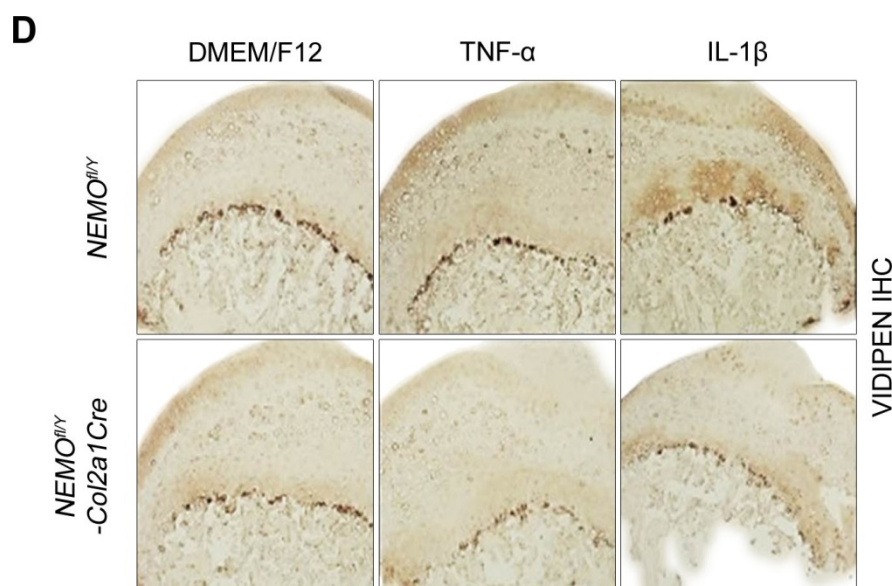


Figure 44: Reduced aggrecanlysis in NEMO-deficient hip explants upon cytokines treatment. Femoral heads were harvested from 4-week-old control and *NEMO^{fl/Y}Col2a1Cre* mice and cultured in serum-free DMEM with or without treatment with TNF- α (100 ng/ml) and IL-1 (10 ng/ml). (A) Safranin orange staining indicated only moderate loss of sulfated GAGs in mutant explants. (B) Immunostaining demonstrates that aggrecan retains in the mutant cartilage matrix after cytokine treatments. (C) Increased protrusion of the ADAMTS4/5-induced aggrecan degradation neopeptide TEGE was observed in control but not in *NEMO^{fl/Y}Col2a1cre* explants. (D) Cytokines treatments increase the exposure of the MMP-induced aggrecan degradation neopeptide VIDIPEN in control but not in of *NEMO^{fl/Y}Col2a1cre* explants.

To determine the glycosaminoglycans (GAG) concentration in media of wild-type and *NEMO*-deficient groups, sulfate GAG (sGAG) assay was performed. In response to TNF- α and IL-1 stimuli, sGAG in media from cartilage of *NEMO*-deficient groups was much less than amount of GAG released into media largely increased in wild-type group (Figure 45). To our expectation, the loss of cartilage ECM triggered by inflammatory cytokines, could be effectively eased by blocking NF- κ B canonical pathway during early stage of inflammation.

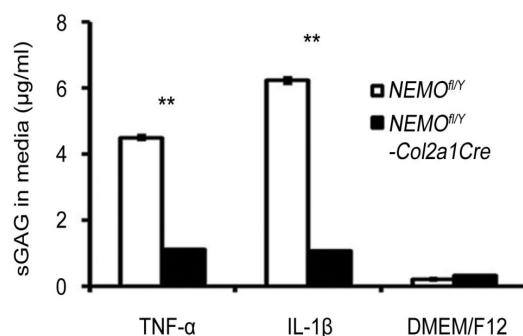
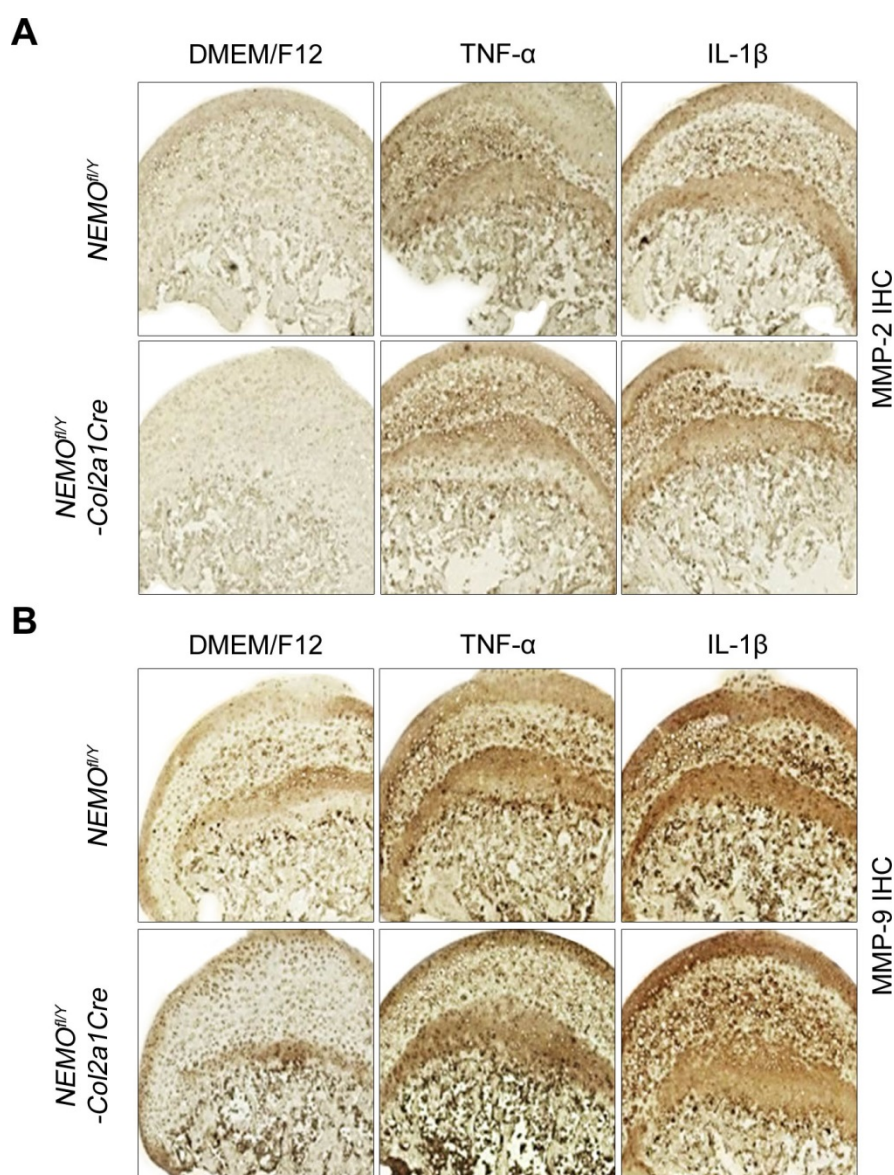


Figure 45: Less soluble GAGs were detected in condition medium of *NEMO^{fl/Y}Col2a1cre* against cytokine-induced proteoglycan degradation. The blockade of NF- κ B canonical pathway could effectively reduce proteoglycan breakdown during early stage of inflammation.

Next, we have investigated the expression and activity of selected matrix metalloproteinases (MMP) using immunohistochemistry and gel zymography. Using antibodies against gelatinases (MMP2 and MMP9, Figure 46A and 46B) and collagenases (MMP13, Figure 46C), we could not detect any genotype-specific difference in the expression of these MMPs upon immunostaining. Collagen and gelatin gel zymography further demonstrated normal activation of collagenases and gelatinases in mutant explants treated with the cytokines (Figure 46E). However, we did observe reduced expression of the aggrecan-degrading MMP3 in IL-1 β and TNF α stimulated mutant explants compared with wild type (Figure 46D). These results indicated that IL-1 β and TNF α stimulation of aggrecanases and MMP3 was partially regulated by NF- κ B and blocking NEMO may be an important approach for the development of intervention strategies for OA.



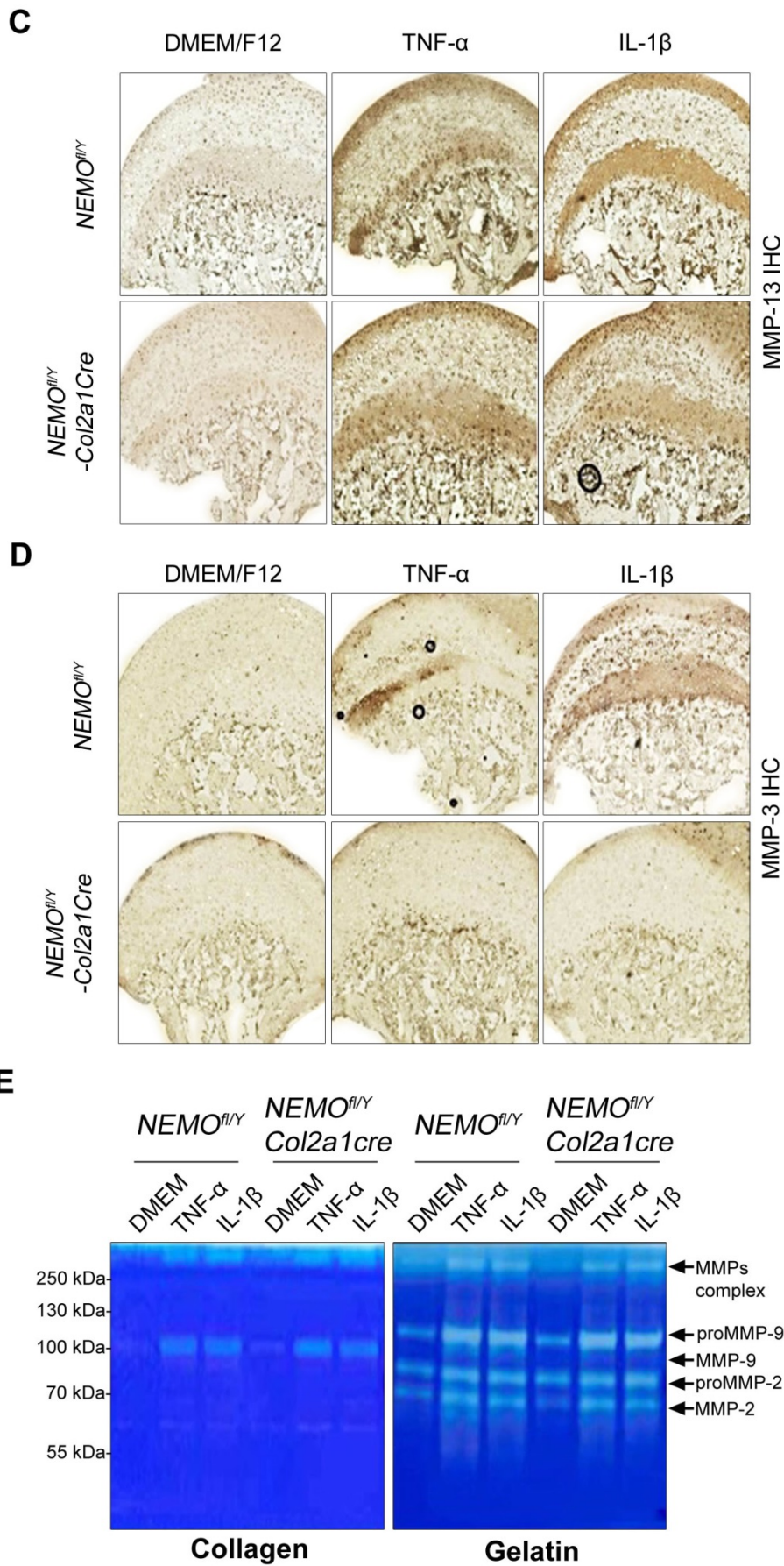


Figure 46: Cytokines-induced expression of MMP3 was decreased in mutant explants. No difference in the expression of MMP2 (A), MMP9 (B) and MMP13 (C) was observed between control and mutant explants after TNF- α (100 ng/ml) and IL-1 (10 ng/ml) treatment. (D) IL-1 β and TNF α

elevate MMP3 expression in control but not in *NEMO^{fl/y}Col2a1cre* explants. (E) Collagen and gelatin zymography demonstrate no obvious difference in the activity of collagenases and gelatinases in control and mutant explants.

4.5. Regulation of NF- κ B in cartilage responses upon ex vivo induced hip injury

Against mechanical stress, ARG-1, HAS-2, IL-18 and MMP-3 were significantly regulated in hip cap of *NEMO^{fl/y}Col2a1Cre* mice compare to wild-type

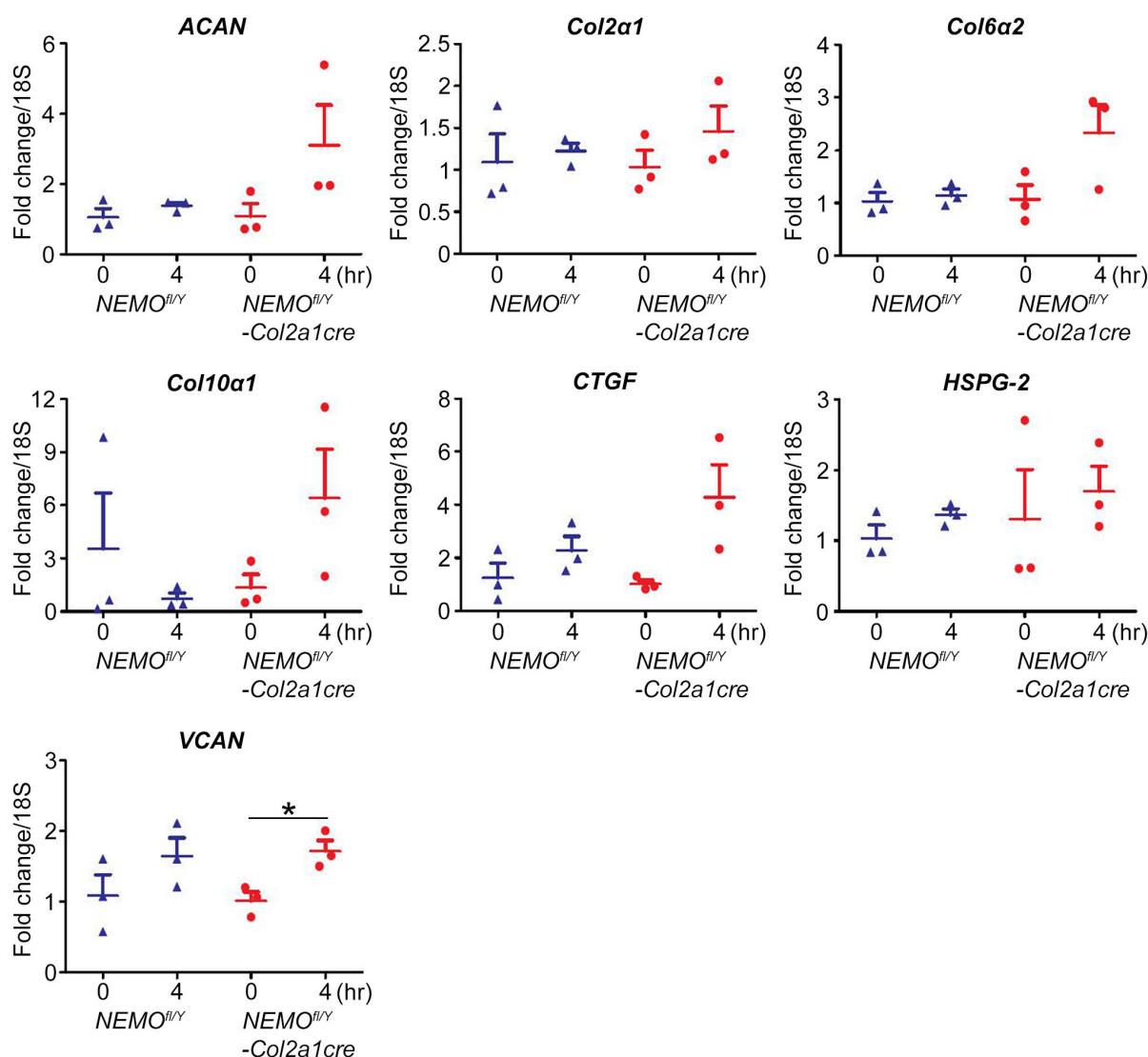
Joint injury significantly increased the risk of OA, therefore dissecting the pathways that were induced after trauma was important for understanding cartilage degeneration. It had been previously shown that physical damage of the articular cartilage rapidly activates the three major MAP kinases (ERK1/2, Jnk, p38) as well as NF- κ B, which in turn triggered intracellular inflammatory signaling pathways (Gruber et al., 2004). To clarify the role of NF- κ B in this process, we applied a mechanical injury model developed by Tonia L. Vincent (Kennedy Institute of Rheumatology Division, Imperial College School of Medicine, London, UK). Briefly, intact femora were isolated from 4-week-old wild-type and *NEMO^{fl/y}Col2a1Cre* mice, and the injury was induced by forcing the hip cartilage from the underlying femoral head. The cartilaginous femoral heads were either immediately frozen in liquid nitrogen (negative control) or cultured in serum-free DMEM for 4 hours before snap freezing. RNA was extracted from the pulverized samples and RT-PCR was performed for a set of 47 pre-determined genes, which were known to be strongly regulated following injury using microfluidic Taqman low-density arrays.

According to the microarray data, there were only few genes significantly regulated in NEMO-deficient group compared to wild-type. The only suppressed gene in *NEMO^{fl/y}Col2a1Cre* hip upon injury was *arginase 1 (ARG-1)*. Hyaluronan synthase-2 (*HAS-2*), *interlukin-18 (IL-18)* and *matrix metalloprotease-3 (MMP-3)* were up-regulated genes in NEMO-deficient group compared to wild-type (Figure 47). *Arginase1* encoded arginase, which was an enzyme participating in urea cycle, a series of reactions that occurs in liver cells. Basically, ARG-1 was characterized by its role in metabolism. However, the role ARG-1 among mechanical stress in articular cartilage was still largely unknown. HAS-2 encoded hyaluronan synthase that was

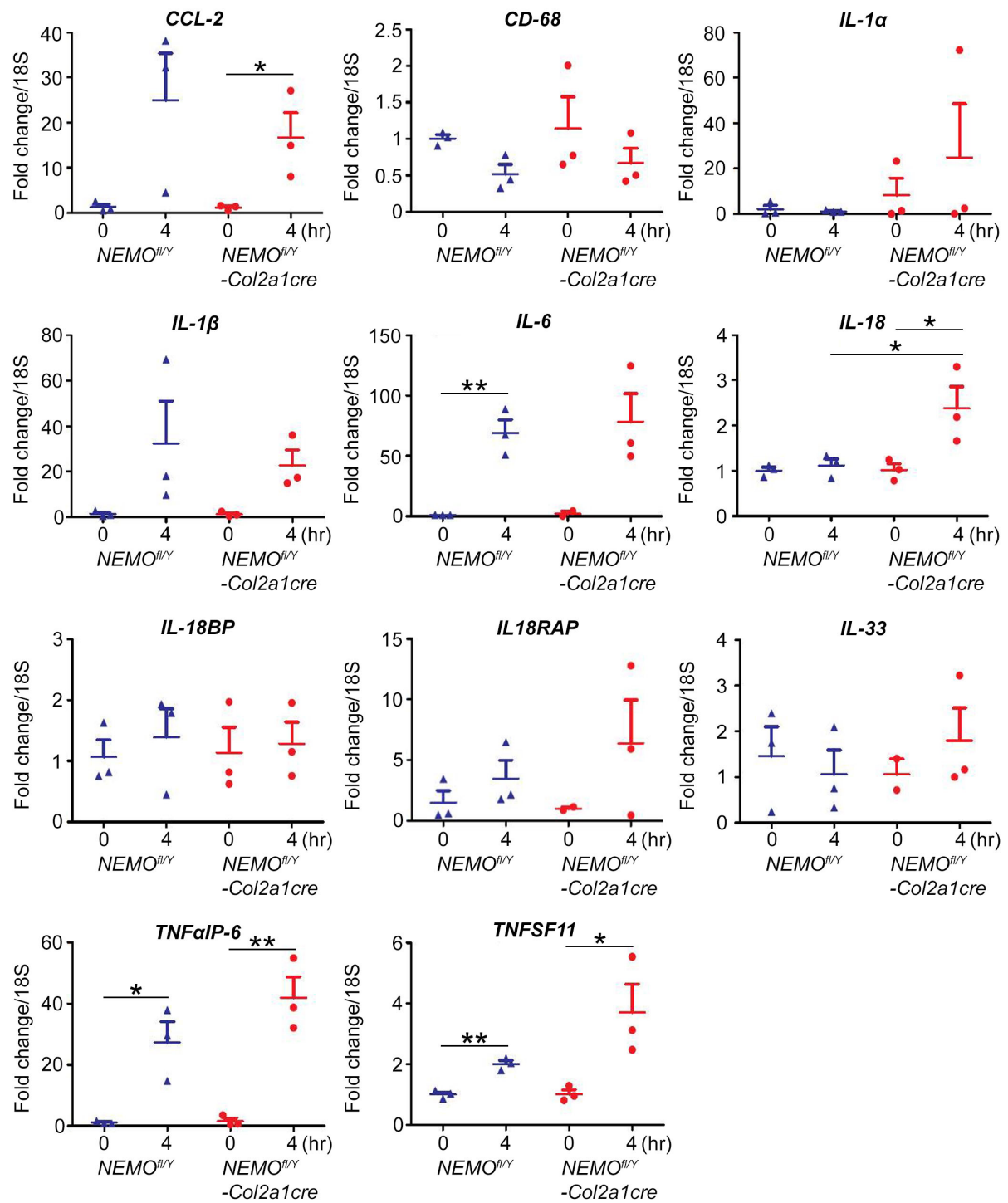
responsible for production of hyaluronan, which was a component of cartilage ECM. Enhanced- regulation of HAS-2 gene in articular cartilage of *NEMO^{fl/y} Col2a1Cre* mice was suggested a repair mechanism against the mechanical stress. Consequently, HAS-2 might continuously produce hyaluronan to replenish the loss of cartilage ECM resulted from mechanical stress.

MMP-3 was known to play important role in degradation of cartilage ECM among injury. Enhanced MMP-3 expression in mutant articular cartilage implied an acceleration of cartilage ECM breakdown among mechanical stress. IL-18, a structure homolog of IL-1, was up-regulated as well. By sharing structure similarity with IL-1, IL-18 might be able to trigger the same signaling as IL-1 induced during injury. However, the role of IL-18 in injury-induced cartilage ECM degradation was remained unclear.

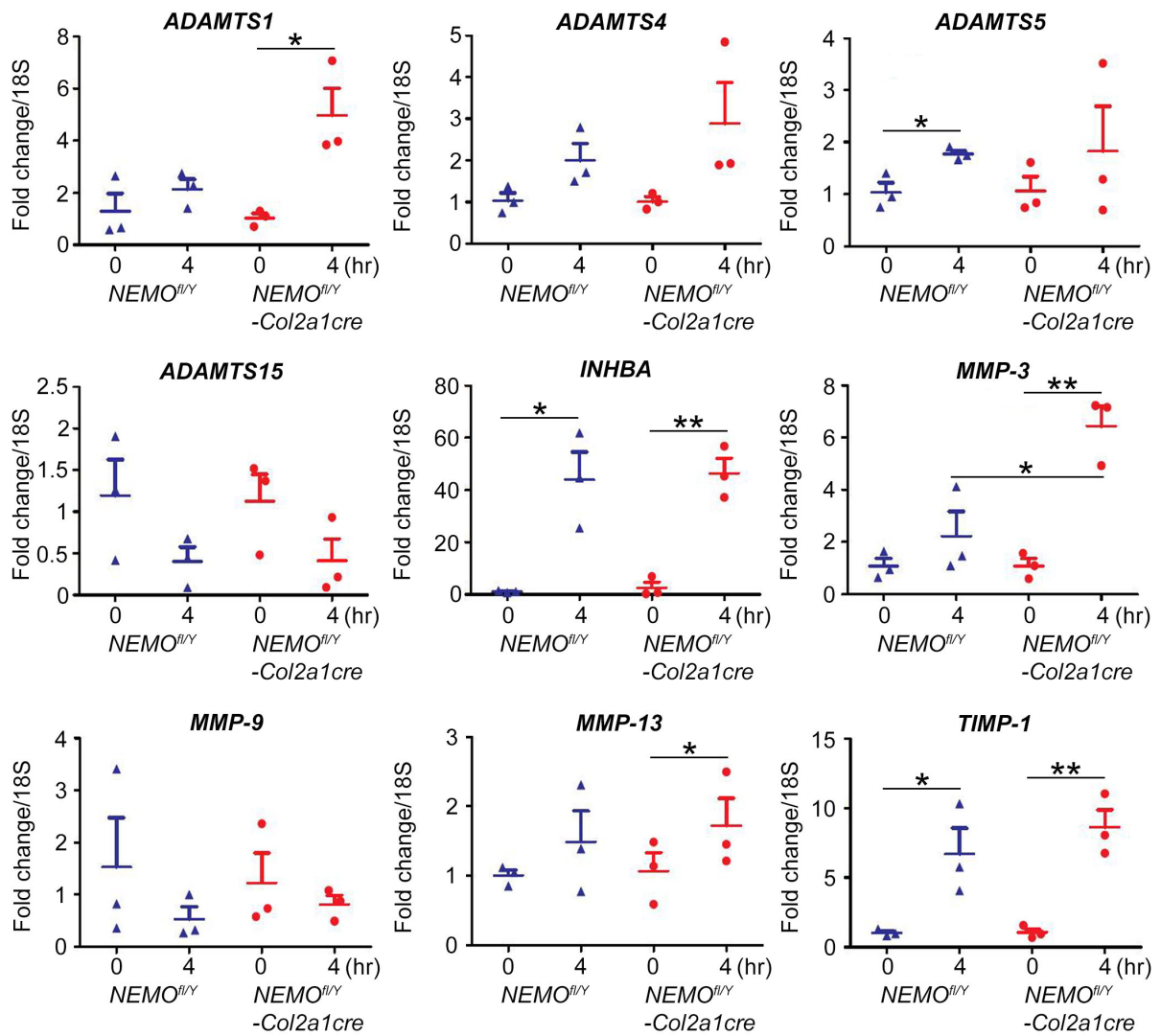
ECM and ECM associated proteins



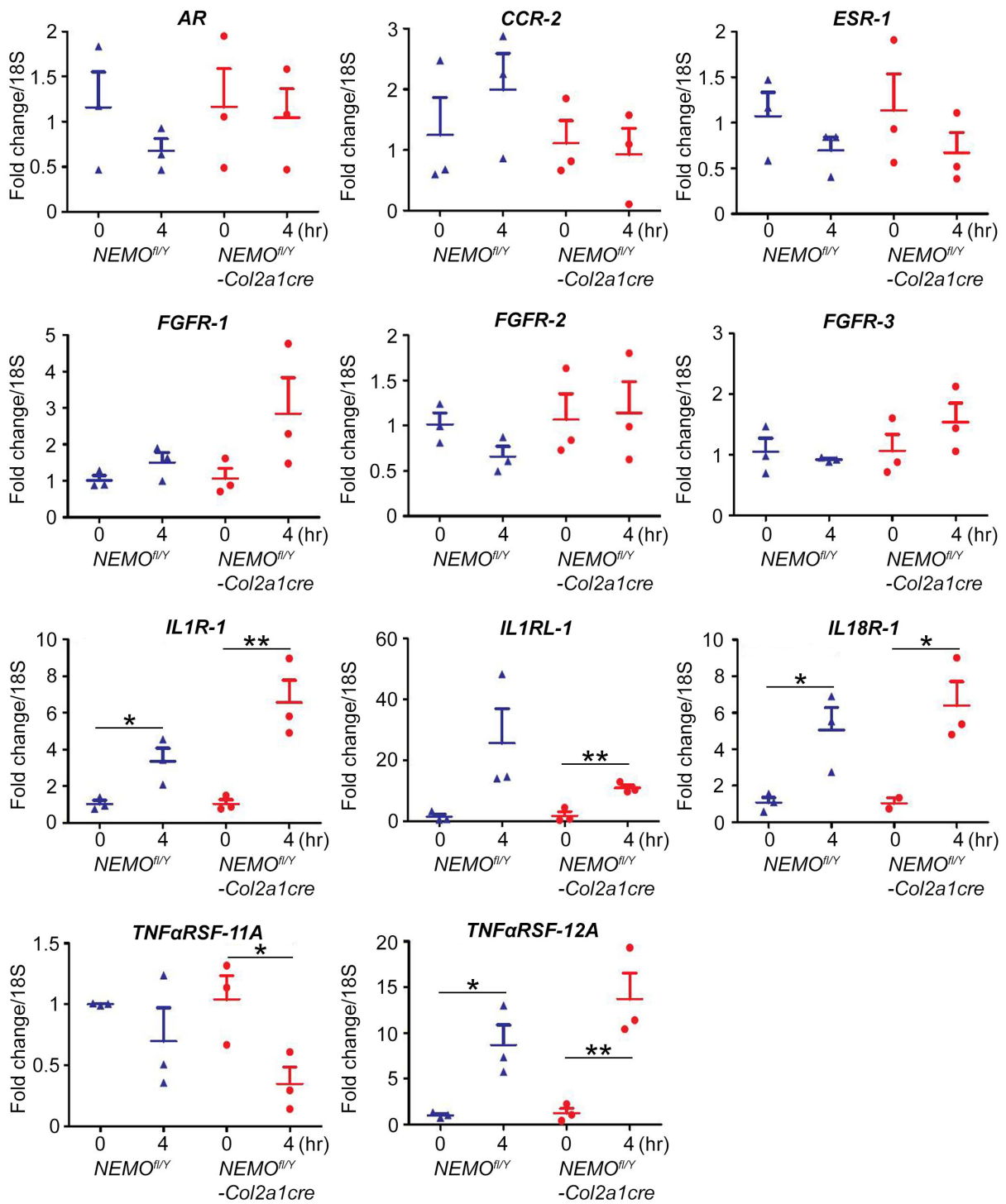
Inflammatory cytokines and associated proteins



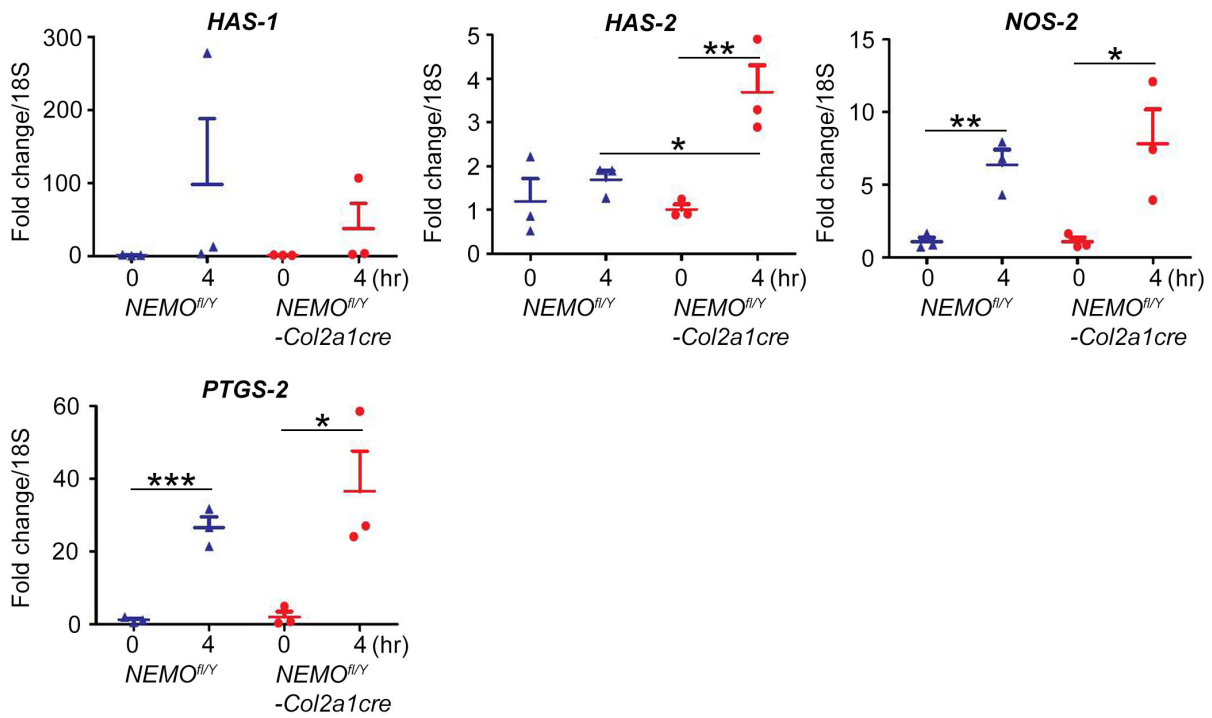
Proteinases and proteinase inhibitors



Receptors



Synthesases



Diverse proteins

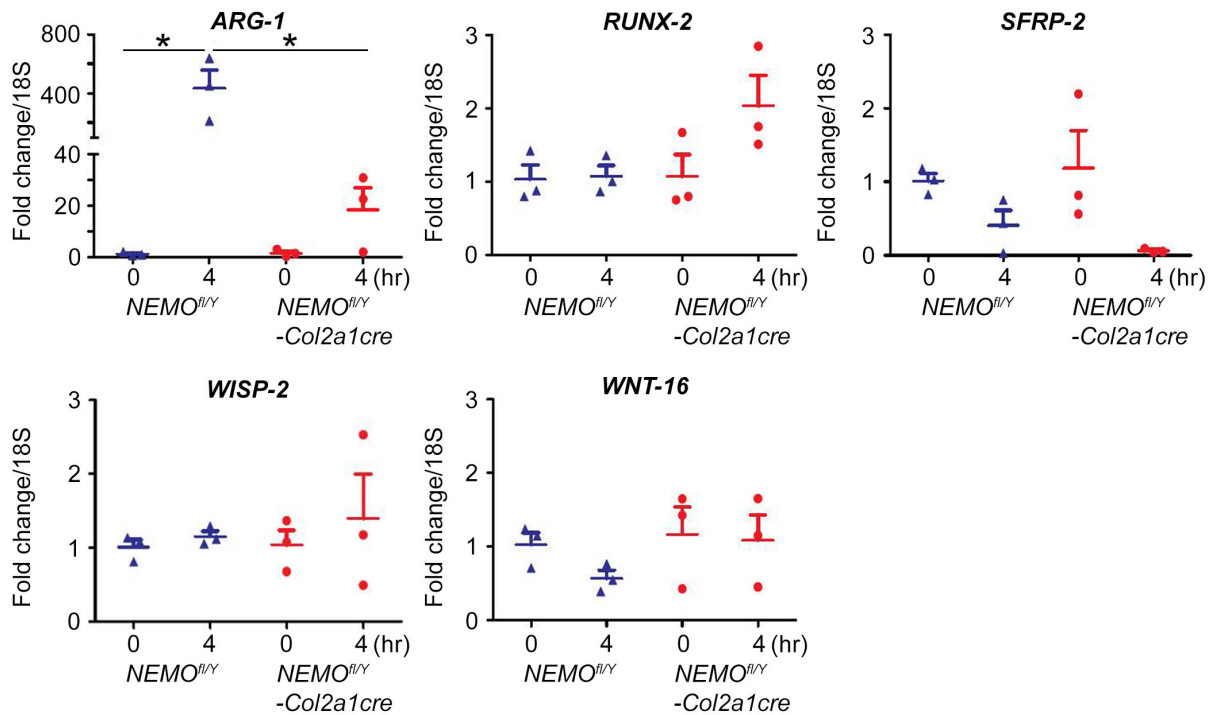


Figure 47: RT-PCR of 47 pre-determined, osteoarthritis-related genes using TaqMan microfluidic cards. It demonstrated that ARG-1 was the only down-regulated gene in *NEMO^{fl/y}Col2a1cre* group compared to control; HAS-2, IL-18 and MMP-3 were the up-regulated genes response to mechanical damage in *NEMO^{fl/y}Col2a1cre* group.

4.6. The role of NF- κ B canonical pathway in spontaneous OA model

***NEMO*-deficiency has no impact on age-associated, spontaneous osteoarthritis in mice**

Idiopathic OA is normally slow progressing; increased mechanical loading upon traumatic lesions could accelerate the disease. To assess the role of NEMO/canonical NF- κ B in spontaneous osteoarthritis, H&E and toluidine blue stained sections of *NEMO^{fl/y}* and *NEMO^{fl/y}Col2a1Cre* knee joints were examined for histological evidence of articular cartilage (AC) degeneration at age of 1 and 1.5 year. The knee joint overview of *NEMO^{fl/y}* and *NEMO^{fl/y}Col2a1Cre* mice were similar with no significant difference (Figure 48). The collateral ligament and synovial tissue from both groups were still health, even at age of 1.5 year. The H&E and toluidine blue stained sections showed that all of the mice including 1- and 1.5-year-old displayed surface irregularity or rift to the transition zone and almost the same proteoglycans level of articular cartilage (Figure 49A and 50A). Hypercellularity was noticed in both 1- and 1.5- year old models. According to the scoring system previously described in materials and methods, cartilage erosion and total OA score of 1-year-old and 1.5-year-old articular cartilage were evaluated. Grade 2 erosions, represented as cleft to the transition zone, were observed in *NEMO^{fl/y}* and *NEMO^{fl/y}Col2a1Cre* mice at age of 1 and 1.5 year (Figure 49B and 50B). Both groups of 1-year-old and 1.5 year-old were with total OA score 6-7, which indicating mild OA progression (Figure 49C and 50C). Analysis of AC thickness (Figure 49D and 50D) and uncalcified/calcified region (Figure 49E and 50E) showed no difference as well. Results of AC thickness and uncalcified/calcified region measurement were almost the same between *NEMO^{fl/y}* and *NEMO^{fl/y}Col2a1Cre* mice at age of 1 and 1.5 year. To summarize, no statistically difference of cartilage erosion, total OA score, AC thickness and uncalcified/calcified region of AC was found between *NEMO^{fl/y}* and *NEMO^{fl/y}Col2a1Cre* mice.

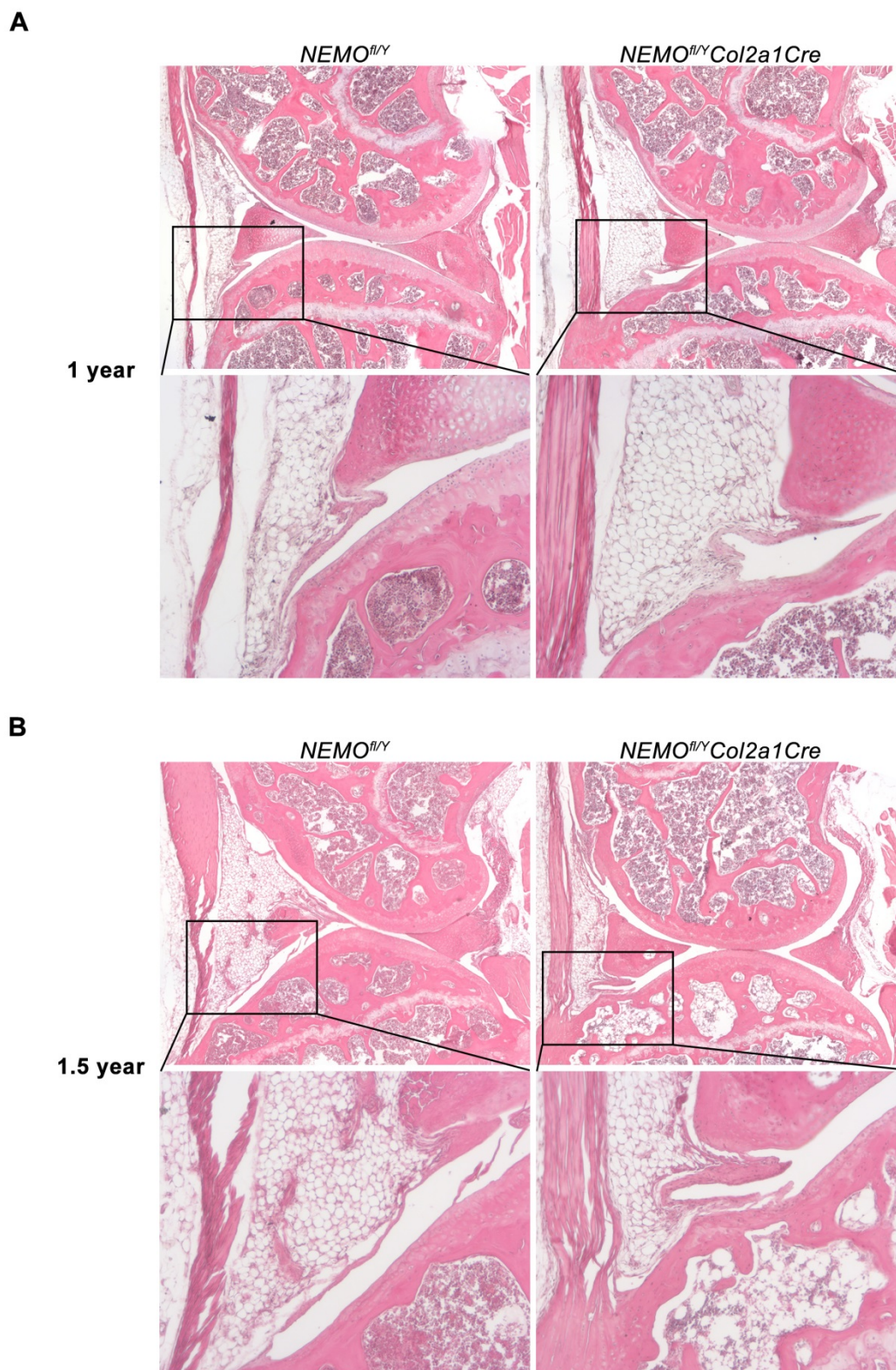


Figure 48: Knee overview of 1- and 1.5-year-old mice. *NEMO*-deficiency did not influence spontaneous knee osteoarthritis in mice. Representative H&E stained knee sections from (A) 1- and (B) 1.5-year-old mice of *NEMO^{fl/y}* and *NEMO^{fl/y}Col2a1Cre* mice were comparable. No significant difference was observed in collateral ligament, synovial tissue (at higher magnification) and articular cartilage.

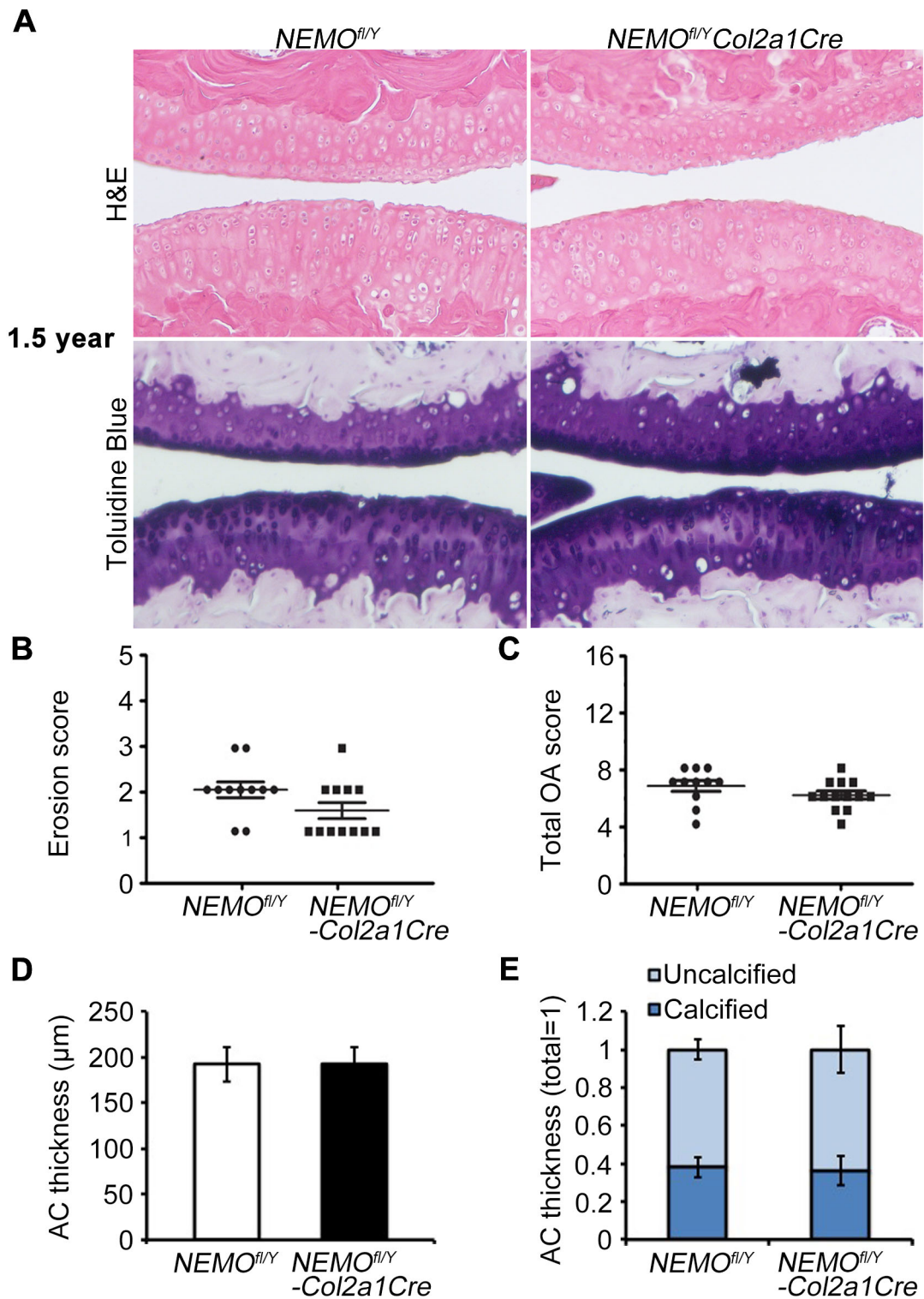


Figure 50: Evaluation of cartilage erosion, OA progression and AC composition at age of 1.5 year. (A) H&E and toluidine blue stained knee sections showed comparable cartilage damage in both groups. (B) According to erosion assessment, the level of cartilage damage was into transition zone. (C) Total OA score revealed that *NEMO^{fl/y}* and *NEMO^{fl/y} Col2a1Cre* mice were with mild OA. (D) The AC thickness of wild type and NEMO-deficiency mice were almost the same. (E) The ratio of uncalcified and calcified region in AC was comparable as well.

To examine the cartilage ECM breakage, IHC staining of aggrecan neopeptide such as G1-TEGE and VIDIPEN were performed. At age of 1- and 1.5-year-old wild type and *NEMO^{fl/y}Col2a1Cre* mice, TEGE-stained signals were evenly distributed in articular cartilage (Figure 51A). VIDIPEN was sporadically detected in 1-year-old AC and largely increased in 1.5-year-old AC (Figure 51B).

The following immunostaining for aggrecanases MMP-2, -9 and -13 did not reveal significant differences between *NEMO^{fl/y}* and *NEMO^{fl/y}Col2a1Cre* mice (Figure 52). To conclude, these results have suggested that *NEMO* is likely a dispensable factor in spontaneous knee osteoarthritis.

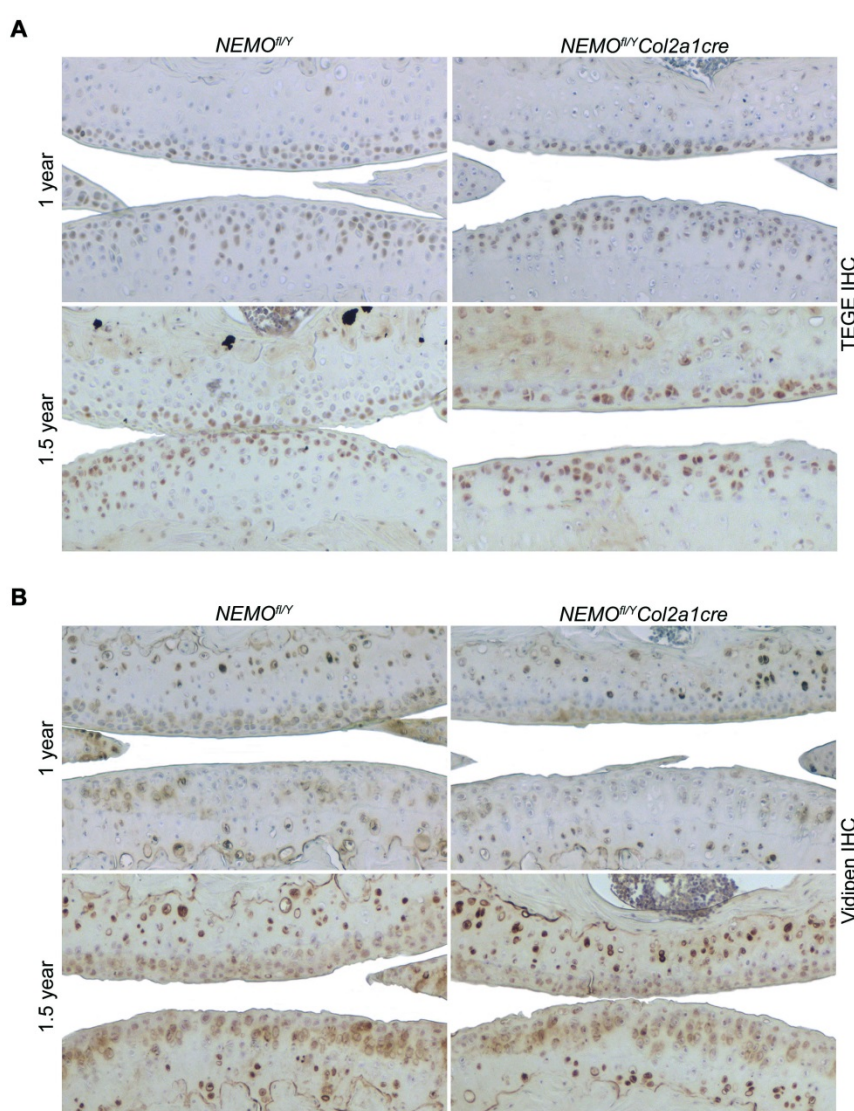


Figure 51: IHC staining of aggrecan neopeptides. (A) In 1- and 1.5-year-old models, the signals of G1-TEGE were evenly distributed near the surface of articular cartilage. (B) Signals of VIDIPEN were sporadically found in 1-year-old cartilage and heavily increased in 1.5-year-old cartilage. Both groups at age of 1 and 1.5 year showed comparable G1-TEGE and VIDIPEN signals.

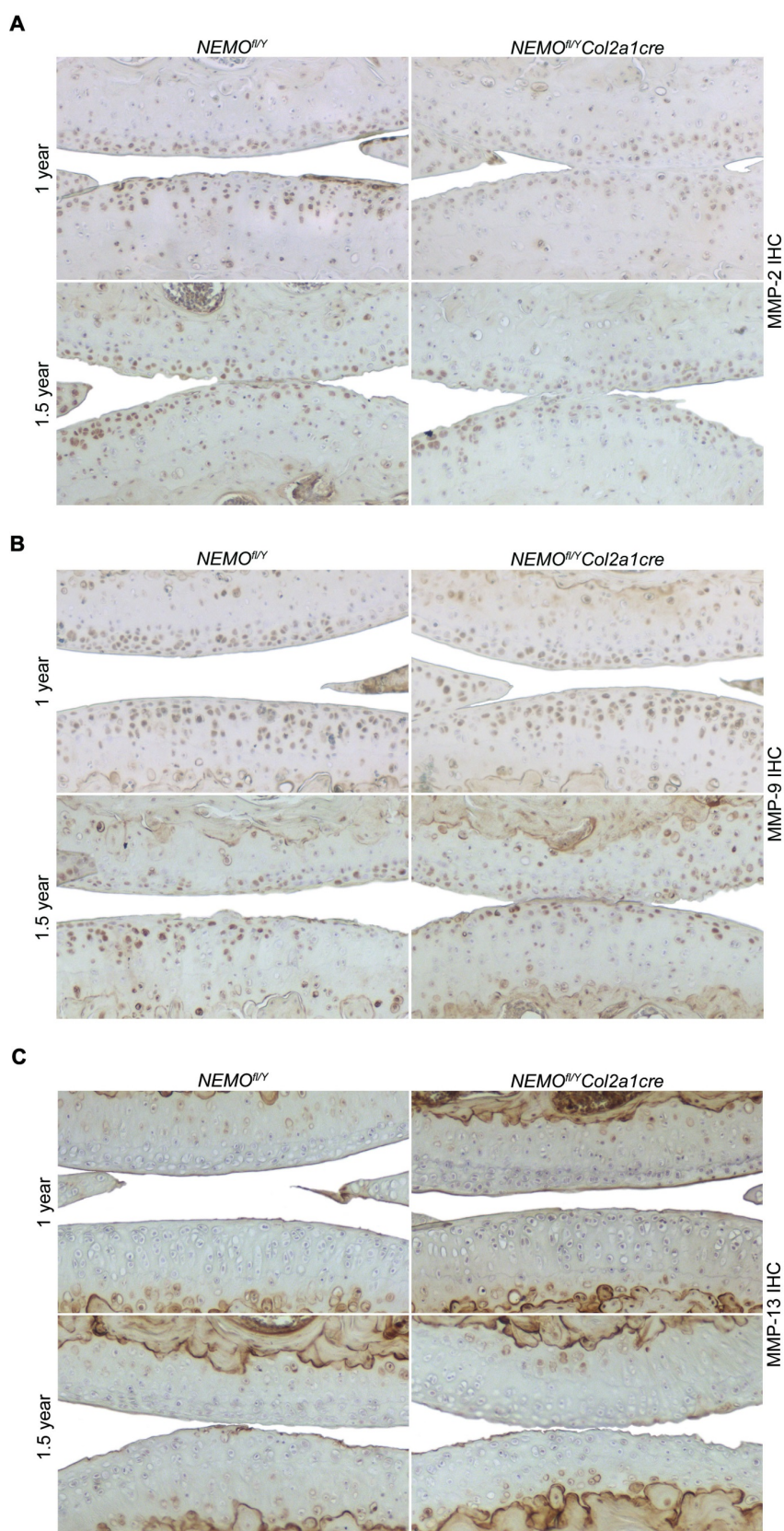


Figure 52: IHC staining of aggrecanases. (A) The signals of MMP2 were similar to G1-TEGE, which were distributed near the surface. (B) The signals of MMP-9 were pronounced in 1-year-old cartilage and slightly reduced in 1.5-year-old group. (C) MMP-13 was predominantly detected in subchondral bone. Comparison of *NEMO^{fl/y}* and *NEMO^{fl/y} Col2a1Cre* at age of 1 and 1.5 year, expression of MMP-2, -9 and -13 were similar and no significant difference.

5. Discussion

Nuclear factor- κ B proteins control the expression of numerous genes in respond to stress conditions such as inflammation, infection or injury. In the recent years, pharmacological blockade of NF- κ B canonical pathway has been suggested as a potential therapeutic treatment against bone degenerative disorders such as rheumatoid arthritis and osteoarthritis. In spite of the suggested beneficial role of diminished NF- κ B activation in amelioration of cartilage degradation, the role of the canonical NF- κ B pathway in normal skeletal development still remains unclear, mainly because of the shortage of appropriate model animal. Using a *Col2a1Cre* transgenic mouse line, in this study we have successfully deleted the floxed *Nemo* gene in cartilage, which allowing us to clarify the role of canonical NF- κ B signaling in skeletal physiology.

5.1. The NEMO-mediated, canonical NF- κ B pathway regulates postnatal growth of endochondral bones via the control of growth plate functions

Previous studies have been revealed that conventional knock-outs of *RelA* (p65) and *NEMO* in mice result in diminished activation of the canonical NF- κ B pathway and cause embryonic lethality between gestation days 12 and 16 (Beg et al., 1995; Rudolph et al., 2000). The embryonic lethality in both mutant strains was found due to apoptosis of hepatocytes and severe liver degeneration. Interestingly, no other abnormalities, including any skeletal defects, were reported in the p65-null and NEMO-null mice. In our study, conditional inactivation of *NEMO* in chondrocytes led to normal embryogenesis without signs of any skeletal malformations. Investigation of the skeleton of *NEMO^{fl/y}Col2a1Cre* embryos and newborn animals using various techniques including whole-mount skeletal staining, morphometry, histological analysis, and proliferation assays showed that the skeletal appearance and skeletal growth of the mutants comparable to that of the wild-type mice. This observation indicates that NEMO/canonical NF- κ B is dispensable for fetal skeletogenesis.

In contrast to the embryonic stages, *NEMO^{fl/y}Col2a1Cre* mice exhibited progressive growth retardation which begun at around 1 week of age and persisted throughout the whole life. Besides the skeletal phenotype, NEMO-deficient animals were fertile, had normal life span and showed no abnormal organ functions. On histological level, the observed postnatal dwarfism was characterized with shortened growth plate and reduced lengths of both the proliferating and hypertrophic zones. The growth plate shortening was accompanied with reduced BrdU incorporation rate in the proliferative zone, indicating that the canonical NF- κ B pathway modulates the mitotic activity of proliferative chondrocytes. We have also found that p16 (also called cyclin-dependent kinase inhibitor 2A) mRNA is up-regulated in NEMO-deficient chondrocytes strongly implying a role of canonical NF- κ B signaling in the control of cyclin dependent kinases. It has been shown in various cellular systems that p16 plays critical regulatory function in cell cycle by suppressing G1/S transition (Hara et al., 1996; Rayess et al., 2012). A previous study has showed that expression of p16 and NF- κ B p65 is inversely correlated in melanocytes during melanoma progression (Ghiorzo et al., 2004). The fact that p16 was up-regulated in the cartilage of *NEMO^{fl/y}Col2a1Cre* mice, further demonstrate that NEMO/ canonical NF- κ B is a generalized signaling mechanisms which modulates cell cycle progression in different cell types, including chondrocytes. Mechanistically, several studies have indicated that p16 up-regulation keeps retinoblastoma proteins (pRB) un-phosphorylated, which results in decelerated progression from G1 to S phase. Whether or not the same mechanisms acting in the NEMO-deficient chondrocytes remains unresolved and needs to be elucidated in the future.

BMP-2, a member of the TGF β superfamily of growth factors, is known to play an important role in regulating embryonic and postnatal bone growth. A recent report has showed that BMP-2 expression is regulated by NF- κ B signaling in growth plate chondrocytes both in vitro and in vivo (Feng et al., 2003). The NF- κ B subunits p50 and p65 bind to regulatory elements of the *BMP-2* gene, and possibly regulating *BMP-2* expression. Importantly, p50/p52 double knockout mice with insufficient NF- κ B activation display reduced BrdU incorporation rate in proliferative growth plate chondrocytes accompanied by decreased *BMP-2* expression. In our study, we have not investigated BMP-2 expression in postnatal *NEMO^{fl/y}Col2a1Cre* chondrocytes. However, we did not find a difference in chondrocyte proliferation upon BMP-2 treatment between NEMO-deficient and control metatarsal explants suggesting that

the ablation of the canonical p50/p65 pathway may not be crucial for BMP-2 induced growth. Nevertheless, the relation between *BMP-2* expression and canonical NF- κ B signaling in postnatal *NEMO^{fl/Y}Col2a1Cre* growth plate chondrocytes should be investigated with more details in the future.

5.2. NEMO/canonical NF- κ B signaling modulates chondrocyte survival in postnatal growth plate

Under normal circumstances, terminally differentiated hypertrophic chondrocytes at the chondro-osseous either die by apoptosis or transdifferentiate into osteoblast (Zhou et al., 2014). Chondrocyte death is not typical in upper growth plate zones, and the appearance of apoptotic cells in the proliferative zone is usually associated with growth plate dysfunction. In the growth plate of *NEMO^{fl/Y}Col2a1Cre* mice, we have detected apoptotic chondrocytes scattered through the proliferative and upper hypertrophic zones by TUNEL assay. Although the rate of apoptosis was low in the mutant growth plate, we hypothesize that a constant cell death in the proximal growth plate zones could also contribute, besides the proliferation defect, to the dwarf phenotype of *NEMO^{fl/Y}Col2a1Cre* mice. Several studies have indicated the participation of NF- κ B subunits in the control of apoptosis (Beg and Baltimore, 1996; Van Antwerp et al., 1996; Wang et al., 1996). Recently, it has been shown that p65 is constitutively activated by the NK homo-protein Nkx3.2 to support chondrocyte survival in proliferative chondrocytes (Park et al., 2007). The expression of Nkx3.2 is reduced in mature chondrocytes (Church et al., 2005; Provot et al., 2006). Moreover, chondrocyte apoptosis and NF- κ B activation are inversely related during cartilage maturation. Interestingly, the constitutive activation of NF- κ B mediated by Nkx3.2 in chondrocytes also requires IKK- β and NEMO (Yong et al., 2011). Apart from Nkx3.2-mediated survival effect, it has known that several distinct elements are also involved in regulation of viability including β 1-integrin and HIF-1 α (Hirsch et al., 1997; Schipani et al., 2001). In our *NEMO*-deficient chondrocytes, Nkx3.2-mediated survival pathways might be blocked as well as canonical NF- κ B signaling and could account for the increased apoptotic rate in the proliferative and upper hypertrophic zones of *NEMO^{fl/Y}Col2a1Cre* growth plate owing to the lack of NEMO expression and canonical NF- κ B activation (Figure 53). However, further investigation is required to confirm this assumption.

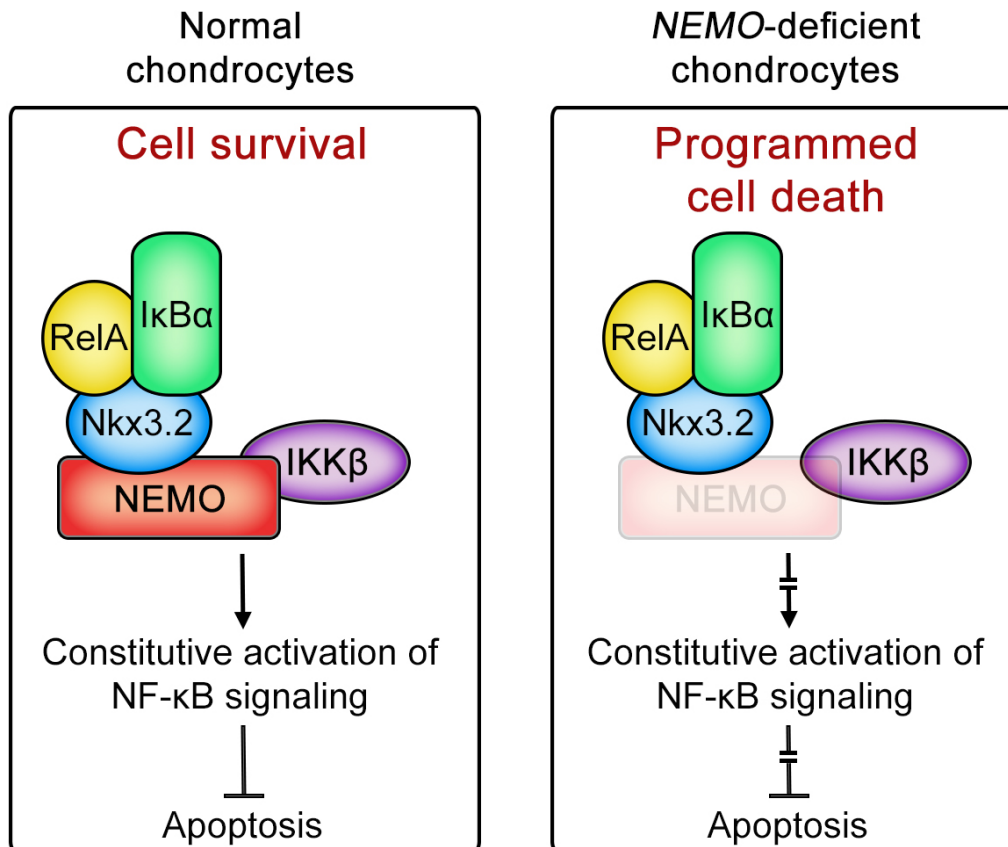


Figure 53: NEMO is involved in Nkx3.2-mediated constitutive activation of NF-κB signaling. Nkx3.2, specifically expresses in proliferative chondrocytes in association with the NEMO-IKKβ complex, and constitutively activates RelA and maintains chondrocyte viability. However, the *NEMO*-deficient chondrocytes are more vulnerable to apoptosis due to the destruction of NF-κB-Nkx3.2-NEMO-IKKβ complex, which is likely responsible for the increased apoptotic rate in the proliferative zone of *NEMO*-deficient growth plate. Figure is adapted and modified from (Park et al., 2007).

5.3. Primary *NEMO*^{fl/y} *Col2a1Cre* chondrocytes exhibit severe death phenotype upon exposure to TNF-α

Inflammation enhances cartilage degradation in the processes of osteoarthritis and rheumatoid arthritis, therefore blocking inflammatory cytokines such as tumor necrosis factor (TNF, TNF α) or interleukin-1 (IL-1) is a potential therapeutic approach for the prevention of the progression of these diseases. TNF signaling proceeds through NEMO/ NF-κB dependent and independent pathways, which are not only regulates the expression of pro-inflammatory proteins but are also involved in the control of death-survival decision of the cells.

In most cell types, upon TNF engagement by TNF receptor-1 (TNFR-1), NF-κB activation is initiated by the binding of TNFR-1 associated death domain protein

(TRADD) to the cytoplasmic part of TNFR-1, which subsequently recruits receptor-interacting serine-threonine protein kinase 1 (RIPK-1), TNFR-associated factor 2 (TRAF-2) and the E3 type ubiquitin ligase cIAP1 or cIAP2 (Devin et al., 2000; Hsu et al., 1996; Kelliher et al., 1998; Ting et al., 1996). After RIPK-1 undergoing poly-ubiquitination (Bertrand et al., 2008; Lee et al., 2004b; Wang et al., 2008; Wertz et al., 2004), it interacts with the ubiquitin-binding domains of NEMO (Laplantine et al., 2009). The binding of NEMO to RIPK-1 is a critical step to recruit the whole IKK complex and activation of the canonical NF- κ B pathway (Ea et al., 2006; Li et al., 2006). RIPK-1/NEMO-induced NF- κ B activation leads to the expression of several anti-apoptotic genes (e.g. IAPs, Bcl-2 family subunits, cFLIP) and thus promotes cell survival (Micheau et al., 2001; Wang et al., 1998). TNF-induced NF- κ B activation was considered as a late-stage pro-survival checkpoint in T lymphocytes (O'Donnell et al., 2007). Apart from participating in NF- κ B-regulated pro-survival function, NEMO was reported to possess a relatively early pro-survival activity that is independent from the canonical NF- κ B pathway (Legarda-Addison et al., 2009). RIPK-1 is able to bind caspase-8 initiating a classical apoptosis pathway. NEMO, before TNF-induced NF- κ B activation, masks caspase-8 binding sites on RIPK-1, therefore it suppress apoptotic activity. The pro-apoptotic activity of RIPK-1 is appears when NEMO is absent (Legarda-Addison et al., 2009) or ubiquitination is not present (Bertrand et al., 2008; O'Donnell et al., 2007; Wang et al., 2008). Consequently, a novel role of NEMO in pro-survival pathway has been suggested. According to above evidences, TNF signal transduction likely has two checkpoints. (1) Binding with of NEMO and attachment of non-degradative ubiquitin chains in RIPK-1 (early checkpoint). Afterwards, IKK complex is recruited by NEMO-RIPK-1 which in turn leads to (2) up-regulation of NF- κ B-mediated pro-survival genes (late checkpoint). Different from the temporary pro-survival effect provided by the primary checkpoint, the secondary checkpoint offers sustained expression of pro-survival genes. Hence, TNF-stimulated apoptosis could occur if one of the pro-survival checkpoints is abolished. Furthermore, a recent study using T lymphoma cells demonstrated that NEMO-deficiency results in hypersensitivity to necroptosis (or regulated necrosis) in the absence of caspase (apoptosis) inhibitors, which, again, does not depend on the activation of the canonical NF- κ B pathway (O'Donnell et al., 2012). In summarizing the literature data, NEMO and NEMO/NF- κ B signaling cascades fine-tunes the TNF-dependent outcome of cell survival or death (apoptosis or necroptosis). In our study, we have investigated

the response of primary NEMO-deficient chondrocytes to TNF- α exposure in monolayer culture. As the lack of NEMO interferes with both the pro-survival function of TNF/NF- κ B signaling and the anti-apoptotic/anti-necrotic function of RIPK-1, it is not surprising that the mutant cells showed massive cell death after TNF- α treatment (Figure 54). However, the used methodology to stain live, apoptotic, and necrotic cells do not allow to clearly discriminating among the potential cell death pathways in the absence of NEMO. The predominant staining of ethidium homodimer and the lack of significant annexin V-positive cell membrane could be interpreted as very late stage apoptosis with already prominent cell membrane degradation or late stage necroptosis. Clearly, further investigation is required to devote into this interesting issue. Importantly, blockage of the canonical NF- κ B pathway in arthritic disorders by inhibiting NEMO function may induce chondrocyte death in the articular cartilage and counteract its beneficial effect on suppressing the expression of catabolic proteins in an inflammatory environment (see later).

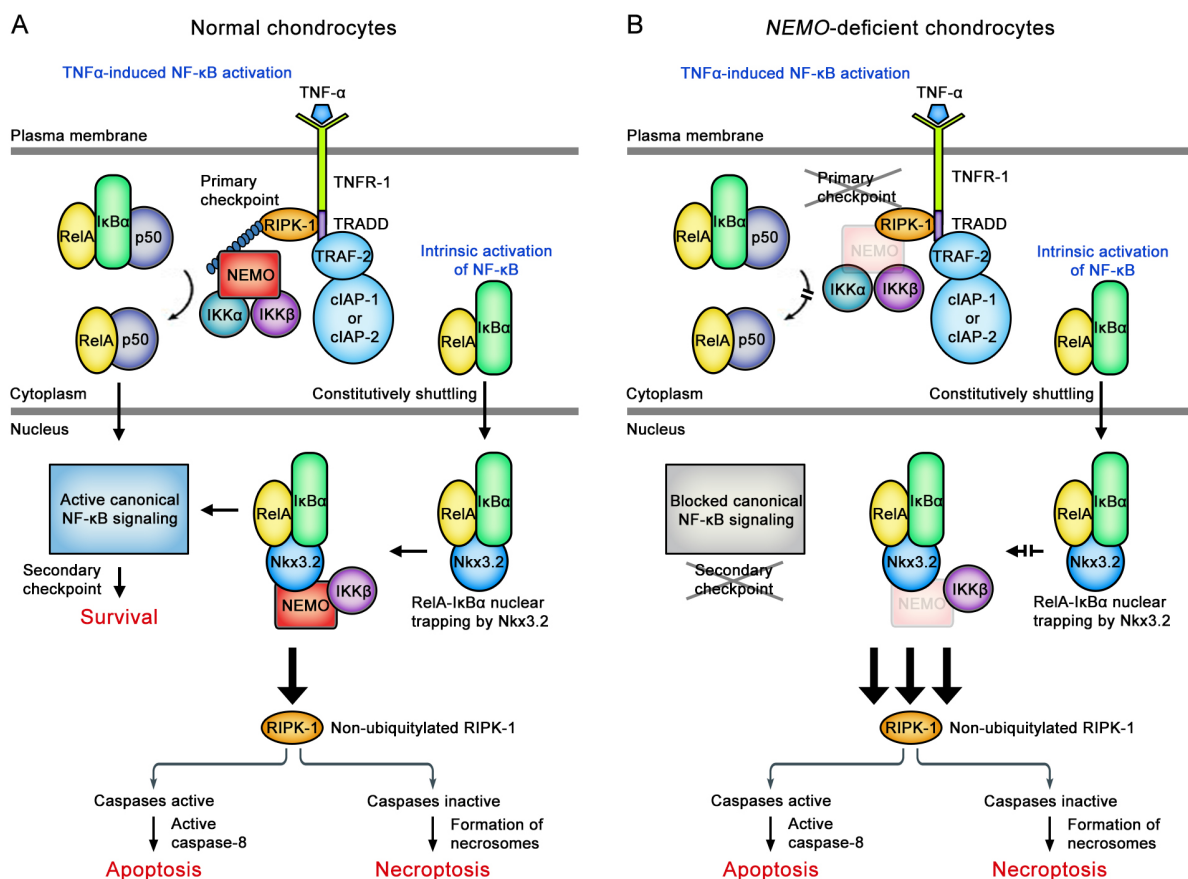


Figure 54: NEMO plays a key role in pro-survival activities against TNF- α stimuli. (A) In response to TNF- α induction, the poly-ubiquitylation of RIPK-1 and its binding with NEMO are regarded as the primary or early pro-survival checkpoint. The NF- κ B-regulated pro-survival activities are served as the secondary or late pro-survival checkpoint. The lack of either checkpoint (or excessive TNF- α stimuli) results in apoptosis or necroptosis. (B) In NEMO-deficient chondrocytes, the canonical and intrinsic

activations of NF- κ B are both abolished, which eliminate both survival checkpoints and lead to massive apoptosis/necroptosis. Figure is adapted and modified from (Brenner et al., 2015).

5.4. NEMO modulates growth plate architecture

The proper geometry, size, number and orientation of growth plate chondrocytes are important factors which ensure longitudinal growth (Ascenzi et al., 2011; Ivkovic et al., 2003). As a result of spatially coordinated proliferation and remodeling at the proximal and distal growth plate, respectively, the length of endochondral bones is gradually increasing during embryonic and early postnatal development. The normal epiphyseal growth plate consists of 3 major layers, namely the resting zone, the proliferating zone, and the hypertrophic zone along the proximo-distal axis of the bone (Karsenty et al., 2009; Kronenberg, 2003). In the proliferative zone, chondrocytes undergo oriented cell division followed by rotational movements, and form linear columns with coin-like arrangements as seen on Figure 8. In 2 to 4 weeks old *NEMO^{fl/y}Col2a1Cre* mice we have observed a slight disorganization of proliferative chondrocytes characterized by a tendency for the formation of less elongated columns. Instead of organized into linear stacks, mutant chondrocytes arranged into more oval clusters indicating failure in cell migration. The mild disarrangement of NEMO-deficient chondrocytes in the proliferative zone might be caused by changes in cell-matrix interactions, in ECM stiffness, or both (Aro et al., 2015; Prein et al., 2016; Raducanu et al., 2009). Using indentation-type atomic force microscopy, we did not find a significant difference in the elasticity of the cartilaginous matrix of the growth plate between mutant and control animals. This may indicate that the hypothetical migration deficit of NEMO-deficient growth plate chondrocytes could be caused by abnormal cell-matrix interactions and/or anchorage-dependent dysfunction of cytoskeletal proteins. Consistent with this hypothesis, we have shown that NEMO deficient chondrocytes display increased binding to ECM ligands such as collagens, fibronectin and laminin in vitro. Furthermore, monitoring chondrocyte migration by life cell imaging on plastic surface in the presence of serum, we have found reduced spontaneous movements of NEMO-null chondrocytes compared to wild type.

Chondrocyte shape and migration are ultimately determined by integrin-mediated cell-matrix interactions. Integrins are heterodimeric transmembrane

receptors composed of alpha and beta subunits with the ability to bind various extracellular matrix ligands. Multiple integrin heterodimers are present in chondrocytes including collagen binding ($\alpha1\beta1$, $\alpha2\beta1$, $\alpha10\beta1$), fibronectin binding ($\alpha5\beta1$, $\alpha v\beta3$ $\alpha v\beta5$) and laminin binding integrins. Integrins connect the cartilage ECM to the intracellular cytoskeletal system, and transmit chemical and biomechanical signals from the pericellular environment into the cell interior via focal adhesion complexes and various intracellular signaling pathways. This signaling network, called outside-in signaling, controls diverse cellular functions such as proliferation, survival, polarity and movement. Perturbed or diminished integrin signaling has severe influence on cytoskeletal dynamics controlled by the Rho family of small GTPases, or on calcium inflow important for proper cell behavior. The signaling process occurs via phosphorylation of kinases such as focal adhesion kinase (FAK) or mitogen-activated protein kinases (MAPKs) and could modulate the expression of transcription factors (e.g. NF- κ B family subunits). Previous studies in genetically modified mice have identified that the lack of $\beta1$ integrins, the largest integrin subfamily, on chondrocytes severely impairs chondrocyte function in the growth plate and in the articular cartilage. Conditional-knockout of the $\beta1$ subunit in chondrocytes ($\beta1^{fl/fl}Col2a1Cre$ mice) (Aszodi et al., 2003) or in limb bud mesenchymal precursor cells ($\beta1^{fl/fl}Prx1Cre$ mice) (Raducanu et al., 2009) resulted in chondrocyte proliferation, survival, adhesion and migration defects. Importantly, in both mouse model the orientation and columnar organization of growth plate chondrocytes were abnormal, which in some respect, resemble to the phenotype observed in the *NEMO*-deficient growth plate. Furthermore, accumulating evidence has pointed out the significance of integrins in determination of cell polarity in various tissues (Streuli, 2009) such as keratinocytes (Lechler and Fuchs, 2005), mammary gland cells (Taddei et al., 2008) or *Drosophila* follicular epithelial cells (Fernandez-Minan et al., 2007) through regulating the orientation of the mitotic spindle apparatus (Toyoshima and Nishida, 2007). In our *NEMO^{fl/y}Col2a1Cre* mice we found much milder growth plate phenotype compared to the phenotypes reported in mice with chondrocyte-specific deletion of $\beta1$ integrins. Indeed, the distribution of the integrin-associated focal adhesion protein paxillin in cultured chondrocytes (Figure 43D) and the activation of integrin signaling molecules such as MAPKs, AKT and FAK were apparently normal in *NEMO^{fl/y}Col2a1Cre* mice (Figure 41B), suggesting that an

abnormal integrin function is probably not causative for the observed growth plate anomalies.

Cdc42 and Rac1, two members of Rho GTPases, controls cytoskeletal organization important for cell shape determination and cell movements. Mice lacking either Cdc42 or Rac1 also exhibit growth plate defects with misoriented chondrocyte columns (Nagahama et al., 2016; Wang et al., 2007), implying that cytoskeletal dynamics is important for normal morphogenesis of the growth plate. The abnormal migration and spreading behavior of Nemo-null chondrocytes in vitro may indicate impaired function of Rho GTPases and the cytoskeletal system (Figure 43A,B). In this study we have not determined the activation status of Rho GTPases, but immunofluorescence staining of the actin cytoskeletal system by phalloidin in Nemo-deficient chondrocytes did not indicate any obvious abnormalities of stress fiber, micro-spike and lamellopodia formation, controlled by RhoA, Cdc42 and Rac1, respectively (Figure 43D). Nevertheless, additional studies should be performed in order to investigate any possible connection between canonical NF- κ B signaling and Rho GTPases-mediated, cytoskeleton-dependent migration behavior of chondrocytes.

5.5. Efficient ablation of *NEMO* in chondrocytes alleviate proteoglycan loss upon pro-inflammatory cytokine treatment in hip explant culture

Pro-inflammatory cytokines IL-1 β and TNF- α enhance the catabolic activities of cartilage and are known as critical players in cartilage degradation during arthritis with inflammatory component. Previous studies have shown the involvement of canonical NF- κ B signaling in cartilage breakdown in response to stimulations with IL-1 β or TNF- α . In experiments of human OA chondrocytes, synovial and chondrosarcoma cells, NF- κ B was reported to modulate the expression of matrix metalloproteinases including MMP-1, -2, -3, -9 and -13 (Amos et al., 2006; Liacini et al., 2003; Vincenti and Brinckerhoff, 2002). Furthermore, it has been shown that NF- κ B signaling also participates in the activation of ADAMTS-4 and -5, two critical members of the “a disintegrin and metalloprotease with thrombospondin motifs” family, which mediate aggrecan degradation during OA (Verma and Dalal, 2011; Yaykasli et al., 2015). Numerous publications have suggested the therapeutic

potential of blocking NF- κ B signaling in the treatment of rheumatic diseases. To confirm this hypothesis, hip explant model with pro-inflammatory cytokines induction was used in our study to examine the early onset of cartilage degradation. Treatments of the hip explants with IL-1 β and TNF- α ex vivo resulted in massive proteoglycan breakdown in the wild type group characterized by high amount of GAGs in the culture medium (Figure 45); reduced Safranin Orange staining and strong exposure of aggrecan degradation neo-epitopes including VIDIPEN and TEGE (Figure 44). NEMO-deficient cartilage displayed significantly reduced GAGs release into the medium, and showed less intensive immunostaining for the VIDIPEN and TEGE neo-epitopes in response to the stimulation of IL-1 β and TNF- α (Figures 44 and 45). The neo-epitopes VIDIPEN and TEGE are generated by the action of MMP-3 and ADAMTS-4/5, respectively (Nagase and Kashiwagi, 2003; Westling et al., 2002). Our immunohistochemical staining demonstrated that the expression of MMP-3 induced by IL-1 β and TNF- α was greatly reduced by blocking canonical NF- κ B signaling (Figure 46). In contrast, the deposition of MMP-2, -9 and -13 in were comparable between wild type and Nemo mutant explants. The expression of ADAMTS-4/5 was not assessed in our study due to the lack of antibodies working on section immunohistochemical staining. In summary, however, our results are consistent with previous studies (Marcu et al., 2010; Roman-Blas and Jimenez, 2006), and clearly demonstrate that the blockade of canonical NF- κ B signaling can effectively protect the cartilage from pro-inflammatory cytokines induced proteoglycan loss by reducing expression of critical degradation enzymes such as MMP3 and probably ADAMTS-4/5. It should also mention that the protection against IL1 β - and TNF α -induced proteoglycan breakdown was only partial, implying that we cannot fully prevent IL1 β - and TNF α - triggered cartilage degradation by suppressing the NF- κ B canonical pathway. Nevertheless, our findings strongly suggest that elimination of the canonical NF- κ B signaling in articular cartilage chondrocytes has the therapeutic potential to ameliorate IL1 β - and TNF α -induced cartilage degradation during OA progression.

The blockade of NF- κ B canonical signaling in rheumatoid diseases of the joint is still controversial owing to the unselective elimination of its various advantages (e.g. on chondrocyte survival), and issues of practical applications such as targeted delivery of the blocking agent(s) (Roman-Blas and Jimenez, 2006). Thus, subsequent

investigations are required to gain more detailed insights into the utility of NF- κ B blockade for the development of effective therapeutic strategies against OA and RA.

5.6. An *ex vivo* hip avulsion model does not indicate a particular importance of NF- κ B canonical signaling in injury induced activation of inflammatory gene expression.

Joint damage due to injury significantly elevates the risk of osteoarthritis; therefore analyzing the pathways that are induced upon trauma has unquestionable importance for better understanding cartilage degeneration. A previously study has showed that physical damage of the articular cartilage rapidly activates the three major MAP kinases (Erk, Jnk, p38) as well as NF- κ B, which in turn triggers intracellular inflammatory signaling pathways (Gruber et al., 2004). Taking into account the advantage of using mice with ablated Nemo/canonical NF- κ B pathway, we have performed an avulsion injury model to assess the contribution of NF- κ B to injury-induced gene expression profile. We have performed expression analysis on a pre-determined, injury-induced panel of genes and, surprisingly, we found that very few genes showed differential expression in NEMO-deficient explants compared with control explants. The only gene suppressed in *NEMO^{fl/y}Col2a1Cre* hips upon explantation of the cartilaginous cap of the hip was *Arginase 1*. In wild-type, *ARG-1* was the most upregulated gene upon injury. ARG-1 is known to participate in hepatic urea cycle, immune system and inflammation responses (Munder, 2009). The function of ARG-1 protein in cartilage so far is still unclear. Curiously, it seems to be regulated in a similar fashion to ADAMTS5, although ADAMTS5 was not significantly suppressed in our experiment. We suggest that the up-regulation of *ARG-1* in wild-type group is possibly due to the inflammation followed by mechanical-induced cartilage damage. Less-regulated *ARG-1* in *NEMO^{fl/y}Col2a1Cre* hip cap might represent lower catabolic metabolism compared to the wild-type group.

We have observed the up-regulation of *Hyaluronan synthase 2 (HAS-2)* in *NEMO^{fl/y}Col2a1Cre* hip caps suggesting the activation of a mechanism which aims to compensate mechanical stress-induced cartilage damage. HAS-2 protein is responsible for hyaluronan (HA) production, which possess multiple functions such as ECM cue for cell migration, space cram and joint lubrication (Spicer and Nguyen,

1999; Watanabe and Yamaguchi, 1996). HA is constitutively generated in the period of injuries to build a scaffold for the growth of fibroblasts and angiogenesis. Elevation of HA concentration in the blood is related to OA and RA. The up-regulation of HAS-2 in *NEMO^{fl/Y}Col2a1Cre* articular cartilage may enrich cartilage ECM and provides a protective mechanism against mechanical stress. Thus, apparently the canonical NF- κ B pathway has a negative influence on hyaluronan-mediated anabolic processes induced upon injury.

MMP-3 and *IL-18* were also up-regulated in *NEMO^{fl/Y}Col2a1Cre* hip caps compared to wild-type. Degradation of aggrecan in degenerative articular cartilage was mainly due to the actions of MMPs and ADAMTSs (Struglics et al., 2006). MMPs are also known to cut collagen II into smaller parts, which could be cleaved by gelatinases (Tchetverikov et al., 2005). In injured or post-compressed human cartilage, the expression of MMP-3 is up-regulated, which is similar to MMP-3 enhancement in the synovial fluid of traumatized-knee (Chubinskaya et al., 1999). The up-regulation of MMP-3 mRNA in *NEMO^{fl/Y}Col2a1Cre* hips upon injury may promote cartilage ECM breakdown. Interestingly, Nemo deficiency results in decreased deposition of MMP-3 in hips exposed to inflammatory cytokines (see before); and in elevated MMP-3 gene expression in hip caps exposed to mechanical stress. This discrepancy may indicate a differential role of the canonical NF- κ B signaling in the control of MMP-3 expression, depending on the nature of external stimuli (inflammatory *versus* mechanical).

IL-1 β is initially produced as a non-active molecule which needs to be further processed to become fully functional. (Black et al., 1988; Hazuda et al., 1989; Mosley et al., 1987). Such processing is carried out by the IL-1 β converting enzyme (ICE or caspase-1) (Black et al., 1989; Miller et al., 1993). Aside from IL-1, IL-18 (interferon gamma inducer) was also found as the substrate of ICE (Dinarello, 1998; Fantuzzi and Dinarello, 1999). IL-1 and IL-18 are structurally-similar, and both initially generated as non-active precursors (Ghayur et al., 1997; Gu et al., 1997). ICE is produced both in the cartilage and the synovial membrane; and the expression of ICE is significantly increased in OA-affected joints. ICE is proposed to be essential for maturation of IL-1 β and IL-18 in OA-affected joints (Saha et al., 1999). Moreover, the expression of IL-1 β , IL-18 and ICE was remarkably increased in OA-affected cartilage. (Saha et al., 1999). Although these observations indicate that IL-18 may

play a role in OA progression, its exact function in OA is still unclear. The fact that upon injury IL-18 is up-regulated in NEMO-null hips compared to wild-type implicates that NF- κ B signaling negatively regulates the expression of this cytokine in a mechanically challenged environment.

Taken together, our *ex vivo* hip injury model demonstrated the upregulation of one “good” gene and two “bad” genes in the absence of NEMO. As for *ARG-1*, it is speculative whether these changes in gene expression are stood for beneficial or harmful response against mechanical stress in the cartilaginous *NEMO^{fl/Y}Col2a1Cre* hip cap. *HAS-2* up-regulation can be recognized as a beneficial factor against the up-regulation of the harmful *MMP-3* and *IL-18*. Interestingly, although Gruber et al., (2014) previously showed that the activation of the NF- κ B signaling pathway among the immediate response to mechanical injury of the articular cartilage, our expression analysis indicates that NEMO/canonical NF- κ B has little influence on the expression of typical genes activated upon mechanical stress.

5.7. NEMO/canonical NF- κ B-deficiency has no apparent consequence on spontaneous, age-associated OA progression in mice

Human osteoarthritis is a slowly progressing degenerative disorder of the articular cartilage in association with, but not caused by aging. Age-related changes in the cartilage ECM, chondrocyte senescence, genetic and epigenetic factors are all contribute for the onset and progression of the diseases (Loeser, 2013). Recent studies have indicated that age-related, or spontaneous, osteoarthritis may be promoted by low level of inflammation of the joint (Greene and Loeser, 2015). This age-associated inflammation is called “inflamm-aging” and NF- κ B signaling could be involved in its regulation. In order to assess the role of Nemo/ NF- κ B in spontaneous osteoarthritis, we have monitored osteoarthritis-like changes of the knee in aging wild-type and *NEMO^{fl/Y}Col2a1Cre* mice. Evaluating distinct levels of cartilage damage, tidemark integrity, chondrocyte cellularity, GAG content and osteophyte formation, these parameters give an overall estimation of OA progression. For our surprise, the assessment of OA progression indicated that *NEMO^{fl/Y}Col2a1Cre* mice displayed comparable cartilage erosion, chondrocyte cellularity and proteoglycan

loss as wild-type mice. No osteophyte formation is found in control and mutant mice. Importantly, careful analysis of the synovial tissue of the joint, we have found no evidence for inflammation or synovial changes in the genotypes. These results demonstrate that NEMO may have a dispensable role in naturally occurring primary osteoarthritis, at least in our rodent model.

However, the impact of canonical NF- κ B signaling in the development of secondary OA is still unclear. To further address this topic and investigate the effect of blocking canonical NF- κ B pathway in post-traumatic OA, we will induce OA by surgical procedures in wild-type and *NEMO*-deficient mice. Transection of the anterior cruciate ligament transection (ACLT) in mouse results in severe OA development post-surgery, thus the ACLT mouse model creates a time-pressing window for studying the early symptoms of OA. Compared to ACLT model, destabilization of the medial meniscus (DMM) surgical instability model offers slower progression of OA and excellent reproducibility. Moreover, the OA symptoms and slow progression of mice receiving DMM surgery are similar to the mice from spontaneous OA models, which make the DMM model more suitable for assessing the early features of secondary OA than ACLT model. Therefore, the DMM model of osteoarthritis (Glasson et al., 2007) will be used in future experiments to confirm the potential of blocking NF- κ B canonical signaling.

6. Conclusion

1. The normal appearance of the pre-natal skeleton in *NEMO^{fl/Y}Col2a1Cre* mice implies that the canonical NF-κB signaling is dispensable embryonic development of endochondral bones.
2. The dwarf phenotype of *NEMO^{fl/Y}Col2a1Cre* mice after birth demonstrates that Nemo/ NF-κB controls postnatal growth of the endochondral skeleton.
3. The canonical NF-κB signaling modulates proliferation of postnatal growth plate chondrocytes through the control of p16 expression.
4. In the absence of Nemo/canonical NF-κB signaling, cell survival of growth plate chondrocytes is compromised.
5. In TNF-α induced cell death, *NEMO^{fl/Y}Col2a1Cre* chondrocytes were more sensitive to apoptosis.
6. Nemo/NF-κB is important for postnatal growth plate morphogenesis by modulating the formation of longitudinal chondrocytes columns.
7. Canonical NF-κB signaling/Nemo play roles for chondrocyte adhesion and spreading.
8. Nemo-deficiency does not alter the biomechanical properties of the postnatal growth plate ECM.
9. Ablation of *NEMO* in chondrocytes results in partial protection against pro-inflammatory cytokine-induced proteoglycan loss in hip explants, suggesting that suppressing the canonical NF-κB cascade by blocking NEMO is a potential therapeutic intervention strategy to ameliorate inflammation-driven arthritis.
10. Nemo/NF-κB has a minor role for injury-induced inflammatory gene expression in a murine articular cartilage avulsion model.
11. In rodent, canonical NF-κB signaling is dispensable for age-related spontaneous osteoarthritis.

In summary, here we have reported that NEMO-deficient mice display a moderate postnatal dwarfism phenotype due to impaired proliferation and apoptosis of growth plate chondrocytes. Reduced migration and enhanced ECM ligand binding affinity of chondrocytes are likely responsible for the slightly disorganized columns in the growth plate of NEMO-deficient mice. Thus, the phenotype of *NEMO^{fl/Y}Col2a1Cre* mice demonstrates a moderate role of NF-κB canonical pathway in development of

CONCLUSION

the postnatal endochondral skeleton. We have proved by mouse genetics that NEMO/NF- κ B is indispensable for mediating pro-inflammatory cytokines-triggered catabolism of the articular cartilage, but it has little effect in trauma-induced gene expression and age-associated, spontaneous osteoarthritis.

7. Summary

NF- κ B proteins are known to mediate expression of numerous genes responding to stress conditions such as inflammation, infection or injury. Studies of bone degenerative diseases have indicated the blockade of NF- κ B canonical signaling as a potential strategy against arthritis. Owing to the absence of suitable animal models, the role of NF- κ B signaling in normal skeletal physiology is still not completely understood. In this study, the X chromosome-localized gene encoding NF- κ B essential modulator (NEMO), a key regulator of the canonical NF- κ B pathway, was conditionally knocked-out using a chondrocyte-specific *Col2a1cre* transgene in mice. *NEMO^{fl/y}Col2a1cre* mice showed the absence of the canonical NF- κ B activation in chondrocytes; and exhibited moderate dwarfism postnatally characterized by shortened growth plate, mild disorganization of columnar chondrocytes and increased apoptosis/necrosis. Primary chondrocytes isolated from costal cartilage displayed reduced migration and proliferation. Pro-inflammatory cytokines induced proteoglycan depletion, monitored by the exposure of the aggrecan degradation neopeptides and glycosaminoglycan release, was significantly less in *NEMO*-deficient hip explants compared with controls. Using an ex vivo hip avulsion model, microarray analysis demonstrated only a few changes in the expression of injury-induced genes compared to wild type. Assessing age-associated, spontaneous osteoarthritis of the knee joint, *NEMO^{fl/y}Col2a1cre* mice displayed comparable articular cartilage destruction with controls. Taken together, the *NEMO*-deficient conditional mouse model demonstrated that: 1) the canonical NF- κ B signaling plays an important role in postnatal skeletal growth; 2) the catabolic effects of pro-inflammatory cytokines in cartilage can be partially eased by blocking the canonical NF- κ B pathway; 3) Nemo-dependent NF- κ B activation has moderate role for gene induction upon injury; and 4) *NEMO*/canonical NF- κ B signaling is dispensable for spontaneous knee arthritis. The *NEMO^{fl/y}Col2a1cre* mice, thus, provide a valuable model system for better understanding the role of canonical NF- κ B for the development and function of the cartilaginous skeleton.

8. Zusammenfassung

Proteine der NF- κ B-Familie beeinflussen die Expression einer Vielzahl von Genen, die auf zelluläre Stresssituationen wie Inflammation, Infektion oder Verletzungen reagieren. Studien von degenerativen Knochenerkrankungen haben die Bedeutung der Blockade des kanonischen NF- κ B Signalwegs als potentiell Ziel zur Behandlung von Osteoarthritis und rheumatoide Arthritis verdeutlicht. Durch den Mangel an geeigneten Tiermodellen ist die Rolle des NF- κ B Signalwegs in der normalen Skelettphysiologie noch immer nicht vollkommen verstanden. In der vorliegenden Studie wurde das X-chromosomalliegende Gen *NEMO* (NF- κ B essential modulator), ein Schlüsselregulator im kanonischen NF- κ B Signalweg, konditional, durch die Verwendung einer knorpelspezifischen *Col2a1cre* transgenen Mauslinie, gelöscht. *NEMO^{fl/y}Col2a1cre* Mäuse zeigten ein Ausbleiben der kanonischen NF- κ B Aktivierung in Chondrozyten und entwickelten postnatal einen mäßigen Kleinwuchs, der durch eine verkürzte Wachstumsfuge, eine leichte Unordnung der säulenförmigen Chondrozyten und eine erhöhte Nekrose/Apoptose verursacht wurde. Primäre Chondrozyten, die aus Rippenknorpel isoliert wurden, zeigten eine reduzierte Migration sowie Proliferation. Pro-inflammatorische Zytokine induzierten Proteoglykanverminderung, dass durch die Freisetzung von Aggrecan-Neoepitopen und Glykosaminoglykanen nachgewiesen wurde, war signifikant weniger in *NEMO*-defizienten Hüftkopffexplantaten im Vergleich zu den Kontrollen. Durch die Verwendung eines Hüftkopfdistorsionsmodells konnte eine Mikroarrayanalyse einige kleine Veränderungen in der Expression von verletzungsbedingten Genen im Vergleich zu Wildtypen aufgezeigt werden. Des Weiteren konnte durch die Beurteilung von altersbedingter, spontaner Osteoarthritis der Kniegelenke eine vergleichbare Zerstörung des artikulären Knorpels in *NEMO^{fl/y}Col2a1cre* Mäusen und Kontrolltieren festgestellt werden. Zusammenfassend zeigte das *NEMO*-defiziente konditionale Mausmodell, dass 1) der kanonische NF- κ B Signalweg eine wichtige Rolle für das postnatale Skelettwachstum spielt; 2) der katabolische Effekt von pro-inflammatorische Zytokinen im Knorpel durch die Blockierung des NF- κ B Signalwegs verringert werden kann; 3) die Aktivierung von NF- κ B durch NEMO eine moderate Rolle in der Geninduktion nach Verletzungen hat; und 4) NEMO-vermittelte kanonische NF- κ B Signaltransduktion entbehrlich für spontane Kniearthrose ist.

NEMO^{fl/y}*Col2a1cre* Mäuse stellen somit ein nützliches Modellsystem dar, um die Rolle von kanonischem NF-κB in der Entwicklung und Funktion des Knorpelskeletts zu verstehen.

9. Reference

- Abad, V., J.L. Meyers, M. Weise, R.I. Gafni, K.M. Barnes, O. Nilsson, J.D. Bacher, and J. Baron. 2002. The role of the resting zone in growth plate chondrogenesis. *Endocrinology*. 143:1851-1857.
- Alford, J.W., and B.J. Cole. 2005a. Cartilage restoration, part 1: basic science, historical perspective, patient evaluation, and treatment options. *The American journal of sports medicine*. 33:295-306.
- Alford, J.W., and B.J. Cole. 2005b. Cartilage restoration, part 2: techniques, outcomes, and future directions. *The American journal of sports medicine*. 33:443-460.
- Amos, N., S. Lauder, A. Evans, M. Feldmann, and J. Bondeson. 2006. Adenoviral gene transfer into osteoarthritis synovial cells using the endogenous inhibitor I κ B reveals that most, but not all, inflammatory and destructive mediators are NF κ B dependent. *Rheumatology (Oxford, England)*. 45:1201-1209.
- Andersen, P.E., Jr., and M. Hauge. 1989. Congenital generalised bone dysplasias: a clinical, radiological, and epidemiological survey. *Journal of medical genetics*. 26:37-44.
- Arendt, E., and R. Dick. 1995. Knee injury patterns among men and women in collegiate basketball and soccer. NCAA data and review of literature. *The American journal of sports medicine*. 23:694-701.
- Aro, E., A.M. Salo, R. Khatri, M. Finnila, I. Miinalainen, R. Sormunen, O. Pakkanen, T. Holster, R. Soininen, C. Prein, H. Clausen-Schaumann, A. Aszodi, J. Tuukkanen, K.I. Kivirikko, E. Schipani, and J. Myllyharju. 2015. Severe Extracellular Matrix Abnormalities and Chondrodysplasia in Mice Lacking Collagen Prolyl 4-Hydroxylase Isoenzyme II in Combination with a Reduced Amount of Isoenzyme I. *The Journal of biological chemistry*. 290:16964-16978.
- Arokoski, J., I. Kiviranta, J. Jurvelin, M. Tammi, and H.J. Helminen. 1993. Long-distance running causes site-dependent decrease of cartilage glycosaminoglycan content in the knee joints of beagle dogs. *Arthritis and rheumatism*. 36:1451-1459.
- Ascenzi, M.G., C. Blanco, I. Drayer, H. Kim, R. Wilson, K.N. Retting, K.M. Lyons, and G. Mohler. 2011. Effect of localization, length and orientation of chondrocytic primary cilium on murine growth plate organization. *Journal of theoretical biology*. 285:147-155.
- Aszodi, A., E.B. Hunziker, C. Brakebusch, and R. Fassler. 2003. Beta1 integrins regulate chondrocyte rotation, G1 progression, and cytokinesis. *Genes & development*. 17:2465-2479.
- Aszodi, A., K.R. Legate, I. Nakchbandi, and R. Fassler. 2006. What mouse mutants teach us about extracellular matrix function. *Annual review of cell and developmental biology*. 22:591-621.
- Ateshian, G.A., W.H. Warden, J.J. Kim, R.P. Grelsamer, and V.C. Mow. 1997. Finite deformation biphasic material properties of bovine articular cartilage from confined compression experiments. *Journal of biomechanics*. 30:1157-1164.
- Auphan, N., J.A. DiDonato, C. Rosette, A. Helmborg, and M. Karin. 1995. Immunosuppression by glucocorticoids: inhibition of NF- κ B activity through induction of I κ B synthesis. *Science (New York, N.Y.)*. 270:286-290.

- Aupperle, K., B. Bennett, Z. Han, D. Boyle, A. Manning, and G. Firestein. 2001. NF-kappa B regulation by I kappa B kinase-2 in rheumatoid arthritis synoviocytes. *Journal of immunology (Baltimore, Md. : 1950)*. 166:2705-2711.
- Ayral, X. 2001. Injections in the treatment of osteoarthritis. *Best practice & research. Clinical rheumatology*. 15:609-626.
- Bacher, S., and M.L. Schmitz. 2004. The NF-kappaB pathway as a potential target for autoimmune disease therapy. *Current pharmaceutical design*. 10:2827-2837.
- Badley, E.M., and P.P. Wang. 1998. Arthritis and the aging population: projections of arthritis prevalence in Canada 1991 to 2031. *The Journal of rheumatology*. 25:138-144.
- Ballock, R.T., and R.J. O'Keefe. 2003. The biology of the growth plate. *The Journal of bone and joint surgery. American volume*. 85-a:715-726.
- Barbosa-Buck, C.O., I.M. Orioli, M. da Graca Dutra, J. Lopez-Camelo, E.E. Castilla, and D.P. Cavalcanti. 2012. Clinical epidemiology of skeletal dysplasias in South America. *American journal of medical genetics. Part A*. 158a:1038-1045.
- Bartz, R.L., and L. Laudicina. 2005. Osteoarthritis after sports knee injuries. *Clinics in sports medicine*. 24:39-45.
- Beg, A.A., and D. Baltimore. 1996. An essential role for NF-kappaB in preventing TNF-alpha-induced cell death. *Science (New York, N.Y.)*. 274:782-784.
- Beg, A.A., W.C. Sha, R.T. Bronson, S. Ghosh, and D. Baltimore. 1995. Embryonic lethality and liver degeneration in mice lacking the RelA component of NF-kappa B. *Nature*. 376:167-170.
- Bengtsson, E., A. Aspberg, D. Heinegard, Y. Sommarin, and D. Spillmann. 2000. The amino-terminal part of PRELP binds to heparin and heparan sulfate. *The Journal of biological chemistry*. 275:40695-40702.
- Bensen, W.G., J.J. Fiechtner, J.I. McMillen, W.W. Zhao, S.S. Yu, E.M. Woods, R.C. Hubbard, P.C. Isakson, K.M. Verburg, and G.S. Geis. 1999. Treatment of osteoarthritis with celecoxib, a cyclooxygenase-2 inhibitor: a randomized controlled trial. *Mayo Clinic proceedings*. 74:1095-1105.
- Bertrand, M.J., S. Milutinovic, K.M. Dickson, W.C. Ho, A. Boudreault, J. Durkin, J.W. Gillard, J.B. Jaquith, S.J. Morris, and P.A. Barker. 2008. cIAP1 and cIAP2 facilitate cancer cell survival by functioning as E3 ligases that promote RIP1 ubiquitination. *Molecular cell*. 30:689-700.
- Bi, W., J.M. Deng, Z. Zhang, R.R. Behringer, and B. de Crombrughe. 1999. Sox9 is required for cartilage formation. *Nature genetics*. 22:85-89.
- Bianchi, G., S. Paderni, D. Tigani, and M. Mercuri. 1999. Osteochondritis dissecans of the lateral femoral condyle. *La Chirurgia degli organi di movimento*. 84:183-187.
- Black, R.A., S.R. Kronheim, M. Cantrell, M.C. Deeley, C.J. March, K.S. Prickett, J. Wignall, P.J. Conlon, D. Cosman, T.P. Hopp, and et al. 1988. Generation of biologically active interleukin-1 beta by proteolytic cleavage of the inactive precursor. *The Journal of biological chemistry*. 263:9437-9442.
- Black, R.A., S.R. Kronheim, and P.R. Sleath. 1989. Activation of interleukin-1 beta by a co-induced protease. *FEBS letters*. 247:386-390.
- Boden, B.P., A.W. Pearsall, W.E. Garrett, Jr., and J.A. Feagin, Jr. 1997. Patellofemoral Instability: Evaluation and Management. *The Journal of the American Academy of Orthopaedic Surgeons*. 5:47-57.
- Bonizzi, G., and M. Karin. 2004. The two NF-kappaB activation pathways and their role in innate and adaptive immunity. *Trends in immunology*. 25:280-288.

- Brandt, K.D., G.N. Smith, Jr., and L.S. Simon. 2000. Intraarticular injection of hyaluronan as treatment for knee osteoarthritis: what is the evidence? *Arthritis and rheumatism*. 43:1192-1203.
- Bremner, P., and M. Heinrich. 2002. Natural products as targeted modulators of the nuclear factor-kappaB pathway. *The Journal of pharmacy and pharmacology*. 54:453-472.
- Brenner, D., H. Blaser, and T.W. Mak. 2015. Regulation of tumour necrosis factor signalling: live or let die. *Nature reviews. Immunology*. 15:362-374.
- Breur, G.J., B.A. VanEnkevort, C.E. Farnum, and N.J. Wilsman. 1991. Linear relationship between the volume of hypertrophic chondrocytes and the rate of longitudinal bone growth in growth plates. *Journal of orthopaedic research : official publication of the Orthopaedic Research Society*. 9:348-359.
- Briggs, M.D., S.M. Hoffman, L.M. King, A.S. Olsen, H. Mohrenweiser, J.G. Leroy, G.R. Mortier, D.L. Rimoïn, R.S. Lachman, E.S. Gaines, and et al. 1995. Pseudoachondroplasia and multiple epiphyseal dysplasia due to mutations in the cartilage oligomeric matrix protein gene. *Nature genetics*. 10:330-336.
- Brighton, C.T. 1978. Structure and function of the growth plate. *Clinical orthopaedics and related research*:22-32.
- Brighton, C.T., and R.M. Hunt. 1986. Histochemical localization of calcium in the fracture callus with potassium pyroantimonate. Possible role of chondrocyte mitochondrial calcium in callus calcification. 703-715 pp.
- Brighton, C.T., and R.M. Hunt. 1991. Early histological and ultrastructural changes in medullary fracture callus. *The Journal of bone and joint surgery. American volume*. 73:832-847.
- Brittberg, M., A. Lindahl, A. Nilsson, C. Ohlsson, O. Isaksson, and L. Peterson. 1994. Treatment of deep cartilage defects in the knee with autologous chondrocyte transplantation. *The New England journal of medicine*. 331:889-895.
- Buckwalter, J.A. 1999. Evaluating methods of restoring cartilaginous articular surfaces. *Clinical orthopaedics and related research*:S224-238.
- Buckwalter, J.A., and H.J. Mankin. 1998. Articular cartilage: tissue design and chondrocyte-matrix interactions. *Instructional course lectures*. 47:477-486.
- Buckwalter, J.A., and J.A. Martin. 2006. Osteoarthritis. *Advanced drug delivery reviews*. 58:150-167.
- Burleigh, A., A. Chanalaris, M.D. Gardiner, C. Driscoll, O. Boruc, J. Saklatvala, and T.L. Vincent. 2012. Joint immobilization prevents murine osteoarthritis and reveals the highly mechanosensitive nature of protease expression in vivo. *Arthritis and rheumatism*. 64:2278-2288.
- Burns, K.A., and F. Martinon. 2004. Inflammatory diseases: is ubiquitinated NEMO at the hub? *Current biology : CB*. 14:R1040-1042.
- Butt, H.J.a.J., M. 1995. Calculation of thermal noise in atomic force microscopy. *Nanotechnology*. 6:1-7.
- Calfee-Mason, K.G., B.T. Spear, and H.P. Glauert. 2004. Effects of vitamin E on the NF-kappaB pathway in rats treated with the peroxisome proliferator, ciprofibrate. *Toxicology and applied pharmacology*. 199:1-9.
- Candela, M.E., L. Cantley, R. Yasuaha, M. Iwamoto, M. Pacifici, and M. Enomoto-Iwamoto. 2014. Distribution of slow-cycling cells in epiphyseal cartilage and requirement of beta-catenin signaling for their maintenance in growth plate. *Journal of orthopaedic research : official publication of the Orthopaedic Research Society*. 32:661-668.

- Carcamo, J.M., A. Pedraza, O. Borquez-Ojeda, and D.W. Golde. 2002. Vitamin C suppresses TNF alpha-induced NF kappa B activation by inhibiting I kappa B alpha phosphorylation. *Biochemistry*. 41:12995-13002.
- Chard, J., and P. Dieppe. 2001. Glucosamine for osteoarthritis: magic, hype, or confusion? It's probably safe-but there's no good evidence that it works. *BMJ (Clinical research ed.)*. 322:1439-1440.
- Chen, Z.J. 2005. Ubiquitin signalling in the NF-kappaB pathway. *Nature cell biology*. 7:758-765.
- Chow, J.C., M.E. Hantes, J.B. Houle, and C.G. Zalavras. 2004. Arthroscopic autogenous osteochondral transplantation for treating knee cartilage defects: a 2- to 5-year follow-up study. *Arthroscopy : the journal of arthroscopic & related surgery : official publication of the Arthroscopy Association of North America and the International Arthroscopy Association*. 20:681-690.
- Chubinskaya, S., K.E. Kuettner, and A.A. Cole. 1999. Expression of matrix metalloproteinases in normal and damaged articular cartilage from human knee and ankle joints. *Laboratory investigation; a journal of technical methods and pathology*. 79:1669-1677.
- Church, V., K. Yamaguchi, P. Tsang, K. Akita, C. Logan, and P. Francis-West. 2005. Expression and function of Bapx1 during chick limb development. *Anatomy and embryology*. 209:461-469.
- Creamer, P. 1999. Intra-articular corticosteroid treatment in osteoarthritis. *Current opinion in rheumatology*. 11:417-421.
- Cuschieri, J., D. Gourlay, I. Garcia, S. Jelacic, and R.V. Maier. 2004. Implications of proteasome inhibition: an enhanced macrophage phenotype. *Cellular immunology*. 227:140-147.
- Cushnaghan, J., and P. Dieppe. 1991. Study of 500 patients with limb joint osteoarthritis. I. Analysis by age, sex, and distribution of symptomatic joint sites. *Annals of the rheumatic diseases*. 50:8-13.
- Cuzzocrea, S., P.K. Chatterjee, E. Mazzon, L. Dugo, I. Serraino, D. Britti, G. Mazzullo, A.P. Caputi, and C. Thiemermann. 2002. Pyrrolidine dithiocarbamate attenuates the development of acute and chronic inflammation. *British journal of pharmacology*. 135:496-510.
- Day, R., B. Morrison, A. Luza, O. Castaneda, A. Strusberg, M. Nahir, K.B. Helgetveit, B. Kress, B. Daniels, J. Bolognese, D. Krupa, B. Seidenberg, and E. Ehrich. 2000. A randomized trial of the efficacy and tolerability of the COX-2 inhibitor rofecoxib vs ibuprofen in patients with osteoarthritis. Rofecoxib/Ibuprofen Comparator Study Group. *Archives of internal medicine*. 160:1781-1787.
- De Bosscher, K., M.L. Schmitz, W. Vanden Berghe, S. Plaisance, W. Fiers, and G. Haegeman. 1997. Glucocorticoid-mediated repression of nuclear factor-kappaB-dependent transcription involves direct interference with transactivation. *Proceedings of the National Academy of Sciences of the United States of America*. 94:13504-13509.
- De Bosscher, K., W. Vanden Berghe, and G. Haegeman. 2000a. Mechanisms of anti-inflammatory action and of immunosuppression by glucocorticoids: negative interference of activated glucocorticoid receptor with transcription factors. *Journal of neuroimmunology*. 109:16-22.
- De Bosscher, K., W. Vanden Berghe, L. Vermeulen, S. Plaisance, E. Boone, and G. Haegeman. 2000b. Glucocorticoids repress NF-kappaB-driven genes by disturbing the interaction of p65 with the basal transcription machinery, irrespective of coactivator levels in the cell. *Proceedings of the National Academy of Sciences of the United States of America*. 97:3919-3924.

- de Crombrugge, B., V. Lefebvre, and K. Nakashima. 2001. Regulatory mechanisms in the pathways of cartilage and bone formation. *Current opinion in cell biology*. 13:721-727.
- Devin, A., A. Cook, Y. Lin, Y. Rodriguez, M. Kelliher, and Z. Liu. 2000. The distinct roles of TRAF2 and RIP in IKK activation by TNF-R1: TRAF2 recruits IKK to TNF-R1 while RIP mediates IKK activation. *Immunity*. 12:419-429.
- Dinarello, C.A. 1998. Interleukin-1 beta, interleukin-18, and the interleukin-1 beta converting enzyme. *Annals of the New York Academy of Sciences*. 856:1-11.
- Ding, L., D. Guo, and G.A. Homandberg. 2009. Fibronectin fragments mediate matrix metalloproteinase upregulation and cartilage damage through proline rich tyrosine kinase 2, c-src, NF-kappaB and protein kinase Cdelta. *Osteoarthritis and cartilage / OARS, Osteoarthritis Research Society*. 17:1385-1392.
- Dobrzanski, P., R.P. Ryseck, and R. Bravo. 1994. Differential interactions of Rel-NF-kappa B complexes with I kappa B alpha determine pools of constitutive and inducible NF-kappa B activity. *The EMBO journal*. 13:4608-4616.
- Dodds, G.S. 1930. Row formation and other types of arrangement of cartilage cells in endochondral ossification. *The Anatomical record*. 46:385-399.
- Drawer, S., and C.W. Fuller. 2001. Propensity for osteoarthritis and lower limb joint pain in retired professional soccer players. *British journal of sports medicine*. 35:402-408.
- Ea, C.K., L. Deng, Z.P. Xia, G. Pineda, and Z.J. Chen. 2006. Activation of IKK by TNFalpha requires site-specific ubiquitination of RIP1 and polyubiquitin binding by NEMO. *Molecular cell*. 22:245-257.
- Elliott, P.J., T.M. Zollner, and W.H. Boehncke. 2003. Proteasome inhibition: a new anti-inflammatory strategy. *Journal of molecular medicine (Berlin, Germany)*. 81:235-245.
- Engstrom, B., M. Forssblad, C. Johansson, and H. Tornkvist. 1990. Does a major knee injury definitely sideline an elite soccer player? *The American journal of sports medicine*. 18:101-105.
- Epinat, J.C., and T.D. Gilmore. 1999. Diverse agents act at multiple levels to inhibit the Rel/NF-kappaB signal transduction pathway. *Oncogene*. 18:6896-6909.
- Eyre, D. 2002. Collagen of articular cartilage. *Arthritis research*. 4:30-35.
- Eyre, D.R., M.A. Weis, and J.J. Wu. 2006. Articular cartilage collagen: an irreplaceable framework? *European cells & materials*. 12:57-63.
- Falah, M., G. Nierenberg, M. Soudry, M. Hayden, and G. Volpin. 2010. Treatment of articular cartilage lesions of the knee. *International Orthopaedics*. 34:621-630.
- Fantuzzi, G., and C.A. Dinarello. 1999. Interleukin-18 and interleukin-1 beta: two cytokine substrates for ICE (caspase-1). *Journal of clinical immunology*. 19:1-11.
- Farnum, C.E., and N.J. Wilsman. 1993. Determination of proliferative characteristics of growth plate chondrocytes by labeling with bromodeoxyuridine. *Calcified tissue international*. 52:110-119.
- Farquharson, C., and D. Jefferies. 2000. Chondrocytes and longitudinal bone growth: the development of tibial dyschondroplasia. *Poultry science*. 79:994-1004.
- Feldmann, M., E. Andreakos, C. Smith, J. Bondeson, S. Yoshimura, S. Kiriakidis, C. Monaco, C. Gasparini, S. Sacre, A. Lundberg, E. Paleolog, N.J. Horwood, F.M. Brennan, and B.M. Foxwell. 2002. Is NF-kappaB a useful therapeutic target in rheumatoid arthritis? *Annals of the rheumatic diseases*. 61 Suppl 2:ii13-18.
- Felson, D.T., R.C. Lawrence, P.A. Dieppe, R. Hirsch, C.G. Helmick, J.M. Jordan, R.S. Kington, N.E. Lane, M.C. Nevitt, Y. Zhang, M. Sowers, T. McAlindon, T.D. Spector, A.R. Poole, S.Z. Yanovski, G. Ateshian, L. Sharma, J.A. Buckwalter,

- K.D. Brandt, and J.F. Fries. 2000. Osteoarthritis: new insights. Part 1: the disease and its risk factors. *Annals of internal medicine*. 133:635-646.
- Feng, J.Q., L. Xing, J.H. Zhang, M. Zhao, D. Horn, J. Chan, B.F. Boyce, S.E. Harris, G.R. Mundy, and D. Chen. 2003. NF-kappaB specifically activates BMP-2 gene expression in growth plate chondrocytes in vivo and in a chondrocyte cell line in vitro. *The Journal of biological chemistry*. 278:29130-29135.
- Fernandez-Minan, A., M.D. Martin-Bermudo, and A. Gonzalez-Reyes. 2007. Integrin signaling regulates spindle orientation in *Drosophila* to preserve the follicular-epithelium monolayer. *Current biology : CB*. 17:683-688.
- Firestein, G.S. 2004. NF-kappaB: Holy Grail for rheumatoid arthritis? *Arthritis and rheumatism*. 50:2381-2386.
- Frank, E.H., and A.J. Grodzinsky. 1987. Cartilage electromechanics--I. Electrokinetic transduction and the effects of electrolyte pH and ionic strength. *Journal of biomechanics*. 20:615-627.
- Frantz, B., E.C. Nordby, G. Bren, N. Steffan, C.V. Paya, R.L. Kincaid, M.J. Tocci, S.J. O'Keefe, and E.A. O'Neill. 1994. Calcineurin acts in synergy with PMA to inactivate I kappa B/MAD3, an inhibitor of NF-kappa B. *The EMBO journal*. 13:861-870.
- Fritz, J., C. Gaissmaier, B. Schewe, and K. Weise. 2006. [Cartilage repair in the knee joint]. *Der Unfallchirurg*. 109:563-574; quiz 575-566.
- Fujihara, S.M., J.S. Cleaveland, L.S. Grosmaire, K.K. Berry, K.A. Kennedy, J.J. Blake, J. Loy, B.M. Rankin, J.A. Ledbetter, and S.G. Nadler. 2000. A D-amino acid peptide inhibitor of NF-kappa B nuclear localization is efficacious in models of inflammatory disease. *Journal of immunology (Baltimore, Md. : 1950)*. 165:1004-1012.
- Garg, A., and B.B. Aggarwal. 2002. Nuclear transcription factor-kappaB as a target for cancer drug development. *Leukemia*. 16:1053-1068.
- Gerondakis, S., M. Grossmann, Y. Nakamura, T. Pohl, and R. Grumont. 1999. Genetic approaches in mice to understand Rel/NF-kappaB and IkappaB function: transgenics and knockouts. *Oncogene*. 18:6888-6895.
- Ghayur, T., S. Banerjee, M. Hugunin, D. Butler, L. Herzog, A. Carter, L. Quintal, L. Sekut, R. Talanian, M. Paskind, W. Wong, R. Kamen, D. Tracey, and H. Allen. 1997. Caspase-1 processes IFN-gamma-inducing factor and regulates LPS-induced IFN-gamma production. *Nature*. 386:619-623.
- Ghiorzo, P., M. Mantelli, S. Gargiulo, C. Gramigni, L. Pastorino, B. Banelli, B. Villaggio, M.C. Coccia, A.R. Sementa, C. Garre, and G. Bianchi-Scarra. 2004. Inverse correlation between p16INK4A expression and NF-kappaB activation in melanoma progression. *Human pathology*. 35:1029-1037.
- Ghosh, S., and M. Karin. 2002. Missing pieces in the NF-kappaB puzzle. *Cell*. 109 Suppl:S81-96.
- Gilbert, J.E. 1998. Current treatment options for the restoration of articular cartilage. *The American journal of knee surgery*. 11:42-46.
- Glasson, S.S., T.J. Blanchet, and E.A. Morris. 2007. The surgical destabilization of the medial meniscus (DMM) model of osteoarthritis in the 129/SvEv mouse. *Osteoarthritis and cartilage / OARS, Osteoarthritis Research Society*. 15:1061-1069.
- Gossec, L., and M. Dougados. 2004. Intra-articular treatments in osteoarthritis: from the symptomatic to the structure modifying. *Annals of the rheumatic diseases*. 63:478-482.

- Greene, M.A., and R.F. Loeser. 2015. Aging-related inflammation in osteoarthritis. *Osteoarthritis and cartilage / OARS, Osteoarthritis Research Society*. 23:1966-1971.
- Gruber, J., T.L. Vincent, M. Hermansson, M. Bolton, R. Wait, and J. Saklatvala. 2004. Induction of interleukin-1 in articular cartilage by explantation and cutting. *Arthritis & Rheumatism*. 50:2539-2546.
- Gu, Y., K. Kuida, H. Tsutsui, G. Ku, K. Hsiao, M.A. Fleming, N. Hayashi, K. Higashino, H. Okamura, K. Nakanishi, M. Kurimoto, T. Tanimoto, R.A. Flavell, V. Sato, M.W. Harding, D.J. Livingston, and M.S. Su. 1997. Activation of interferon-gamma inducing factor mediated by interleukin-1beta converting enzyme. *Science (New York, N.Y.)*. 275:206-209.
- Gunther, K.P., T. Sturmer, S. Sauerland, I. Zeissig, Y. Sun, S. Kessler, H.P. Scharf, H. Brenner, and W. Puhl. 1998. Prevalence of generalised osteoarthritis in patients with advanced hip and knee osteoarthritis: the Ulm Osteoarthritis Study. *Annals of the rheumatic diseases*. 57:717-723.
- Hall, B.K., and T. Miyake. 2000. All for one and one for all: condensations and the initiation of skeletal development. *BioEssays : news and reviews in molecular, cellular and developmental biology*. 22:138-147.
- Hara, E., R. Smith, D. Parry, H. Tahara, S. Stone, and G. Peters. 1996. Regulation of p16CDKN2 expression and its implications for cell immortalization and senescence. *Molecular and cellular biology*. 16:859-867.
- Hayden, M.S., and S. Ghosh. 2004. Signaling to NF-kappaB. *Genes & development*. 18:2195-2224.
- Hayes, W.C., and A.J. Bodine. 1978. Flow-independent viscoelastic properties of articular cartilage matrix. *Journal of biomechanics*. 11:407-419.
- Hayes, W.C., and L.F. Mockros. 1971. Viscoelastic properties of human articular cartilage. *Journal of applied physiology*. 31:562-568.
- Hazuda, D., R.L. Webb, P. Simon, and P. Young. 1989. Purification and characterization of human recombinant precursor interleukin 1 beta. *The Journal of biological chemistry*. 264:1689-1693.
- Heinegard, D., and T. Saxne. 2011. The role of the cartilage matrix in osteoarthritis. *Nature reviews. Rheumatology*. 7:50-56.
- Heliovaara, M., M. Makela, O. Impivaara, P. Knekt, A. Aromaa, and K. Sievers. 1993. Association of overweight, trauma and workload with coxarthrosis. A health survey of 7,217 persons. *Acta orthopaedica Scandinavica*. 64:513-518.
- Hertwig, O. 1893. Ueber den Werth der ersten Furchungszellen für die Organbildung des Embryo Experimentelle Studien am Frosch-und Tritonei. *Archiv für mikroskopische Anatomie*. 42:662-807.
- Hirsch, M.S., L.E. Lunsford, V. Trinkaus-Randall, and K.K. Svoboda. 1997. Chondrocyte survival and differentiation in situ are integrin mediated. *Developmental dynamics : an official publication of the American Association of Anatomists*. 210:249-263.
- Hoffmann, A., T.H. Leung, and D. Baltimore. 2003. Genetic analysis of NF-kappaB/Rel transcription factors defines functional specificities. *The EMBO journal*. 22:5530-5539.
- Horton, W.A. 2003. Skeletal development: insights from targeting the mouse genome. *Lancet (London, England)*. 362:560-569.
- Howlett, C.R. 1979. The fine structure of the proximal growth plate of the avian tibia. *Journal of anatomy*. 128:377-399.

- Hsu, H., J. Huang, H.B. Shu, V. Baichwal, and D.V. Goeddel. 1996. TNF-dependent recruitment of the protein kinase RIP to the TNF receptor-1 signaling complex. *Immunity*. 4:387-396.
- Hunziker, E.B. 1994. Mechanism of longitudinal bone growth and its regulation by growth plate chondrocytes. *Microscopy research and technique*. 28:505-519.
- Huppi, K., S.E. Martin, and N.J. Caplen. 2005. Defining and assaying RNAi in mammalian cells. *Molecular cell*. 17:1-10.
- Iorio, R., W.J. Robb, W.L. Healy, D.J. Berry, W.J. Hozack, R.F. Kyle, D.G. Lewallen, R.T. Trousdale, W.A. Jiranek, V.P. Stamos, and B.S. Parsley. 2008. Orthopaedic surgeon workforce and volume assessment for total hip and knee replacement in the United States: preparing for an epidemic. *The Journal of bone and joint surgery. American volume*. 90:1598-1605.
- Iotsova, V., J. Caamano, J. Loy, Y. Yang, A. Lewin, and R. Bravo. 1997. Osteopetrosis in mice lacking NF-kappaB1 and NF-kappaB2. *Nature medicine*. 3:1285-1289.
- Ivkovic, S., B.S. Yoon, S.N. Popoff, F.F. Safadi, D.E. Libuda, R.C. Stephenson, A. Daluiski, and K.M. Lyons. 2003. Connective tissue growth factor coordinates chondrogenesis and angiogenesis during skeletal development. *Development (Cambridge, England)*. 130:2779-2791.
- Jackson, D.W., P.A. Lalor, H.M. Aberman, and T.M. Simon. 2001. Spontaneous repair of full-thickness defects of articular cartilage in a goat model. A preliminary study. *The Journal of bone and joint surgery. American volume*. 83-A:53-64.
- Jacobs, M.D., and S.C. Harrison. 1998. Structure of an IkappaBalpha/NF-kappaB complex. *Cell*. 95:749-758.
- James, C.B., and T.L. Uhl. 2001. A Review of Articular Cartilage Pathology and the Use of Glucosamine Sulfate. *Journal of Athletic Training*. 36:413-419.
- Janssens, S., and J. Tschopp. 2006. Signals from within: the DNA-damage-induced NF-kappaB response. *Cell death and differentiation*. 13:773-784.
- Jenkins, R.N., S.L. Osborne-Lawrence, A.K. Sinclair, R.L. Eddy, Jr., M.G. Byers, T.B. Shows, and A.D. Duby. 1990. Structure and chromosomal location of the human gene encoding cartilage matrix protein. *The Journal of biological chemistry*. 265:19624-19631.
- Jepsen, J.S., and J. Wengel. 2004. LNA-antisense rivals siRNA for gene silencing. *Current opinion in drug discovery & development*. 7:188-194.
- Jones, S.J., R.A. Lyons, J. Sibert, R. Evans, and S.R. Palmer. 2001. Changes in sports injuries to children between 1983 and 1998: comparison of case series. *Journal of public health medicine*. 23:268-271.
- Jordan, K.M., N.K. Arden, M. Doherty, B. Bannwarth, J.W. Bijlsma, P. Dieppe, K. Gunther, H. Hauselmann, G. Herrero-Beaumont, P. Kaklamanis, S. Lohmander, B. Leeb, M. Lequesne, B. Mazieres, E. Martin-Mola, K. Pavelka, A. Pendleton, L. Punzi, U. Serni, B. Swoboda, G. Verbruggen, I. Zimmerman-Gorska, M. Dougados, and E. Standing Committee for International Clinical Studies Including Therapeutic Trials. 2003. EULAR Recommendations 2003: an evidence based approach to the management of knee osteoarthritis: Report of a Task Force of the Standing Committee for International Clinical Studies Including Therapeutic Trials (ESCISIT). *Annals of the rheumatic diseases*. 62:1145-1155.
- Karsenty, G., H.M. Kronenberg, and C. Settembre. 2009. Genetic control of bone formation. *Annual review of cell and developmental biology*. 25:629-648.
- Kaufman, M.H. 1992. The atlas of mouse development. London: Academic Press.

- Kawai, N., H. Takahashi, H. Nishida, and H. Yokosawa. 2005. Regulation of NF-kappaB/Rel by IkappaB is essential for ascidian notochord formation. *Developmental biology*. 277:80-91.
- Kawai, T., and S. Akira. 2006. TLR signaling. *Cell death and differentiation*. 13:816-825.
- Kawakami, A., T. Nakashima, H. Sakai, A. Hida, S. Urayama, S. Yamasaki, H. Nakamura, H. Ida, Y. Ichinose, T. Aoyagi, I. Furuichi, M. Nakashima, K. Migita, Y. Kawabe, and K. Eguchi. 1999. Regulation of synovial cell apoptosis by proteasome inhibitor. *Arthritis and rheumatism*. 42:2440-2448.
- Keller, R., L. Davidson, A. Edlund, T. Elul, M. Ezin, D. Shook, and P. Skoglund. 2000. Mechanisms of convergence and extension by cell intercalation. *Philosophical transactions of the Royal Society of London. Series B, Biological sciences*. 355:897-922.
- Kelliher, M.A., S. Grimm, Y. Ishida, F. Kuo, B.Z. Stanger, and P. Leder. 1998. The death domain kinase RIP mediates the TNF-induced NF-kappaB signal. *Immunity*. 8:297-303.
- Kember, N.F. 1971. Cell population kinetics of bone growth: the first ten years of autoradiographic studies with tritiated thymidine. *Clinical orthopaedics and related research*. 76:213-230.
- Kember, N.F., J.K. Kirkwood, P.J. Duignan, D. Godfrey, and D.J. Spratt. 1990. Comparative cell kinetics of avian growth plates. *Research in veterinary science*. 49:283-288.
- Kiviranta, I., M. Tammi, J. Jurvelin, J. Arokoski, A.M. Saamanen, and H.J. Helminen. 1992. Articular cartilage thickness and glycosaminoglycan distribution in the canine knee joint after strenuous running exercise. *Clinical orthopaedics and related research*:302-308.
- Knudson, W., and R.F. Loeser. 2002. CD44 and integrin matrix receptors participate in cartilage homeostasis. *Cellular and molecular life sciences : CMLS*. 59:36-44.
- Krakow, D., and D.L. Rimoin. 2010. The skeletal dysplasias. *Genetics in medicine : official journal of the American College of Medical Genetics*. 12:327-341.
- Krappmann, D., and C. Scheidereit. 2005. A pervasive role of ubiquitin conjugation in activation and termination of IkappaB kinase pathways. *EMBO reports*. 6:321-326.
- Kronenberg, H.M. 2003. Developmental regulation of the growth plate. *Nature*. 423:332-336.
- Kuhn, K., S. Hashimoto, and M. Lotz. 2000. IL-1 beta protects human chondrocytes from CD95-induced apoptosis. *Journal of immunology (Baltimore, Md. : 1950)*. 164:2233-2239.
- Kujala, U.M., J. Kaprio, and S. Sarna. 1994. Osteoarthritis of weight bearing joints of lower limbs in former elite male athletes. *BMJ (Clinical research ed.)*. 308:231-234.
- Kujala, U.M., J. Kettunen, H. Paananen, T. Aalto, M.C. Battie, O. Impivaara, T. Videman, and S. Sarna. 1995. Knee osteoarthritis in former runners, soccer players, weight lifters, and shooters. *Arthritis and rheumatism*. 38:539-546.
- Lai, W.M., J.S. Hou, and V.C. Mow. 1991. A triphasic theory for the swelling and deformation behaviors of articular cartilage. *Journal of biomechanical engineering*. 113:245-258.
- Landínez-Parra, N.S., D.A. Garzón-Alvarado, and J.C. Vanegas-Acosta. 2012. Mechanical Behavior of Articular Cartilage.

- Lane, J.G., J.B. Massie, S.T. Ball, M.E. Amiel, A.C. Chen, W.C. Bae, R.L. Sah, and D. Amiel. 2004. Follow-up of osteochondral plug transfers in a goat model: a 6-month study. *The American journal of sports medicine*. 32:1440-1450.
- Langenskiold, A. 1998. Role of the ossification groove of Ranvier in normal and pathologic bone growth: a review. *Journal of pediatric orthopedics*. 18:173-177.
- Laplantine, E., E. Fontan, J. Chiaravalli, T. Lopez, G. Lakisic, M. Veron, F. Agou, and A. Israel. 2009. NEMO specifically recognizes K63-linked poly-ubiquitin chains through a new bipartite ubiquitin-binding domain. *The EMBO journal*. 28:2885-2895.
- Largo, R., M.A. Alvarez-Soria, I. Diez-Ortego, E. Calvo, O. Sanchez-Pernaute, J. Egido, and G. Herrero-Beaumont. 2003. Glucosamine inhibits IL-1beta-induced NFkappaB activation in human osteoarthritic chondrocytes. *Osteoarthritis and cartilage / OARS, Osteoarthritis Research Society*. 11:290-298.
- Lechler, T., and E. Fuchs. 2005. Asymmetric cell divisions promote stratification and differentiation of mammalian skin. *Nature*. 437:275-280.
- Lee, C., W.L. Straus, R. Balshaw, S. Barlas, S. Vogel, and T.J. Schnitzer. 2004a. A comparison of the efficacy and safety of nonsteroidal antiinflammatory agents versus acetaminophen in the treatment of osteoarthritis: a meta-analysis. *Arthritis and rheumatism*. 51:746-754.
- Lee, T.H., J. Shank, N. Cusson, and M.A. Kelliher. 2004b. The kinase activity of Rip1 is not required for tumor necrosis factor-alpha-induced IkappaB kinase or p38 MAP kinase activation or for the ubiquitination of Rip1 by Traf2. *The Journal of biological chemistry*. 279:33185-33191.
- Lefebvre, V., R.R. Behringer, and B. de Crombrughe. 2001. L-Sox5, Sox6 and Sox9 control essential steps of the chondrocyte differentiation pathway. *Osteoarthritis and cartilage / OARS, Osteoarthritis Research Society*. 9 Suppl A:S69-75.
- Legarda-Addison, D., H. Hase, M.A. O'Donnell, and A.T. Ting. 2009. NEMO/IKKgamma regulates an early NF-kappaB-independent cell-death checkpoint during TNF signaling. *Cell death and differentiation*. 16:1279-1288.
- Legate, K.R., S.A. Wickstrom, and R. Fassler. 2009. Genetic and cell biological analysis of integrin outside-in signaling. *Genes & development*. 23:397-418.
- Lewandrowski, K.U., J. Muller, and G. Schollmeier. 1997. Concomitant meniscal and articular cartilage lesions in the femorotibial joint. *The American journal of sports medicine*. 25:486-494.
- Lewis, A.J., and A.M. Manning. 1999. New targets for anti-inflammatory drugs. *Current opinion in chemical biology*. 3:489-494.
- Li, H., M. Kobayashi, M. Blonska, Y. You, and X. Lin. 2006. Ubiquitination of RIP is required for tumor necrosis factor alpha-induced NF-kappaB activation. *The Journal of biological chemistry*. 281:13636-13643.
- Li, Q., Q. Lu, J.Y. Hwang, D. Buscher, K.F. Lee, J.C. Izpisua-Belmonte, and I.M. Verma. 1999a. IKK1-deficient mice exhibit abnormal development of skin and skeleton. *Genes & development*. 13:1322-1328.
- Li, Q., D. Van Antwerp, F. Mercurio, K.F. Lee, and I.M. Verma. 1999b. Severe liver degeneration in mice lacking the IkappaB kinase 2 gene. *Science (New York, N.Y.)*. 284:321-325.
- Liacini, A., J. Sylvester, W.Q. Li, W. Huang, F. Dehnade, M. Ahmad, and M. Zafarullah. 2003. Induction of matrix metalloproteinase-13 gene expression by TNF-alpha is mediated by MAP kinases, AP-1, and NF-kappaB transcription factors in articular chondrocytes. *Experimental cell research*. 288:208-217.

- Lianxu, C., J. Hongti, and Y. Changlong. 2006. NF-kappaBp65-specific siRNA inhibits expression of genes of COX-2, NOS-2 and MMP-9 in rat IL-1beta-induced and TNF-alpha-induced chondrocytes. *Osteoarthritis and cartilage / OARS, Osteoarthritis Research Society*. 14:367-376.
- Lin, J., W. Zhang, A. Jones, and M. Doherty. 2004. Efficacy of topical non-steroidal anti-inflammatory drugs in the treatment of osteoarthritis: meta-analysis of randomised controlled trials. *BMJ (Clinical research ed.)*. 329:324.
- Linn, F.C., and L. Sokoloff. 1965. MOVEMENT AND COMPOSITION OF INTERSTITIAL FLUID OF CARTILAGE. *Arthritis and rheumatism*. 8:481-494.
- Lo, G.H., M. LaValley, T. McAlindon, and D.T. Felson. 2003. Intra-articular hyaluronic acid in treatment of knee osteoarthritis: a meta-analysis. *Jama*. 290:3115-3121.
- Loeser, R.F. 2013. Aging processes and the development of osteoarthritis. *Current opinion in rheumatology*. 25:108-113.
- Lohmander, L.S., N. Dalen, G. Englund, M. Hamalainen, E.M. Jensen, K. Karlsson, M. Odensten, L. Ryd, I. Sernbo, O. Suomalainen, and A. Tegnander. 1996. Intra-articular hyaluronan injections in the treatment of osteoarthritis of the knee: a randomised, double blind, placebo controlled multicentre trial. Hyaluronan Multicentre Trial Group. *Annals of the rheumatic diseases*. 55:424-431.
- Lohmander, L.S., H. Roos, L. Dahlberg, L.A. Hoerrner, and M.W. Lark. 1994. Temporal patterns of stromelysin-1, tissue inhibitor, and proteoglycan fragments in human knee joint fluid after injury to the cruciate ligament or meniscus. *Journal of orthopaedic research : official publication of the Orthopaedic Research Society*. 12:21-28.
- Makarov, S.S. 2001. NF-kappa B in rheumatoid arthritis: a pivotal regulator of inflammation, hyperplasia, and tissue destruction. *Arthritis research*. 3:200-206.
- Mankin, H.J., V.C. Mow, J.A. Buckwalter, and J.P. Lannotti. 1994. Form and function of articular cartilage. In *Orthopaedic Basic Science*. American Academy of Orthopaedic Surgeons, Rosemont, IL. 1-44.
- Mann, H.H., S. Ozbek, J. Engel, M. Paulsson, and R. Wagener. 2004. Interactions between the cartilage oligomeric matrix protein and matrilins. Implications for matrix assembly and the pathogenesis of chondrodysplasias. *The Journal of biological chemistry*. 279:25294-25298.
- Manna, S.K., A. Mukhopadhyay, and B.B. Aggarwal. 2000. Leflunomide suppresses TNF-induced cellular responses: effects on NF-kappa B, activator protein-1, c-Jun N-terminal protein kinase, and apoptosis. *Journal of immunology (Baltimore, Md. : 1950)*. 165:5962-5969.
- Marcu, K.B., M. Otero, E. Olivotto, R.M. Borzi, and M.B. Goldring. 2010. NF-kappaB signaling: multiple angles to target OA. *Current drug targets*. 11:599-613.
- Maroudas, A. 1979. Physicochemical properties of articular cartilage. In *Adult Articular Cartilage*. United Kingdom: Cambridge University Press, Kent. 215-290.
- Maroudas, A., and P. Bullough. 1968. Permeability of articular cartilage. *Nature*. 219:1260-1261.
- Maroudas, A., E. Wachtel, G. Grushko, E.P. Katz, and P. Weinberg. 1991. The effect of osmotic and mechanical pressures on water partitioning in articular cartilage. *Biochimica et biophysica acta*. 1073:285-294.
- Mason, L., R.A. Moore, J.E. Edwards, S. Derry, and H.J. McQuay. 2004. Topical NSAIDs for chronic musculoskeletal pain: systematic review and meta-analysis. *BMC musculoskeletal disorders*. 5:28.
- Masuda, K., R.L. Sah, M.J. Hejna, and E.J. Thonar. 2003. A novel two-step method for the formation of tissue-engineered cartilage by mature bovine

- chondrocytes: the alginate-recovered-chondrocyte (ARC) method. *Journal of orthopaedic research : official publication of the Orthopaedic Research Society*. 21:139-148.
- McAdams, T.R., K. Mithoefer, J.M. Scopp, and B.R. Mandelbaum. 2010. Articular Cartilage Injury in Athletes. *Cartilage*. 1:165-179.
- McAlindon, T.E., M.P. LaValley, J.P. Gulin, and D.T. Felson. 2000. Glucosamine and chondroitin for treatment of osteoarthritis: a systematic quality assessment and meta-analysis. *Jama*. 283:1469-1475.
- McManus, M.T., and P.A. Sharp. 2002. Gene silencing in mammals by small interfering RNAs. *Nature reviews. Genetics*. 3:737-747.
- Meierhofer, C., and C.J. Wiedermann. 2003. New insights into the pharmacological and toxicological effects of thalidomide. *Current opinion in drug discovery & development*. 6:92-99.
- Mendes, A.F., M.M. Caramona, A.P. de Carvalho, and M.C. Lopes. 2002. Diacerhein and rhein prevent interleukin-1beta-induced nuclear factor-kappaB activation by inhibiting the degradation of inhibitor kappaB-alpha. *Pharmacology & toxicology*. 91:22-28.
- Merx, H., K.E. Dreinhofer, and K.P. Gunther. 2007. [Socioeconomic relevance of osteoarthritis in Germany]. *Zeitschrift fur Orthopadie und Unfallchirurgie*. 145:421-429.
- Messner, K., and J. Gillquist. 1996. Cartilage repair. A critical review. *Acta orthopaedica Scandinavica*. 67:523-529.
- Meyer, S., N.G. Kohler, and A. Joly. 1997. Cyclosporine A is an uncompetitive inhibitor of proteasome activity and prevents NF-kappaB activation. *FEBS letters*. 413:354-358.
- Micheau, O., S. Lens, O. Gaide, K. Alevizopoulos, and J. Tschopp. 2001. NF-kappaB signals induce the expression of c-FLIP. *Molecular and cellular biology*. 21:5299-5305.
- Millennium, W.H.O.S.G.o.t.B.o.M.C.a.t.S.o.t.N. 2003. The burden of musculoskeletal conditions at the start of the new millennium. *World Health Organization technical report series*. 919:i-x, 1-218, back cover.
- Miller, D.K., J.M. Ayala, L.A. Egger, S.M. Raju, T.T. Yamin, G.J. Ding, E.P. Gaffney, A.D. Howard, O.C. Palyha, A.M. Rolando, and et al. 1993. Purification and characterization of active human interleukin-1 beta-converting enzyme from THP.1 monocytic cells. *The Journal of biological chemistry*. 268:18062-18069.
- Mithofer, K., L. Peterson, B.R. Mandelbaum, and T. Minas. 2005. Articular cartilage repair in soccer players with autologous chondrocyte transplantation: functional outcome and return to competition. *The American journal of sports medicine*. 33:1639-1646.
- Mor, A., S.B. Abramson, and M.H. Pillinger. 2005. The fibroblast-like synovial cell in rheumatoid arthritis: a key player in inflammation and joint destruction. *Clinical immunology (Orlando, Fla.)*. 115:118-128.
- Morris, N.P., Keene, D. R., Horton, W. A. 2002. Cartilage morphology. In: Royce, P. M., Steinmann, B., eds. Extracellular matrix and heritable disorders of connective tissue. 2nd edn. New York: Alan R Liss.
- Morriss-Kay, G.M. 2001. Derivation of the mammalian skull vault. *Journal of anatomy*. 199:143-151.
- Mosley, B., D.L. Urdal, K.S. Prickett, A. Larsen, D. Cosman, P.J. Conlon, S. Gillis, and S.K. Dower. 1987. The interleukin-1 receptor binds the human interleukin-1 alpha precursor but not the interleukin-1 beta precursor. *The Journal of biological chemistry*. 262:2941-2944.

- Moti, A.W., and L.J. Micheli. 2003. Meniscal and articular cartilage injury in the skeletally immature knee. *Instructional course lectures*. 52:683-690.
- Mow, V.C., M.H. Holmes, and W.M. Lai. 1984. Fluid transport and mechanical properties of articular cartilage: a review. *Journal of biomechanics*. 17:377-394.
- Mow, V.C., S.C. Kuei, W.M. Lai, and C.G. Armstrong. 1980. Biphasic creep and stress relaxation of articular cartilage in compression? Theory and experiments. *Journal of biomechanical engineering*. 102:73-84.
- Mow, V.C., and A. Ratcliffe. 1997. Structure and Function of Articular Cartilage and Meniscus. Lippincott-Raven, Philadelphia, PA.
- Mow, V.C., A. Ratcliffe, and A.R. Poole. 1992. Cartilage and diarthrodial joints as paradigms for hierarchical materials and structures. *Biomaterials*. 13:67-97.
- Munder, M. 2009. Arginase: an emerging key player in the mammalian immune system. *British journal of pharmacology*. 158:638-651.
- Nagahama, R., A. Yamada, J. Tanaka, R. Aizawa, D. Suzuki, H. Kassai, M. Yamamoto, K. Mishima, A. Aiba, K. Maki, and R. Kamijo. 2016. Rho GTPase protein Cdc42 is critical for postnatal cartilage development. *Biochemical and biophysical research communications*. 470:813-817.
- Nagase, H., and M. Kashiwagi. 2003. Aggrecanases and cartilage matrix degradation. *Arthritis research & therapy*. 5:94-103.
- Neame, P.J., H. Tapp, and A. Azizan. 1999. Noncollagenous, nonproteoglycan macromolecules of cartilage. *Cellular and molecular life sciences : CMLS*. 55:1327-1340.
- Neame, R., W. Zhang, and M. Doherty. 2004. A historic issue of the Annals: three papers examine paracetamol in osteoarthritis. *Annals of the rheumatic diseases*. 63:897-900.
- O'Donnell, M.A., H. Hase, D. Legarda, and A.T. Ting. 2012. NEMO inhibits programmed necrosis in an NFkappaB-independent manner by restraining RIP1. *PLoS one*. 7:e41238.
- O'Donnell, M.A., D. Legarda-Addison, P. Skountzos, W.C. Yeh, and A.T. Ting. 2007. Ubiquitination of RIP1 regulates an NF-kappaB-independent cell-death switch in TNF signaling. *Current biology : CB*. 17:418-424.
- Odenbring, S., N. Egund, A. Lindstrand, L.S. Lohmander, and H. Willen. 1992. Cartilage regeneration after proximal tibial osteotomy for medial gonarthrosis. An arthroscopic, roentgenographic, and histologic study. *Clinical orthopaedics and related research*:210-216.
- Ogden, J., and L. Rosenberg. 1988. Defining the growth plate. Raven Press, New York, NY, USA.
- Ohlsson, C., A. Nilsson, O. Isaksson, and A. Lindahl. 1992. Growth hormone induces multiplication of the slowly cycling germinal cells of the rat tibial growth plate. *Proceedings of the National Academy of Sciences of the United States of America*. 89:9826-9830.
- Olivotto, E., R.M. Borzi, R. Vitellozzi, S. Pagani, A. Facchini, M. Battistelli, M. Penzo, X. Li, F. Flamigni, J. Li, E. Falcieri, A. Facchini, and K.B. Marcu. 2008. Differential requirements for IKKalpha and IKKbeta in the differentiation of primary human osteoarthritic chondrocytes. *Arthritis and rheumatism*. 58:227-239.
- Orioli, I.M., E.E. Castilla, and J.G. Barbosa-Neto. 1986. The birth prevalence rates for the skeletal dysplasias. *Journal of medical genetics*. 23:328-332.
- Ortega, N., D.J. Behonick, and Z. Werb. 2004. Matrix remodeling during endochondral ossification. *Trends in cell biology*. 14:86-93.

- Park, J., M. Gebhardt, S. Golovchenko, F. Perez-Branguli, T. Hattori, C. Hartmann, X. Zhou, B. deCrombrugge, M. Stock, H. Schneider, and K. von der Mark. 2015. Dual pathways to endochondral osteoblasts: a novel chondrocyte-derived osteoprogenitor cell identified in hypertrophic cartilage. *Biology open*. 4:608-621.
- Park, M., Y. Yong, S.W. Choi, J.H. Kim, J.E. Lee, and D.W. Kim. 2007. Constitutive RelA activation mediated by Nkx3.2 controls chondrocyte viability. *Nature cell biology*. 9:287-298.
- Pasparakis, M., T. Luedde, and M. Schmidt-Suppran. 2006. Dissection of the NF-kappaB signalling cascade in transgenic and knockout mice. *Cell death and differentiation*. 13:861-872.
- Patel, D.V., N.M. Breazeale, C.T. Behr, R.F. Warren, T.L. Wickiewicz, and S.J. O'Brien. 1998. Osteonecrosis of the knee: current clinical concepts. *Knee surgery, sports traumatology, arthroscopy : official journal of the ESSKA*. 6:2-11.
- Pattoli, M.A., J.F. MacMaster, K.R. Gregor, and J.R. Burke. 2005. Collagen and aggrecan degradation is blocked in interleukin-1-treated cartilage explants by an inhibitor of IkappaB kinase through suppression of metalloproteinase expression. *The Journal of pharmacology and experimental therapeutics*. 315:382-388.
- Payne, D.N., and I.M. Adcock. 2001. Molecular mechanisms of corticosteroid actions. *Paediatric respiratory reviews*. 2:145-150.
- Pearle, A.D., R.F. Warren, and S.A. Rodeo. 2005. Basic science of articular cartilage and osteoarthritis. *Clinics in sports medicine*. 24:1-12.
- Perkins, N.D. 2003. Oncogenes, tumor suppressors and p52 NF-kappaB. *Oncogene*. 22:7553-7556.
- Perkins, N.D. 2006. Post-translational modifications regulating the activity and function of the nuclear factor kappa B pathway. *Oncogene*. 25:6717-6730.
- Perkins, N.D. 2007. Integrating cell-signalling pathways with NF-kappaB and IKK function. *Nature reviews. Molecular cell biology*. 8:49-62.
- Perkins, N.D., and T.D. Gilmore. 2006. Good cop, bad cop: the different faces of NF-kappaB. *Cell death and differentiation*. 13:759-772.
- Pfuntner, A., L.M. Wier, and C. Steiner. 2006. Costs for Hospital Stays in the United States, 2011: Statistical Brief #168. *In Healthcare Cost and Utilization Project (HCUP) Statistical Briefs*, Rockville MD.
- Piasecki, D.P., K.P. Spindler, T.A. Warren, J.T. Andrish, and R.D. Parker. 2003. Intraarticular injuries associated with anterior cruciate ligament tear: findings at ligament reconstruction in high school and recreational athletes. An analysis of sex-based differences. *The American journal of sports medicine*. 31:601-605.
- Pinkenburg, O., J. Platz, C. Beisswenger, C. Vogelmeier, and R. Bals. 2004. Inhibition of NF-kappaB mediated inflammation by siRNA expressed by recombinant adeno-associated virus. *Journal of virological methods*. 120:119-122.
- Pirog, K.A., and M.D. Briggs. 2010. Skeletal dysplasias associated with mild myopathy-a clinical and molecular review. *Journal of biomedicine & biotechnology*. 2010:686457.
- Poole, C.A., M.H. Flint, and B.W. Beaumont. 1987. Chondrons in cartilage: ultrastructural analysis of the pericellular microenvironment in adult human articular cartilages. *Journal of orthopaedic research : official publication of the Orthopaedic Research Society*. 5:509-522.

- Prein, C., N. Warmbold, Z. Farkas, M. Schieker, A. Aszodi, and H. Clausen-Schaumann. 2016. Structural and mechanical properties of the proliferative zone of the developing murine growth plate cartilage assessed by atomic force microscopy. *Matrix biology : journal of the International Society for Matrix Biology*. 50:1-15.
- Provot, S., H. Kempf, L.C. Murtaugh, U.I. Chung, D.W. Kim, J. Chyung, H.M. Kronenberg, and A.B. Lassar. 2006. Nkx3.2/Bapx1 acts as a negative regulator of chondrocyte maturation. *Development (Cambridge, England)*. 133:651-662.
- Raducanu, A., and A. Aszodi. 2008. Knock-Out Mice in Osteoarthritis Research. *Current Rheumatology Reviews*. 4:183-192.
- Raducanu, A., E.B. Hunziker, I. Drosse, and A. Aszodi. 2009. Beta1 integrin deficiency results in multiple abnormalities of the knee joint. *The Journal of biological chemistry*. 284:23780-23792.
- Rajewsky, K., H. Gu, R. Kuhn, U.A. Betz, W. Muller, J. Roes, and F. Schwenk. 1996. Conditional gene targeting. *The Journal of clinical investigation*. 98:600-603.
- Rasmussen, S.A., F.R. Bieber, B.R. Benacerraf, R.S. Lachman, D.L. Rimoin, and L.B. Holmes. 1996. Epidemiology of osteochondrodysplasias: changing trends due to advances in prenatal diagnosis. *American journal of medical genetics*. 61:49-58.
- Rayess, H., M.B. Wang, and E.S. Srivatsan. 2012. Cellular senescence and tumor suppressor gene p16. *International Journal of Cancer. Journal International du Cancer*. 130:1715-1725.
- Richette, P., T. Bardin, and C. Stheneur. 2008. Achondroplasia: from genotype to phenotype. *Joint, bone, spine : revue du rhumatisme*. 75:125-130.
- Riyazi, N., F.R. Rosendaal, E. Slagboom, H.M. Kroon, F.C. Breedveld, and M. Kloppenburg. 2008. Risk factors in familial osteoarthritis: the GARP sibling study. *Osteoarthritis and cartilage / OARS, Osteoarthritis Research Society*. 16:654-659.
- Robi, K., N. Jakob, K. Matevz, and V. Matjaz. 2013. The Physiology of Sports Injuries and Repair Processes.
- Rodriguez, J.I., E. Delgado, and R. Paniagua. 1985. Changes in young rat radius following excision of the perichondrial ring. *Calcified tissue international*. 37:677-683.
- Roman-Blas, J.A., and S.A. Jimenez. 2006. NF-kappaB as a potential therapeutic target in osteoarthritis and rheumatoid arthritis. *Osteoarthritis and cartilage / OARS, Osteoarthritis Research Society*. 14:839-848.
- Romberger, D.J. 1997. Fibronectin. *The international journal of biochemistry & cell biology*. 29:939-943.
- Roos, E.M., and L. Dahlberg. 2005. Positive effects of moderate exercise on glycosaminoglycan content in knee cartilage: a four-month, randomized, controlled trial in patients at risk of osteoarthritis. *Arthritis and rheumatism*. 52:3507-3514.
- Roos, H. 1998. Are there long-term sequelae from soccer? *Clinics in sports medicine*. 17:819-831, viii.
- Roughley, P.J. 2001. Articular cartilage and changes in arthritis: noncollagenous proteins and proteoglycans in the extracellular matrix of cartilage. *Arthritis research*. 3:342-347.
- Rudolph, D., W.C. Yeh, A. Wakeham, B. Rudolph, D. Nallainathan, J. Potter, A.J. Elia, and T.W. Mak. 2000. Severe liver degeneration and lack of NF-kappaB

- activation in NEMO/IKKgamma-deficient mice. *Genes & development*. 14:854-862.
- Saha, N., F. Moldovan, G. Tardif, J.P. Pelletier, J.M. Cloutier, and J. Martel-Pelletier. 1999. Interleukin-1beta-converting enzyme/caspase-1 in human osteoarthritic tissues: localization and role in the maturation of interleukin-1beta and interleukin-18. *Arthritis and rheumatism*. 42:1577-1587.
- Sakai, K., L. Hiripi, V. Glumoff, O. Brandau, R. Eerola, E. Vuorio, Z. Bosze, R. Fassler, and A. Aszodi. 2001. Stage- and tissue-specific expression of a Col2a1-Cre fusion gene in transgenic mice. *Matrix biology : journal of the International Society for Matrix Biology*. 19:761-767.
- Samad, T.A., K.A. Moore, A. Sapirstein, S. Billet, A. Allchorne, S. Poole, J.V. Bonventre, and C.J. Woolf. 2001. Interleukin-1beta-mediated induction of Cox-2 in the CNS contributes to inflammatory pain hypersensitivity. *Nature*. 410:471-475.
- Scheinman, R.I., P.C. Cogswell, A.K. Lofquist, and A.S. Baldwin, Jr. 1995. Role of transcriptional activation of I kappa B alpha in mediation of immunosuppression by glucocorticoids. *Science (New York, N.Y.)*. 270:283-286.
- Schipani, E., H.E. Ryan, S. Didrickson, T. Kobayashi, M. Knight, and R.S. Johnson. 2001. Hypoxia in cartilage: HIF-1alpha is essential for chondrocyte growth arrest and survival. *Genes & development*. 15:2865-2876.
- Schmidt-Suppran, M., W. Bloch, G. Courtois, K. Addicks, A. Israel, K. Rajewsky, and M. Pasparakis. 2000. NEMO/IKK gamma-deficient mice model incontinentia pigmenti. *Molecular cell*. 5:981-992.
- Schopf, L., A. Savinainen, K. Anderson, J. Kujawa, M. DuPont, M. Silva, E. Siebert, S. Chandra, J. Morgan, P. Gangurde, D. Wen, J. Lane, Y. Xu, M. Hepperle, G. Harriman, T. Ocain, and B. Jaffee. 2006. IKKbeta inhibition protects against bone and cartilage destruction in a rat model of rheumatoid arthritis. *Arthritis and rheumatism*. 54:3163-3173.
- Setton, L.A., V.C. Mow, and D.S. Howell. 1995. Mechanical behavior of articular cartilage in shear is altered by transection of the anterior cruciate ligament. *Journal of orthopaedic research : official publication of the Orthopaedic Research Society*. 13:473-482.
- Sil, A.K., S. Maeda, Y. Sano, D.R. Roop, and M. Karin. 2004. I kappa B kinase-alpha acts in the epidermis to control skeletal and craniofacial morphogenesis. *Nature*. 428:660-664.
- Simon, B.R., R.S. Coats, and S.L. Woo. 1984. Relaxation and creep quasilinear viscoelastic models for normal articular cartilage. *Journal of biomechanical engineering*. 106:159-164.
- Smith, A.D., and S.S. Tao. 1995. Knee injuries in young athletes. *Clinics in sports medicine*. 14:629-650.
- Smolen, J.S., and G. Steiner. 2003. Therapeutic strategies for rheumatoid arthritis. *Nature reviews. Drug discovery*. 2:473-488.
- Song, W., C.W. Fhu, K.H. Ang, C.H. Liu, N.A. Johari, D. Lio, S. Abraham, W. Hong, S.E. Moss, J. Greenwood, and X. Wang. 2015. The fetal mouse metatarsal bone explant as a model of angiogenesis. *Nature protocols*. 10:1459-1473.
- Sophia Fox, A.J., A. Bedi, and S.A. Rodeo. 2009. The Basic Science of Articular Cartilage: Structure, Composition, and Function. *Sports Health*. 1:461-468.
- Spicer, A.P., and T.K. Nguyen. 1999. Mammalian hyaluronan synthases: investigation of functional relationships in vivo. *Biochemical Society transactions*. 27:109-115.

- Stanitski, C.L. 1995. Articular hypermobility and chondral injury in patients with acute patellar dislocation. *The American journal of sports medicine*. 23:146-150.
- Stanton, H., S.B. Golub, F.M. Rogerson, K. Last, C.B. Little, and A.J. Fosang. 2011. Investigating ADAMTS-mediated aggrecanolysis in mouse cartilage. *Nature protocols*. 6:388-404.
- Steadman, J.R., B.S. Miller, S.G. Karas, T.F. Schlegel, K.K. Briggs, and R.J. Hawkins. 2003. The microfracture technique in the treatment of full-thickness chondral lesions of the knee in National Football League players. *The journal of knee surgery*. 16:83-86.
- Streuli, C.H. 2009. Integrins and cell-fate determination. *Journal of cell science*. 122:171-177.
- Struglics, A., S. Larsson, M.A. Pratta, S. Kumar, M.W. Lark, and L.S. Lohmander. 2006. Human osteoarthritis synovial fluid and joint cartilage contain both aggrecanase- and matrix metalloproteinase-generated aggrecan fragments. *Osteoarthritis and cartilage / OARS, Osteoarthritis Research Society*. 14:101-113.
- Su, M.S., and A. Semerjian. 1991. Activation of transcription factor NF kappa B in Jurkat cells is inhibited selectively by FK 506 in a signal-dependent manner. *Transplantation proceedings*. 23:2912-2915.
- Taddei, I., M.A. Deugnier, M.M. Faraldo, V. Petit, D. Bouvard, D. Medina, R. Fassler, J.P. Thiery, and M.A. Glukhova. 2008. Beta1 integrin deletion from the basal compartment of the mammary epithelium affects stem cells. *Nature cell biology*. 10:716-722.
- Tak, P.P., D.M. Gerlag, K.R. Aupperle, D.A. van de Geest, M. Overbeek, B.L. Bennett, D.L. Boyle, A.M. Manning, and G.S. Firestein. 2001. Inhibitor of nuclear factor kappaB kinase beta is a key regulator of synovial inflammation. *Arthritis and rheumatism*. 44:1897-1907.
- Tchetverikov, I., L.S. Lohmander, N. Verzijl, T.W. Huizinga, J.M. TeKoppele, R. Hanemaaijer, and J. DeGroot. 2005. MMP protein and activity levels in synovial fluid from patients with joint injury, inflammatory arthritis, and osteoarthritis. *Annals of the rheumatic diseases*. 64:694-698.
- Tegeder, I., J. Pfeilschifter, and G. Geisslinger. 2001. Cyclooxygenase-independent actions of cyclooxygenase inhibitors. *FASEB journal : official publication of the Federation of American Societies for Experimental Biology*. 15:2057-2072.
- Ting, A.T., F.X. Pimentel-Muiños, and B. Seed. 1996. RIP mediates tumor necrosis factor receptor 1 activation of NF-kappaB but not Fas/APO-1-initiated apoptosis. *The EMBO journal*. 15:6189-6196.
- Tomita, T., E. Takeuchi, N. Tomita, R. Morishita, M. Kaneko, K. Yamamoto, T. Nakase, H. Seki, K. Kato, Y. Kaneda, and T. Ochi. 1999. Suppressed severity of collagen-induced arthritis by in vivo transfection of nuclear factor kappaB decoy oligodeoxynucleotides as a gene therapy. *Arthritis and rheumatism*. 42:2532-2542.
- Torzilli, P.A. 1985. Influence of cartilage conformation on its equilibrium water partition. *Journal of orthopaedic research : official publication of the Orthopaedic Research Society*. 3:473-483.
- Torzilli, P.A., R. Grigiene, J. Borrelli, Jr., and D.L. Helfet. 1999. Effect of impact load on articular cartilage: cell metabolism and viability, and matrix water content. *Journal of biomechanical engineering*. 121:433-441.
- Toyoshima, F., and E. Nishida. 2007. Integrin-mediated adhesion orients the spindle parallel to the substratum in an EB1- and myosin X-dependent manner. *The EMBO journal*. 26:1487-1498.

- Uthoff, H.K. 1988. Development of the growth plate during intrauterine life. In: Uthoff HK, Wiley JJ, eds. Behavior of the growth plate. New York: Raven Press 17-24.
- Van Antwerp, D.J., S.J. Martin, T. Kafri, D.R. Green, and I.M. Verma. 1996. Suppression of TNF-alpha-induced apoptosis by NF-kappaB. *Science (New York, N.Y.)*. 274:787-789.
- Vane, J.R., Y.S. Bakhle, and R.M. Botting. 1998. Cyclooxygenases 1 and 2. *Annual review of pharmacology and toxicology*. 38:97-120.
- Vanky, P., U. Brockstedt, A. Hjerpe, and B. Wikstrom. 1998. Kinetic studies on epiphyseal growth cartilage in the normal mouse. *Bone*. 22:331-339.
- Venkataraman, L., S.J. Burakoff, and R. Sen. 1995. FK506 inhibits antigen receptor-mediated induction of c-rel in B and T lymphoid cells. *The Journal of experimental medicine*. 181:1091-1099.
- Verma, P., and K. Dalal. 2011. ADAMTS-4 and ADAMTS-5: key enzymes in osteoarthritis. *Journal of cellular biochemistry*. 112:3507-3514.
- Vincenti, M.P., and C.E. Brinckerhoff. 2002. Transcriptional regulation of collagenase (MMP-1, MMP-13) genes in arthritis: integration of complex signaling pathways for the recruitment of gene-specific transcription factors. *Arthritis research*. 4:157-164.
- Vos, T., A.D. Flaxman, M. Naghavi, R. Lozano, C. Michaud, M. Ezzati, K. Shibuya, J.A. Salomon, S. Abdalla, V. Aboyans, J. Abraham, I. Ackerman, R. Aggarwal, S.Y. Ahn, M.K. Ali, M. Alvarado, H.R. Anderson, L.M. Anderson, K.G. Andrews, C. Atkinson, L.M. Baddour, A.N. Bahalim, S. Barker-Collo, L.H. Barrero, D.H. Bartels, M.G. Basanez, A. Baxter, M.L. Bell, E.J. Benjamin, D. Bennett, E. Bernabe, K. Bhalla, B. Bhandari, B. Bikbov, A. Bin Abdulhak, G. Birbeck, J.A. Black, H. Blencowe, J.D. Blore, F. Blyth, I. Bolliger, A. Bonaventure, S. Boufous, R. Bourne, M. Boussinesq, T. Braithwaite, C. Brayne, L. Bridgett, S. Brooker, P. Brooks, T.S. Brugha, C. Bryan-Hancock, C. Bucello, R. Buchbinder, G. Buckle, C.M. Budke, M. Burch, P. Burney, R. Burstein, B. Calabria, B. Campbell, C.E. Canter, H. Carabin, J. Carapetis, L. Carmona, C. Cella, F. Charlson, H. Chen, A.T. Cheng, D. Chou, S.S. Chugh, L.E. Coffeng, S.D. Colan, S. Colquhoun, K.E. Colson, J. Condon, M.D. Connor, L.T. Cooper, M. Corriere, M. Cortinovis, K.C. de Vaccaro, W. Couser, B.C. Cowie, M.H. Criqui, M. Cross, K.C. Dabhadkar, M. Dahiya, N. Dahodwala, J. Damsere-Derry, G. Danaei, A. Davis, D. De Leo, L. Degenhardt, R. Dellavalle, A. Delossantos, J. Denenberg, S. Derrett, D.C. Des Jarlais, S.D. Dharmaratne, M. Dherani, et al. 2012. Years lived with disability (YLDs) for 1160 sequelae of 289 diseases and injuries 1990-2010: a systematic analysis for the Global Burden of Disease Study 2010. *Lancet (London, England)*. 380:2163-2196.
- Wahl, C., S. Liptay, G. Adler, and R.M. Schmid. 1998. Sulfasalazine: a potent and specific inhibitor of nuclear factor kappa B. *The Journal of clinical investigation*. 101:1163-1174.
- Wang, C.Y., M.W. Mayo, and A.S. Baldwin, Jr. 1996. TNF- and cancer therapy-induced apoptosis: potentiation by inhibition of NF-kappaB. *Science (New York, N.Y.)*. 274:784-787.
- Wang, C.Y., M.W. Mayo, R.G. Korneluk, D.V. Goeddel, and A.S. Baldwin, Jr. 1998. NF-kappaB antiapoptosis: induction of TRAF1 and TRAF2 and c-IAP1 and c-IAP2 to suppress caspase-8 activation. *Science (New York, N.Y.)*. 281:1680-1683.

- Wang, G., A. Woods, H. Agoston, V. Ulici, M. Glogauer, and F. Beier. 2007. Genetic ablation of Rac1 in cartilage results in chondrodysplasia. *Developmental biology*. 306:612-623.
- Wang, L., F. Du, and X. Wang. 2008. TNF-alpha induces two distinct caspase-8 activation pathways. *Cell*. 133:693-703.
- Warner, T.D., F. Giuliano, I. Vojnovic, A. Bukasa, J.A. Mitchell, and J.R. Vane. 1999. Nonsteroid drug selectivities for cyclo-oxygenase-1 rather than cyclo-oxygenase-2 are associated with human gastrointestinal toxicity: a full in vitro analysis. *Proceedings of the National Academy of Sciences of the United States of America*. 96:7563-7568.
- Watanabe, K., and Y. Yamaguchi. 1996. Molecular identification of a putative human hyaluronan synthase. *The Journal of biological chemistry*. 271:22945-22948.
- Watson, M., S.T. Brookes, A. Faulkner, and J. Kirwan. 2006. WITHDRAWN: Non-aspirin, non-steroidal anti-inflammatory drugs for treating osteoarthritis of the knee. *The Cochrane database of systematic reviews*:CD000142.
- Wertz, I.E., K.M. O'Rourke, H. Zhou, M. Eby, L. Aravind, S. Seshagiri, P. Wu, C. Wiesmann, R. Baker, D.L. Boone, A. Ma, E.V. Koonin, and V.M. Dixit. 2004. De-ubiquitination and ubiquitin ligase domains of A20 downregulate NF-kappaB signalling. *Nature*. 430:694-699.
- Westling, J., A.J. Fosang, K. Last, V.P. Thompson, K.N. Tomkinson, T. Hebert, T. McDonagh, L.A. Collins-Racie, E.R. LaVallie, E.A. Morris, and J.D. Sandy. 2002. ADAMTS4 cleaves at the aggrecanase site (Glu373-Ala374) and secondarily at the matrix metalloproteinase site (Asn341-Phe342) in the aggrecan interglobular domain. *The Journal of biological chemistry*. 277:16059-16066.
- Wiberg, C., A.R. Klatt, R. Wagener, M. Paulsson, J.F. Bateman, D. Heinegard, and M. Morgelin. 2003. Complexes of matrilin-1 and biglycan or decorin connect collagen VI microfibrils to both collagen II and aggrecan. *The Journal of biological chemistry*. 278:37698-37704.
- Wieland, H.A., M. Michaelis, B.J. Kirschbaum, and K.A. Rudolphi. 2005. Osteoarthritis - an untreatable disease? *Nature reviews. Drug discovery*. 4:331-344.
- Wilsman, N.J., C.E. Farnum, E.M. Green, E.M. Lieferman, and M.K. Clayton. 1996. Cell cycle analysis of proliferative zone chondrocytes in growth plates elongating at different rates. *Journal of orthopaedic research : official publication of the Orthopaedic Research Society*. 14:562-572.
- Woo, S.L., T.Q. Lee, M.A. Gomez, S. Sato, and F.P. Field. 1987. Temperature dependent behavior of the canine medial collateral ligament. *Journal of biomechanical engineering*. 109:68-71.
- Wu, S., D. Fadoju, G. Rezvani, and F. De Luca. 2008. Stimulatory effects of insulin-like growth factor-I on growth plate chondrogenesis are mediated by nuclear factor-kappaB p65. *The Journal of biological chemistry*. 283:34037-34044.
- Wu, S., A. Morrison, H. Sun, and F. De Luca. 2011. Nuclear factor-kappaB (NF-kappaB) p65 interacts with Stat5b in growth plate chondrocytes and mediates the effects of growth hormone on chondrogenesis and on the expression of insulin-like growth factor-1 and bone morphogenetic protein-2. *The Journal of biological chemistry*. 286:24726-24734.
- Wu, Z.H., Y. Shi, R.S. Tibbetts, and S. Miyamoto. 2006. Molecular linkage between the kinase ATM and NF-kappaB signaling in response to genotoxic stimuli. *Science (New York, N.Y.)*. 311:1141-1146.

- Yamamoto, Y., and R.B. Gaynor. 2001. Therapeutic potential of inhibition of the NF-kappaB pathway in the treatment of inflammation and cancer. *The Journal of clinical investigation*. 107:135-142.
- Yang, L., K.Y. Tsang, H.C. Tang, D. Chan, and K.S. Cheah. 2014. Hypertrophic chondrocytes can become osteoblasts and osteocytes in endochondral bone formation. *Proceedings of the National Academy of Sciences of the United States of America*. 111:12097-12102.
- Yaykasli, K.O., O.F. Hatipoglu, E. Yaykasli, K. Yildirim, E. Kaya, M. Ozsahin, M. Uslu, and E. Gunduz. 2015. Leptin induces ADAMTS-4, ADAMTS-5, and ADAMTS-9 genes expression by mitogen-activated protein kinases and NF-kB signaling pathways in human chondrocytes. *Cell biology international*. 39:104-112.
- Yong, Y., S.W. Choi, H.J. Choi, H.W. Nam, J.A. Kim, D.U. Jeong, D.Y. Kim, Y.S. Kim, and D.W. Kim. 2011. Exogenous signal-independent nuclear I kappa B kinase activation triggered by Nkx3.2 enables constitutive nuclear degradation of I kappa B-alpha in chondrocytes. *Molecular and cellular biology*. 31:2802-2816.
- Zerkak, D., and M. Dougados. 2004. The use of glucosamine therapy in osteoarthritis. *Current pain and headache reports*. 8:507-511.
- Zhang, W., A. Jones, and M. Doherty. 2004. Does paracetamol (acetaminophen) reduce the pain of osteoarthritis? A meta-analysis of randomised controlled trials. *Annals of the rheumatic diseases*. 63:901-907.
- Zhang, Y., and J.M. Jordan. 2008. Epidemiology of osteoarthritis. *Rheumatic diseases clinics of North America*. 34:515-529.
- Zhang, Y., and J.M. Jordan. 2010. Epidemiology of osteoarthritis. *Clinics in geriatric medicine*. 26:355-369.
- Zhou, X., K. von der Mark, S. Henry, W. Norton, H. Adams, and B. de Crombrughe. 2014. Chondrocytes transdifferentiate into osteoblasts in endochondral bone during development, postnatal growth and fracture healing in mice. *PLoS genetics*. 10:e1004820.

10. List of abbreviations

AC	Articular cartilage
ACL	Anterior cruciate ligament
ACLT	Anterior cruciate ligament transection
ADAMTS-5	A disintegrin and metalloproteinase with thrombospondin motifs 5
AFM	Atomic force microscopy
AKT	Protein kinase B (PKB)
ARG-1	Arginase-1
ATM	Ataxia telangiectasia mutated
BCL	B-cell lymphoma
BMP-2	Bone morphogenetic protein 2
BrdU	5-bromo-2'-deoxyuridine
BSA	Bovine serum albumin
CD95	Cluster of differentiation 95
cFLIP	Cellular FLICE (FADD-like IL-1 β -converting enzyme)-inhibitory protein
Col	Collagen
CK-2	Casein kinase-II
CRE	Chromosome recombinase
COMP	Cartilage oligo matrix protein
COX-2	Cyclooxygenase 2
DDR-2	Discoidin domain-containing receptor 2
DAPI	4,6-diamidino-2-phenylindole
DMEM	Dulbeco's minimal essential medium
DNA	Deoxyribonucleic acid
dNTP	Deoxyribonucleotide triphosphate
dKO	Double knockout
DMM	Destabilization of the medial meniscus
DMSO	Dimethyl sulfoxide
DTT	Dithiothreitol
dsRNA	Double strand RNA

LIST OF ABBREVIATIONS

ECM	Extracellular matrix
EDTA	Ethylenediaminetetraacetic acid
e.g.	Exempli gratia (for example)
ELISA	Enzyme-linked immunosorbent assay
ERK	Extracellular signal-regulated kinases
FAK	Focal adhesion kinase
FBS	Fetal bovine serum
FGF	Fibroblast growth factor
FGFR	Fibroblast growth factor receptor
FITC	Fluorescein isothiocyanate
Fn	Fibronectin
GADPH	Glyceraldehyde 3-phosphate dehydrogenase
GAG	Glycosaminoglycan
gDNA	Genomic DNA
gp-39	Glycoprotein 39
GTP	Guanosine triphosphate
HA	hyaluronan
HAS-2	Hyaluronan synthase 2
HER-2	Human epidermal growth factor receptor 2
HLH	Helix-loop-helix
HZ	Hypertrophic zone
H&E	Hematoxyl & eosin
ICE	IL-1 β converting enzyme
IGF	Insulin-like growth factor
IL	Interleukin
I κ B	Nuclear factor of kappa light polypeptide gene enhancer in B-cells inhibitor
IKK	I κ B kinases
iNOS	Inducible nitric oxide synthase
ITM	Interterritorial matrix
Jnk	c-Jun N-terminal kinase
KO	Knockout
LMP	Latent membrane protein
LNA	Lock nucleic acid-antisense

LIST OF ABBREVIATIONS

LPS	Lipopolysaccharide
LZ	RelB-transactivation domain
MAPK	Mitogen-activated protein kinase
MEF	Mouse embryonic fibroblasts
MGP	Matrix gla protein
ML	Mediolateral
MMP	Matrix metalloproteinase
mRNA	Messenger RNA
MSC	Mesenchymal stem cell
NBD	NEMO binding domain
Nemo	NF-kappa-B essential modulator, also known as IKK- γ
NF- κ B	Nuclear factor kappa-light-chain-enhancer of activated B cells
NIK-1	NF- κ B-inducing kinase 1
NKx3.2	NK3 homeobox 2, also called Bapx-1
NLS	Nuclear localization signal
NO	Nitrogen oxide
NSAID	Non-steroidal anti-inflammatory drug
OA	Osteoarthritis
OD	Osteochondritis dissecans
ODN	Oligodeoxynucleotides
OPN	Osteopontin
p16	Cyclin-dependent kinase inhibitor 2A
PBS	Phosphate-buffered saline
PCM	Pericellular matrix
PD	Proximaldistal
PEST	Domain rich in proline (P), glutamate (E), serine (S) and threonine (T).
PFA	Paraformaldehyde
PGE	Prostaglandin E
PGs	Proteoglycans
PI3K	Phosphoinositide 3-kinase
PM	Periterritorial matrix
PRb	Retinoblastoma protein

LIST OF ABBREVIATIONS

PTHrP	Parathyroid hormone-related peptide
PVDF	Polyvinylidene fluoride
PZ	Proliferating zone of growth plate
RA	Rheumatoid arthritis
RHD	Rel-homology domain
RIPK-1	Receptor-interacting protein kinase 1
RNA	Ribonucleic acid
RNAi	RNA interference
RT	Room temperature
RT-PCR	Reverse transcriptase polymerase chain reaction
RZ	Resting zone of growth plate
SDS	Sodium dodecyl sulfate
siRNA	Small interfering RNA
SCW	Streptococcal cell wall
SOX	Sex determining region Y box 9
SUMO	Small ubiquitin-like modifier protein
TAD	Transcriptional activation domain
TCR	T-cell receptor
TGP	Total growth plate
TIMP	Tissue inhibitors of metalloproteinases
TLDA	
TNF- α	Tumor necrosis factor alpha
TNFR	Tumor necrosis factor receptor
TRAP	Tartrate resistant acid phosphatase
TUNEL	Terminal deoxynucleotidyl transferase dUTP nick end labeling
ZF	Zinc-finger domain

11. Acknowledgement

First, I would like to thank my family for supporting me spiritually and giving me advices. Study abroad with people all around the world is my dream. Thank to Deutsche Akademischer Austauschdienst (DAAD), the scholarship of doctoral students makes it come true. I am very honored to be the recipient of this award. It has lightened my life costs in Germany and allows me to focus on my research project. I hope one day I will be able to help students achieve their goals just as DAAD has helped me.

I would like to express my sincere gratitude to my supervisors Prof. Dr. med. Mathias Schieker and PD Dr. Attila Aszodi for the continuous support of my Ph.D study and research project, with their patience, motivation, and immense knowledge. Their guidance helped me in all the time of research and writing of this thesis. My sincere thanks also go to Prof. Tonia Vincent and Prof. Hauke Clausen-Schaumann, who cooperate in this research project. Thank to Zsuzsanna Farkas and Carina Prein for their contribution of IHC experiments and AFM operation. Without they precious support, they gave much strength to this research as well. During these four years, I had the pleasure to work with many colleagues in the lab. Thank you for the stimulating discussions, for the time we worked together, and for all the good time we shared.

Last but not the least, I would like to thank my friends that I met in Germany and those ones from Taiwan. You all encourage and support me in some way during the past four years. To my girl, who sees the worst part of me, thank you for standing on my side.

12. Declaration

I, the undersigned, hereby declare that this dissertation is entitled, “The role of NF- κ B signaling in cartilage development and function” is my own work, and that all the sources I have used or quoted have been indicated or acknowledged properly by means of included references.

Munich, 06. 11. 2017

Place, date

Feng-Koo Hsieh